

# **Appendix A**

## **Hydraulic Design**

**Draft Interim Feasibility Report  
DeLong Mountain Terminal, Alaska  
Navigation Improvements**

## Table of Contents

1.0 INTRODUCTION .....	1
1.1 Project Purpose.....	1
1.2 Background .....	1
1.3 Description of Project Area .....	3
2.0 NEEDS AND OPPORTUNITIES .....	5
3.0 STUDY CONSTRAINTS.....	6
4.0 CLIMATOLOGY, METEOROLOGY, HYDROLOGY .....	6
4.1 Temperature.....	6
4.2 Fog.....	6
4.3 Ice Conditions.....	6
4.3.1 Ice Thickness .....	7
4.3.2 Ice Ridges and Rubble .....	7
4.3.3 Rafted Ice .....	7
4.3.4 Ice Flexural Strength .....	7
4.3.5 Open Water Season .....	8
4.3.6 Historical Shipping Season.....	8
4.4 Geology and Soils.....	9
4.5 History of Erosion .....	11
4.6 Tides.....	12
4.7 Wind.....	13
4.7.1 Basin Scale Winds.....	14
4.7.2 Regional Scale Winds.....	17
4.7.3 Summary Wind Data .....	22
5.0 Wave Climate.....	27
5.1 Ice.....	27
5.2 Low Frequency Energy .....	29
5.3 Hindcast Model Description.....	35
5.3.1 Basin.....	36
5.3.2 Region .....	37
5.3.3 Subregion.....	37
5.3.4 Model Validation.....	37
5.4 Average Wave Climate.....	56
5.5 Nearshore Wave Transformation.....	65
5.6 Extreme Storms .....	69
5.7 Determination of Weather Days Based on Waves.....	75
6.0 Currents and Water Levels.....	78
6.1 Measured Currents.....	78
6.1.1 Observations During Times of Ice Cover .....	84
6.2 Current and Water Surface Modeling.....	85
6.2.1 Model Verification .....	88
6.3 ADCIRC Currents for Hypothetical Year .....	95
6.4 ADCIRC Currents for Storm Events .....	96
6.5 ADCIRC Water Surface Elevation .....	97
7.0 SEDIMENT MOVEMENT .....	99
7.1 Nearshore Sediment.....	99
7.2 Sediment Grain Size and Spatial Distribution .....	99
7.3 Erosion Rate Data.....	100
7.4 Sediment Transport Methods and Models.....	101
7.5 Channel Infilling Assumptions, and Representations.....	106
7.5.1 Representation of Bed Material.....	106
7.5.2 Application of Environmental Conditions .....	107
7.5.3 Other Parameters. ....	107

Draft Feasibility Report  
Appendix A: Hydraulic Design, Delong Mountain Terminal, Alaska

7.5.4 Model Accuracy and Uncertainty .....	108
7.6 Longshore Transport .....	108
7.6.1 Wave Transformation .....	108
7.6.2 Beach Profile .....	108
7.6.3 Longshore Transport Sediment Characteristics .....	109
7.6.4 Longshore Transport Estimates .....	109
7.6.5 Uncertainty in Longshore Transport Estimates .....	112
7.7 "Hypothetical" Year Simulations .....	113
7.7.1 Hypothetical Year Channel-Infilling Results .....	113
7.8 Channel Infilling Estimates for Extreme Events .....	115
7.8.1 Synthetic Storms .....	116
7.8.2 Synthetic Storm Results .....	117
7.9 Event-Based Extremal Analysis of Channel Infilling .....	121
7.9.1 Input Conditions .....	121
7.9.2 Results of the Event-Based Analysis of Channel Infilling .....	123
7.9.3 Sensitivity and Uncertainty .....	133
7.10 Infilling Under Ice Cover .....	134
<b>8.0 CHANNEL DESIGN .....</b>	<b>135</b>
8.1 Design Vessel Criteria .....	135
8.2 Configuration and Use .....	135
8.2.1 Channel Width .....	141
8.2.2 Channel Depth .....	142
8.2.3 Ships Factors .....	143
8.2.4 Channel Location .....	144
8.2.5 Turning Basin .....	145
8.2.6 Sideslopes and Bank Stability .....	145
8.3 Initial Dredging Quantity .....	145
8.4 CHANNEL NAVIGATION .....	146
8.4.1 Analysis of Currents With Respect to Navigation .....	146
8.4.2 Joint Probability of Currents and Wind .....	147
8.4.3 Ship Simulation .....	149
8.4.4 Tug Boat Assistance .....	169
8.4.5 Navigation Aids .....	169
8.5 Vessel Motion Study .....	170
8.5.1 Parameters Tested .....	170
8.5.2 Vessel Motion in the Dredged Channel .....	172
8.5.3 Moored Vessel Motion .....	172
8.6 Construction Considerations .....	172
8.7 Disposal of Dredge Material .....	173
8.8 Dredged Channel Project Cost .....	174
<b>9.0 Breakwater DESIGN .....</b>	<b>174</b>
9.1 Alignment, Length & Usability .....	177
9.2 Underlayer Design .....	177
9.3 Toe Design .....	177
9.4 Armor Stone .....	177
9.5 Navigation Aids .....	178
9.6 Construction Considerations .....	178
9.7 Breakwater Cost .....	181
<b>10.0 GEOTECHNICAL CONSIDERATIONS .....</b>	<b>182</b>
10.1 Site Geology and Soils .....	182
10.2 Boring Locations and Material Summary .....	182
<b>11.0 Maintenance Dredging .....</b>	<b>182</b>
11.1 Sedimentation Associated With Shore Connected Direct Loading Facility .....	183
11.1.1 Littoral Zone .....	183
11.1.2 Wave and Current Induced Sediment Transport Seaward of the Littoral Zone .....	184

Draft Feasibility Report  
Appendix A: Hydraulic Design, Delong Mountain Terminal, Alaska

11.1.3 Side Slope Sloughing Due To Waves And Vessel Activity .....	187
11.1.4 Required Overdepth Dredging Options .....	189
11.1.5 Required Overdepth Dredging For Efficient Maintenance .....	192
11.1.6 Annual Dredging Cost For Deep Water Facility .....	197
11.1.7 Dredge Required for the Shore Connected Direct Loading Facility .....	198
11.2 Sedimentation Associated With The Breakwater And Barge Loading Facility.....	200
11.2.1 Sediment Transport Within the Littoral Zone.....	200
11.2.2 Wave and Current Induced Sediment Transport Seaward of the Littoral Zone.....	200
11.2.3 Annual Maintenance Cost For Breakwater and Barge Loading Facility .....	200
11.2.4 Dredge Associated with the Breakwater/Barge Loading Facility.....	200
12.0 Risk and Uncertainty.....	201

## 1.0 INTRODUCTION

This hydraulic design appendix describes the technical aspects of the DeLong Mountain Terminal (DMT) navigation improvements. It provides the background for determining the Federal interest in construction of a port improvement project.

The Alaska Industrial Development and Export Authority (AIDEA) owns the existing DeLong Mountain Transportation System (DMTS), which includes a dedicated roadway and a small port facility. Teck Cominco Alaska (TCAK) primarily uses the port facility for loading zinc and lead concentrate from the mine for shipment.

To determine the feasibility of a project to improve shipping, model studies were conducted on the winds, waves, currents, and sediment movement at the site. A ship simulation study was also performed to verify the tug horsepower and channel dimensions.

### 1.1 Project Purpose

The following objectives were identified for the port improvements before beginning this engineering analysis.

1. Develop a port facility to accommodate the current loading of zinc and lead at the site with provisions for future expansion to accommodate an increase in throughput and diversification of the products shipped through the port.
2. Design and construct improvements to provide a safe and efficient port facility that satisfies the above objectives in an environmentally and economically sound manner. Over forty port improvements were screened to ensure the correct port improvements were evaluated in more detail for the National Economic Development (NED) and locally preferred plan. This resulted in five port improvements being analyzed in more detail. Hydraulic analysis in support of those alternatives is provided herein.

### 1.2 Background

Current Portsite operations have vessels loaded by transshipment from lightering barges in a designated anchorage area, located just over 3 miles offshore. The anchorage area accommodates four vessels moored 0.5 to 1 mile apart. By keeping the vessel over 3 miles offshore, foreign crews do not have to clear customs upon arrival.

Foss Maritime (Foss) owns and operates the lightering barge system under long-term contract to TCAK. The lightering fleet includes two 5,500 dead weight ton (DWT) self-unloading, non-ice class barges. The barges are attended by up to four conventional, deep-sea tugs. Two of the tugs are dedicated to towing the barges, one tug is a rover for berthing assistance at the barge berth and the vessel, and the fourth is used to tow the

Draft Feasibility Report  
Appendix A: Hydraulic Design, Delong Mountain Terminal, Alaska

stern of the deep-sea vessel to make a lee, to partially shelter the barge during transshipment.

The start of the shipping season depends on the date when ice is sufficiently clear for tugs, lightering barges, and vessels to operate at the site. Between 1990 and 1999, the theoretical earliest date for shipping has varied from June 10 to July 14. Subsistence hunting of marine mammals is an additional consideration for starting shipping operations, and TCAK will not start shipping until the local subsistence hunting committee confirms that shipping will not affect their activities.

Actual commencement of concentrate transshipment has varied from July 4 to July 15. To date, the actual starting dates have been governed by ice or pre-arranged scheduling of vessels, and shipping operations have not been delayed by subsistence hunting.

The end of the shipping season is governed by ice formation to the south in the Bering Straits and by ice formation along the shores of the Chukchi Sea. Timing of the last ship has to be planned using satellite ice data to avoid the risk of damage or entrapment of the vessel, tugs, and lightering barges north of the Bering Straits. From 1990 to 1999, the latest day possible for lightering varied from October 1 to November 16.

In late 1997, Cominco Alaska (now known as Teck Cominco Alaska Incorporated (TCAK)) initiated conceptual studies for upgrading the ship loading system at the DMT to handle increased concentrate production. The existing two-barge lightering system was judged to be inadequate to reliably export the anticipated increased production that would accompany the upgraded loading system. The study concluded that a direct loading facility was the preferred option to increase the export capacity. This judgment was based on the following assumptions:

- a normal shipping window of 85 days (July 7-September 30)
- a weather allowance of 25 days (based on historical records)
- a net usable shipping window of 60 days
- a calculation of 79 days to load the expanded production with two barges, 19 days in excess of the 60-day estimated net usable shipping window.

In March 1998, Cominco Alaska authorized H.A. Simons to complete a preliminary offshore field investigation, which included gathering basic geotechnical and environmental data. H.A. Simons in June 1998 started what they called a bankable feasibility study that examined a dredged channel leading to a direct loading facility.

During the latter half of 1999, the Alaska Industrial Development and Export Authority (AIDEA) and Cominco Alaska approached the U.S. Army Corps of Engineers (USACE) regarding the possibility of obtaining federal funding for navigation improvements at the Portsite. In November 1999, USACE completed a reconnaissance level study to determine if there was a federal interest in improving the navigation system of the DMT. The conclusion of the study was that there was a Federal interest.

In January 2000, USACE and AIDEA entered into a formal “Feasibility Cost Sharing Agreement” contract. While USACE has primary responsibility for the study, AIDEA, as the local sponsor, provides input to the study through provision of in-kind services.

Reference to a proposed channel in this appendix is based on the early examination of a direct loading facility.

### 1.3 Description of Project Area

The DMT is on the eastern shore of the Chukchi Sea, north of the Bering Strait and 90 miles north of the Arctic Circle (figures 1 and 2). The site is bounded on each side by the Cape Krusenstern National Wildlife Refuge. It is approximately 15 miles (24.1 km) southeast of Kivalina, 82 miles (132 km) northwest of Kotzebue, and 650 air miles (1046 km) northwest of Anchorage, Alaska. The site is accessible only by air or water. Air transport to the site is by charter to the Red Dog Mine. A 50-mile (80.5 km) gravel road extends from the mine to the Ports site (figure 3).



Figure 1. State of Alaska Location Map

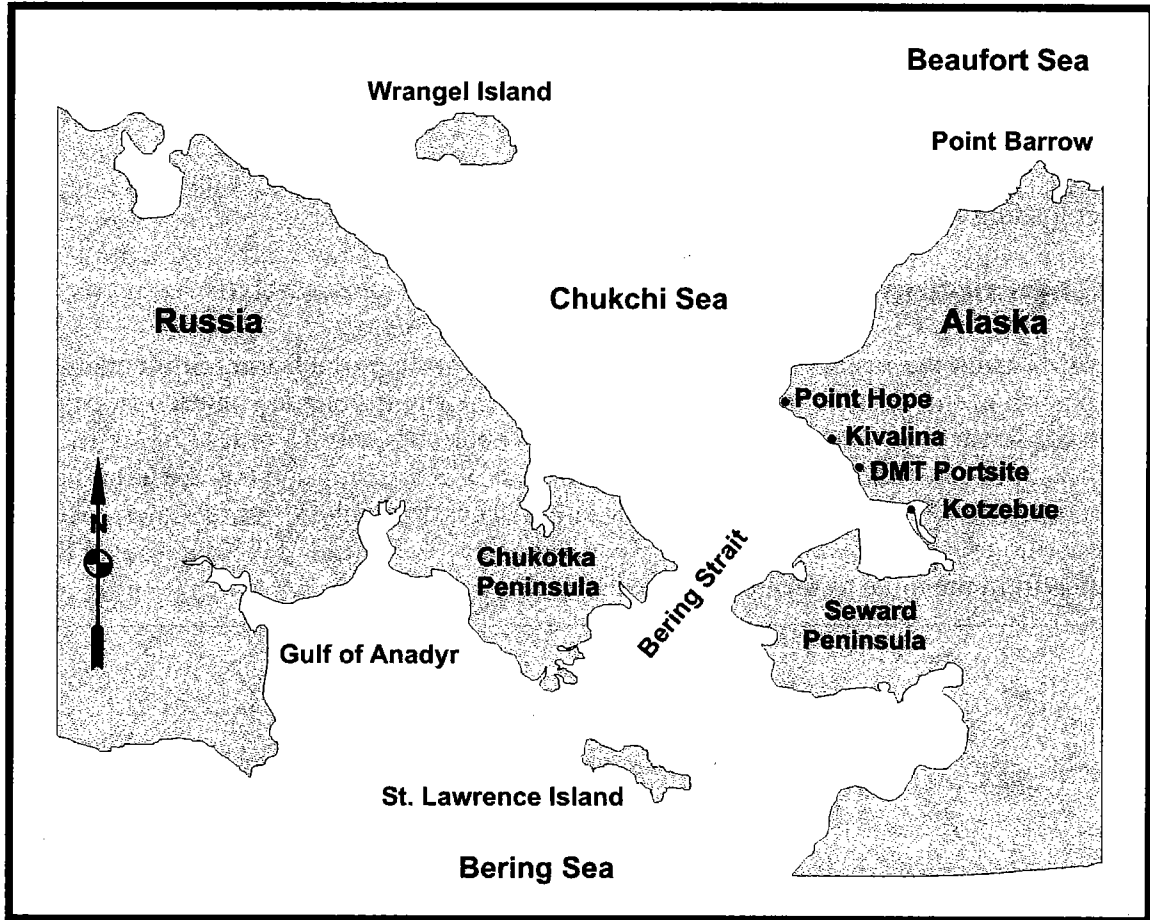


Figure 2. Project site and surrounding area

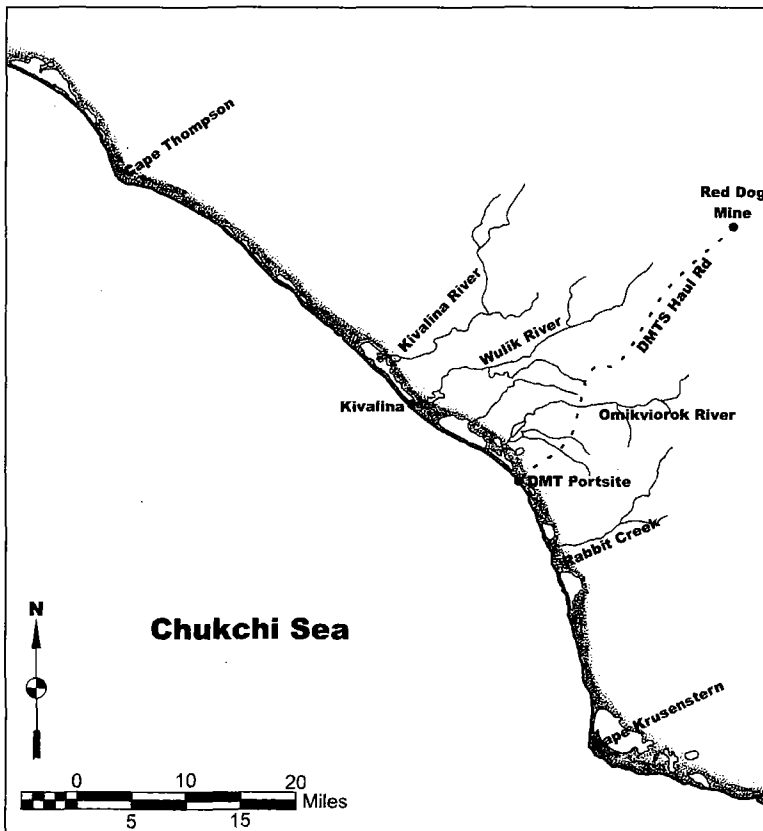


Figure 3. Vicinity Map.

## 2.0 NEEDS AND OPPORTUNITIES

Identification of the opportunities, problems, needs, and concerns in the study area provided the major issues and direction of the study effort. The northwest arctic region of Alaska contains several world class metallogenic belts and hydrocarbon deposits including:

- the zinc belt containing the Red Dog Mine, Lik/Su, Alvinella, Drenchwater, and other lead deposits;
- the polymetallic belt (with copper as the major metal) containing Bornite, Omar, Arctic, Sun, Smucker, and other deposits;
- the Western Arctic coal deposits.

AIDEA developed the Portsite to provide transportation infrastructure to support development of the resources of this region. Further resource development, such as additional Red Dog expansions, development of Lik/Su, connection to the Arctic and Bornite deposit developments, or the transshipment of coal from the proposed Deadfall Syncline development (in the western arctic coal deposits) would require upgrading of the current and proposed Portsite ship loading capacity.

In addition to supporting development of the region's resources, there is an opportunity to economically improve the existing fuel distribution system for some villages of the Northwest Arctic Borough (NAB) using the Portsite as the distribution hub.

### **3.0 STUDY CONSTRAINTS**

During the DeLong Mountain Terminal Feasibility Study, a number of study constraints were identified. These included:

- (1) The work season start is controlled by the completion of subsistence hunting of marine mammals.
- (2) The work season end is governed by icing in the Bering Strait. This generally occurs earlier than icing at the DMT site and could result in a ship being trapped in the Chukchi Sea.

### **4.0 CLIMATOLOGY, METEOROLOGY, HYDROLOGY**

#### **4.1 Temperature**

The DeLong Mountain Terminal lies in the transitional climate zone, which is characterized by long, cold winters and cool summers. The average low temperature during January is  $-15^{\circ}\text{F}$  ( $-26.1^{\circ}\text{C}$ ); the average high during July is  $57^{\circ}\text{F}$  ( $13.9^{\circ}\text{C}$ ). Temperature extremes can range from  $-54^{\circ}\text{F}$  to  $85^{\circ}\text{F}$  ( $-47.8^{\circ}\text{C}$  to  $29.4^{\circ}\text{C}$ ). Snowfall averages 57 inches (144.8 cm), with 8.6 inches (21.8 cm) of precipitation per year. (Alaska Department of Community and Economic Development-Kivalina)

#### **4.2 Fog**

According to the Coast Pilot, fog is most frequent during the months of May (10 days), June (11 days), July (9 days), August (9 days), September (6 days), and October (6 days). A pilot at the site notes: "It is heaviest in May and June. Fog is most dense in the morning hours but can last all day. It has occasionally lasted for several days. In July and August in the Bering Strait and Chukchi Sea, visibilities drop below 2 miles 10 to 25 percent of the time." (Personal communication with Captain Hannuksela)

#### **4.3 Ice Conditions**

Ice generally begins accumulating in the south Chukchi Sea in October. It begins forming along the northeast coast of Russia and proceeds down the Chukotsk Peninsula to Cape Dezhnev (figure 4). Generally, by the time ice has reached Cape Dezhnev, ice is also forming along the western Alaska coast. Ice along the Russian coast generally grows faster than the ice along the Alaska coast. Ice on both coasts continues to grow until access to the Chukchi Sea is cut off by ice in the Bering Strait. Shortly after the Bering Strait is iced up the Chukchi Sea ices over.

Ice formation in the Bering Strait governs the termination of the shipping season for the DMT. The transportation manager for TCAK consults the ice reports toward the end of the season to time his final ship orders. This enables ships to load and depart before ice in the Bering Strait blocks the ship's passage or requires the ship to leave the DMT early to avoid being icebound.

#### **4.3.1 Ice Thickness**

Peratrovich, Nottingham, and Drage Inc. (PN&D) measured ice thickness at the Ports site. In addition, PN&D conducted full-scale ice bending tests in 2000.

PN&D measured ice thickness of up to about 5 feet in April 1998 and 2000. Theoretical estimates of maximum ice thickness were also made based on:

- Consideration of theoretical ice-freezing index values
- Comparison of onsite ice measurements with data from the USACE Cold Region Research and Engineering Laboratory (CRREL) ice thickness observation program in Kotzebue.
- Comparison of Ports site temperatures with Kotzebue during 1996-2000

PN&D calculated a 100-year return period freezing index at 7210 °F-days, corresponding to an operating ice thickness design value of 63 inches. Assuming a normal distribution, an extreme ice thickness of 72 inches was estimated for 5000-year freezing index of 7850 °F-days.

#### **4.3.2 Ice Ridges and Rubble**

Measured data on ice ridges and rubble is relatively scarce, and consists of USCG icebreaker voyages, aerial laser profiles, aerial mapping for areas farther offshore, and limited site observations by PN&D in 1985 and 1988.

PN&D observed ridge heights of about 10 feet with ridge widths of less than 100 feet. Ridges consisted of ice blocks with thickness of less than 2 feet. Keel depths of 30 to 35 feet were observed by PN&D using a remote operated vehicle underwater reconnaissance in 1998.

For design purposes, PN&D recommended assuming that keel depths are limited by water depth, up to a maximum of 40 feet, with consolidated thickness of 10 feet and extreme maximum sail height of up to 25 feet.

#### **4.3.3 Rafted Ice**

PN&D encountered rafted ice at 35 feet water depth at the Ports site during 2000, consisting of two or three layers, with a maximum total ice thickness of 78 inches. PN&D recommended that the estimated potential maximum rafted ice thickness of 98 inches be used for this area.

#### **4.3.4 Ice Flexural Strength**

Between April 22 and May 2, 2000, PN&D conducted ice flexural strength testing at the Portsite. Ice temperatures and salinity measurements were also taken.

A total of 20 cantilever ice beams were tested to failure in uplift, to simulate the failure mechanism for the recommended ice structure design that incorporates an upright cone at the waterline of each structure. In addition to generating lower ice loads than a crushing failure, the bending failure in uplift occurs at a lower load than downward bending, due to the relatively higher temperature of seawater and high brine content at the bottom of the ice.

Ice thickness at the time of testing was between 40.5 and 52.8 inches, under snow cover of 0-6 inches. The cumulative freezing index at the port site was 5850°F-days. Cantilever ice beams were cut to a size of about 5 feet wide by 12 to 15 feet long. Flexural strengths of 35 to 73 pounds per square inch were measured, with an average of 52 pounds per square inch and a standard deviation of +/- 9 pounds per square inch.

#### 4.3.5 Open Water Season

Weekly historical ice conditions at the Portsite were extracted from the United States Ice Center's Sea Ice Grid (SIGRID) database from 1972 to 2001. Tables A-1 and A-2 show the earliest and latest open water season dates.

**Table A-1. Open Water Season Dates 1972 to 2001.**

	0 Tenths Ice Cover		5 Tenths Ice Cover	
	Ice Out	Ice In	Ice Out	Ice In
Earliest Date	9 June	4 October	7 June	9 October
Mean Date	6 July	29 October	27 June	4 November
Latest Date	28 July	19 November	18 July	23 November

**Table A-2. Open Water Season Length [days] 1972 to 2001**

	Ice Cover	
	0 Tenths Ice Cover	5 Tenths
Minimum Season	78	108
Mean Season	115	131
Maximum Season	148	160

#### 4.3.6 Historical Shipping Season

The start of the work season is based on the presence of whales and ice in the area. Based on previous years' shipping records, the season typically begins in the beginning of July. Equipment needs to be demobilized from the site before the Bering Straits ices over and prevents travel to or from the site. The start and finish shipping days from 1990 to 2000 are presented in table A-3.

**Table A-3. Historical Shipping Start and Finish Dates**

Year	Start Date	Finish Date	Total Days	Wet Metric Tons Shipped
------	------------	-------------	------------	-------------------------

Draft Feasibility Report  
Appendix A: Hydraulic Design, Delong Mountain Terminal, Alaska

1990	18 July	3 October	77	319,100
1991	4 July	8 October	96	548,200
1992	11 July	30 September	81	469,900
1993	7 July	6 October	91	464,300
1994	15 July	13 October	90	638,300
1995	7 July	30 September	85	727,400
1996	7 July	28 September	83	862,900
1997	4 July	11 October	99	986,000
1998	8 July	18 October	102	971,629
1999	14 July	1 November	110	1,204,100
2000	12 July	16 October	96	1,143,434

#### 4.4 Geology and Soils

The embayed southeastern Chukchi Sea is, in general, a flat, featureless plain with gradients ranging from 4 feet per mile (0.76 m/km) to immeasurably small slopes. The maximum depth is 210 feet (64 meters). A number of features stand out on this flat plain. Well-defined shoals extend north of Cape Prince of Wales and west of Point Hope, and an ill-defined shoal projects westward from Cape Krusenstern. Hope Submarine Valley, with a relief of only 180 feet (54.86 m), lies south and west of Point Hope (figures 4 and 5)

The sediments of the embayed southeastern Chukchi Sea consist of silt, sand, and gravel in decreasing order of abundance. Clay-sized particles are generally absent because weathering processes common to arctic regions produce primarily silty soils. The occurrences of gravel are associated with headland source areas.

Two primary source areas are available to this region: one is the area to the south of Bering Strait, and the other is the near shore cliffs at Cape Thompson and north of Point Hope. Sediment shed from the remainder of the surrounding landmass is effectively trapped on the low, rolling, and poorly drained coastal plain surrounding the Chukchi Sea.

Large quantities of sediment are distributed throughout the central portion of the Chukchi Sea by the current setting northward through the Bering Strait. The speed of the current is greatest in the strait and diminishes to the north around Cape Prince of Wales Shoal. The sediment mean diameter decreases, and sorting improves in a down current direction. (Creager and McManus, Project Chariot)

Along most of the coastline, where no structures have interrupted the coast, the beach is in a quasi-steady state condition. The shoreline is neither accreting as a result of permanent deposition of beach material, nor eroding because of wave action. The energy available in the waves is principally expended in moving beach sediment first toward the sea during times of heavy surf and then restoring it to the beach during the longer periods of relative calm.

The width of the steady-state beaches is related to their exposure to wave action. Sheltered beaches are wide, and exposed beaches tend to be narrow. Sediment related to the present beaches extends only to a water depth of approximately 30 feet (9.14 m). The sediment grades downward from fine gravel in the surf zone to very fine-grained sand. (Moore and

Cole, Geologic Investigations in Support of Project Chariot in the Vicinity of Cape  
Thompson, Northwestern-Alaska – Preliminary Report)

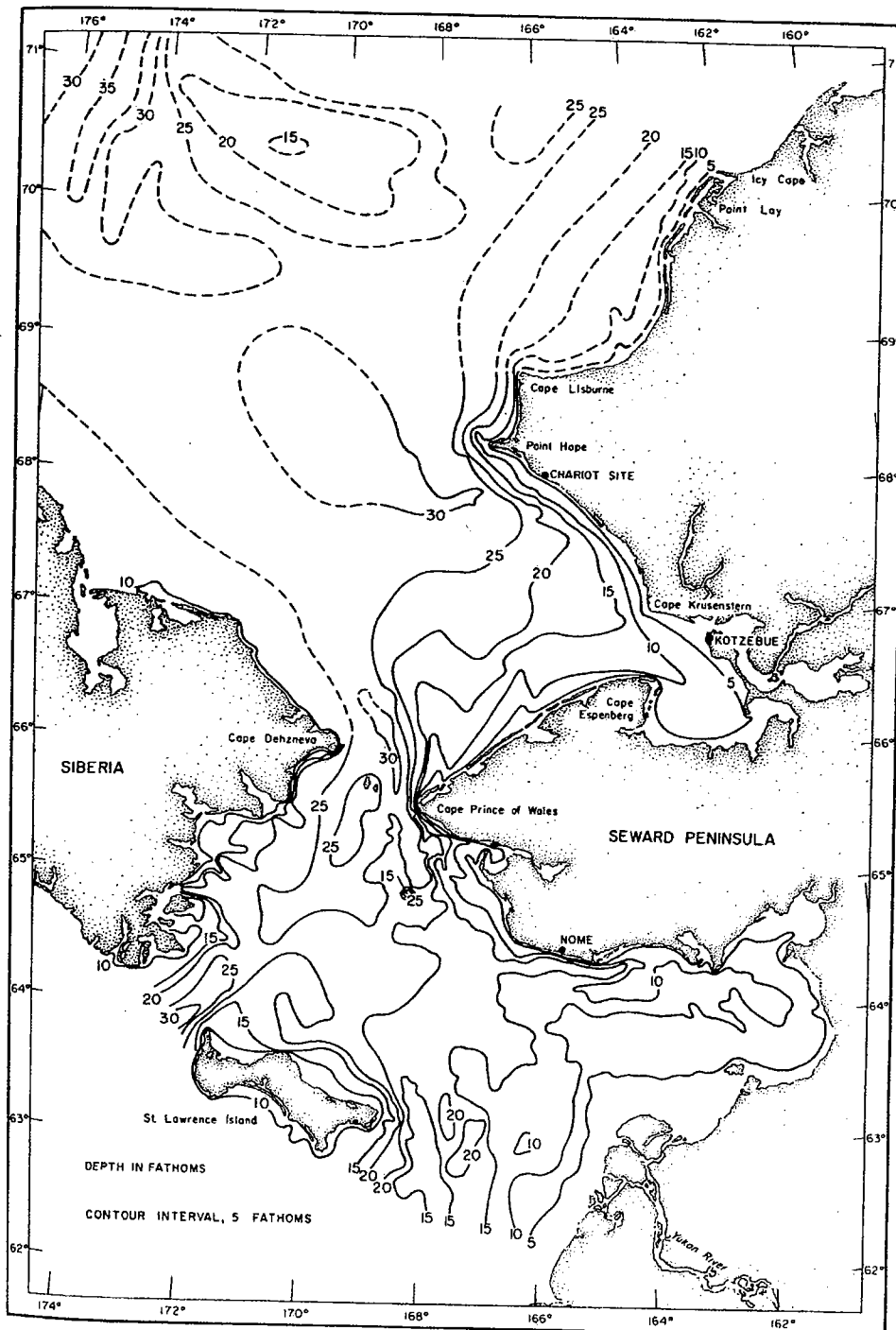


Figure 4 Generalized bathymetry in the Bering Straits and Chukchi Sea. *Oceanography of the Southeastern Chukchi Sea, Fleming and Heggarty*

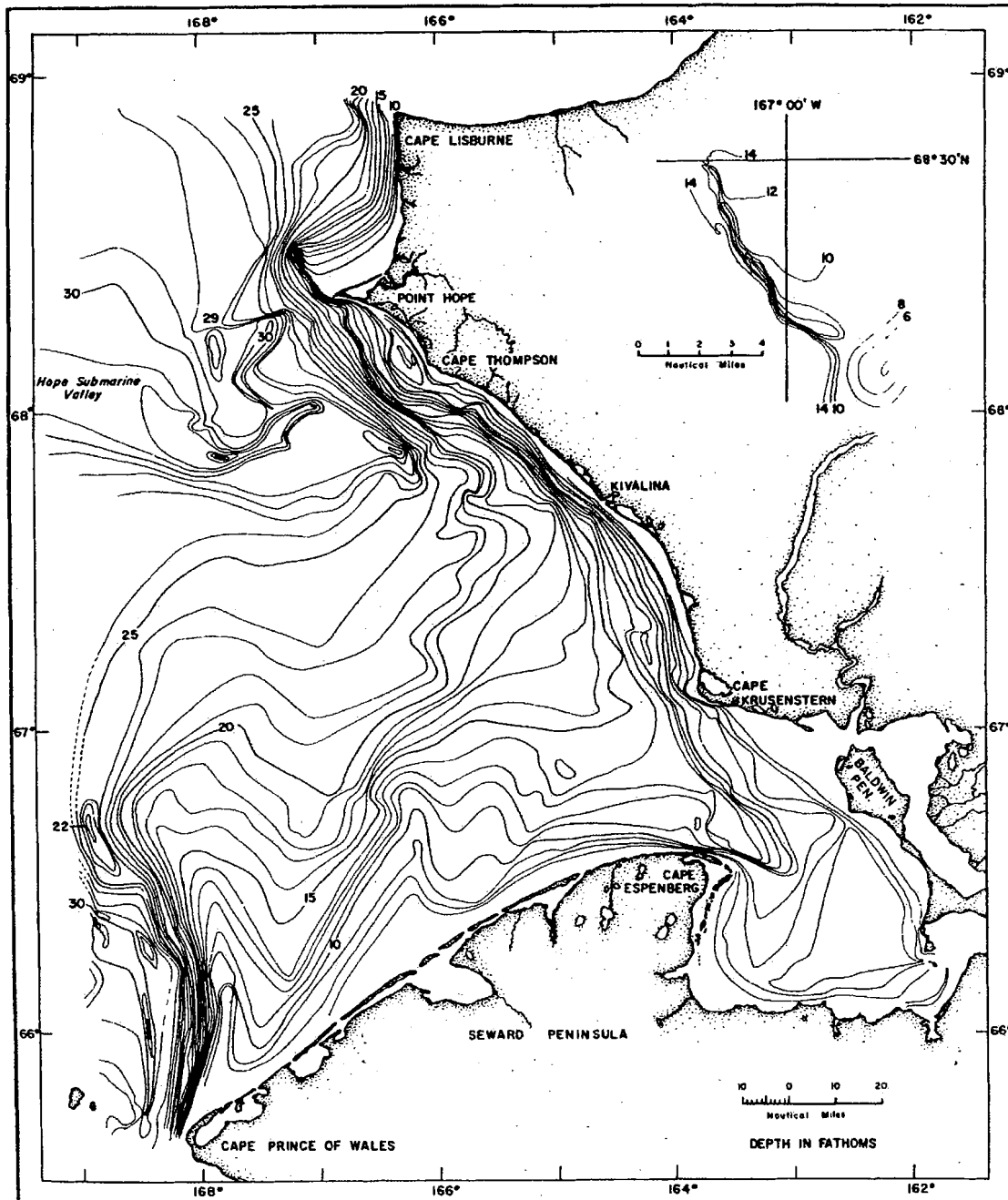


Figure 5 Bathymetry of the southeastern Chukchi Sea. *Geology of the Southeastern Chukchi Sea*, Creager and McManus

## 4.5 History of Erosion

Since construction of the shallow-water dock in 1986, sediment has impounded on the north side of the dock, requiring mechanical bypassing of material to the south. This material impoundment suggests that the net longshore transport at the site is to the south, which is in agreement with the Coastal and Hydraulics Laboratory (CHL) model predictions. Contrary to the net transport, the general trend of the currents at the site is

from south to north. The majority of sediment movement appears to occur during large storm events. The material impoundment and subsequent bypassing is not a yearly maintenance activity, rather it is an event driven activity that is performed on an as needed basis. Most recently bypassing has been performed in October 2002. Prior to that, bypassing was performed in the spring and fall of 1997.

The long-term consequence of a hardened structure along the beach is evident in aerial photographs taken at the site. The once linear beach line in the area of the dock is now non linear with the beach south of the dock appearing to have receded while the beach north of the dock has grown (figure 6).

Any loading facility constructed at the Portsite would include by passing as part of the annual maintenance. The effect of the loading facility constructed at the site will not have the impact of the existing dock.



Figure 6. Portsite shoreline in 2001.

#### 4.6 Tides

The DeLong Mountain Terminal is in an area of semi-diurnal tides with two high waters and two low waters each lunar day.

Tidal parameters at the DeLong Mountain Terminal are similar to those determined by NOAA for Station 949-1253 – Kivalina, Corwin Lagoon Entrance (67°43.6'N, 164°35.5'). The tidal parameters in table 4 were determined by NOAA using data from the period October 1, 1985 to September 30, 1986.

**TABLE A-4. Tidal Parameters – Kivalina, Corwin Lagoon Entrance**

Parameter	Elevation (ft MLLW)	Elevation (m MLLW)
Highest Observed Water Level (11/10/1985)	4.16	1.27
Mean Higher High Water (MHHW)	0.90	0.27
Mean High Water (MHW)	0.77	0.23
Mean Sea Level (MSL)	0.43	0.13
Mean Low Water (MLW)	0.10	0.03
Mean Lower Low Water (MLLW)	0.00	0.00
Lowest Observed Water Level (12/19/1985)	-3.12	-0.95

## 4.7 Wind

A wind hindcast was performed for the years 1985-1999 by Oceanweather Inc. (OWI), under contract to the Coastal Hydraulics Laboratory (CHL) to accurately reflect the forcing mechanism for the wave and current modeling, which in turn provided input to the sediment study. The hindcast was later extended to 2000. The wind data was also directly used in the ship simulation study.

Winds cannot be considered uniform in space. The curvature of wind fields that characterize low-pressure systems can be severe, especially for the meso-scale wind events that frequently influence the Portsites. Large-scale synoptic events, which are generally a rare event for the Chukchi Sea and Kotzebue Sound area, could possibly be represented by spatially constant winds. It is critical for an accurate representation of the winds, that the detailed structure of the small-scale meteorological events be resolved. The accuracy of the winds directly affects the accuracy of the model-generated data. For example, a ten percent uncertainty in the wind speed estimate will lead to an approximate 20 percent uncertainty in the wave height.

Two distinct wind fields were used for modeling; *basin scale* winds fields developed from the National Center for Environmental Prediction/National Center for Atmospheric Research (NCEP/NCAR) Reanalysis Project and *regional scale* wind fields that were developed by Oceanweather Inc. using their Interactive Objective Kinematic Analysis (IKOA) system. The basin scale winds are for synoptic scale features. Regional scale winds will capture the synoptic, meso, and micro scale wind fields, and will incorporate additional data and utilize different processing procedures. The domains for both wind fields used are shown in figure 7. Table 5 lists the geographical boundaries and characteristics of the wind domains.

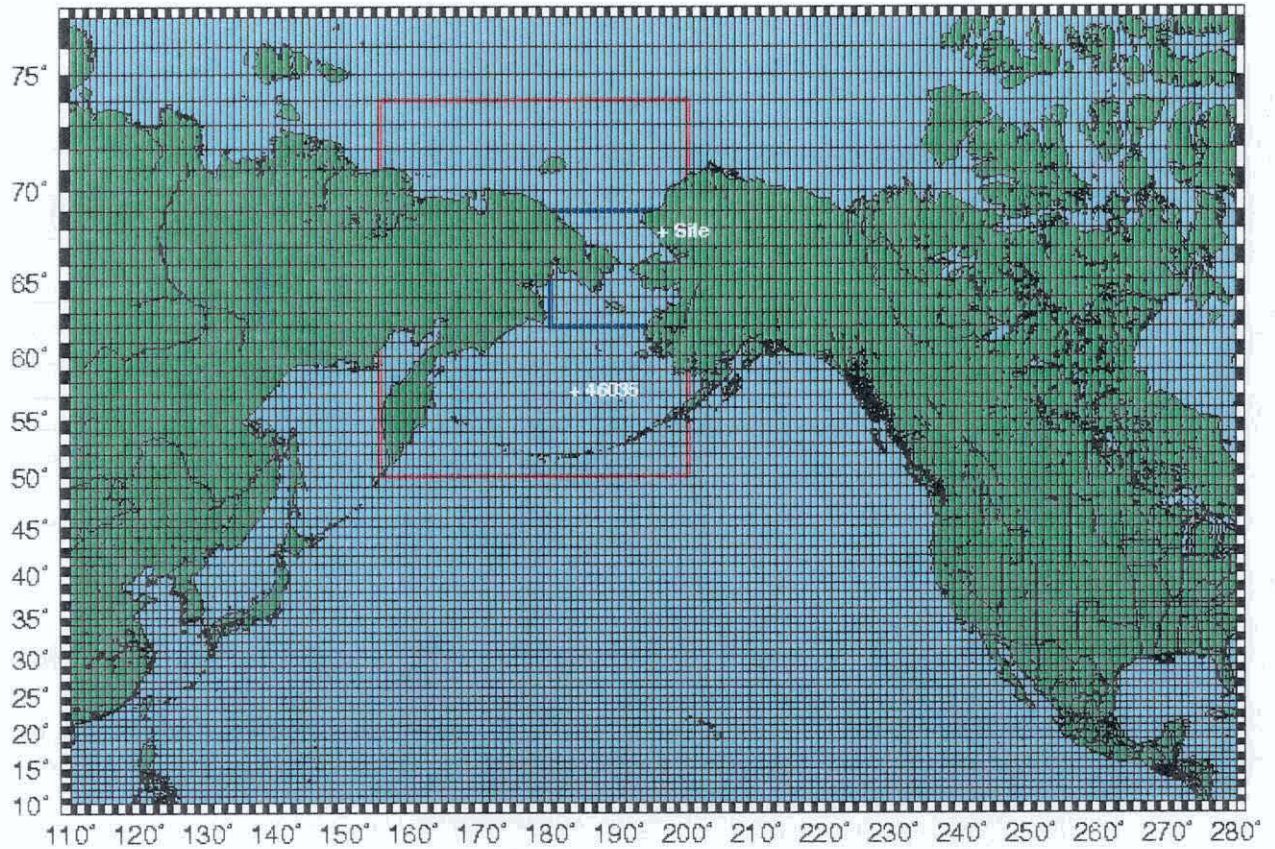


Figure 7. Basin shown by entire grid, region shown in red box, and subregion shown in blue box.

**TABLE A-5. Wind and wave domain description.**

Field Specification	Latitude Boundary		Longitude Boundary		Resolution	
	North	South	West	East	$\Delta x$	$\Delta t$
Basin Winds	79.0°	-2.8°	108.7°	281.2°	1.87/1.9°	6hr
OWI Regional Winds	74°	50°	155E	200°	0.25°	6hr

#### 4.7.1 Basin Scale Winds

The NCEP/NCAR Reanalysis project uses “frozen” methodologies (analysis/forecast) and performs data assimilation using historic data. The intent of using frozen methodologies is that the winds will not suffer from discontinuities generated by ever changing atmospheric models. Data assimilation methods add value by including all available point source measurements, as well as satellite data. Selection of the NCEP/NCAR Reanalysis wind fields adequately serves the purpose of providing a consistent wind field data set to establish basin scale winds.

The NCEP/NCAR Reanalysis 33.3 foot (10 meter) winds are resolved at 6-hour time steps and were taken directly from the database generated for the project. The only modification to these wind fields prior to use in the wave model simulations, was to interpolate them to a fixed spherical grid. The interpolated wind fields were checked against the original data to ensure consistency. Details of the check performed are discussed in the CHL report *Engineering Studies in Support of Delong Mountain Terminal Project*, September 2002.

The principal role of the basin scale domain is to capture synoptic scale meteorological events, and transmit the resulting energy to the regional domain. To illustrate the need for, and effectiveness of, proper scaling of meteorological events, an extremely large scale wind and wave event that affected the Portsite was selected. Figures 8 and 9 display the NCEP/NCAR Reanalyzed wind fields used to drive the basin scale wave model for a particular historic event, at two different times. The origin of this storm was Super Typhoon Patsy (November 1970). After making landfall, the remnants of the storm, steered by the jet stream, migrated back into the Pacific Ocean as an extra-tropical storm system and eventually redeveloped into a strong extra-tropical system. As indicated in figure 8, the maximum lobe in wind speeds was in excess of 38.9 knot (20 m/s) with a predominant wind direction heading toward the Bering Sea. Sixty hours later, this lobe of high winds was located at approximately 60° N latitude, just south of the Bering Strait (figure 9), with a similar intensity and spatial distribution. At the same time, another tropical system was developing just to the west of Japan; however, its net impact was not as severe as Patsy's. In general, specification of small-scale systems (compared to the target grid systems used in basin scale atmospheric modeling) is performed on a manual basis. To represent these types of systems at a basin scale, the tendency is to artificially create regions with strong winds, to approximate the net impact of meso scale features.

If the basin scale domain were excluded, the potential to misrepresent the energy levels in distant swells would increase, or in this case, the storm's impact on the Portsite would be missed completely. As previously noted, the regional scale winds will capture synoptic scale features such as Super Typhoon Patsy. Assuming no ice coverage, this event was the largest considered in the study. While the no ice coverage may or may not be a valid assumption for that particular event, it is valid for the evaluation of conditions at the Portsite given the fact that the ice coverage has been occurring later in the season, making the Portsite more susceptible to impacts from fall storms. This appears to be a steady trend. A United States Navy Report indicates that the polar ice cap could melt to the point where seasonal shipping lanes could open up in the Arctic by 2015.

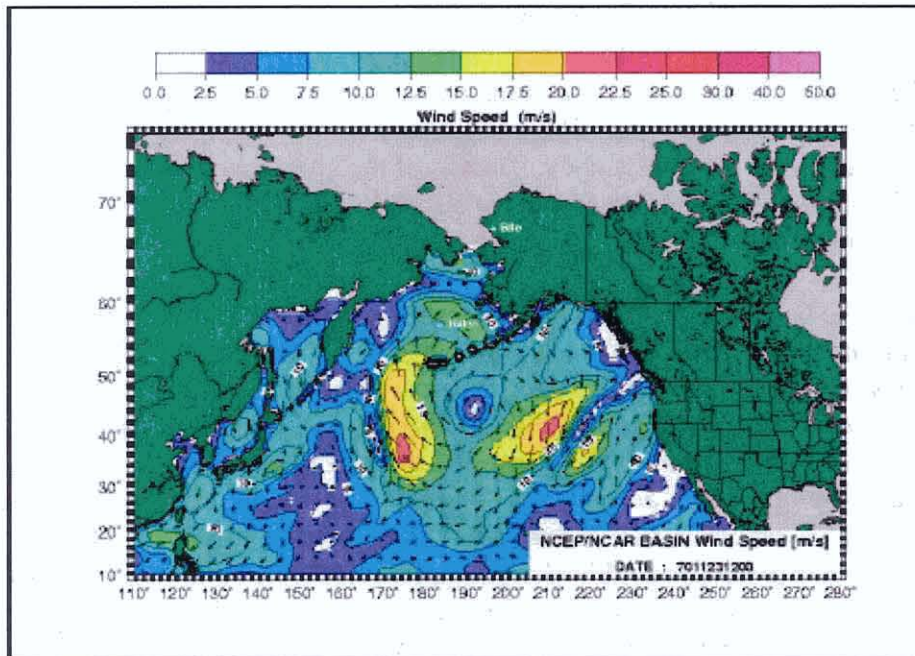


Figure 8. Basin scale wind field example from 23 November 1970, 1200 Universal Time Coordinate (UTC) (wind speeds color contoured, wind directions identified by arrows).

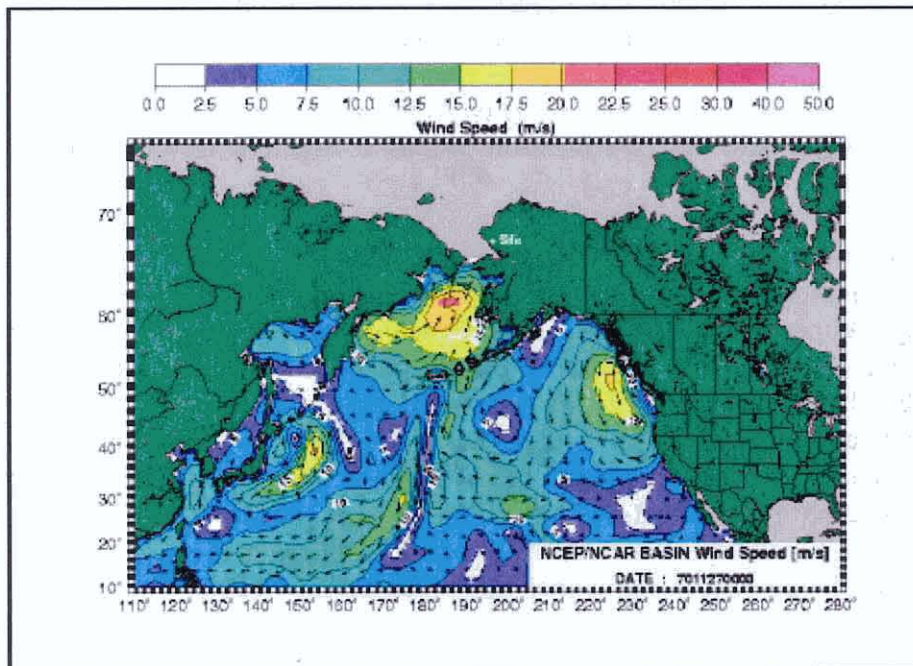


Figure 9. Basin scale wind field example from 27 November 1970, 0000 Universal Time Coordinate (UTC) (wind speeds color contoured, wind directions identified by arrows).

#### 4.7.2 Regional Scale Winds

The regional scale wind fields were developed by Oceanweather Inc. (OWI) using their Interactive Objective Kinematic Analysis (IOKA) system. The domain for the wind field and the geographical constraints are shown in figure 7 and table 5, respectively. The generation of high resolution wind fields in the Bering and Chukchi Seas, as well as the Kotzebue Sound, is critical for the establishment of the local wind generated sea component in the wave hindcast study. As previously noted, the basin scale is represented by large synoptic scale meteorological events, with the exception of tropical systems such as typhoons. In the area of the Portsite, meso- and micro-scale events dominate. The NCEP/NCAR wind fields capture the synoptic and, generally, the tropical systems rather well despite the low-resolution grid used in atmospheric modeling. This is most likely a result of using data assimilation methods and use of scatterometer data derived from satellites. The use of these wind fields in the specification of local conditions would not be sufficiently accurate to describe the winds affecting conditions around the Portsite.

OWI developed the Interactive Objective Kinematic Analysis (IOKA) system to provide wind analysis associated with tropical systems. This system has been modified for nearly all meteorological events including small scale, meso scale, and extra tropical storm systems. Five critical elements are required for the IOKA system:

- Background wind fields
- Point source measurements (airport anemometer records, buoy data)
- Ship records (archived wind speed and direction)
- Scatterometer estimates of the wind speed
- Kinematic control points (KCPs).

These data sets (excluding the KCPs) must be adjusted for stability and brought to a common reference level. Stability accounts for the changes in the boundary layer due to differences between air and water temperatures. If the water temperature is greater than the air temperature, momentum transfers increase at the air sea interface, and the effectiveness of the wind speed increases.

Point source measurements such as buoy data and airport records reflect wind speeds and directions based on short time burst averaging. These short term averages (1 to 10 minute averages) are temporally interpolated to hourly data.

Scatterometer wind fields derived from satellites are not true wind speed measurements. They are derived from inversion techniques and are extremely useful because of the spatial coverage obtained during one satellite pass. The repeat cycle is 35 days (on a 12 hour orbit); therefore, temporally continuous data are not available as in the case of point source measurements. In addition, data from all satellite-based scatterometers do not span the entire 16 year hindcast period, or any of the pre-1985 extreme storms that were considered in the study. Including these data may produce a series of discontinuities in the development of the wind field climatology; however, use of these data adds

considerable value to the final wind products, and outweighs concerns regarding the consistency of the climatological wind products.

Land based wind measurements were also adjusted for boundary layer effects. Every land based, point source measured data set was individually investigated, and adjustments were made as needed. These adjustments depended not only on the wind direction, but also on the wind magnitude. Close to the Portsite, terrain steering of the winds was approximated from extensive work done by OWI in this area. The Portsite anemometer data set was used to verify the approximation.

Because of the small number of point source measurements and the limited temporal coverage of the scatterometer wind estimates, a background wind field representing synoptic to meso scale meteorological conditions was required. The NCEP/NCAR Reanalysis wind field were used. This is the key factor relating the basin and regional scale wind fields.

Once all data sets were transformed to equivalently neutral, stable 33.3 feet (10 meter) winds, the IOKA system is used. Each input wind data product carries a specified weight which can be overridden by an OWI analyst at any time. Background wind fields are ingested into OWI's Graphical Wind Work Station, displaying all the available data sets (point source measurements, scatterometer data). The NCEP/NCAR Reanalysis wind fields are at a 6-hour time step, so all 1-hour point source wind measurements are repositioned via "moving centers relocation". This assures continuity between successive wind fields.

The most powerful tool of the IOKA system is the use of KCPs by the analyst. This tool can input and define ultra fine scale features such as frontal passages, maintain jet streaks, and control orographic effects near coastal boundaries. The analyst can use the KCPs to define data sparse areas using continuity analysis, satellite interpretation, climatology of developing systems, and other analysis tools. The IOKA system contains a looping mechanism that will continually update the new wind field based on revisions performed by the analyst. See figure 10 for an example of a workstation screen.

Draft Feasibility Report  
Appendix A: Hydraulic Design, Delong Mountain Terminal, Alaska

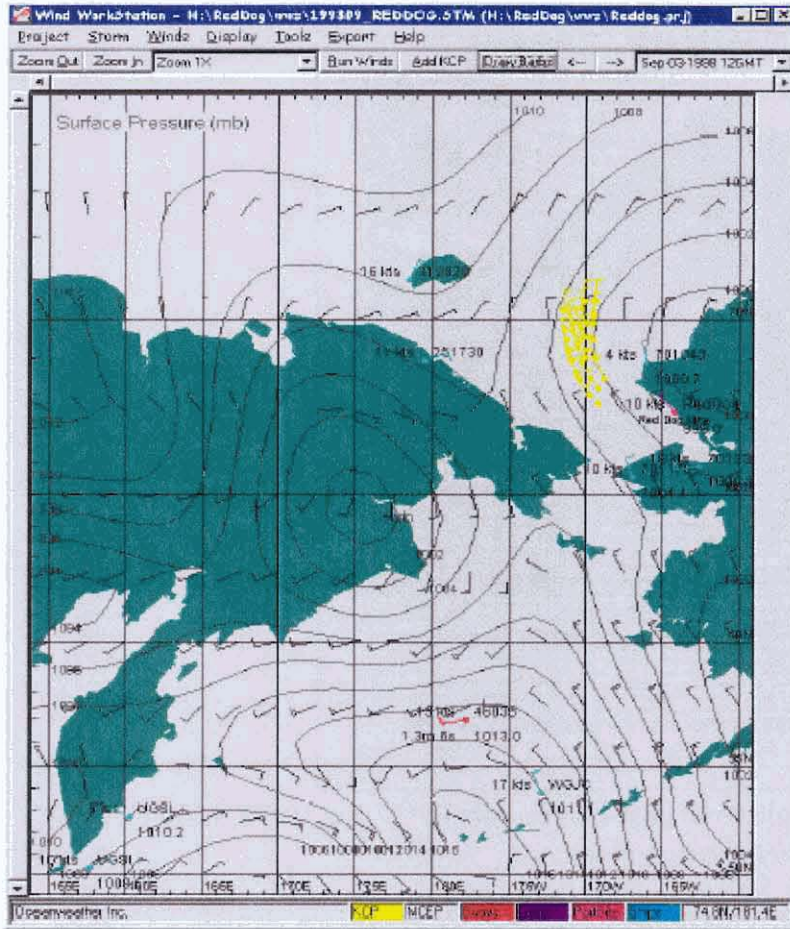


Figure 10. Example of the wind work station pressure contours and associated wind barbs: wind data color coded red (buoy data), blue (land-based stations), yellow (KPCs)

The final step in the construction of the OWI regional wind fields was to spatially interpolate the winds to a target domain and resolution. Based on past studies, a 0.25-degree resolution was selected for the final winds and covered the domain from 10° to 75° N Latitude, 155° to 200° E longitude (the blue box in figure 7). This interpolation procedure used continuity checking procedures, but also retained the structure of each storm for a moving center checking algorithm. The time step for each successive wind field was set to six hours. This was done because the NCEP/NCAR Reanalysis wind fields are resolved at 6-hour time steps. The numbers of point measurements were limited in general; however they were more numerous in the Kotzebue Sound area. The spatial structure of the winds is well established at the 0.25 degree resolution, and continuity between each successive wind field is retained. This is evident in figure 11, where the wind direction vectors are plotted. Note that every other wind vector is shown. One can clearly see the details and spatially varying winds reflected in the OWI regional wind fields. Curvature of the winds is evident and is considerable, particularly in the Chukchi Sea. Any assumption of spatially invariant winds cannot be made for cases like this.

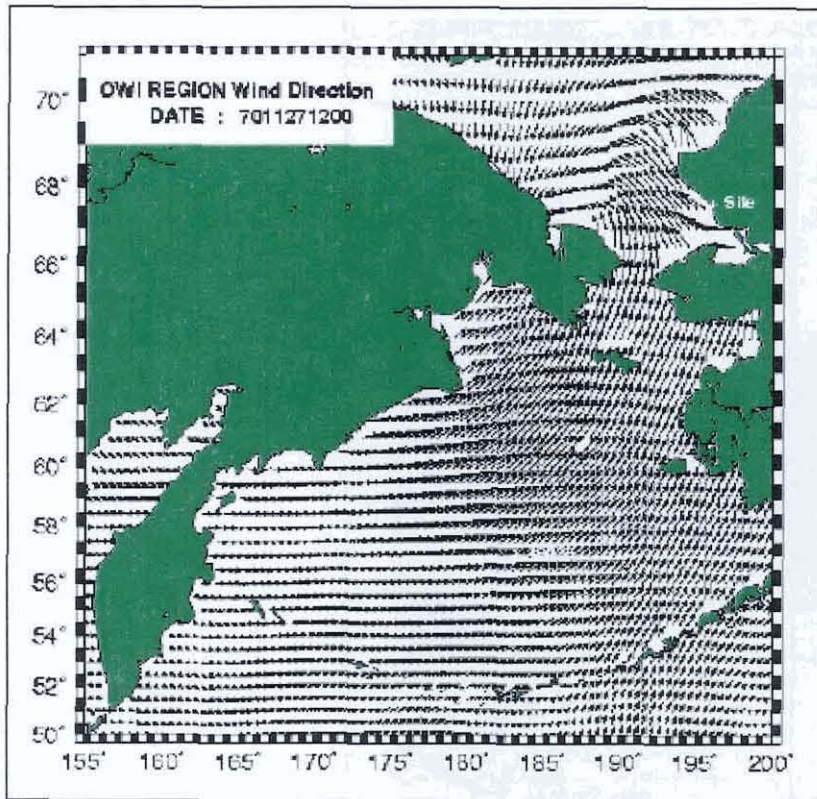


Figure 11. OWI regional scale wind direction vectors for 27 Nov 1970, 1200 UTC (vector length proportional to the magnitude)

Regional wind fields generated for Super typhoon Patsy are shown in figures 12 and 13. There are subtle differences between the basin scale winds and regional scale winds. Comparison of figures 8 and 12 reveal addition lobes of 29-34 knot (15 to 17.5 m/s) wind speeds in the regional field that were not present in the basin scale winds. The detailed structure of the OWI fields compared to the NCEP/NCAR winds shown clearly appears in the area around 64°N latitude. Sixty hours later (27 November 1970, 1200 UTC), the basin and regional winds differ. The lobe of high winds evident in the OWI winds (figure 13) is displaced slightly to the south when compared to the basin winds. The wind intensity is higher in magnitude and elongated.

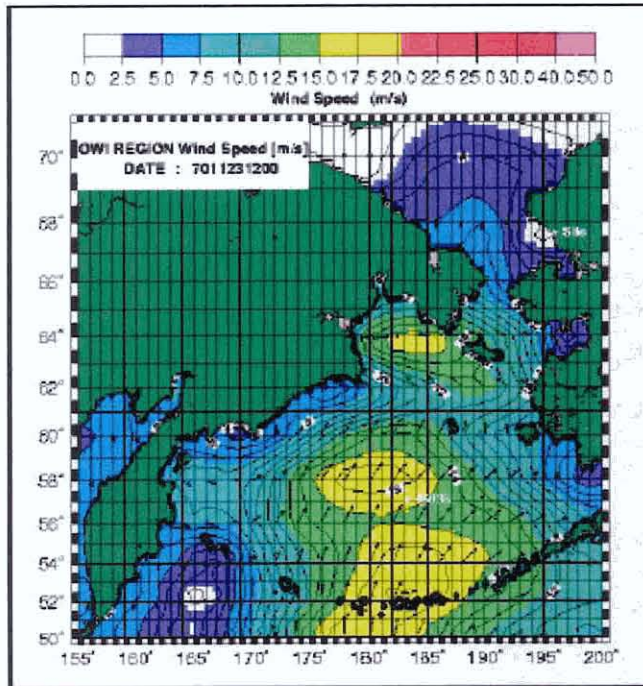


Figure 12. OWI region scale wind field example from 23 November 1970, 1200 Universal Time Coordinate (UTC) (wind speeds color contoured, wind directions identified by arrows).

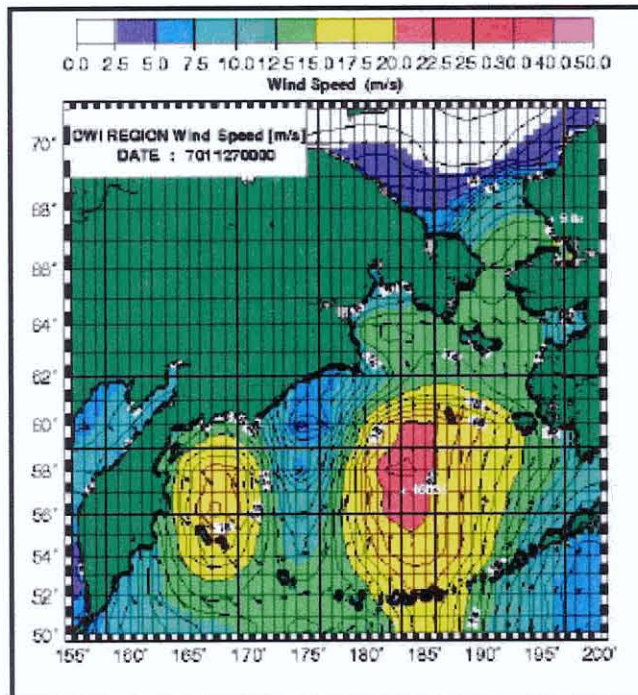


Figure 13. OWI region scale wind field example from 27 November 1970, 0000 Universal Time Coordinate (UTC) (wind speeds color contoured, wind directions identified by arrows).

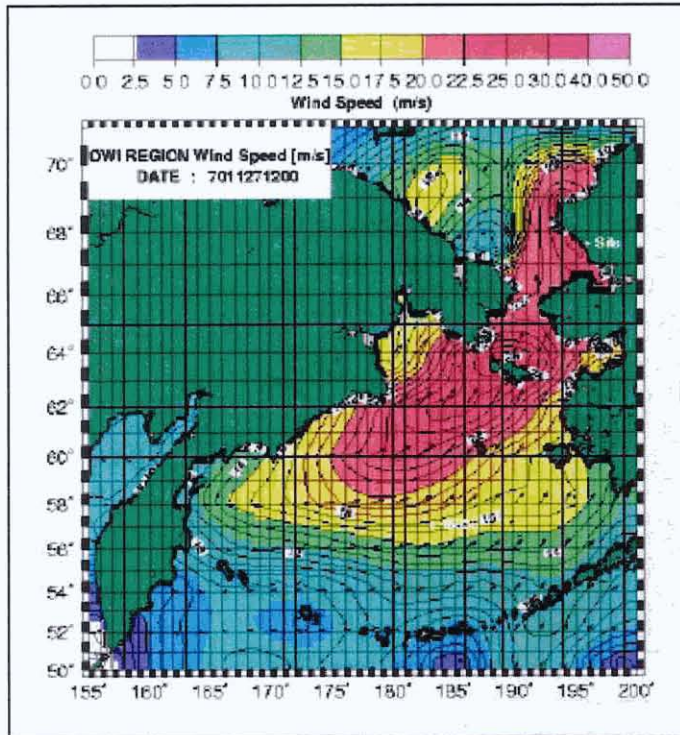


Figure 14. OWI region scale wind field example from 27 November 1970, 1200 Universal Time Coordinate (UTC) (wind speeds color contoured, wind directions identified by arrows).

Regional scale winds 12 hours later (figure 14) show that the storm moved north of the Bering Strait into Kotzebue Sound, offshore of the Portsite area. Wind speeds are in excess of 48.6 knots (25 m/s). The effect of the wind south of the Bering Strait would generate wave energy, somewhat blocked by Saint Lawrence Island, through the Bering Strait directly to the Portsite. In addition, locally generated wind seas would be created, running nearly shore parallel to the site. This shows the relative consistency between the two wind fields, and the importance of modeling the North Pacific Ocean as well as the entire Bering Sea.

#### 4.7.3 Summary Wind Data

Wind data generated for station 5 (figure 28) from the hindcast are shown in tables A-6, 7, and 8. A sample plot of the hindcast and buoy data for the Bering Sea (46035) and a plot of the hindcast and buoy data for the year 2000 deployment at DMT (48011) are shown in figures 15 through 19.

Draft Feasibility Report  
Appendix A: Hydraulic Design, Delong Mountain Terminal, Alaska

**TABLE A-6. Percent Occurrence of wind speeds for 1985-1999 June-November**  
**Latitude: 67.50N Longitude: 195.75E (see figure 28, Station 5 for location)**  
**22.5-DEG Direction bands centered about:**

Center Direction	0	22.5	45	67.5	90	112.5	135	157.5	180	202.5	225	247.5	270	292.5	315	337.5	TOTAL
Wind Speed (knot (m/s))																	
0.00 - 4.84 (0.00 - 2.49)	1.10	1.20	1.28	0.85	0.71	0.54	0.54	0.64	0.91	0.99	0.95	0.68	0.67	0.59	0.63	0.81	13%
4.86 - 9.70 (2.50 - 4.99)	2.08	2.68	1.89	1.68	1.30	0.83	1.07	1.12	1.77	1.89	1.68	1.17	0.97	1.04	1.09	1.45	24%
9.72 - 14.56 (5.00 - 7.49)	2.54	2.91	2.75	1.70	1.47	1.24	1.47	1.42	2.07	2.12	1.66	0.86	0.84	1.12	1.27	1.53	27%
14.58 - 19.42 (7.50 - 9.99)	1.94	2.29	2.55	1.44	1.09	1.12	1.09	0.73	1.25	1.19	0.69	0.38	0.45	0.42	0.81	1.03	18%
19.44 - 24.28 (10.00 - 12.49)	0.94	1.67	2.09	1.21	0.59	0.66	0.76	0.50	0.57	0.54	0.12	0.11	0.16	0.28	0.42	0.37	11%
24.30 - 29.13 (12.50 - 14.99)	0.26	0.58	0.91	0.64	0.41	0.39	0.39	0.24	0.26	0.23	0.05	0.03	0.06	0.06	0.07	0.15	5%
29.16 - 34.00 (15.00 - 17.49)	0.10	0.20	0.51	0.09	0.04	0.16	0.16	0.11	0.08	0.08	0.01	0.03	0.02	0.01	0.03		2%
34.02 - 38.86 (17.50 - 19.99)		0.05	0.04	0.03	0.02	0.07	0.10	0.06			0.01						0%
38.88 - 43.72 (20.00 - 22.49)					0.01	0.02	0.03	0.01									0%
43.74 - 48.58 (22.50 - 24.99)																	0%
48.60 - 53.44 (25.00 - 27.49)																	0%
53.46 - 58.30 (27.50 - 29.99)																	0%
58.32 - GREATER (30.00 - GREATER)																	0%
<b>TOTAL</b>	<b>9.0%</b>	<b>11.6%</b>	<b>12.0%</b>	<b>7.6%</b>	<b>5.6%</b>	<b>5.0%</b>	<b>5.6%</b>	<b>4.8%</b>	<b>6.9%</b>	<b>7.0%</b>	<b>5.2%</b>	<b>3.3%</b>	<b>3.2%</b>	<b>3.5%</b>	<b>4.3%</b>	<b>5.3%</b>	<b>100%</b>

**TABLE A-7. Summary of mean wind speeds (knots (m/s)) by month and year. 1985-1999 June-November**  
**Latitude: 67.50N Longitude: 195.75E (see figure 28, Station 5 for location)**

YEAR	JUN	JUL	AUG	SEP	OCT	NOV	MEAN
1985	6.61 (3.4)	7.17 (3.69)	9.35 (4.81)	14.74 (7.58)	18.62 (9.58)	15.26 (7.85)	11.96 (6.15)
1986	5.48 (2.82)	8.12 (4.18)	14.95 (7.69)	15.10 (7.77)	13.82 (7.11)	14.87 (7.65)	12.05 (6.2)
1987	6.53 (3.36)	11.04 (5.68)	9.82 (5.05)	13.61 (7.00)	14.77 (7.6)	21.42 (11.02)	12.85 (6.61)
1988	5.19 (2.67)	12.23 (6.29)	14.49 (7.45)	13.31 (6.85)	14.50 (7.46)	17.87 (9.19)	12.95 (6.66)
1989	6.35 (3.27)	9.00 (4.63)	9.65 (4.96)	16.44 (8.46)	17.55 (9.03)	18.39 (9.46)	12.89 (6.63)
1990	12.77 (6.57)	9.04 (4.65)	10.42 (5.36)	16.39 (8.43)	16.56 (8.52)	18.02 (9.27)	13.84 (7.12)
1991	4.62 (2.38)	8.80 (4.53)	13.45 (6.92)	15.70 (8.08)	17.22 (8.86)	16.42 (8.45)	12.71 (6.54)
1992	5.54 (2.85)	10.84 (5.58)	10.58 (5.44)	12.77 (6.57)	14.77 (7.6)	17.40 (8.95)	11.97 (6.16)
1993	7.04 (3.62)	7.50 (3.86)	10.81 (5.56)	17.38 (8.94)	15.48 (7.96)	16.09 (8.28)	12.37 (6.36)
1994	5.07 (2.61)	4.70 (2.42)	14.11 (7.26)	15.84 (8.15)	14.41 (7.41)	12.38 (6.37)	11.08 (5.7)
1995	11.30 (5.81)	12.21 (6.28)	8.34 (4.29)	15.35 (7.9)	16.08 (8.27)	15.15 (7.79)	13.06 (6.72)

**TABLE A-8. Summary of maximum wind speed (knots (m/s)) by month and year. 1985-1999 June-November**  
**Latitude: 67.50N Longitude: 195.75E (see figure 28, Station 5 for location)**

YEAR	JUN	JUL	AUG	SEP	OCT	NOV	MAX
1985	20.02 (10.3)	21.97 (11.3)	25.46 (13.1)	29.94 (15.4)	32.85 (16.9)	36.74 (18.9)	36.74 (18.9)
1986	15.94 (8.2)	21.77 (11.2)	26.04 (13.4)	27.80 (14.3)	27.41 (14.1)	27.21 (14)	27.80 (14.3)
1987	20.99 (10.8)	20.99 (10.8)	23.52 (12.1)	26.24 (13.5)	29.55 (15.2)	34.98 (18)	34.98 (18)
1988	12.63 (6.5)	27.99 (14.4)	30.13 (15.5)	33.63 (17.3)	25.29 (13)	32.66 (16.8)	33.63 (17.3)
1989	18.86 (9.7)	20.99 (10.8)	25.29 (13)	31.88 (16.4)	37.71 (19.4)	39.07 (20.1)	39.07 (20.1)
1990	20.80 (10.7)	26.43 (13.6)	27.22 (14)	27.99 (14.4)	32.66 (16.8)	36.16 (18.6)	36.16 (18.6)
1991	13.61 (7)	20.21 (10.4)	28.77 (14.8)	31.10 (16)	34.02 (17.5)	35.58 (18.3)	35.58 (18.3)
1992	16.33 (8.4)	20.99 (10.8)	21.77 (11.2)	24.69 (12.7)	39.65 (20.4)	37.32 (19.2)	39.65 (20.4)
1993	21.97 (11.3)	24.30 (12.5)	36.16 (18.6)	36.74 (18.9)	31.68 (16.3)	36.93 (19)	36.93 (19)
1994	17.11 (8.8)	14.96 (7.7)	31.88 (16.4)	34.79 (17.9)	33.82 (17.4)	32.46 (16.7)	34.79 (17.9)
1995	22.94 (11.8)	26.04 (13.4)	21.77 (11.2)	23.91 (12.3)	31.88 (16.4)	29.75 (15.3)	31.88 (16.4)

Draft Feasibility Report  
 Appendix A: Hydraulic Design, Delong Mountain Terminal, Alaska

**TABLE A-7. Summary of mean wind speeds (knots (m/s)) by month and year. 1985-1999 June-November**  
 Latitude: 67.50N Longitude: 195.75E (see figure 28, Station 5 for location)

YEAR	JUN	JUL	AUG	SEP	OCT	NOV	MEAN
1996	11.41 (5.87)	13.06 (6.72)	14.17 (7.29)	14.83 (7.63)	13.06 (6.72)	19.38 (9.97)	14.30 (7.36)
1997	9.31 (4.79)	10.36 (5.33)	12.44 (6.4)	14.25 (7.33)	13.86 (7.13)	20.18 (10.38)	13.38 (6.88)
1998	5.69 (2.93)	7.89 (4.06)	14.27 (7.34)	15.69 (8.07)	18.80 (9.67)	18.66 (9.6)	13.51 (6.95)
1999	8.32 (4.28)	9.27 (4.77)	11.91 (6.13)	12.77 (6.57)	15.35 (7.9)	11.88 (6.11)	11.58 (5.96)
MEAN	7.43 (3.82)	9.41 (4.84)	11.91 (6.13)	14.95 (7.69)	15.65 (8.05)	16.89 (8.69)	

**TABLE A-8. Summary of maximum wind speed (knots (m/s)) by month and year. 1985-1999 June-November**  
 Latitude: 67.50N Longitude: 195.75E (see figure 28, Station 5 for location)

YEAR	JUN	JUL	AUG	SEP	OCT	NOV	MAX
1996	28.19 (14.5)	34.02 (17.5)	32.27 (16.6)	35.18 (18.1)	41.60 (21.4)	40.62 (20.9)	41.60 (21.4)
1997	22.74 (11.7)	21.97 (11.3)	33.24 (17.1)	29.15 (15)	28.77 (14.8)	39.07 (20.1)	39.07 (20.1)
1998	24.69 (12.7)	15.94 (8.2)	35.77 (18.4)	31.29 (16.1)	36.54 (18.8)	28.96 (14.9)	36.54 (18.8)
1999	28.77 (14.8)	23.32 (12)	26.43 (13.6)	27.22 (14)	25.85 (13.3)	23.91 (12.3)	28.77 (14.8)
MAX	28.77 (14.8)	34.02 (17.5)	36.16 (18.6)	36.74 (18.9)	41.60 (21.4)	40.62 (20.9)	

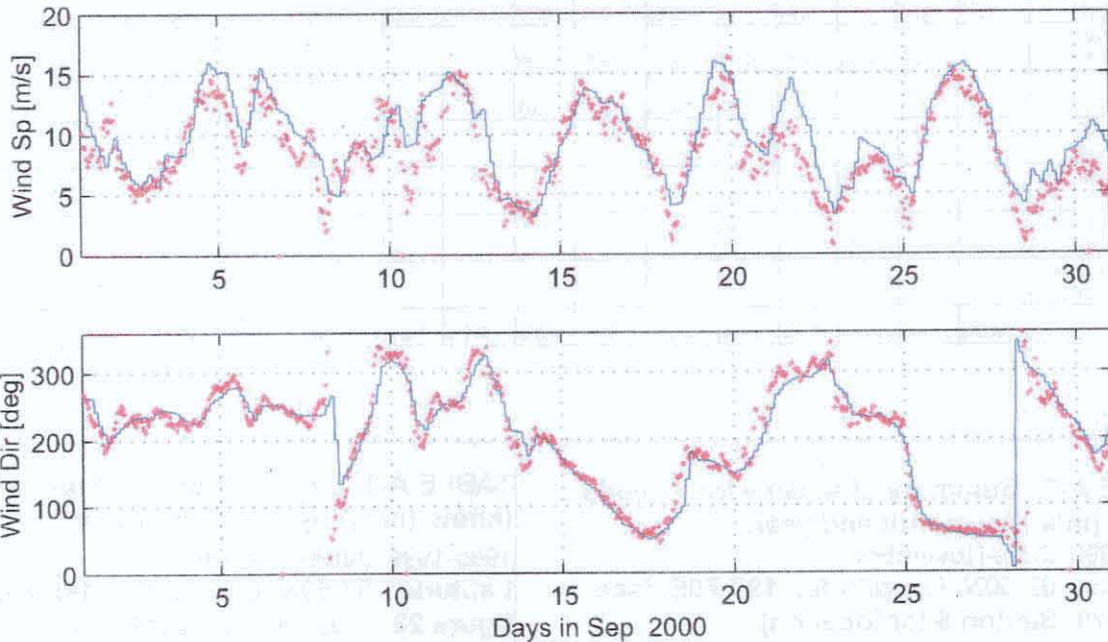


Figure 15. OWI Winds and Bering Sea Buoy (46035) Comparison September 2000  
 OWI Wind = Blue Buoy wind = Red 1 m/s = 1.9 knots

Draft Feasibility Report  
Appendix A: Hydraulic Design, Delong Mountain Terminal, Alaska

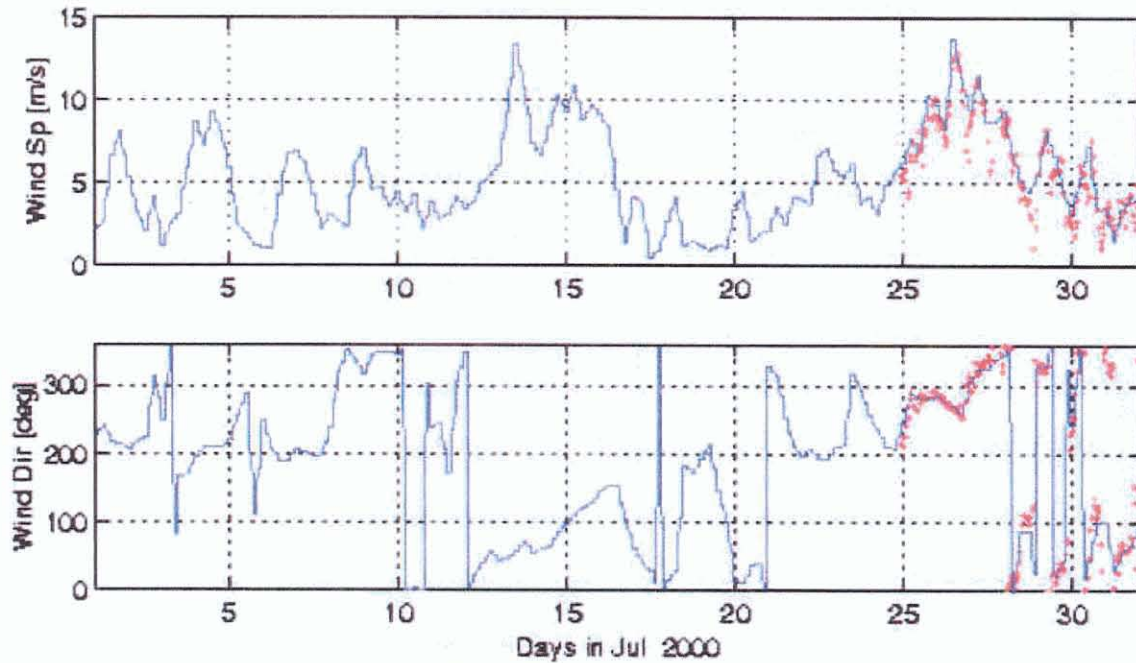


Figure 16. OWI Winds and DMT Buoy Comparison July 2000  
OWI Wind = Blue Buoy wind = Red 1 m/s = 1.9 knots

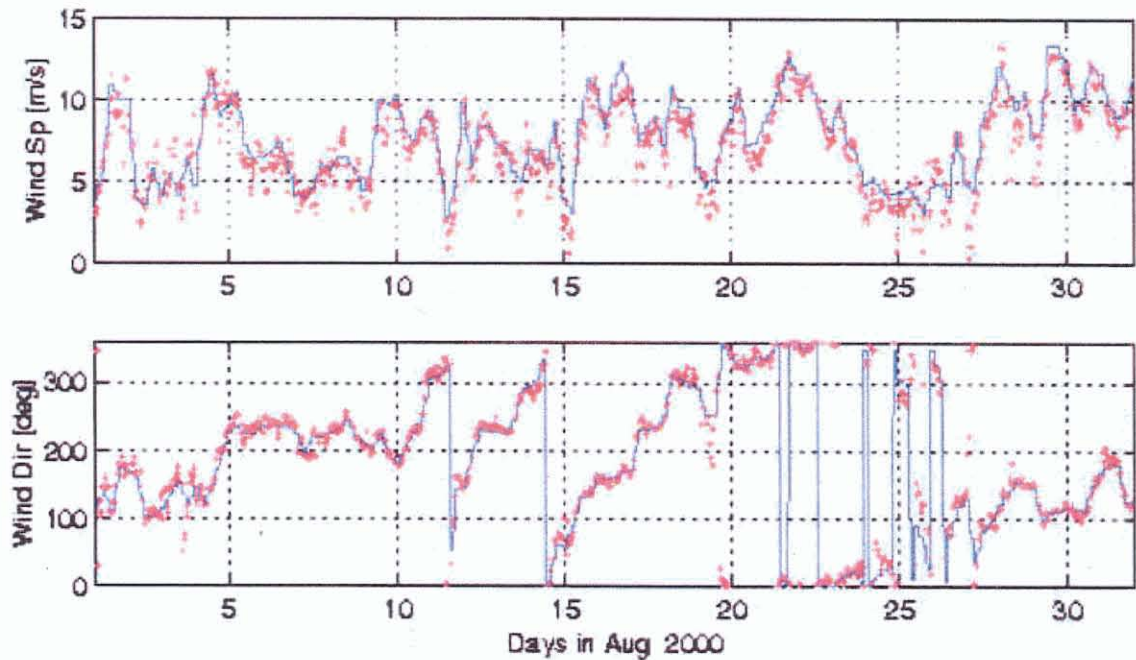


Figure 17. OWI Winds and DMT Buoy Comparison August 2000  
OWI Wind = Blue Buoy wind = Red  
1 m/s = 1.9 knots

Draft Feasibility Report  
Appendix A: Hydraulic Design, Delong Mountain Terminal, Alaska

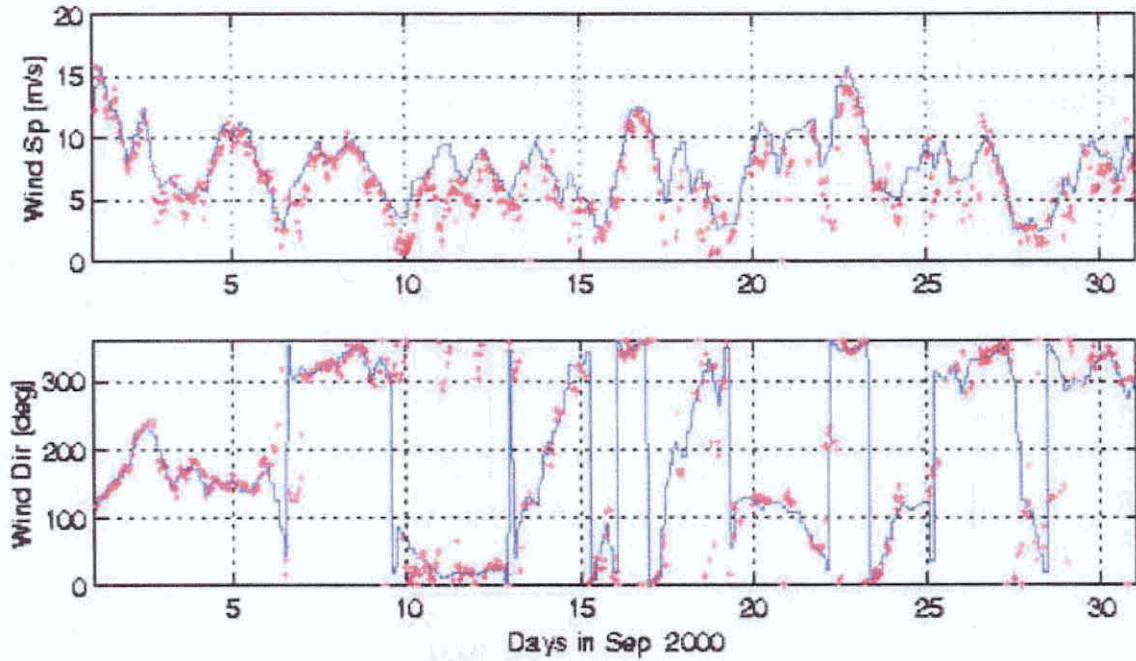


Figure 18. OWI Winds and DMT Buoy Comparison September 2000  
OWI Wind = Blue Buoy wind = Red  
1 m/s = 1.9 knots

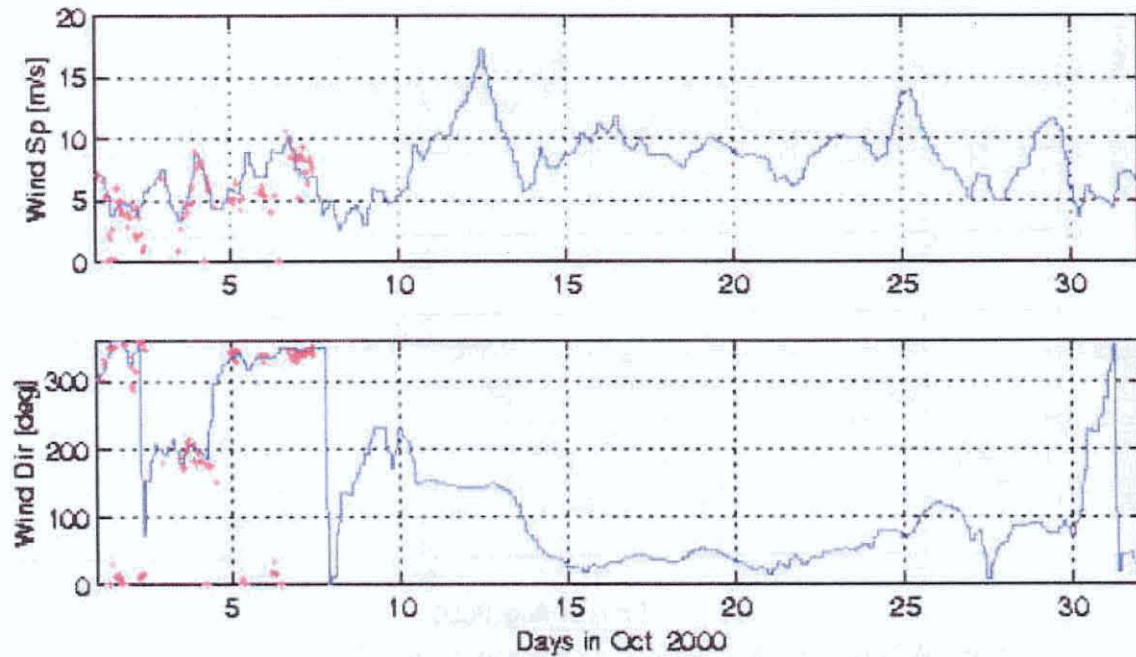


Figure 19. OWI Winds and DMT Buoy Comparison October 2000  
OWI Wind = Blue Buoy wind = Red  
1 m/s = 1.9 knots

## 5.0 WAVE CLIMATE

The DMT area has an extremely complex wave environment. The wave climate at the DMT is dominated by local wind-sea conditions. Meteorological conditions in Kotzebue Sound strongly influence the DMT area. Wave generation in areas to the north, including the Chukchi Sea and Arctic Ocean, have an impact on extremes at the project site. The Bering Sea and Northern Pacific Ocean are also important, where synoptic-scale events are formed and where low frequency energy is radiated from tropical cyclones and large, very powerful tropical storms.

The Coastal and Hydraulics Laboratory (CHL) of the Engineer Research and Development Center (ERDC) developed a 16-year hindcast of the wave climate at the DMT using wind data generated from the wind hindcast. The wave hindcast was verified using National Data Buoy Center (NDBC) buoy data. An NDBC buoy (48011) was deployed at the site for the years 2000 and 2001. The data from this buoy and a buoy in the Bering Sea (46035) were used to validate the hindcast results. Prior studies at the site collected wave data using an Interocean S4ADW Directional Wave Gage and a Seabird SBE-26 Non-directional Wave Gage. Where possible, the data collected from the previous study was compared to the hindcast results.

A number of wave-related design issues needed to be addressed in the wave hindcast, including the presence of long-period swell energy that propagates through the Bering Strait and into the project vicinity, and short-period wave energy generated within the Chukchi Sea by fast-moving, low-pressure systems. Fast-moving systems imply a rapidly changing, highly unsteady wind field (in terms of both speed and direction), and rapidly changing fetch, all of which strongly influence wave conditions at the DMT site.

Severe historic storms dating back to 1954, which were thought to have a significant influence on wave conditions at the DMT site, were also hindcast. Inclusion of the additional storms was done to provide higher confidence in extreme wave estimates (those representing 50-year return-period events) that are critical for design of the loading facility.

### 5.1 Ice

The influence of ice as a limiting factor on the fetch over which waves are generated was accounted for by incorporating monthly ice-cover maps into the hindcast. Ice maps were linked to the regional wave model simulation. The assumption was made that a 50-percent or greater ice concentration was considered as land in the wave model. The ice maps are generated from a number of ice databases summarized in Table A-9. The mean ice coverage for a particular month is used for the entire month, and changed at the beginning of each successive month. An example of an ice map indicating 50-percent or greater concentrations is presented in figure 20.

The simulations for the extreme storm analysis were conducted identical to a 16-year hindcast with one exception. All extreme storms were simulated without ice coverage for

Draft Feasibility Report  
Appendix A: Hydraulic Design, Delong Mountain Terminal, Alaska

the regional domain. This will allow storms that emanate from the Arctic Ocean and Chukchi Sea traveling in a southeasterly direction to fully impact the Portsite rather than being blocked or dampened by the presence of ice. This will also allow tropical systems to proceed through the Bering Straits that might otherwise be blocked by ice in the Straits. This was viewed as a reasonable approach since recent evidence has suggested that the arctic environment is experiencing a warming trend. Details on the treatment of ice in the hindcast may be found in the ERDC report *Engineering Studies in Support of Delong Mountain Terminal Project*.

Table A-9. Ice Data Bases Used to Construct Region / Subregion Ice Maps			
Reference	Database Name	Media	Date Coverage
Walsh and Johnson	End of Month Sea Ice Concentrations for the Arctic	hyperlink	1953-1990
Sigrid	Weekly Sea Ice Concentrations form the Artic and Antarctic Sea Ice Data	CDROM	1972-1994
Nimbus	Oceans Branch, Laboratory for Hydrospheric Processes at NASA GSFC	hyperlink	Oct 1970- Dec 1996
DMSF SSM/I	National Snow and Ice Data Center (mean monthly)	hyperlink	1997- Jun 2000

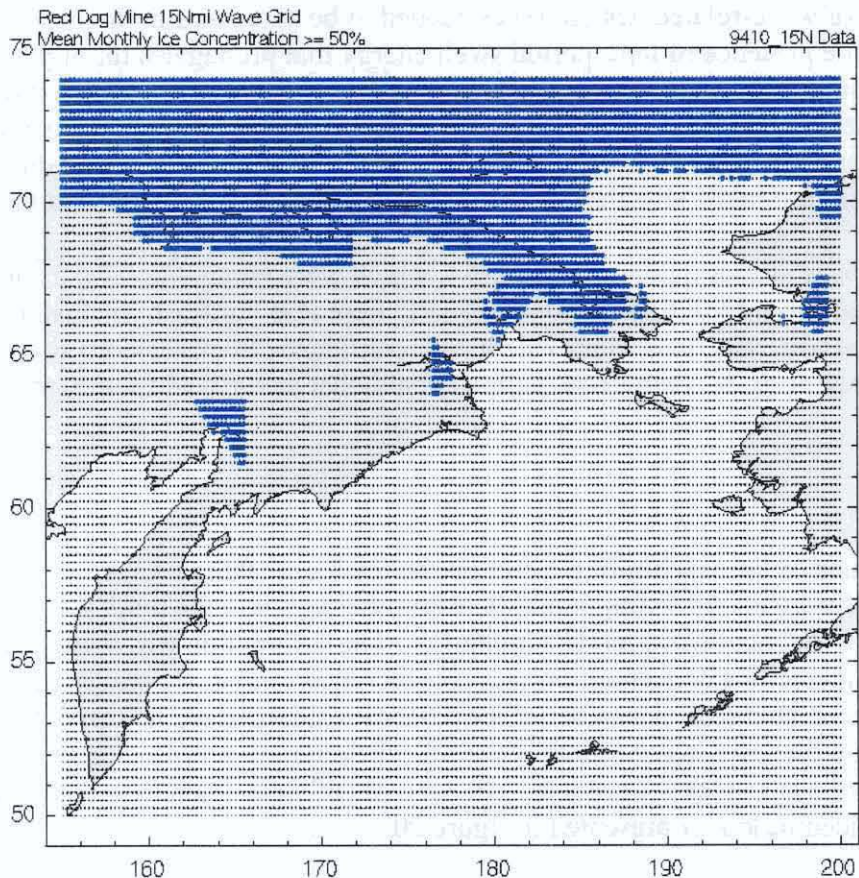


Figure 20. Ice map for Regional Domain October 1994, blue symbols indicate ice concentrations greater than 50 percent

## 5.2 Low Frequency Energy

An analysis of typhoon archives was performed to determine the number of storms that could generate low frequency energy that could potentially impact the DMT site. The presence of low frequency energy at the site was important to determine as it could have a significant impact on ships at berth and barging operations at the Portsite. Low frequency energy will also have a greater potential for sediment transport.

Typhoons were identified for the period June through November 1985-1999. The storm intensity and track were examined, with the path being the key to counting a typhoon as having the potential for migration into the Bering Sea and up to the Chukchi Sea. There was subjectivity associated with this analysis, and the results were considered to be a preliminary indication of those storms that had the potential to produce long-period swells at the DMT. This was used to establish the southerly boundary of the hindcast model grid.

The results of this investigation are presented in figure 21 and should be used only for qualitative purposes. The month of September clearly shows a predominance of typhoon occurrences (approximately 35) compared to other months. August and October have the second-highest frequency with about 20 potential events. The average number of events per year was about seven; however, during the period of 1994-1997, the number increased to nearly 10 per year.

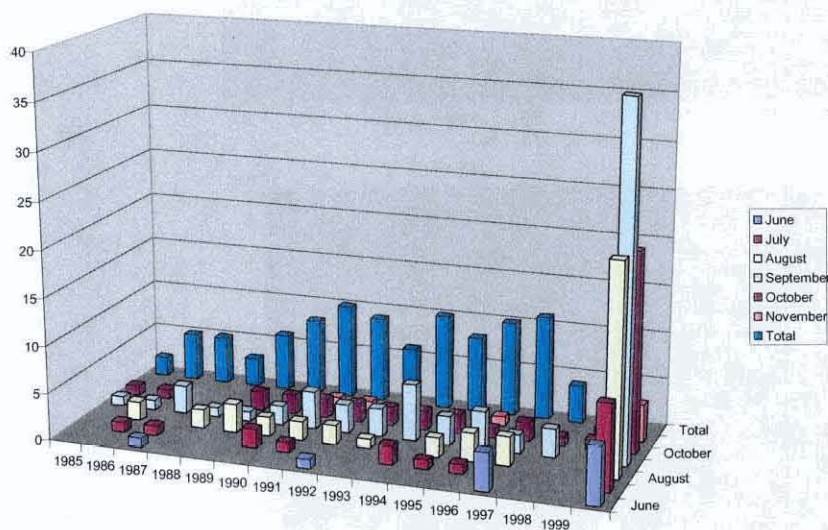


Figure 21. Typhoons potentially affecting the DMT site, by year and month

Assuming the potential for long-period swell energy could be derived from typhoon storm systems, the analysis was continued to determine if that energy could reach the DMT site. Wave energy derived from any storm, local or distant, will follow great circle paths. Earth is a sphere, and hence the path of propagation must be solved in a spherical coordinate system. From geometric principles, the propagation lines were traced on a Mercator projection and selectively pinned at an end point that is just offshore of the Portsite. This method was used to develop figure 22.

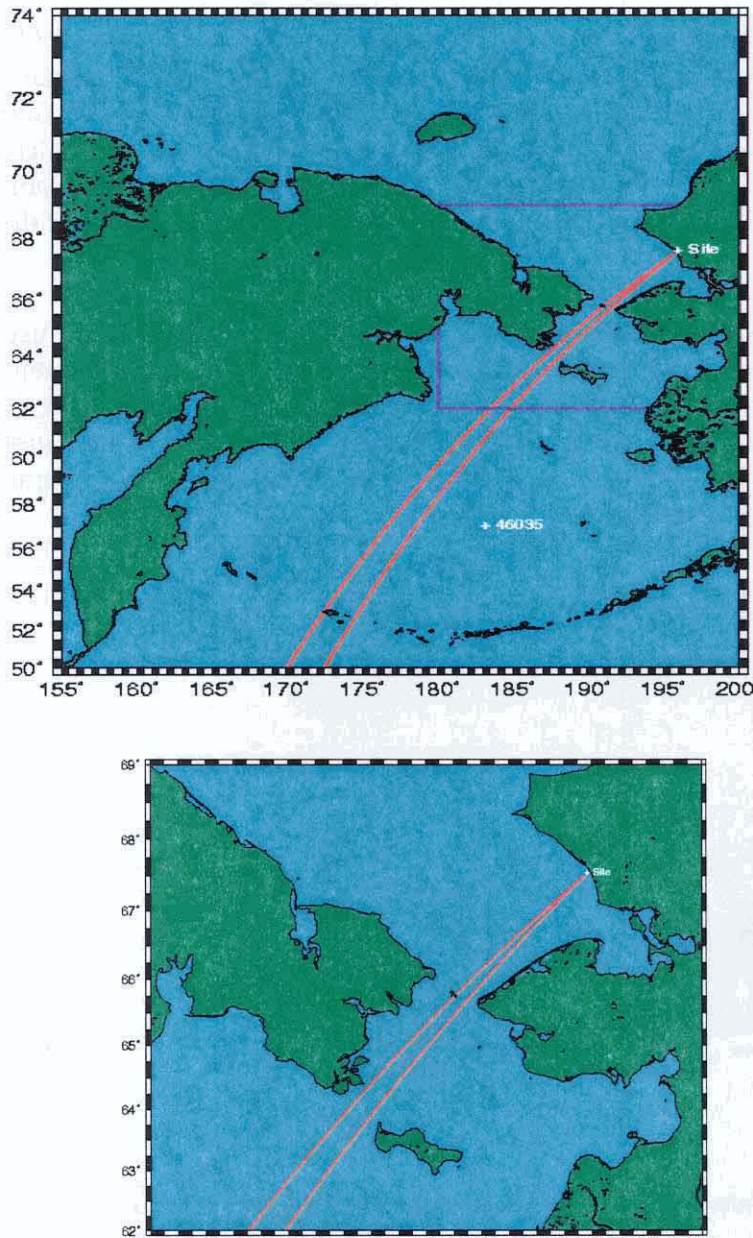


Figure 22. Great circle path to the DMT site (upper panel shows regional domain and subregional domain in blue box, lower panel shows subregion domain)

In light of geographical constraints (land masses), there appears to be a small open water path through the Bering Strait that also misses Saint Lawrence and Big and Little Diomede islands. There is also adequate open water near the western extent of the Aleutian Island Chain to allow this energy to exist in the Bering Sea. However, gradients dramatically increase in the water depths south of the Bering Strait. Water depths are adequately shallow in places to allow for refraction of long-period swell energy, thereby possibly filtering it out or reducing the energy before it could arrive at the DMT site.

Evidence from the 8-year record at the Bering Sea NDBC buoy 46035 (figure 23) shows a net increase in long-period energy for the month of October that is consistent with the previous analysis, and indicates that distant swell can propagate through the gaps in the Aleutian Island Chain. The net increase of the mean dominant wave period for all Octobers could be due to the increase in the wind speeds (lower panel of figure 23). However, the interesting evidence is in the maximum period of 25 seconds, compared with the period in December and January. During those two months, the mean wind speed was nearly 2 knots greater than that found in October. The maximum wind speeds for the months of November and January are nearly 50 knots and more than 50 knots, respectively. This is compared with a maximum of about 44 knots for the month of October. These winds, and accompanying dominant wave periods, suggest that the October swell energy may be derived from sources other than the Bering Sea.

The final question pertaining to the relative energy levels of the long-period swell component can be answered through a correlation analysis of wave spectra from NDBC buoy 46035, the DMT directional wave gauge during the 1998-2000 deployment period, and the buoy (48011) deployed in the Chukchi Sea during 2000.

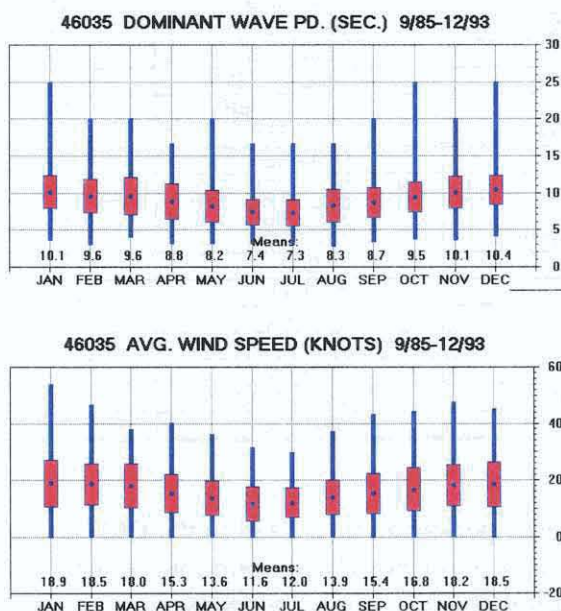


Figure 23. Monthly means and maxima for wave period (upper panel) and average wind speed (lower panel) at NDBC buoy 46035

Draft Feasibility Report  
Appendix A: Hydraulic Design, Delong Mountain Terminal, Alaska

Archived frequency spectra at NDBC 46035 and 48011 were used to calculate energy (figure 24). The buoy data shown in figure 24 are scaled on two different ordinates; the Bering Sea data are scaled on the left side of the plot and the DMT data are scaled on the right. Note the different magnitudes of the scaling, which shows that low-frequency energy at the DMT buoy is roughly 200 times lower than that measured at the Bering Sea buoy.

The observed energy levels derived from NDBC buoy 46035 can be roughly correlated to typhoon occurrences, displayed in table 10. There is a phase lag between the date of low frequency arrival and the peak of the typhoon winds. This is about 72 to 96 hours. The peaks have the proper phase lags from the various typhoons in table A-10. These peaks occur at 12 July; 2, 25 and 29 August; 7, 11, 20, and 27 September. The greatest impact at the Bering Sea buoy (46035) occurs on 29 August.

<b>TABLE A-10. List of Tropical Storms June – Nov 2000</b>			
<b>Typhoon Name</b>	<b>Time Period</b>	<b>Wind Speed (kt)</b>	<b>Cat.</b>
Typhoon KIROGI	02-08 JUL	115	4
Typhoon KAI TAK	04-10 JUL	75	1
TD 07W	13-15 JUL	25	-
TD 08W	16-17 JUL	25	-
TS TEMBIN	17-21 JUL	45	-
TD 10W	20-23 JUL	25	-
TS BOLAVEN	24-30 JUL	50	-
TS CHANCHU	28-29 JUL	40	-
Super Typhoon JELAWAT	01-11 AUG	125	4
TD 14W	08-10 AUG	30	-
Typhoon EWINIAR	09-18 AUG	75	1
TS WENE	15-16 AUG	40	-
TD 17W	18-19 AUG	25	-
Super Typhoon BILIS	18-24 AUG	140	5
TS KAEMI	20-22 AUG	45	-
Typhoon PRAPIROON	26 AUG-01 SEP	85	2
TS MARIA	28 AUG-01 SEP	55	-
Super Typhoon SAOMAI	03-16 SEP	140	5
Typhoon WUKONG	05-10 SEP	95	2
TS BOPHA	05-11 SEP	75	-
Typhoon SONAMU	14-18 SEP	75	1
Super Typhoon SHANSHAN	17-24 SEP	130	4
Tropical Storm 26W	17 SEP-18	50	-
TD 27W	28-30 SEP	30	-
TD 28W	06-12 OCT	30	-
TD 29W	21-21 OCT	30	-
Typhoon YAGI	22-27 OCT	105	3
Typhoon XANGSANE	25 OCT-01 NOV	90	2
TD 30W	25-26 OCT	30	-

The low frequency energy peaks can be related to the DMT site in a similar fashion. This analysis compared the low frequency (long-period wave) energy from decaying typhoons with the occurrence of low frequency energy peaks found in the NDBC buoy data (figure 24). A phase shift of about 24 to 36 hours was used for investigation. Only the peak energy levels in red dashed lines to the right of the Bering Sea buoy peaks should be considered. Only four (2 and 29 August; 20 and 27 September) of the original storm

peaks could be correlated to the data from the Bering Sea buoy. The remaining low frequency energy peaks found in the 48011 data arise at the same time as the 46035 data. This suggests large, synoptic-scale events impacting both locations simultaneously. It is apparent that the constriction in the Bering Strait shelters the DMT site from most of the southerly energy component. Also, the topography (figure 25) in the surrounding area of the Bering Strait acts like a low-pass filter (refractive effects) selectively turning the long-period swell energy toward the Russian coastline.

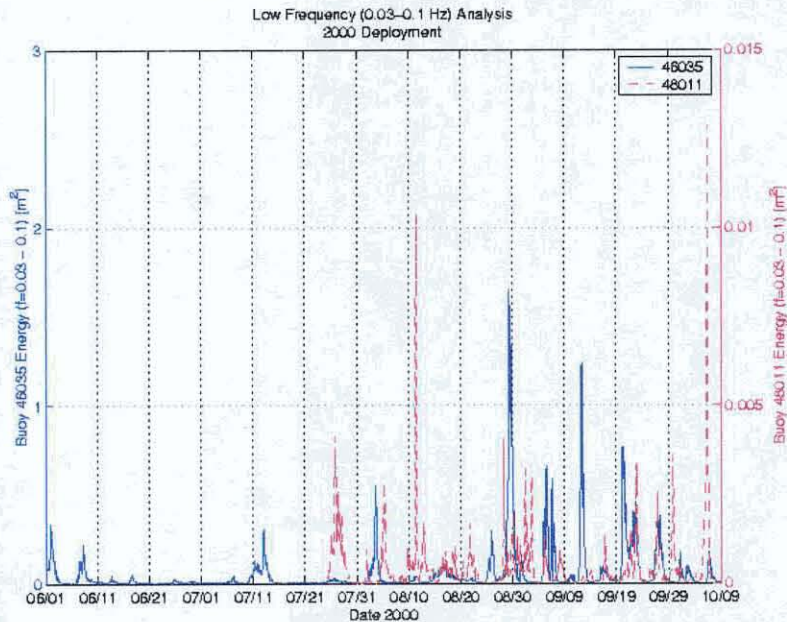


Figure 24. Time comparison of low frequency energy contribution for June through October 2000 at NDBC 46035 (blue), and 48011 (red) buoy sites.

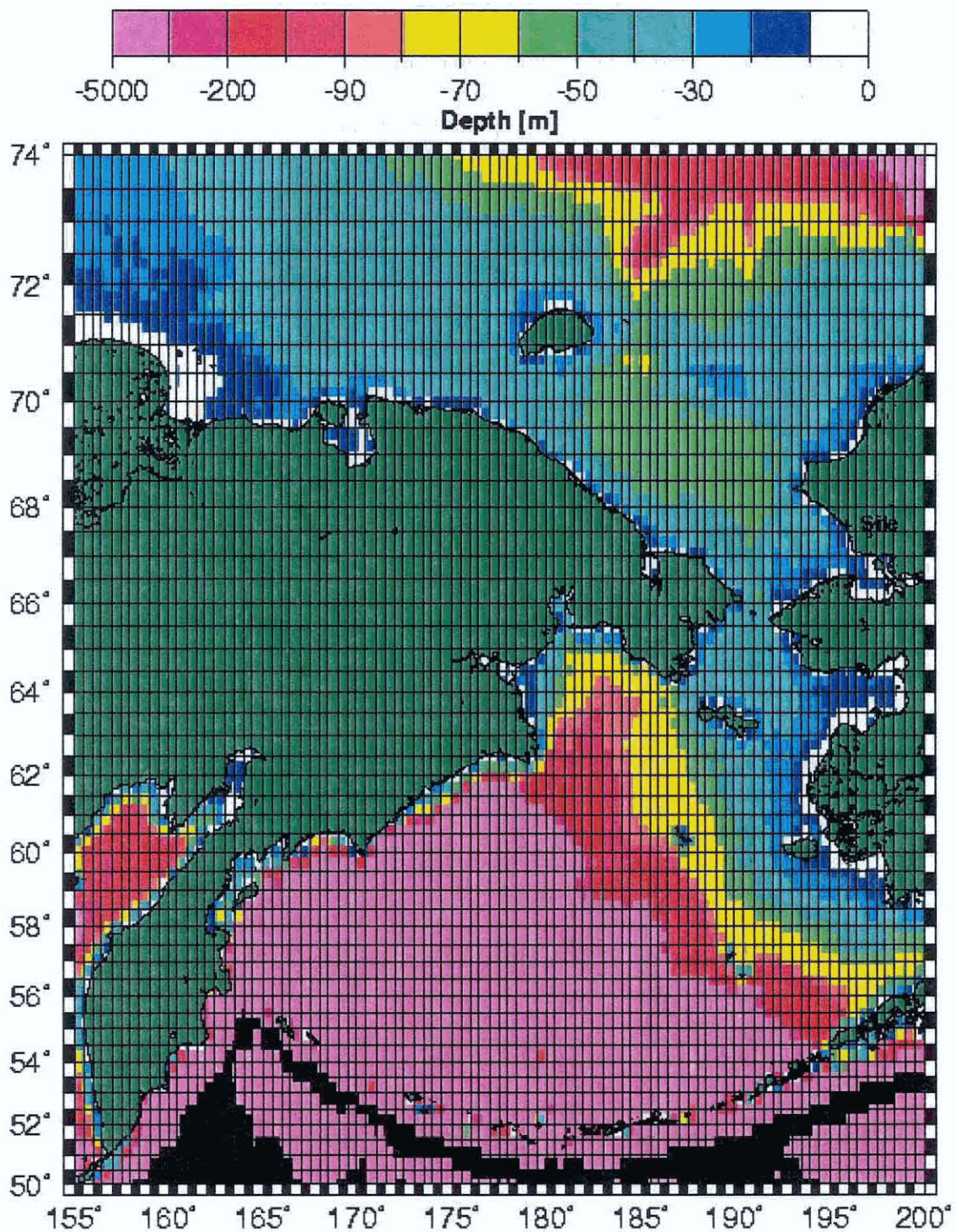


Figure 25. Wave Prediction Model regional water depth grid. Black areas >5000m (\* 1 m = 3.28 ft)

Based on the analysis, it was concluded that the potential for low frequency energy exists at the DMT site. The energy can be related to northern Pacific decaying typhoons. The

data derived from the NDBC 48011 buoy suggest an approximate maximum swell height of 0.66 feet (0.2 meters). This conclusion is based on data acquired during the 2000 open water season.

Examination of the hindcast (1985-2000) indicates that the month of October has the highest propensity for long period waves. From the hindcast statistics, the frequency of occurrence of a 12 second or longer period wave in October was 0.1% for waves 5 meters or greater, 0.1% for waves 1.5 meters to 1.99 meters, and 1.0% for waves 1 meter to 1.49 meters. Waves with a 12 second period below 1 meter occurred 7% of the time.

### 5.3 Hindcast Model Description

The selection of a wave modeling technology depends on four critical factors:

- Operating constraints of a particular project
- Flexibility of the wave model
- Desired accuracy of the wave estimates
- Inclusion of ice cover
- 

The deep-water wave climate at the Portsite was analyzed using the global ocean model, **W**Ave prediction **M**odel (**W**AM). WAM is a third generation wave model which predicts directional spectra as well as wave properties such as significant wave height, mean wave direction and frequency, swell wave height and mean direction. All source terms (wind input, wave-wave interaction, whitcapping, wave bottom effects, and wave breaking) are specified with the same degree of freedom in WAM with which the resulting directional wave spectra are specified. There is no a priori assumption governing the shape of the frequency or directional wave spectrum. WAM has been used extensively at weather prediction centers with the option to include ice coverage. Model Assumptions for WAM are:

- Time dependent wave action balance equation.
- Wave growth based on sea surface roughness and wind characteristics.
- Nonlinear wave and wave interaction by Discrete Interaction Approximation (DIA).
- Free form of spectral shape.
- High dissipation rate to short waves.

A multi-level grid system was used for the wave model, focusing from the North Pacific Ocean into the DMT site. The grid selection process was dictated by scales of meteorological events, and geographic constraints determined from the incorporation of islands, shoreline configurations, and bathymetry. The three grid domains are the basin, region, and subregion. These areas are displayed in figure 26. The domain boundaries, along with the grid resolution employed for each domain, are provided in table A-11.

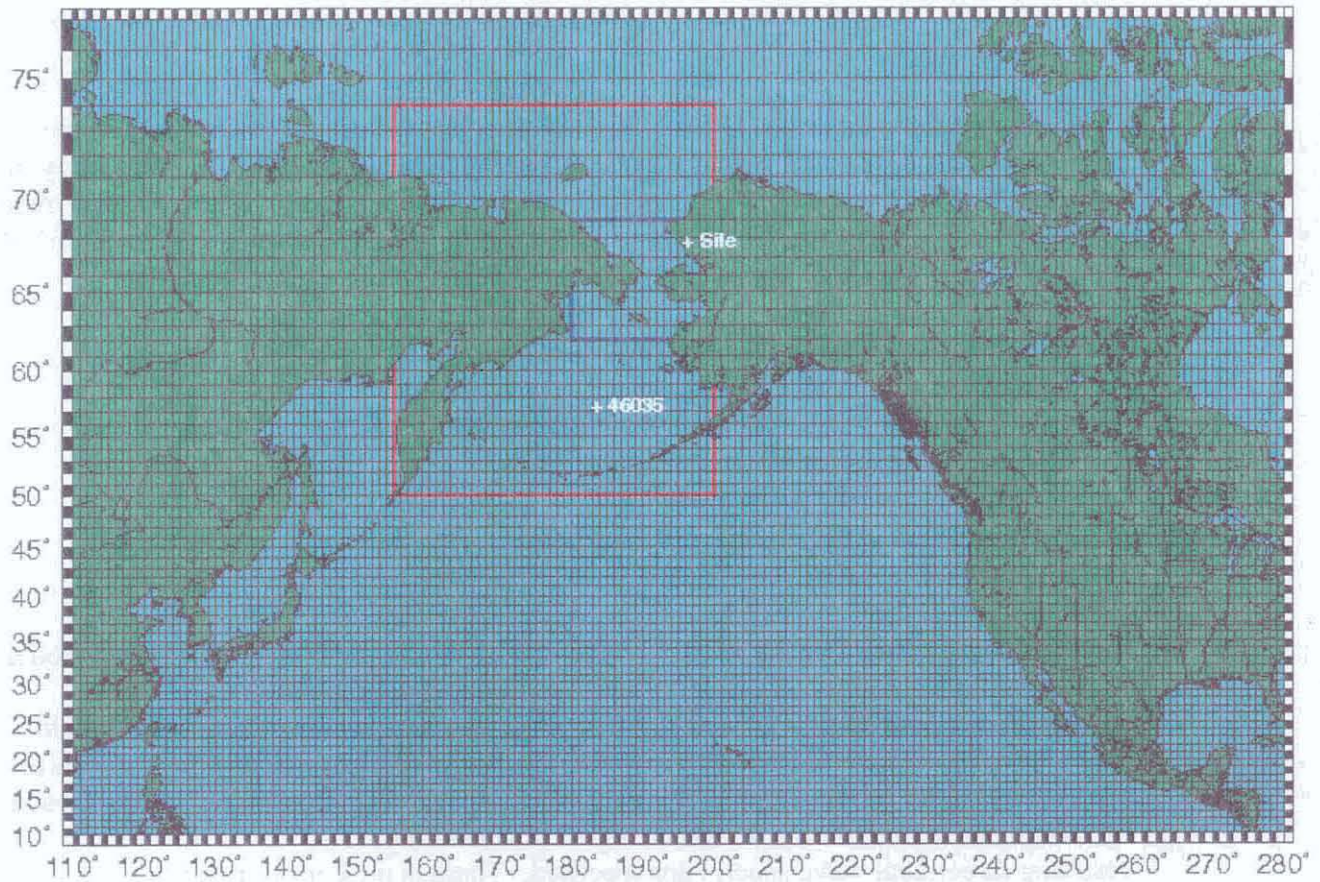


Figure 26. Basin (entire picture), region (red box), and subregion (blue box)

**TABLE A-11. Wave domain description.**

Field Specification	Latitude Boundary		Longitude Boundary		Resolution	
	North	South	West	East	$\Delta x$	$\Delta t$
WAM Basin Waves	75°	10°	110°	280°	1.0°	1200s
WAM Region Waves	71°	50°	155°	200°	0.25°	300s
WAM Subreg Waves	69°	62°	180°	200°	0.0833°	60s

### 5.3.1 Basin

The geographical constraints, islands, shoreline configurations, and bathymetry were treated in a similar form for each of the three domains. The basin scale WAM simulations assume deep-water conditions. All of the 5,942 active water points in this domain are set to 984 yards (900 meters). The depiction of islands is based on World Vector II and CIA digital shoreline databases. In general, most of the islands (e.g. Aleutian Island Chain) were omitted from this grid because they could be considered as sub-scale features. It is important to emphasize that the basin WAM simulation was used

in the DMT project to produce boundary condition information for the regional domain (the red framed region in figure 26), either northerly propagating wave energy that originates in the North Pacific Ocean or energy originating in the Arctic Ocean that propagates to the south.

### **5.3.2 Region**

The regional WAM grid included a careful description of the Aleutian Island Chain, Saint Lawrence Island, a clearly defined Bering Strait, and a refined approximation to the shoreline. Water depths were specified at each of the 9,786 active water points of the regional grid. Wave bottom effects were considered in this domain. Arbitrary water depth effects in the propagation routine such as refraction and shoaling were activated in the regional simulations. The phase and group velocities, along with the wavelength, varied with each grid location, as well as for each frequency band.

The regional WAM bathymetry grid was built from the Digital Bathymetry Data Base Five (DBDBV) obtained from the Naval Oceanographic Office. DBDBV approximates water depths to a 5-min longitude/latitude resolution. There are inherent problems with some of the DBDBV data for water depths shallower than 164 feet (50 meters). The National Ocean Services and National Imagery and Mapping Agency (NIMA) digital databases containing random water depth samplings were used to augment the DBDBV records. The land/water interface was approximated by digital shoreline databases and hand edited where needed to accurately portray the shape of the shoreline and islands. Extreme care was taken in specifying land-water interfaces so that wave energy leakage cross diagonal to the grid was prevented. The final WAM regional bathymetry grid is presented in figure 25. Note the extremely steep depth gradients, south of the Bering Straits, a characteristic that was hypothesized to act as a filter or reduce long period swell energy that originated in the Pacific Ocean and Bering Sea.

### **5.3.3 Subregion**

The subregion WAM grid was constructed in a similar manner as in the regional domain. The subregion contains 12,156 active water points. The subregion grid is a factor of three times denser than the regional WAM grid, and thus can better approximate the geographical constraints of the Bering Strait, and Saint Lawrence and Big and Little Diomedé islands. The water depths and their gradients are better resolved in this grid compared with that of the regional WAM domain.

### **5.3.4 Model Validation**

Measured wave data near the Portsite are limited in spatial and temporal coverage. Data from several deployments of a directional wave gage (S4ADW) in the nearshore zone were available. These data sets cover the open water seasons of 1998 through 2000. An NDBC three meter directional wave buoy (NDBC 48011) was deployed offshore of the Portsite during the open water seasons of 2000 and 2001. Only one point measurement platform exists in the far field (NDBC buoy 46035). These buoy data provided a useful means to test the hypotheses of long-period swell energy propagation and to assess

quality of the regional WAM results. A list of the sites used for comparison, their location, and the deployment period are listed in table A-12. The location of the NDBC buoy 46035 is shown in figure 27 and locations of the WAM save points used for comparison are shown in figure 28.

**Table A-12. Wave Measurement Sites**

Station Number	Location		Depth [ft]	Site No. (figure 28)	Deployment Period
	Longitude [E]	Latitude [N]			
NDBC 46035	182°18'1"	57.0°	12,014	N/A	1985-2000 (data gaps)
S4ADW	195°55'25" 195°55'23" 195°53'41"	67°34'24" 67°34'24" 67°34'11"	36* 65.3** 27.9*	12A	14 July-ice coverage 1998 22 September – ice coverage 1999 29 July – 25 September 2000
NDBC 48011	195°30'1"	67°31'	84	1 (red dot)***	25 July – 13 October 2000

\* Approximated from mean water height data  
 \*\* Suggested by contractor no to use these data because of concerns of deployment water depth and questionable quality  
 \*\*\*Site 1 is location for model and buoy comparison. Site 5 shown on map is used for reporting of wave model statistics referenced later in document.

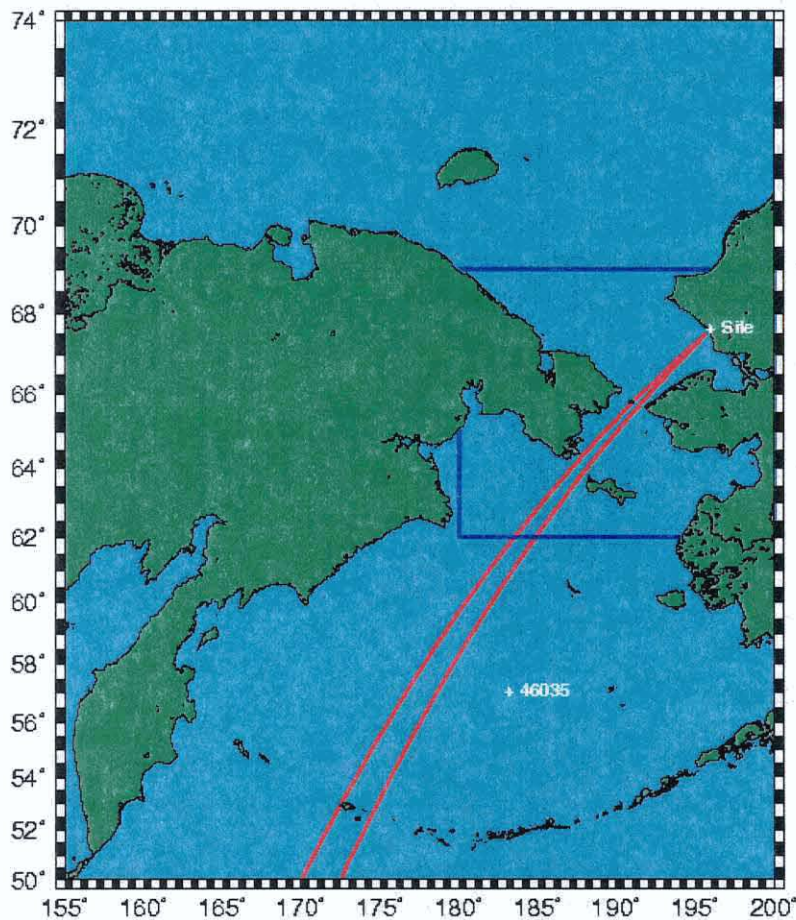


Figure 27 Region with buoy 46035

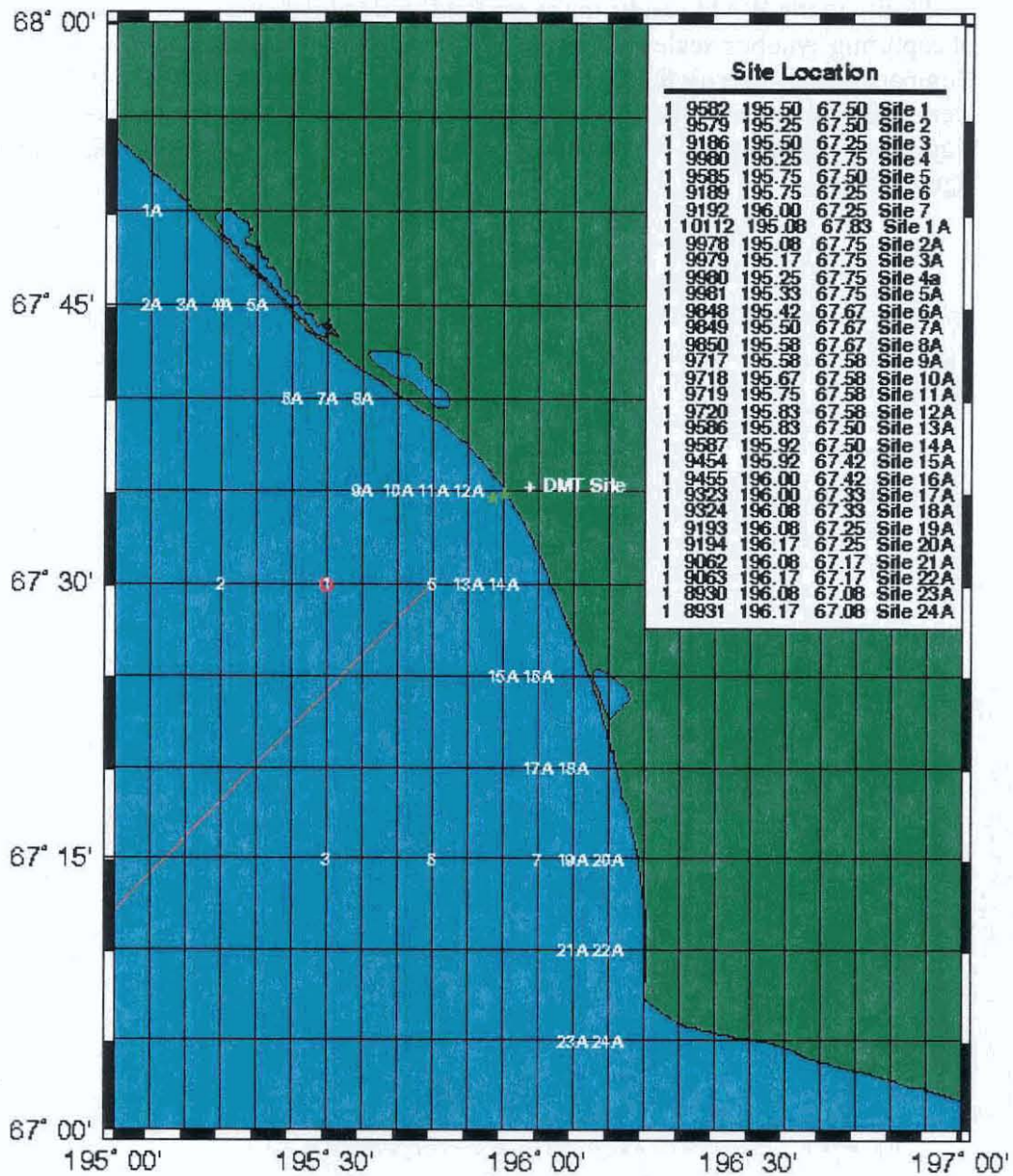


Figure 28 Subregion grid with WAM save points

*NDBC 46035*

The nondirectional NDBC buoy 46035 provided the means for long term analysis of the wave model's performance, since the buoy has been deployed for many years, much longer than any other wave measurement platform in the region. Despite the distance between the Portsite and buoy 46035, comparisons between the model and these

Draft Feasibility Report  
Appendix A: Hydraulic Design, Delong Mountain Terminal, Alaska

measurements are very relevant to the assessment of the hindcast quality. They add credibility to the WAM results in the far field, and validate the basin scale winds in terms of capturing synoptic scale meteorological events and meso scale tropical energy. Comparisons also verify the OWI regional wind field generation. If the WAM results were deficient at the NDBC 46035 site, the likelihood of success at the Portsite would be significantly diminished. Comparisons of the WAM output and buoy 46035 are shown in figures 29-33.

Draft Feasibility Report  
Appendix A: Hydraulic Design, Delong Mountain Terminal, Alaska

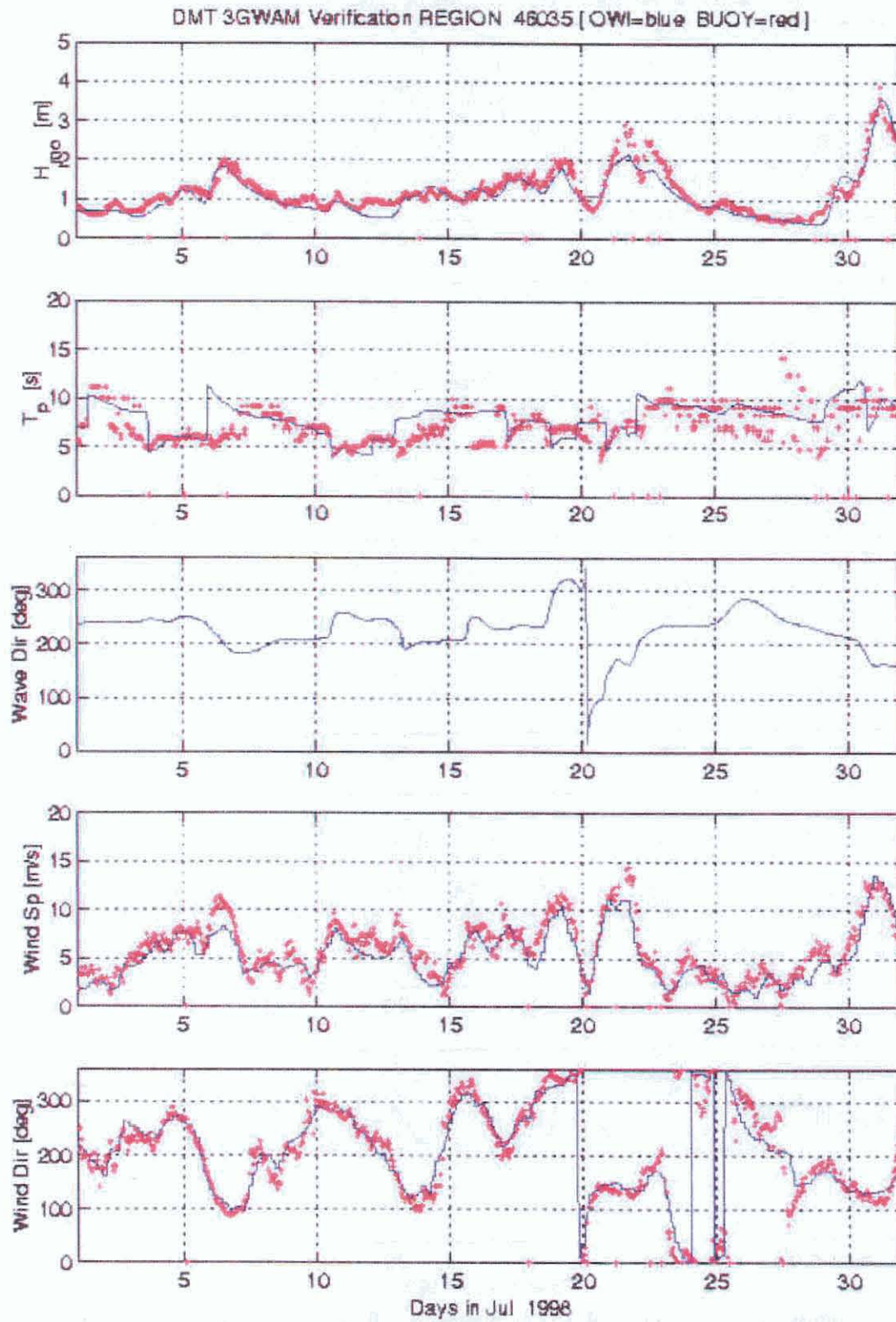


Figure 29 July buoy 46035 and WAM comparison 46035 data in red, hindcast data in blue.

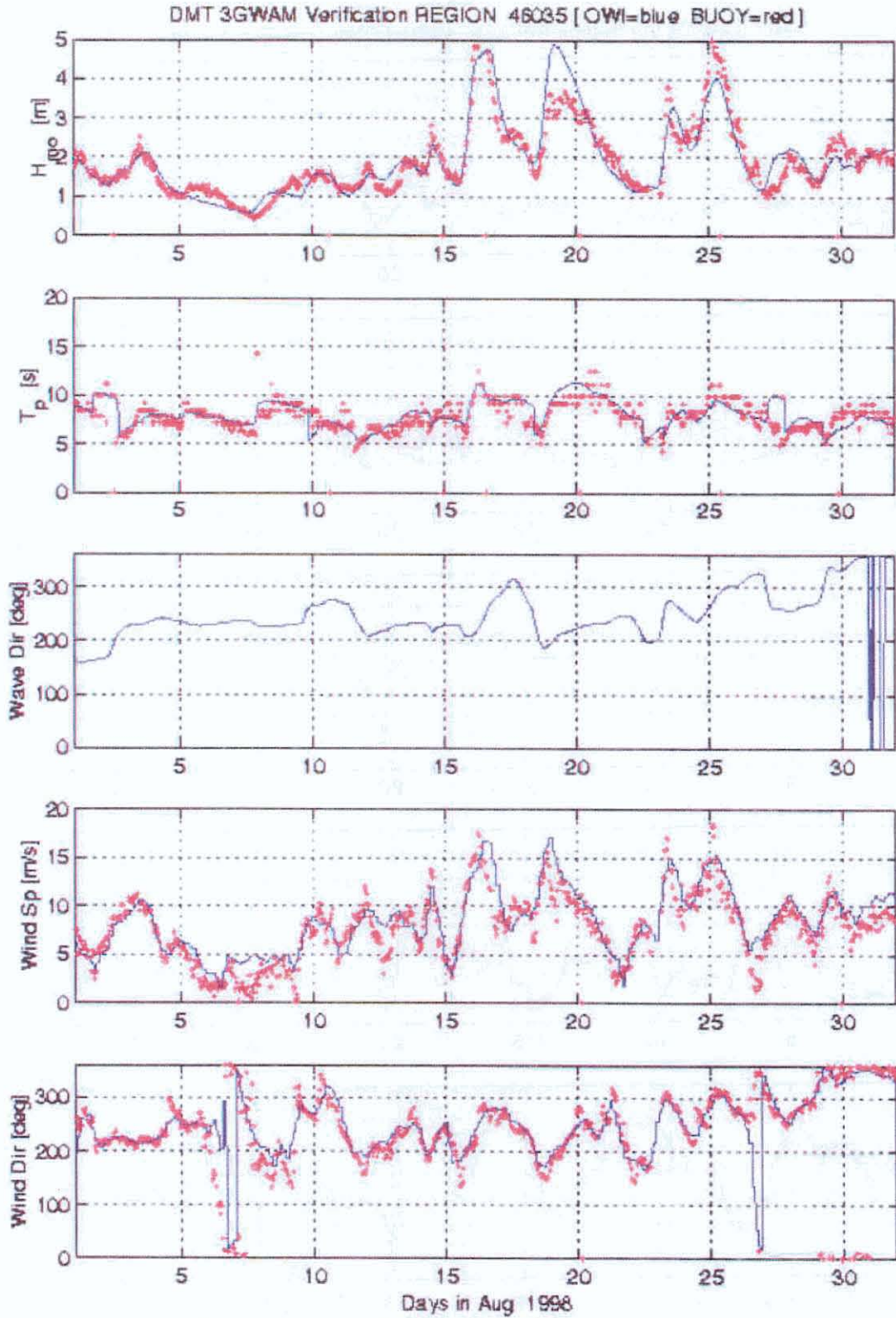


Figure 30 August buoy 46035 and WAM comparison 46035 data in red, hindcast data in blue.

Draft Feasibility Report  
Appendix A: Hydraulic Design, Delong Mountain Terminal, Alaska

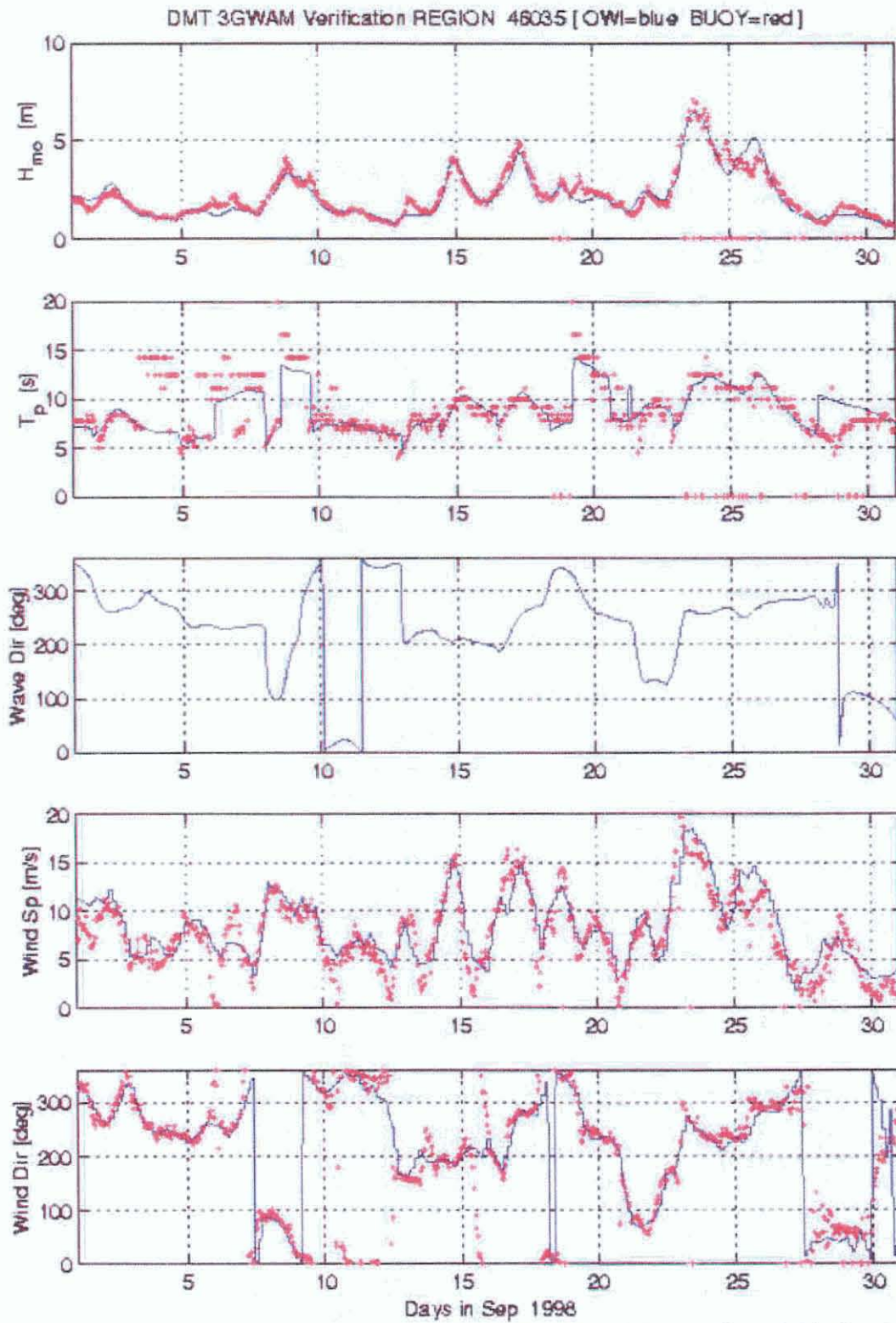


Figure 31 September buoy 46035 and WAM comparison 46035 data in red, hindcast data in blue.

Draft Feasibility Report  
Appendix A: Hydraulic Design, Delong Mountain Terminal, Alaska

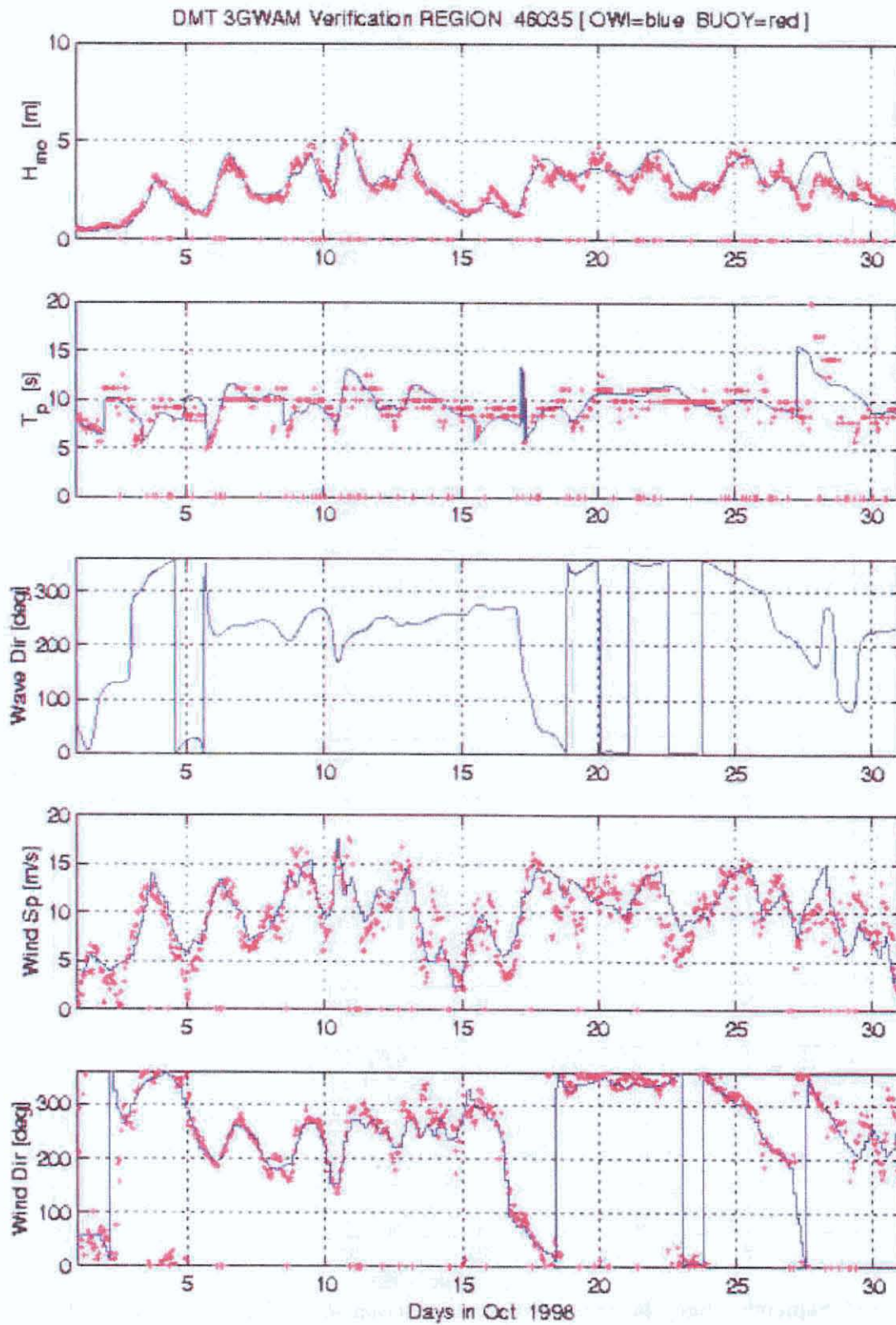


Figure 32 October buoy 46035 and WAM comparison 46035 data in red, hindcast data in blue.

Draft Feasibility Report  
Appendix A: Hydraulic Design, Delong Mountain Terminal, Alaska

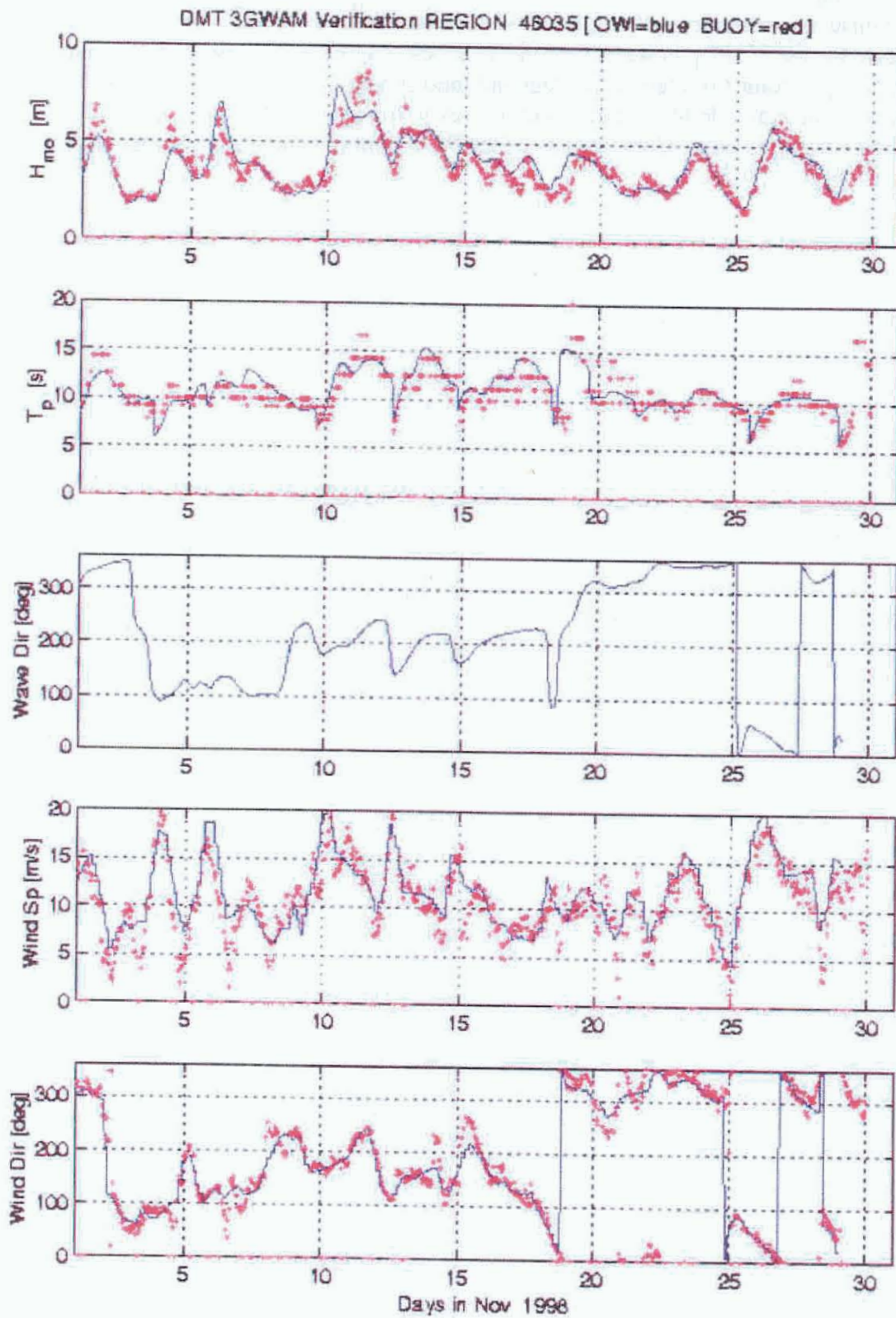


Figure 33 November buoy 46035 and WAM comparison 46035 data in red, hindcast data in blue.

*S4ADW Gage*

At the onset of the hindcast effort, S4ADW directional wave measurements were available for the 1998 open water season. The location of the S4ADW gage and the nearest output point from the WAM regional (and subregional) hindcast were not coincident and water depth was different; however, hindcast quality issues were examined using the data. Comparisons of the WAM out put and S4ADW gage data are shown in figures 34-37.

Draft Feasibility Report  
Appendix A: Hydraulic Design, Delong Mountain Terminal, Alaska

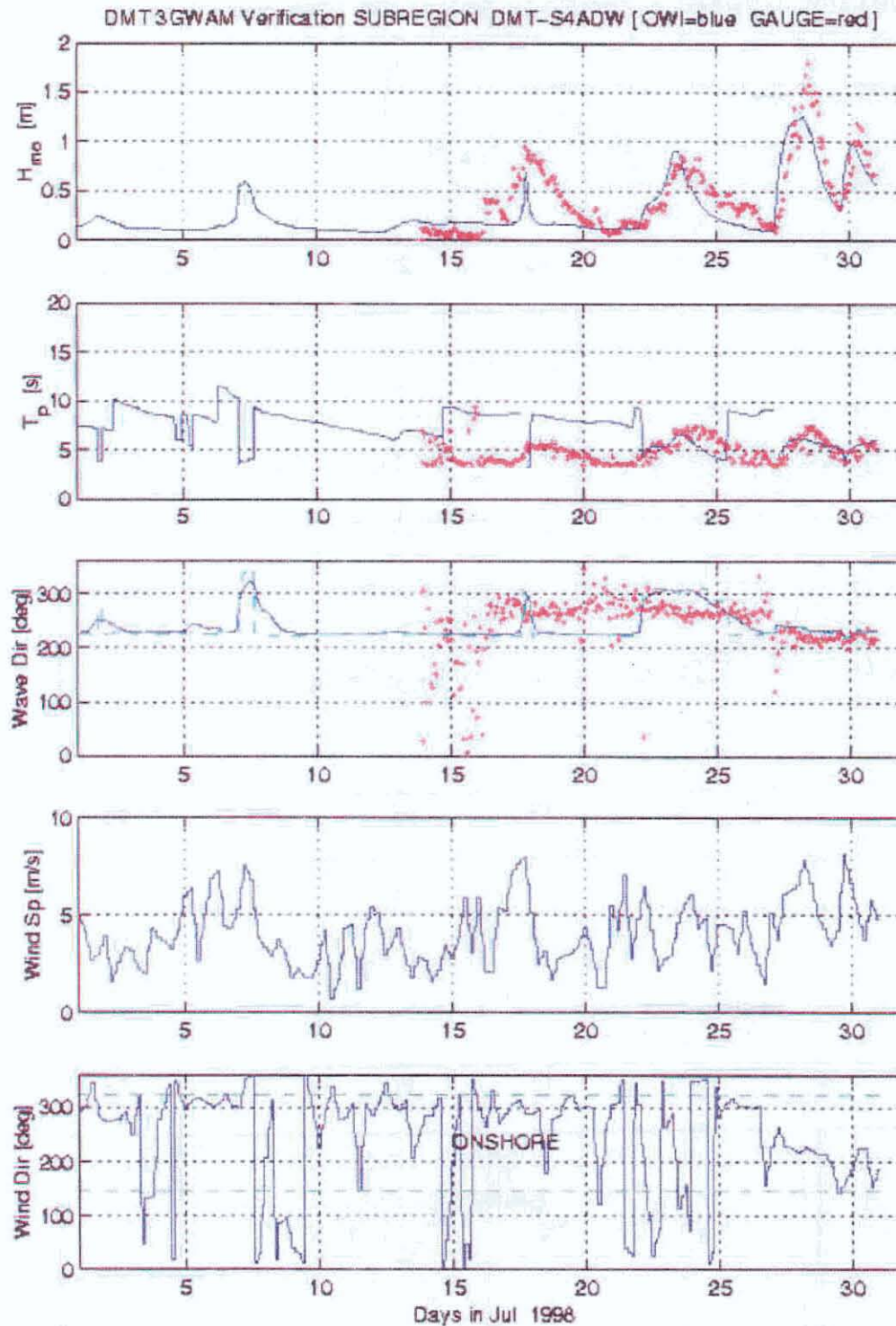


Figure 34 July S4ADW and WAM comparison S4 data in red, hindcast data in blue.

Draft Feasibility Report  
Appendix A: Hydraulic Design, Delong Mountain Terminal, Alaska

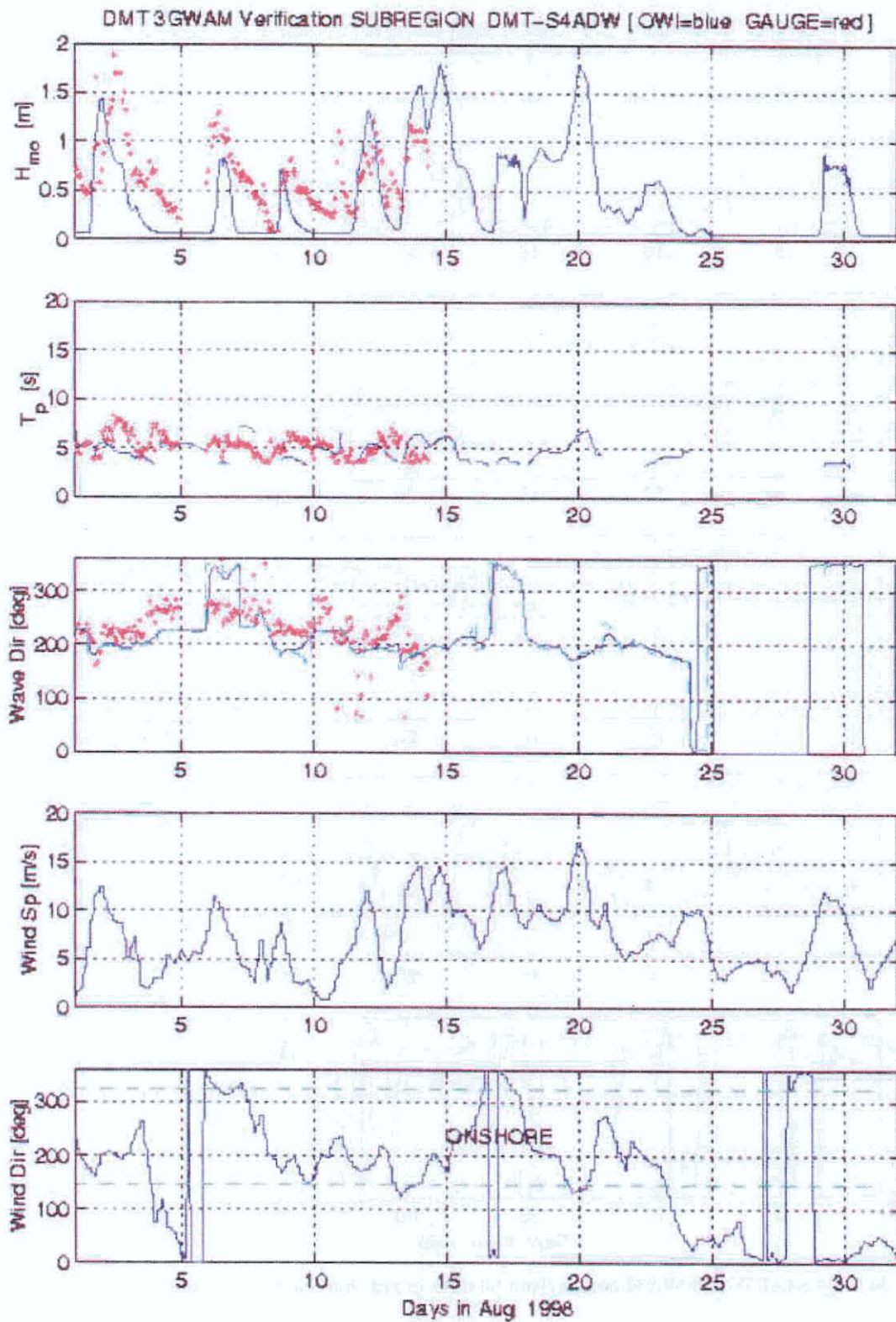


Figure 35 August S4ADW and WAM comparison S4 data in red, hindcast data in blue.

Draft Feasibility Report  
Appendix A: Hydraulic Design, Delong Mountain Terminal, Alaska

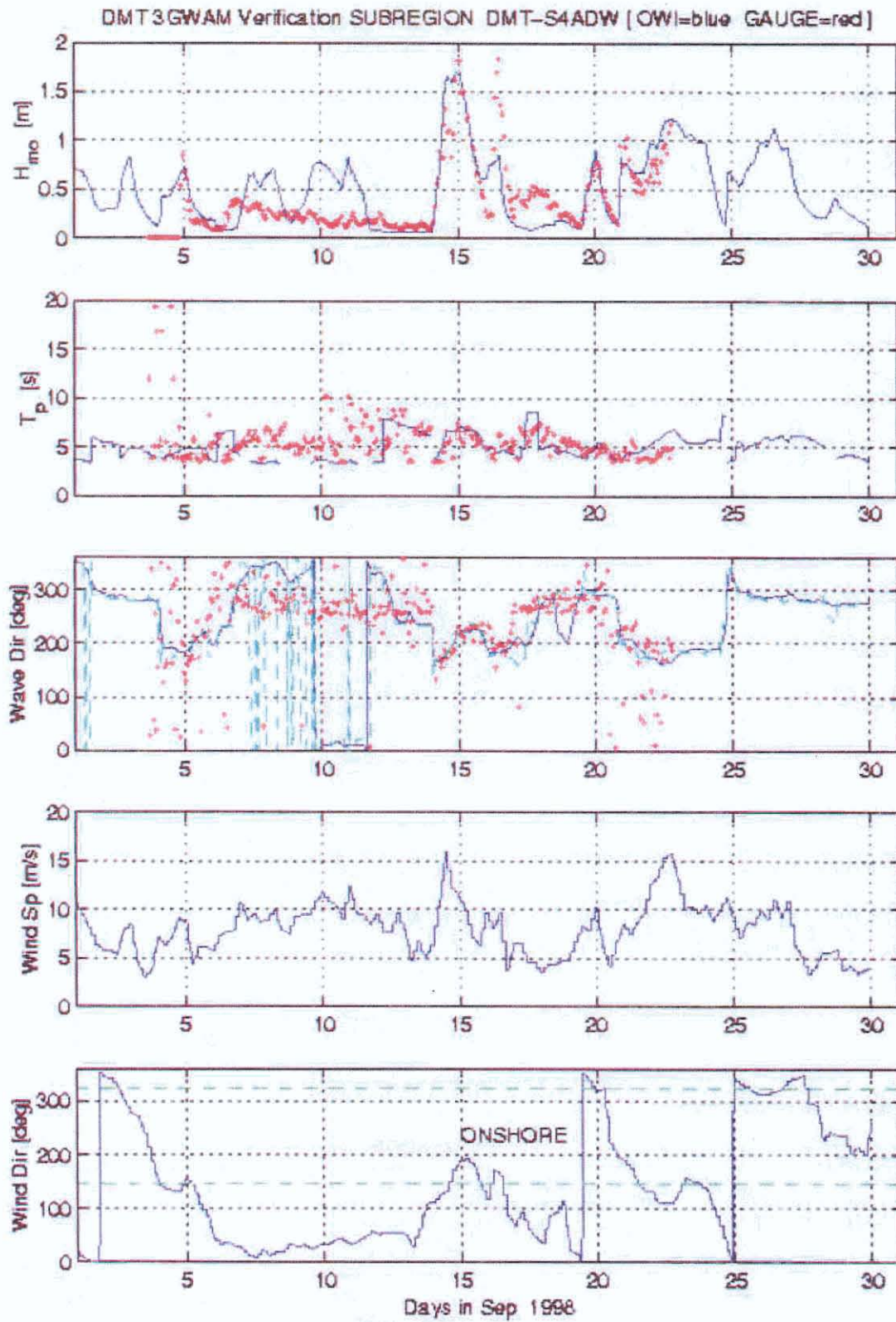


Figure 36 September S4ADW and WAM comparison S4 data in red, hindcast data in blue.

Draft Feasibility Report  
Appendix A: Hydraulic Design, Delong Mountain Terminal, Alaska

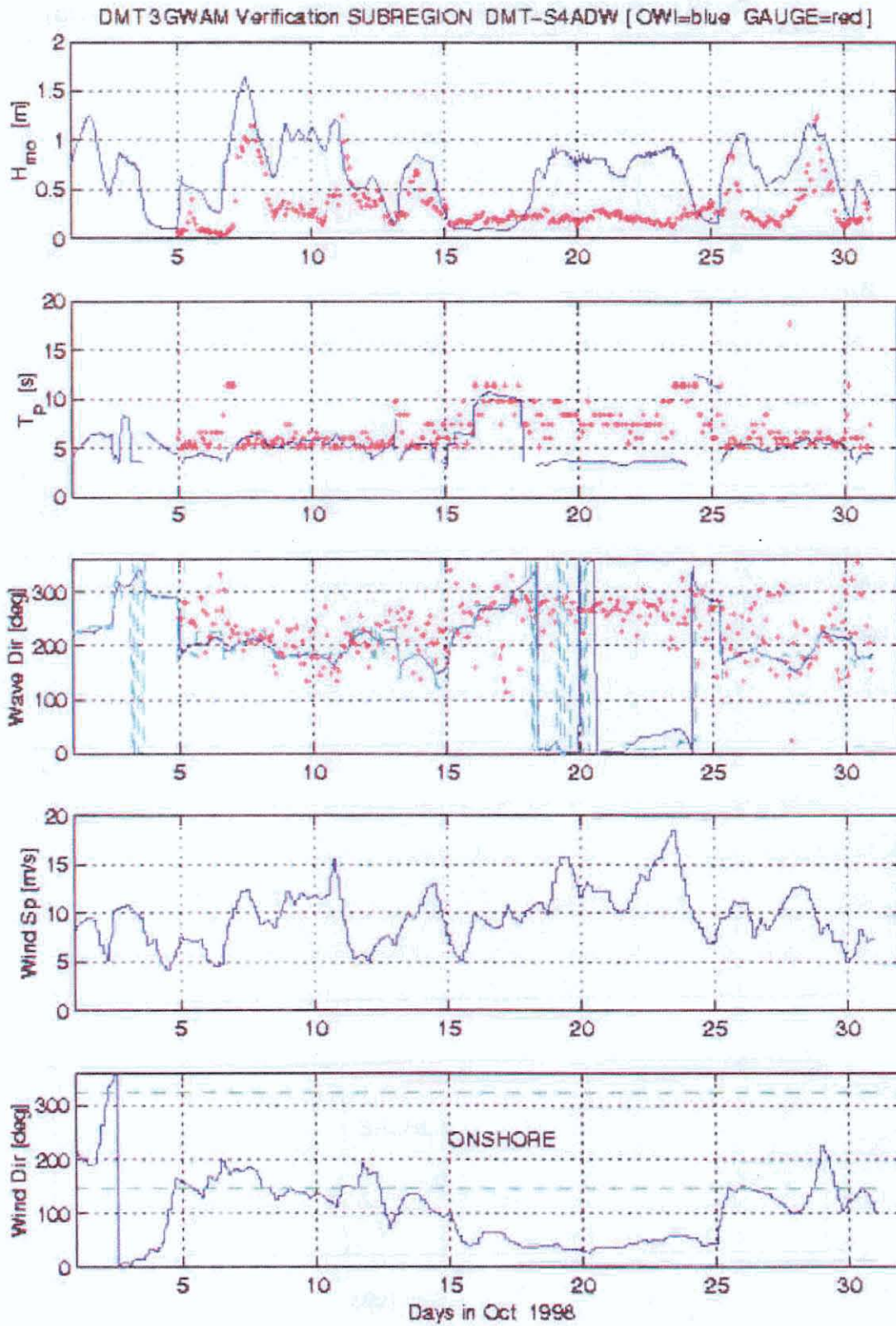


Figure 37 October S4ADW and WAM comparison S4 data in red, hindcast data in blue.

*NDBC 48011*

An NDBC buoy (NDBC 48011) was deployed on 24 July 2000 and became operational on 25 July 2000, measuring wave and meteorological information on an hourly basis. This continued until the buoy was recovered in early October 2000. The meteorological sensors on the buoy measured wind speed, direction, barometric pressure, air and water temperatures at one hour intervals. Directional wave data from the buoy were compared with WAM results at the nearest geographical location of regional and subregional grid intersection. The buoy was deployed again in 2001 to provide more data for comparison. Comparisons of the WAM out put and the buoy 48011 data are shown in figures 38-41.

Draft Feasibility Report  
Appendix A: Hydraulic Design, Delong Mountain Terminal, Alaska

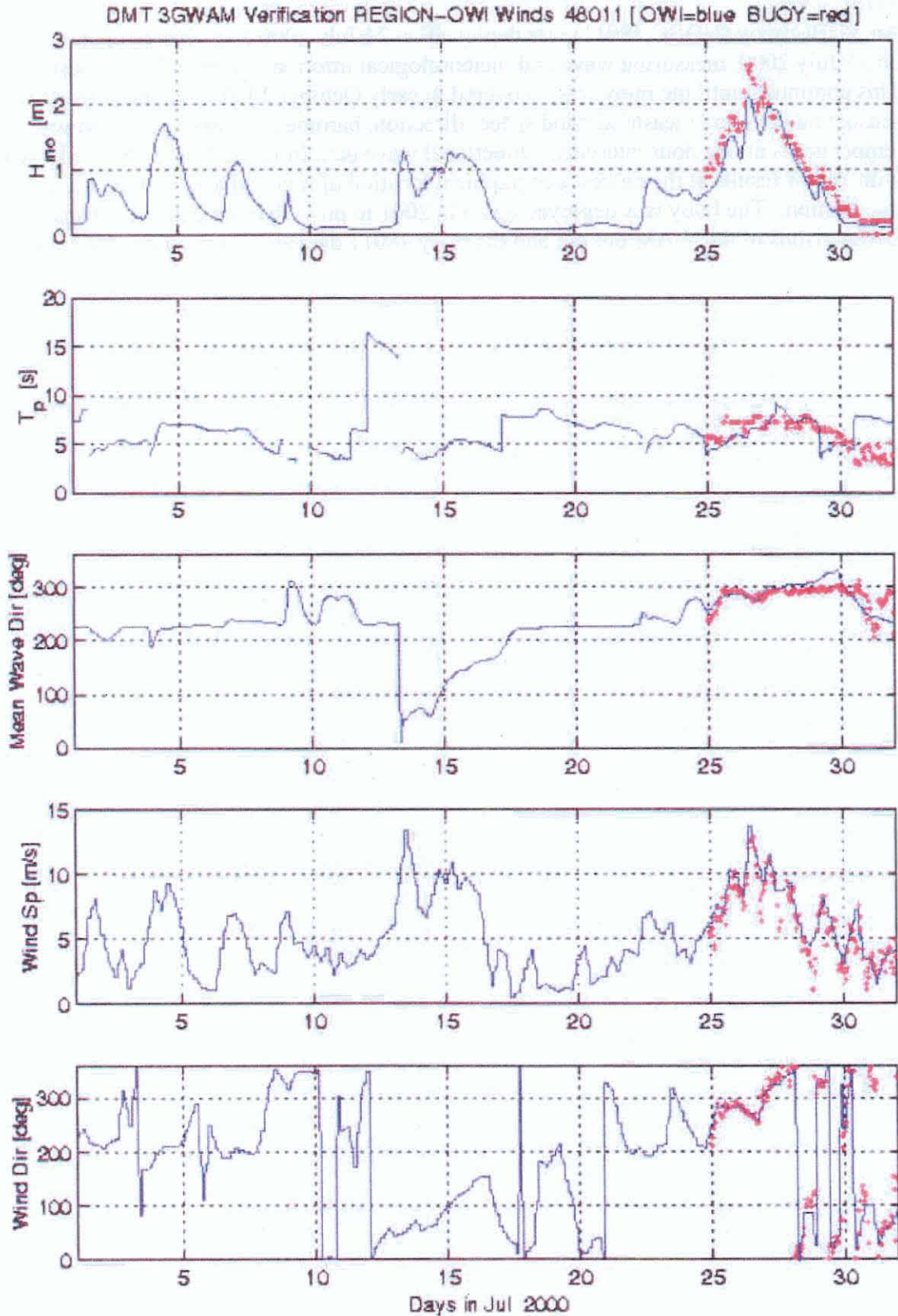


Figure 38 July buoy 48011 and WAM comparison buoy 48011 data in red, hindcast data in blue.

Draft Feasibility Report  
Appendix A: Hydraulic Design, Delong Mountain Terminal, Alaska

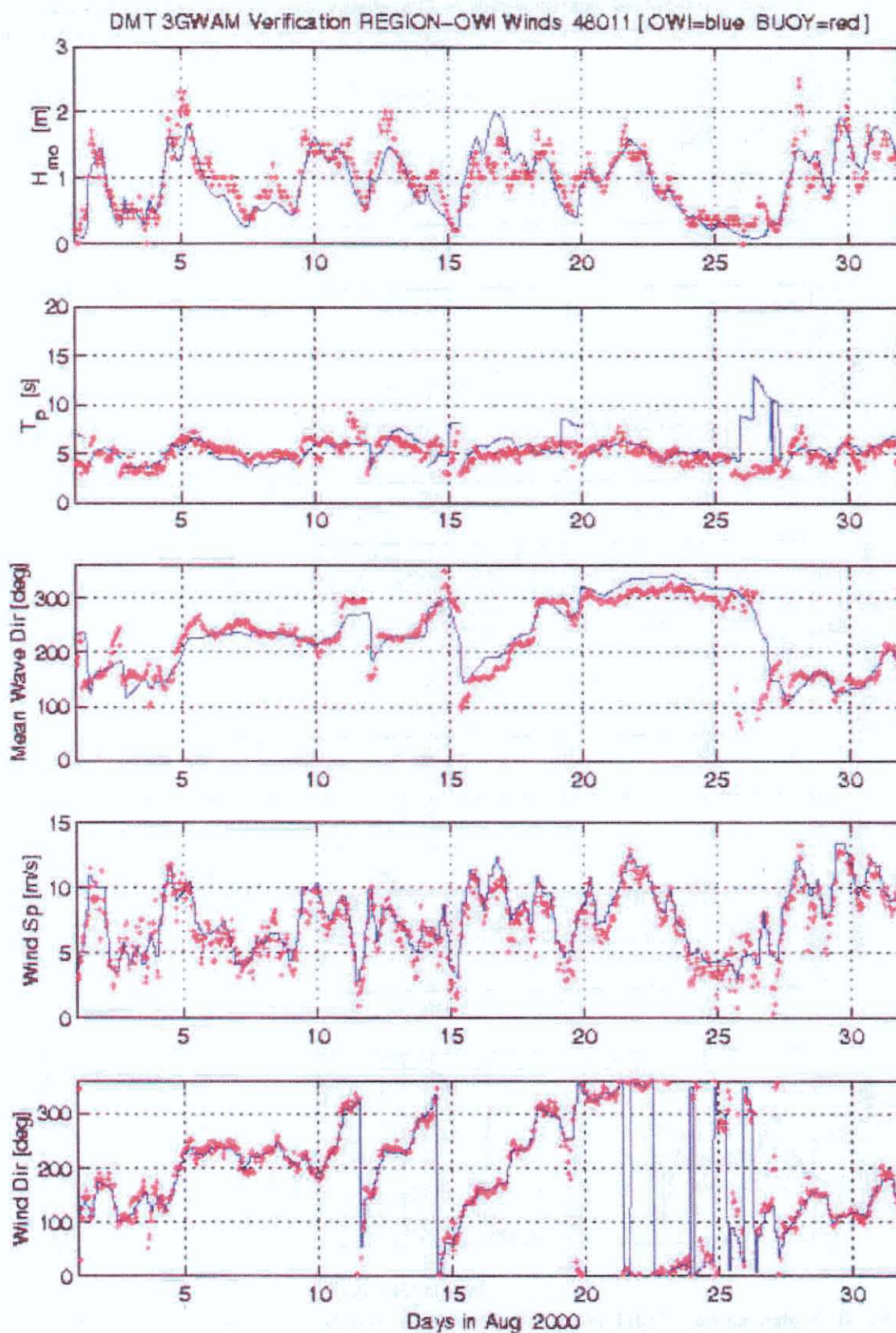


Figure 39 August buoy 48011 and WAM comparison buoy 48011 data in red, hindcast data in blue.

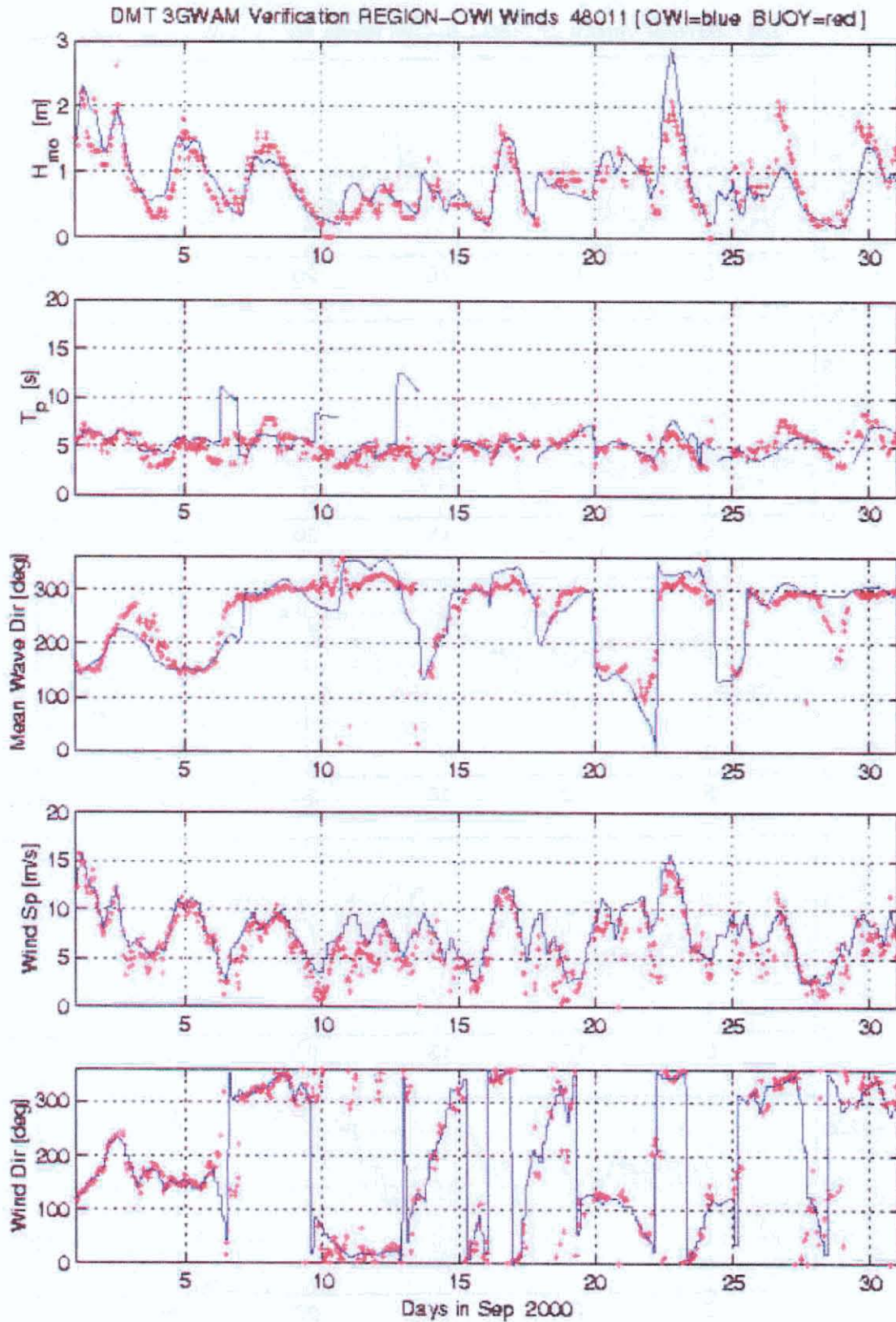


Figure 40 September buoy 48011 and WAM comparison buoy 48011 data in red, hindcast data in blue.

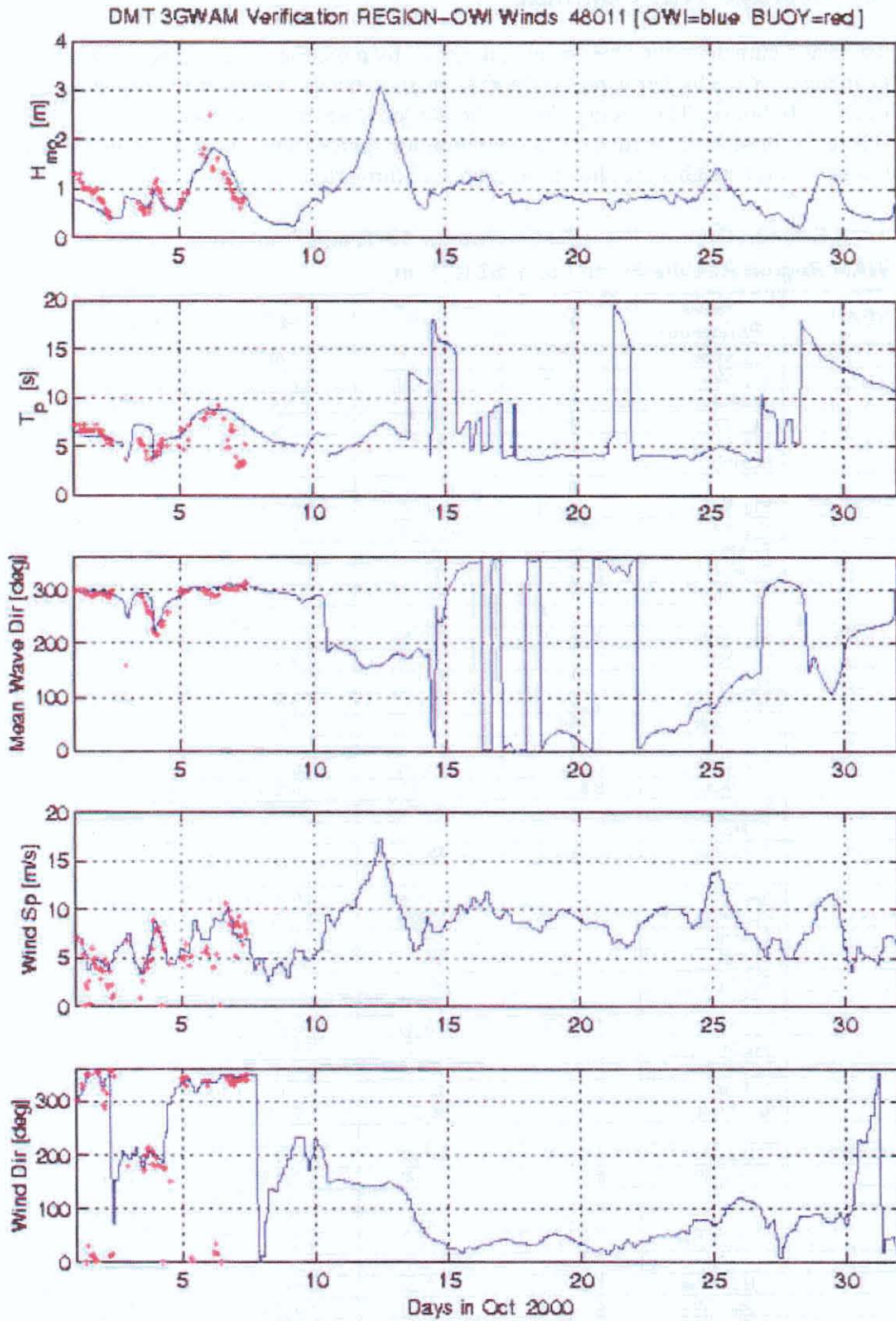


Figure 41 October buoy 48011 and WAM comparison buoy 48011 data in red, hindcast data in blue.

## 5.4 Average Wave Climate

The wave climate at the DMT is characterized by a predominance of waves under 3.3 feet (1 meter). When higher waves (>6.6 ft (>2m)) do occur, it is usually for a short duration of 24 to 48 hours. The average wave climate for 1985-2000 is shown in table A-13. See figure 28 for station location. Seasonal duration tables showing the total and average hours of wave heights are shown in figures 42 through 56.

**TABLE A-13. General Wave Estimates for 16-Year Climatology  
WAM Region Results Station 5, h=62 ft (19m)**

YEAR	Wave Parameter	JUL	AUG	SEP	OCT
1985	H <sub>mo</sub> Mean	1.3 (0.4)	1.3 (0.4)	2.3 (0.7)	3.6 (1.1)
	H <sub>mo</sub> Max	5.9 (1.8)	7.2 (2.2)	9.2 (2.8)	12.8 (3.9)
	T <sub>p</sub> Mean	6.5	6.9	5.4	5.9
	T <sub>p</sub> Max	12+	12+	12+	12+
	% < 3 feet (0.91m)	90.8	87.5	77.4	54.4
1986	H <sub>mo</sub> Mean	1.3 (0.4)	2.3 (0.7)	3.0 (0.9)	2.3 (0.7)
	H <sub>mo</sub> Max	5.9 (1.8)	6.6 (2.0)	9.8 (3.0)	6.6 (2.0)
	T <sub>p</sub> Mean	6.9	5.8	5.6	6.3
	T <sub>p</sub> Max	12+	12+	10	12+
	% < 3 feet	91.1	82.0	67.5	76.0
1987	H <sub>mo</sub> Mean	1.0 (0.3)	1.6 (0.5)	2.3 (0.7)	2.3 (0.7)
	H <sub>mo</sub> Max	3.6 (1.1)	7.5 (2.3)	7.9 (2.4)	7.2 (2.2)
	T <sub>p</sub> Mean	6.6	7.2	6.5	6.7
	T <sub>p</sub> Max	12+	12+	12+	12+
	% < 3 feet	99.0	83.2	75.8	71.2
1988	H <sub>mo</sub> Mean	2.0 (0.6)	2.3 (0.7)	2.0 (0.6)	1.6 (0.5)
	H <sub>mo</sub> Max	9.8 (3.0)	10.5 (3.2)	7.9 (2.4)	5.9 (1.8)
	T <sub>p</sub> Mean	4.7	5.6	6.3	5.4
	T <sub>p</sub> Max	11	12+	12+	12+
	% < 3 feet	88.4	78.1	79.8	95.0
1989	H <sub>mo</sub> Mean	1.3 (0.4)	1.6 (0.5)	2.6 (0.8)	3.0 (0.9)
	H <sub>mo</sub> Max	6.2 (1.9)	8.5 (2.6)	9.8 (3.0)	10.2 (3.1)
	T <sub>p</sub> Mean	6.2	6.8	5.7	7.8
	T <sub>p</sub> Max	11	12+	12+	12+
	% < 3 feet	92.5	90.3	75.8	71.6
1990	H <sub>mo</sub> Mean	1.6 (0.5)	1.6 (0.5)	2.6 (0.8)	2.6 (0.8)
	H <sub>mo</sub> Max	8.2 (2.5)	9.8 (3.0)	6.6 (2.0)	7.9 (2.4)
	T <sub>p</sub> Mean	6.8	7.4	5.1	5.9
	T <sub>p</sub> Max	12+	12+	10	12+
	% < 3 feet	87.3	88.5	76.4	76.7
1991	H <sub>mo</sub> Mean	1.3 (0.4)	1.6 (0.5)	2.0 (0.6)	3.6 (1.1)
	H <sub>mo</sub> Max	5.6 (1.7)	5.9 (1.8)	4.9 (1.5)	14.8 (4.5)
	T <sub>p</sub> Mean	6.6	6.4	5.0	7.2
	T <sub>p</sub> Max	12+	12+	12+	12+
	% < 3 feet	90.4	87.0	93.5	59.4
1992	H <sub>mo</sub> Mean	1.3 (0.4)	1.6 (0.5)	2.0 (0.6)	3.0 (0.9)
	H <sub>mo</sub> Max	4.3 (1.3)	5.9 (1.8)	7.5 (2.3)	14.4 (4.4)
	T <sub>p</sub> Mean	6.7	5.4	7.1	6.4
	T <sub>p</sub> Max	12+	10	12+	12+
	% < 3 feet	95.9	89.2	85.4	72.4

Draft Feasibility Report  
Appendix A: Hydraulic Design, Delong Mountain Terminal, Alaska

**TABLE A-13. General Wave Estimates for 16-Year Climatology  
WAM Region Results Station 5, h=62 ft (19m)**

YEAR	Wave Parameter	JUL	AUG	SEP	OCT
1993	H <sub>mo</sub> Mean	1.3 (0.4)	1.6 (0.5)	3.6 (1.1)	2.6 (0.8)
	H <sub>mo</sub> Max	7.2 (2.2)	10.5 (3.2)	9.8 (3.0)	10.5 (3.2)
	T <sub>p</sub> Mean	7.3	6.2	5.7	7.4
	T <sub>p</sub> Max	12+	10	9	12+
	% < 3 feet	87.1	86.9	52.8	69.9
1994	H <sub>mo</sub> Mean	0.7 (0.2)	3.3 (1.0)	2.6 (0.8)	2.6 (0.8)
	H <sub>mo</sub> Max	2.6 (0.8)	11.2 (3.4)	7.5 (2.3)	9.8 (3.0)
	T <sub>p</sub> Mean	7.9	6.6	5.8	7.4
	T <sub>p</sub> Max	12+	12+	12+	12+
	% < 3 feet	100	61.8	70.7	73.6
1995	H <sub>mo</sub> Mean	2.0 (0.6)	1.0 (0.3)	2.0 (0.6)	2.0 (0.6)
	H <sub>mo</sub> Max	7.2 (2.2)	5.9 (1.8)	4.9 (1.5)	8.2 (2.5)
	T <sub>p</sub> Mean	6.0	7.0	5.9	5.8
	T <sub>p</sub> Max	12+	12+	12+	12+
	% < 3 feet	90.6	96.9	88.5	93.7
1996	H <sub>mo</sub> Mean	2.3 (0.7)	2.3 (0.7)	2.3 (0.7)	2.6 (0.8)
	H <sub>mo</sub> Max	11.8 (3.6)	7.5 (2.3)	7.9 (2.4)	22.0 (6.7)
	T <sub>p</sub> Mean	6.3	6.7	6.5	6.6
	T <sub>p</sub> Max	12+	12+	12+	12+
	% < 3 feet	80.7	73.9	73.0	83.2
1997	H <sub>mo</sub> Mean	1.3 (0.4)	2.0 (0.6)	2.0 (0.6)	2.6 (0.8)
	H <sub>mo</sub> Max	3.3 (1.0)	8.9 (2.7)	8.9 (2.7)	12.5 (3.8)
	T <sub>p</sub> Mean	3.6	3.4	6.1	6.3
	T <sub>p</sub> Max	8.0	7.0	12+	12+
	% < 3 feet	100.	86.1	82.0	76.5
1998	H <sub>mo</sub> Mean	1.0 (0.3)	2.3 (0.7)	2.6 (0.8)	3.3 (1.0)
	H <sub>mo</sub> Max	4.3 (1.3)	9.2 (2.8)	8.5 (2.6)	7.2 (2.2)
	T <sub>p</sub> Mean	7.3	4.5	5.7	5.5
	T <sub>p</sub> Max	12+	12+	12+	12+
	% < 3 feet	96.5	77.0	75.3	51.3
1999	H <sub>mo</sub> Mean	1.0 (0.3)	1.6 (0.5)	1.6 (0.5)	2.0 (0.6)
	H <sub>mo</sub> Max	4.6 (1.4)	5.6 (1.7)	3.3 (1.0)	3.6 (1.1)
	T <sub>p</sub> Mean	4.1	3.5	3.3	5.5
	T <sub>p</sub> Max	11	12+	12+	12+
	% < 3 feet	98.6	90.4	98.4	96.6
2000	H <sub>mo</sub> Mean	1.6 (0.5)	2.6 (0.8)	2.6 (0.8)	2.6 (0.8)
	H <sub>mo</sub> Max	7.2 (2.2)	5.9 (1.8)	8.9 (2.7)	8.5 (2.6)
	T <sub>p</sub> Mean	6.3	5.6	5.4	7.5
	T <sub>p</sub> Max	12+	12+	12+	12+
	% < 3 feet	84.8	59.3	75.3	84.2

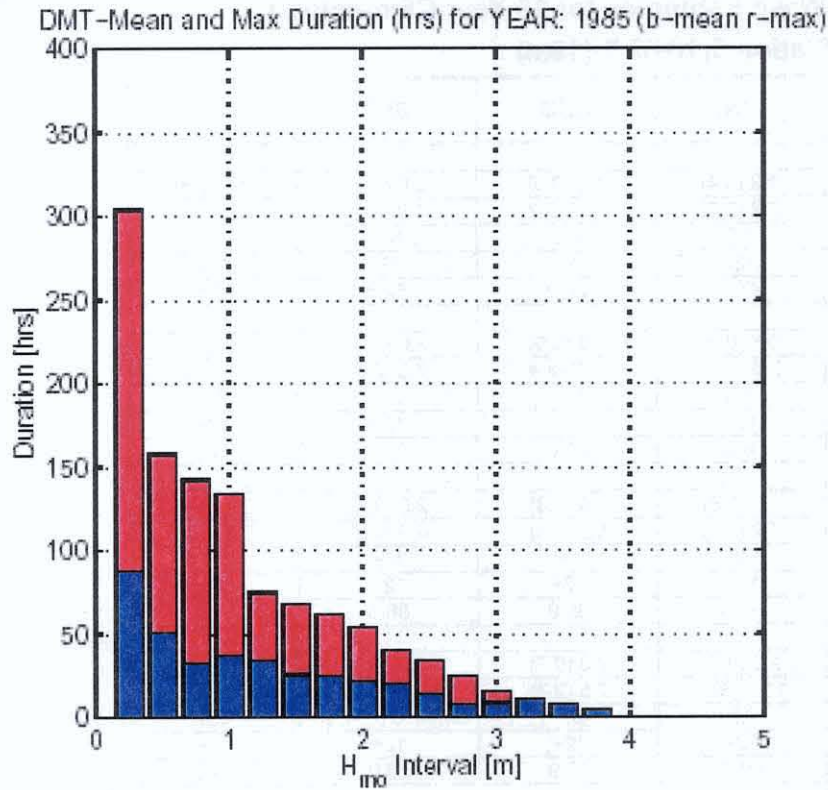


Figure 42 1985 Duration Plot

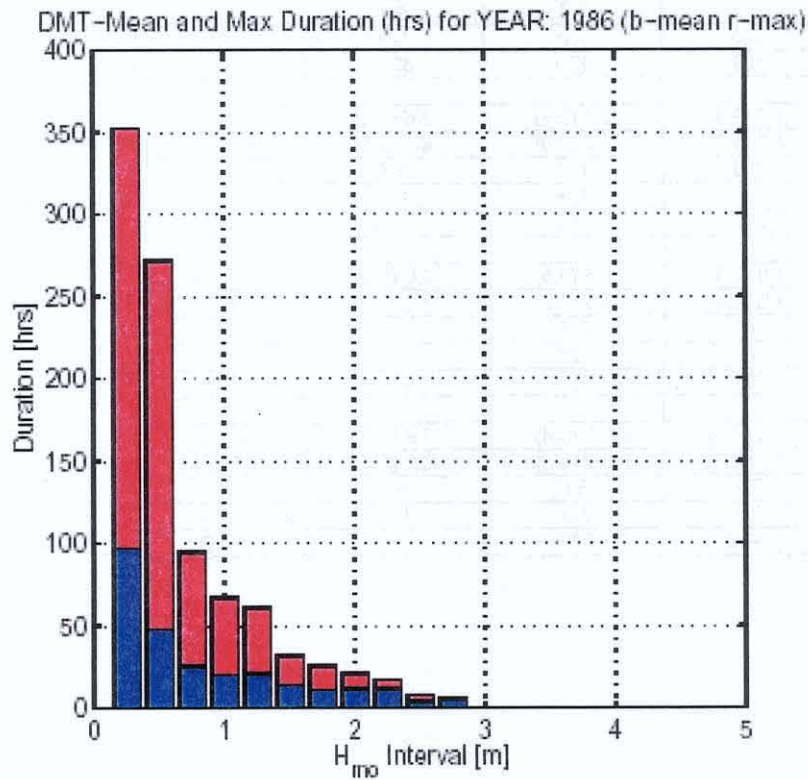


Figure 43 1986 Duration Plot

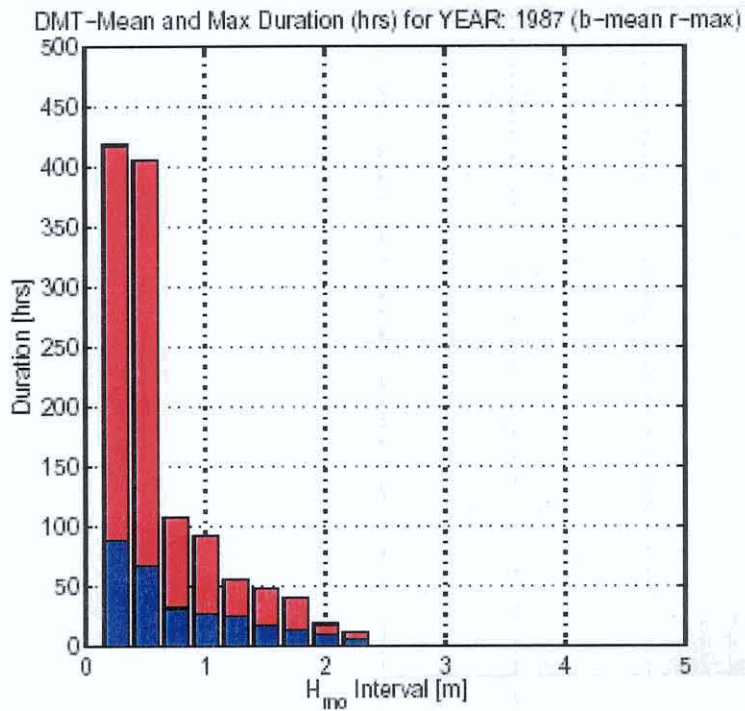


Figure 44 1987 Duration Plot

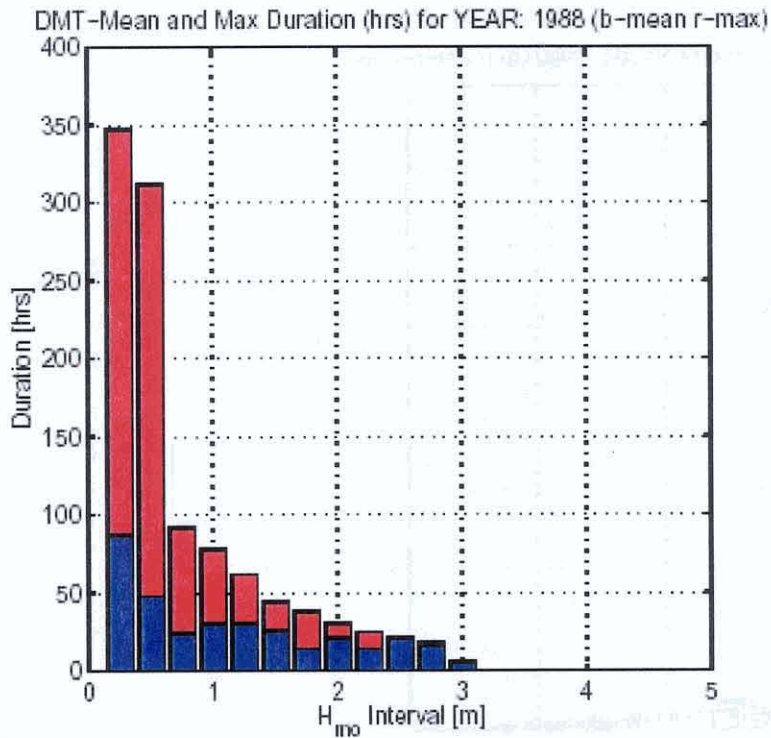


Figure 45 1988 Duration Plot

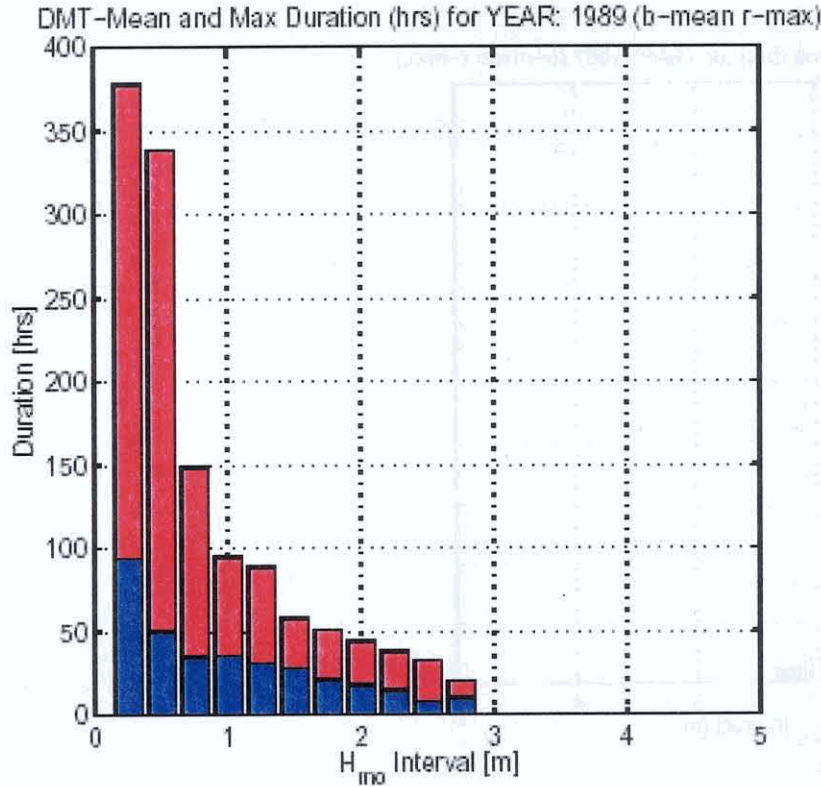


Figure 46 1989 Duration Plot

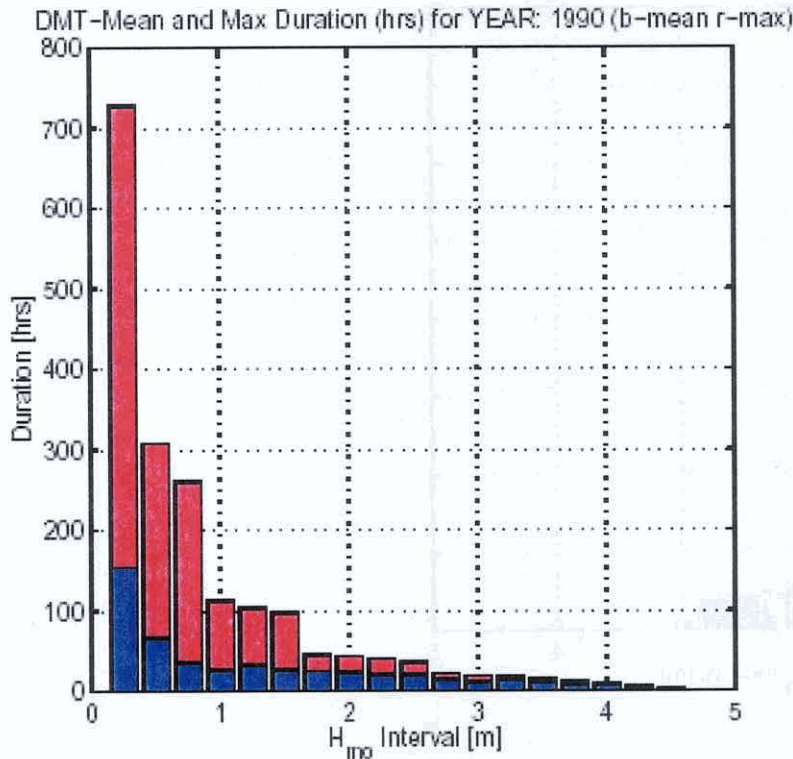


Figure 47 1990 Duration Plot

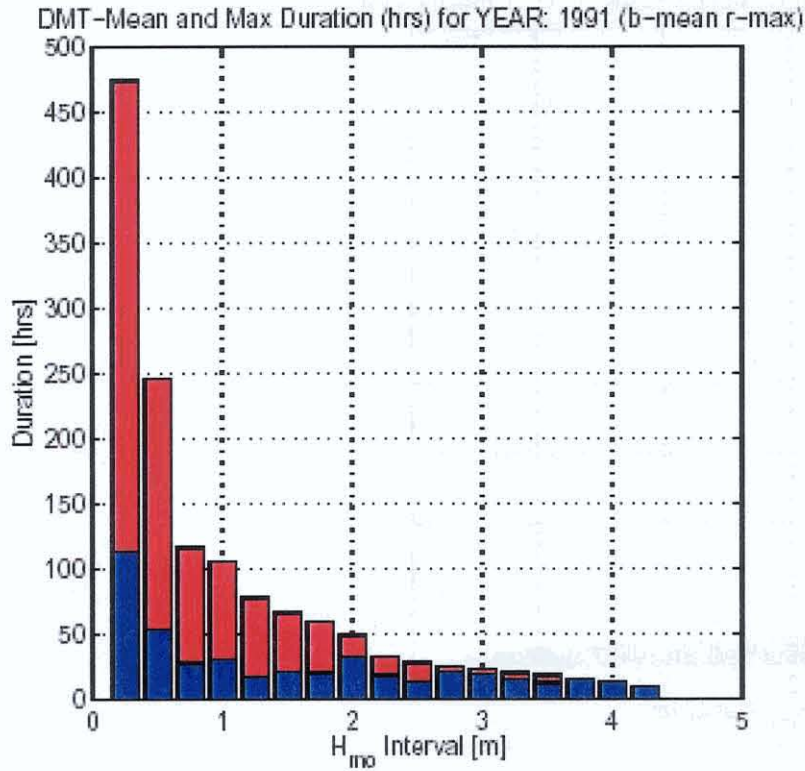


Figure 48 1991 Duration Plot

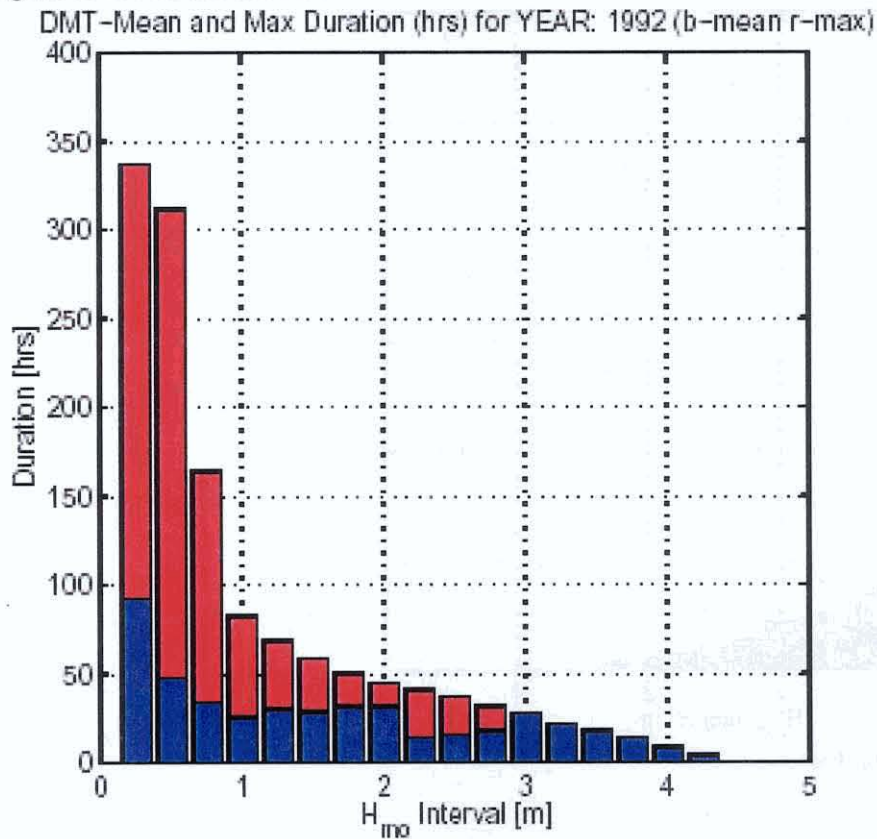


Figure 49 1992 Duration Plot

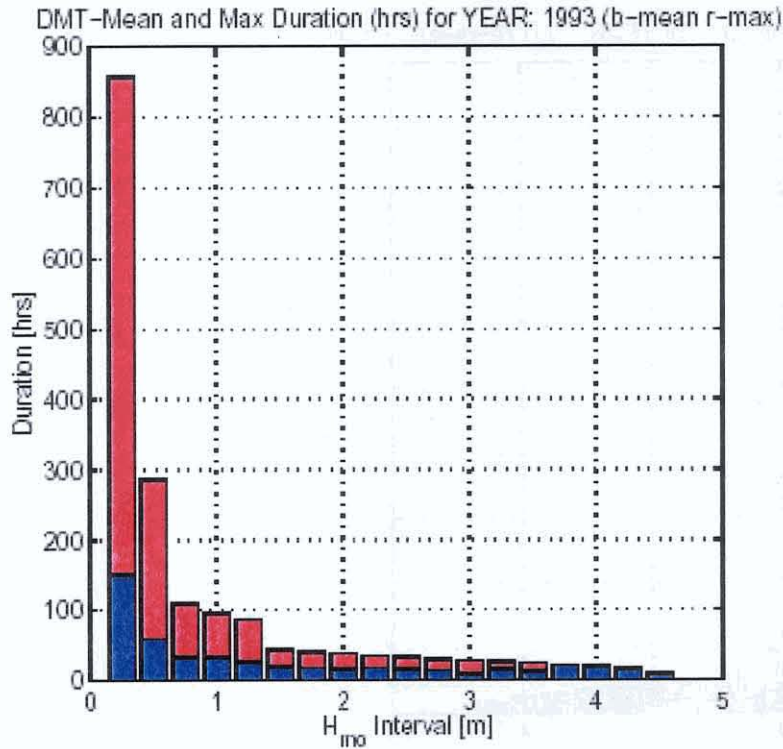


Figure 50 1993 Duration Plot

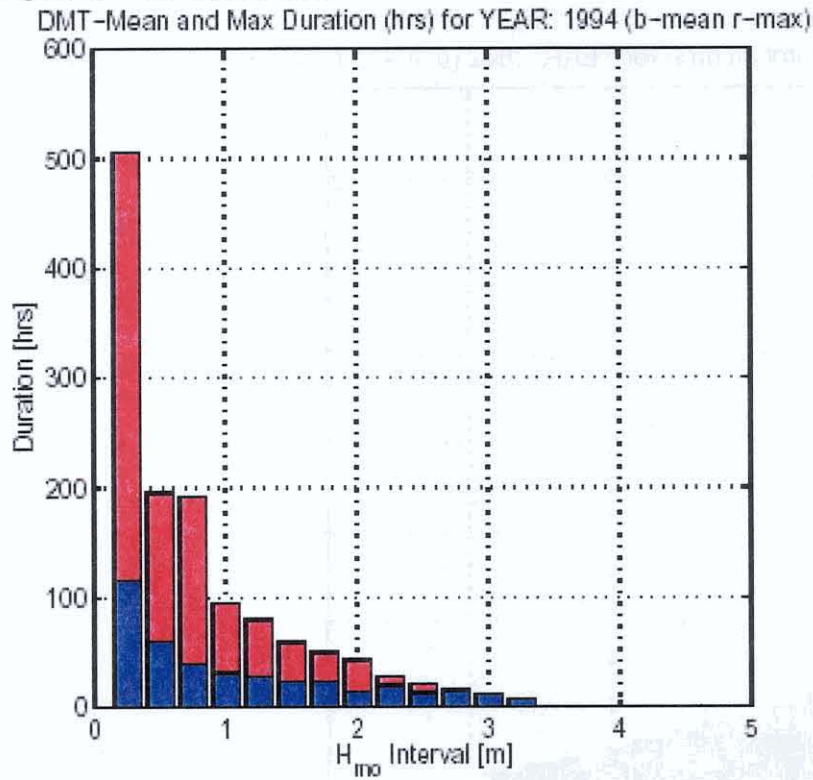


Figure 51 1994 Duration Plot

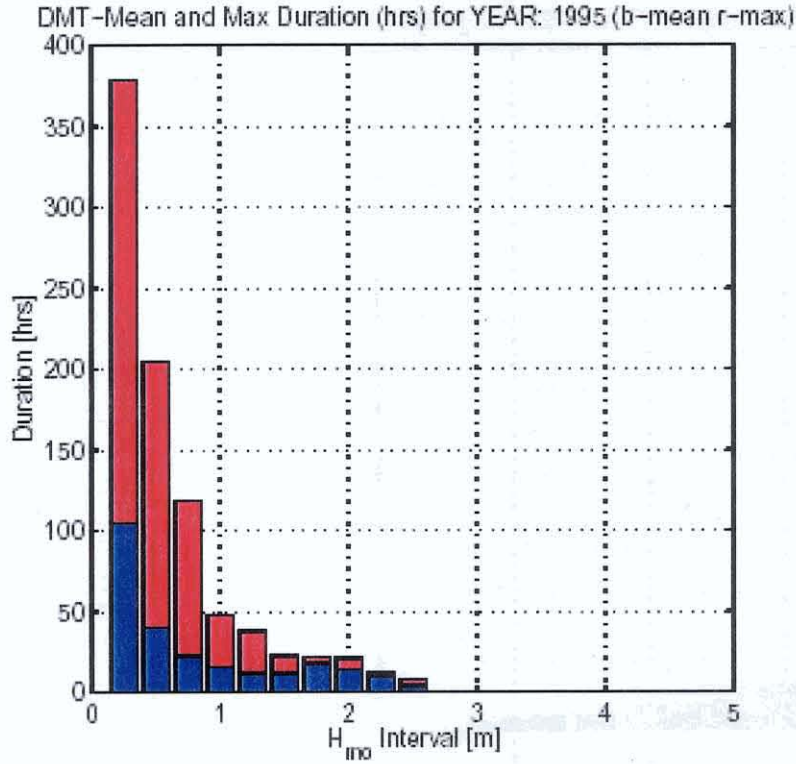


Figure 52 1995 Duration Plot  
 DMT-Mean and Max Duration (hrs) for YEAR: 1996 (b-mean r-max)

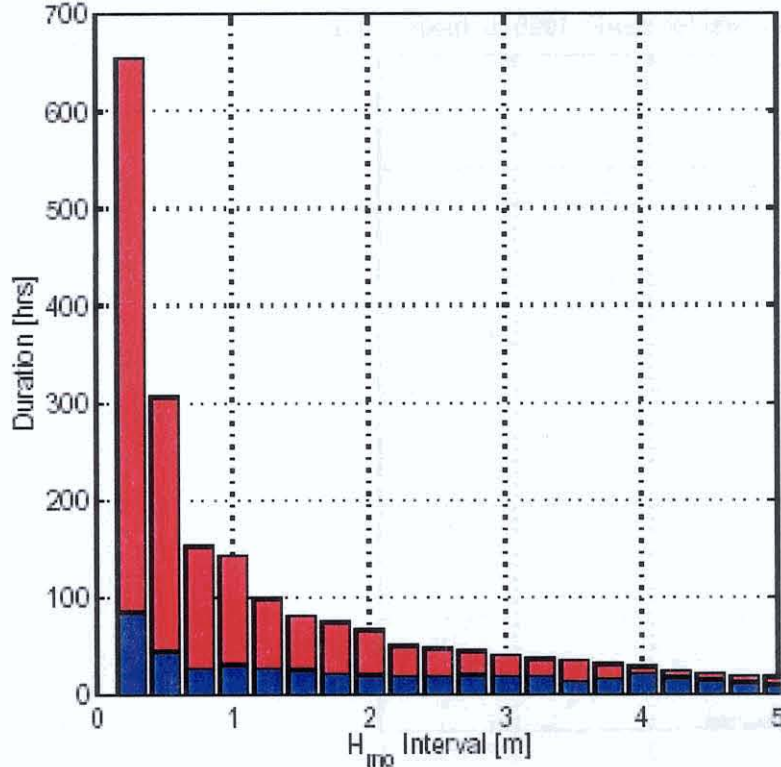


Figure 53 1996 Duration Plot

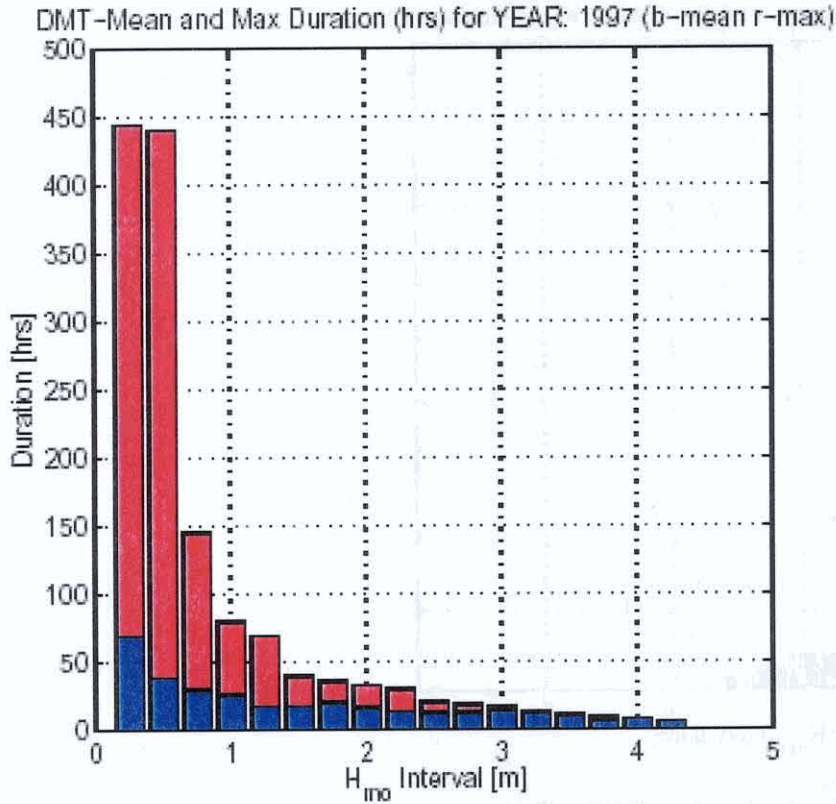


Figure 54 1997 Duration Plot

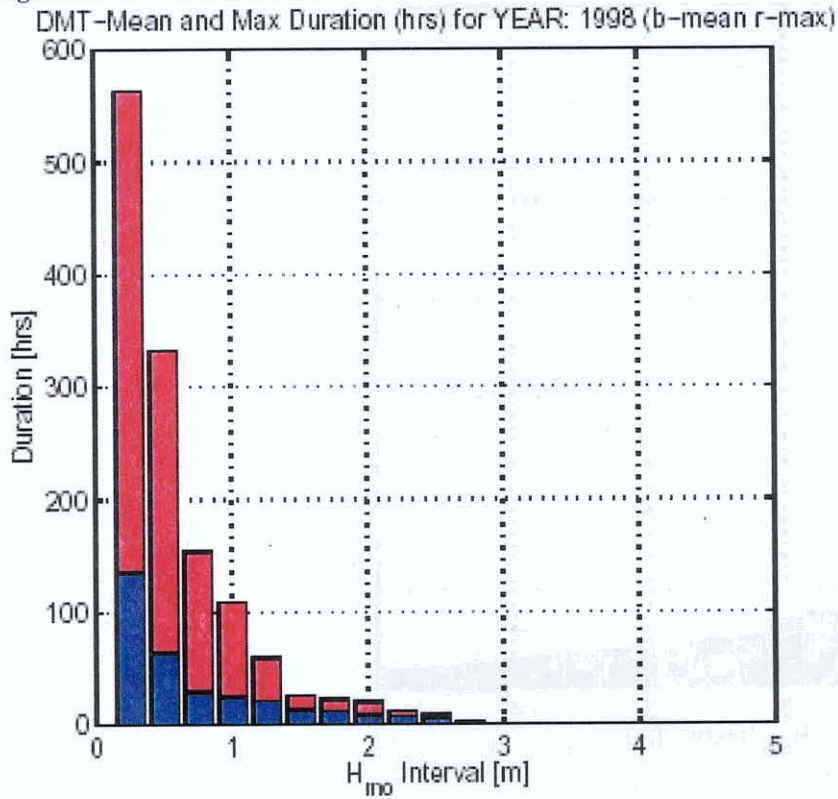


Figure 55 1998 Duration Plot

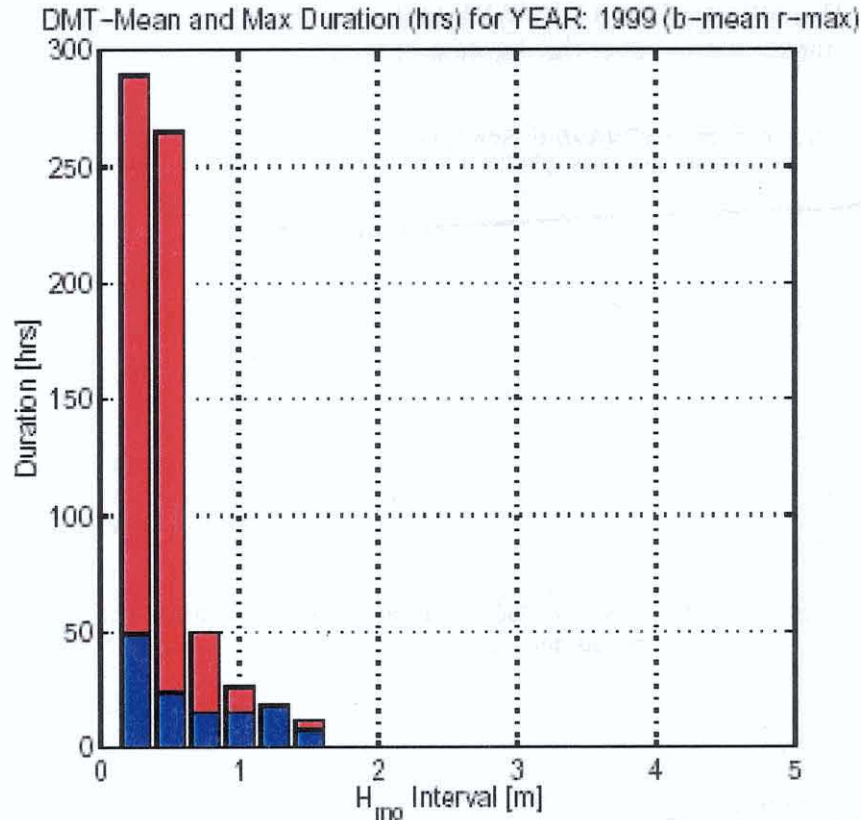


Figure 56 1999 Duration Plot  
 \*(1 m = 3.28 ft)

## 5.5 Nearshore Wave Transformation

The waves from the hindcast were transformed inshore to the -28, -24, -20, and -13-foot (-8.5, -7.3, -6.1, and -4.0 meter) contour using Snell's Law. Details of these results are in the CHL report appendices. This simple transformation assumes that the contours are straight and parallel. The relatively simple planar bathymetry surrounding the proposed DMT navigation channel suggested that Snell's law could be applied with little sacrifice in accuracy.

The use of Snell's Law for a simplified wave transformation was evaluated using a comparison with the Steady-State Spectral Wave (STWAVE) model. STWAVE is a steady state finite difference model based on the wave action balance equation. It simulates depth-induced wave refraction and shoaling, current-induced refraction and shoaling, depth- and steepness-induced wave breaking, wind-wave growth, and wave-wave interaction and white capping that redistribute and dissipate energy in a growing wave field. For the comparison with Snell's Law, a relatively mild storm event was selected. The storm wave conditions are 10-foot (3.0-meter) peak incident  $H_{m0}$ , a 5 second to 9 second period, and a mean wave direction generally to the north northeast. The test conditions were selected from the WAM 16-year hindcast. Figure 57 displays the cross-shore comparison of  $H_{m0}$  and  $\theta_{mean}$  wave direction estimated by STWAVE and Snell's Law.

Figure 58 compares the  $H_{mo}$  estimated from STWAVE to that estimated by Snell's law for simulations of wave transformation over the duration of the storm.

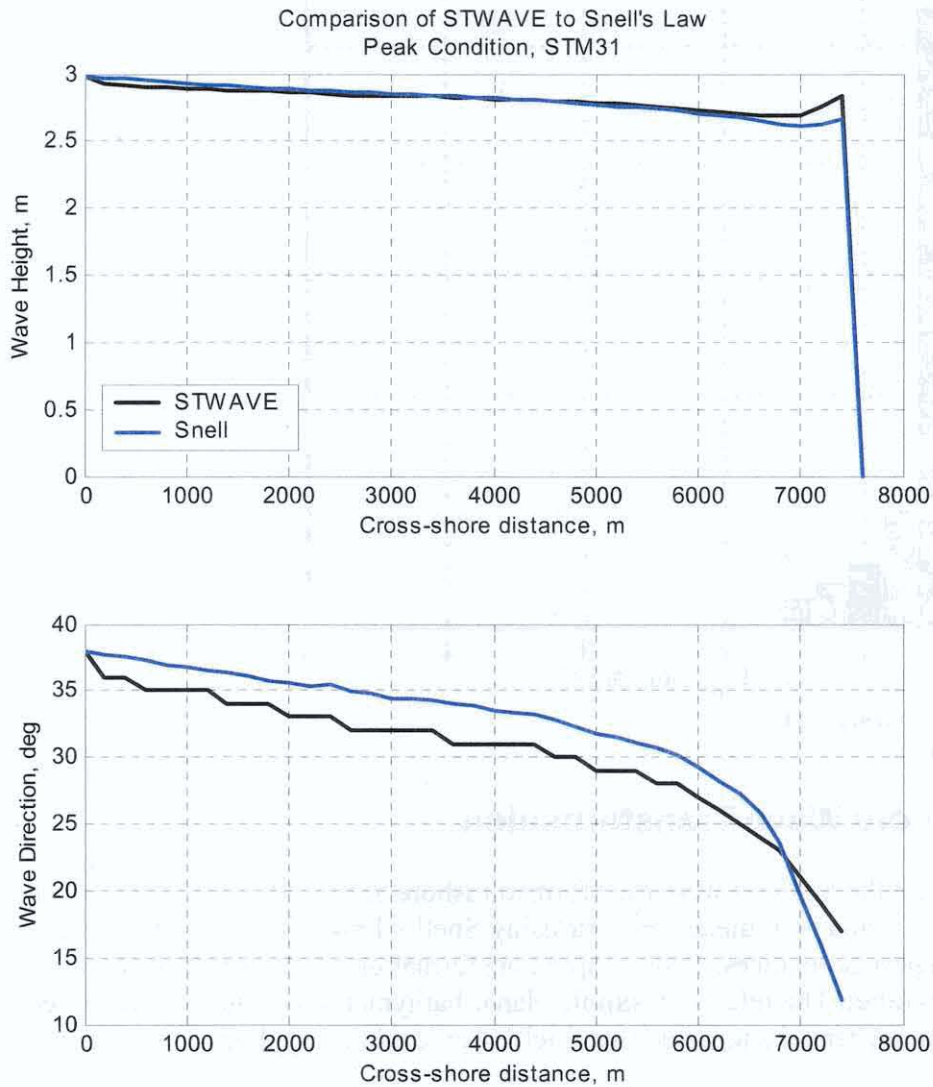
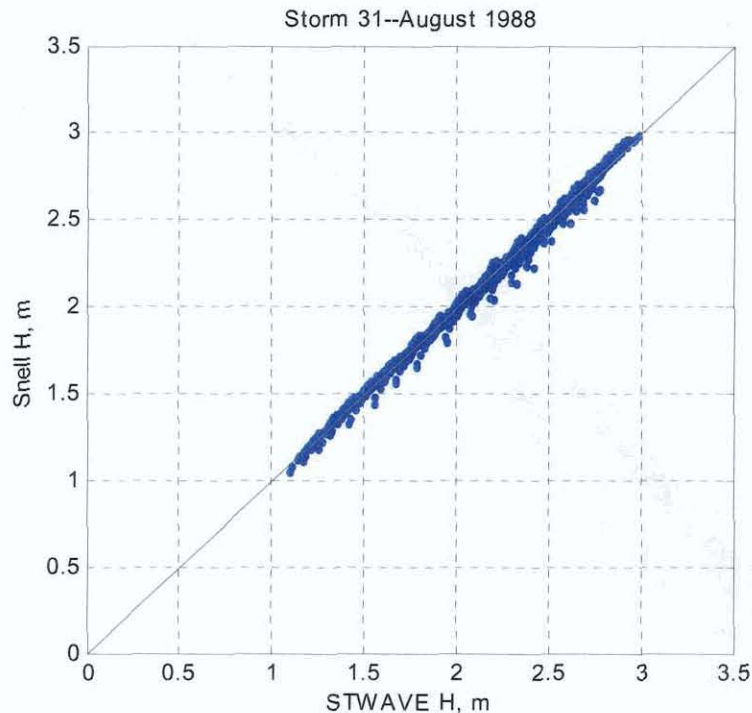


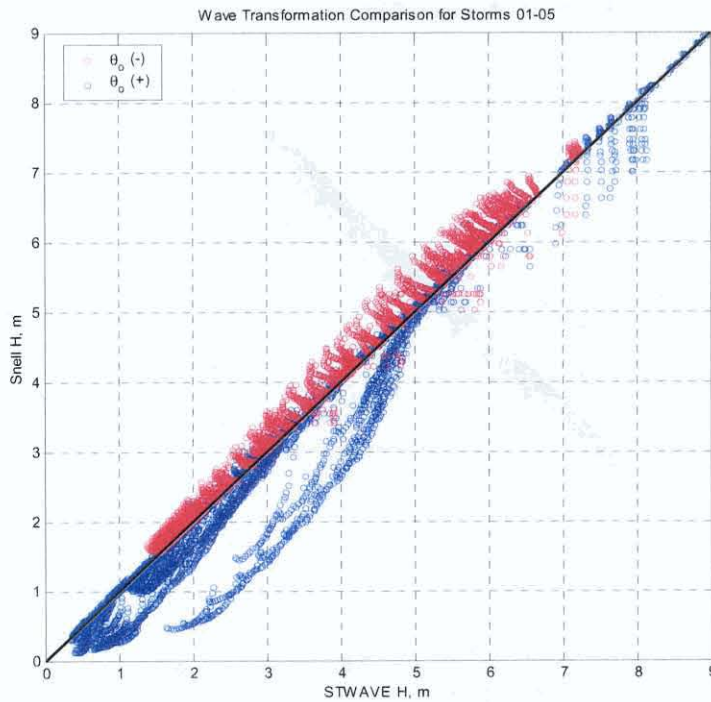
Figure 57. Cross-shore representation of  $H_{mo}$  and  $\theta_{mean}$  wave direction estimated by STWAVE and Snell's Law. Conditions modeled are from the peak wave height of Storm-31, 14 August 1988 1400 UTC. \*(1 m = 3.28 ft)



**Figure 58. Scatter diagram comparing  $H_{mo}$  estimated from STWAVE and Snell's law for the duration of Storm-31 at co-located cross-shore points with depth greater than 6-m. Assumed orientation of bathymetry is 350 true. \*(1 m = 3.28 ft)**

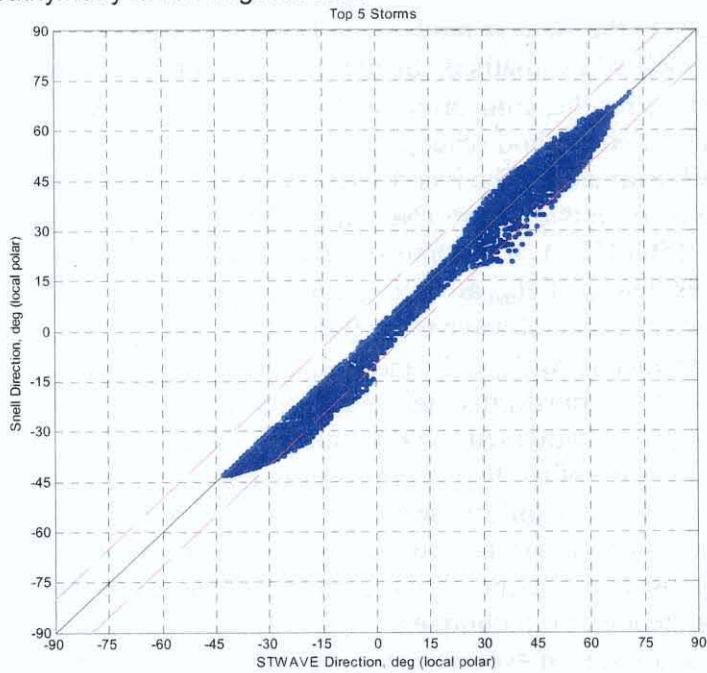
Five of the most energetic conditions in the 16-year hindcast and extremes were simulated with STWAVE and the Snell's Law method. Scatter diagrams are provided in figures 59 and 60 for the  $H_{mo}$  and  $\theta_{mean}$  results, comparing Snell's Law to STWAVE. There are two storms where the simplified method severely under-estimates the  $H_{mo}$  results compared with the STWAVE estimates. The inconsistent Snell's Law results compared with STWAVE are derived from two storms (November 1970, 1400 – 1600 UTC, and November 1974, 0700 – 1500 UTC). The input storm conditions were from the south. The Snell's Law-based estimates of  $H_{mo}$  are biased low (compared with STWAVE) because of the increased influence of wave refraction. The Snell's Law method applies single bulk wave parameters for  $H_{mo}$ ,  $T_p$  and  $\theta_{mean}$  across an assumed plane and parallel bathymetry. STWAVE transforms individual components of the directional wave spectrum across a grid of bathymetry to estimate the wave transformation. The oblique angle of entry of the two storms resulted in the waves being refracted en masse using Snell's Law due to a uniform wave period used, while the STWAVE method allowed individual periods for the wave components across a grid, which resulted in less energy being lost to refraction. This resulted in lower wave heights being predicted for storms entering the area from oblique angles. This was addressed in the sediment transport by analysis of a series of synthetic storms. Details on the synthetic storm analysis are presented in the sediment transport section of this appendix.

Draft Feasibility Report  
 Appendix A: Hydraulic Design, Delong Mountain Terminal, Alaska



*\*(1 m = 3.28 ft)*

Figure 59. Scatter diagram comparing wave height estimated from STWAVE and Snell's law for the top 5-storms at all cross-shore locations with depth greater than 6 m. Assumed orientation of bathymetry is 350 degrees true.



*\*(1 m = 3.28 ft)*

Figure 60. Scatter diagram comparing wave height estimated from STWAVE and Snell's law for the top 5 storms at all cross-shore locations with depth greater than 6-m. Assumed orientation of bathymetry is 350 true.

The model comparisons indicated that Snell's Law is capable of estimating wave transformation mechanisms along the proposed navigation channel within the limits of accuracy of the more complex model, STWAVE. This comparison suggested that Snell's Law was a suitable wave transformation method for estimating channel infilling rates, so analysis of the nearshore wave climate was performed using Snell's Law.

## 5.6 Extreme Storms

The extremal significant wave height estimates were derived from table 14 and used as input to the equation

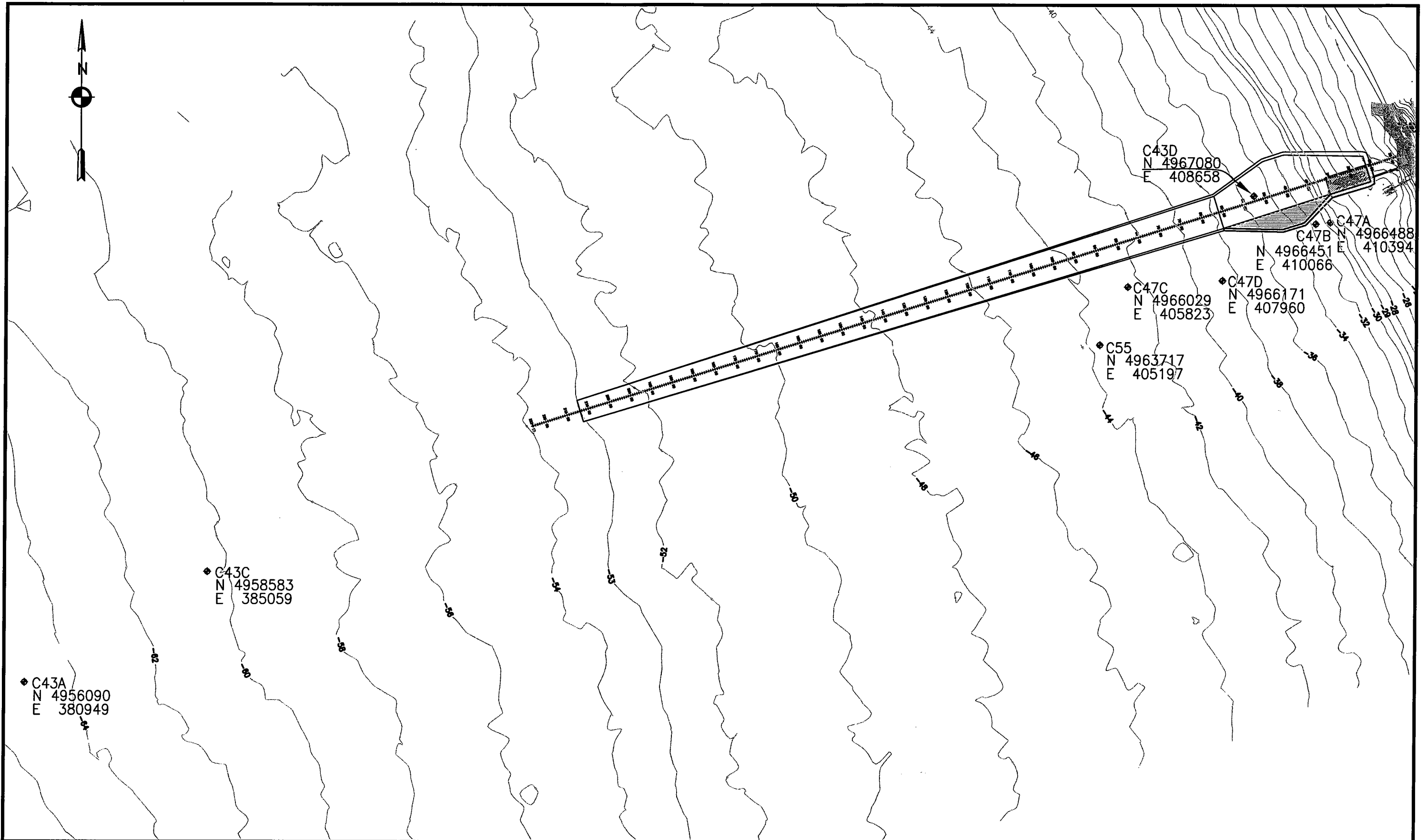
$$RETURN PERIOD_{YEARS} = \frac{RECORD LENGTH + 1}{STORM RANK},$$

where the RECORD LENGTH is equal to 47 years. The return period is plotted in figure 61. It is evident all but one point (November 1970) follow the least squares fit rather well. The November 1970 storm may be indicative of either an outlier, or a storm peak event above the data set limited 47 return period.

The data represent the peak  $H_{m0}$  condition and the accompanying  $T_p$  and  $\sigma_{mean}$ . Percent distributions of the top 1,000 individual  $H_{m0}$  indicate that the extreme wave conditions can generally be considered as locally generated wind seas. The  $T_p$  estimates for these waves range from 7 to 13 seconds with 8 seconds being the most frequently occurring period. There is a slight indication of distant swell energy existing (16 second period and greater); however, the percent occurrence is quite small.

The simulations were conducted identical to a 16-year hindcast with one exception. All extreme storms were simulated without ice coverage for the regional domain. This will produce somewhat conservative results for storms emanating from the Arctic Ocean and Chuckchi Sea and traveling in a southeasterly direction toward the DMT site. This will also allow tropical systems to proceed through the Bering Straits that might otherwise be blocked by ice in the Straits. Mean wave direction (adopting the oceanographic convention, which indicates the direction toward which waves propagate) is shown. In this convention, the approximate shore normal angle is 61 degrees.

This page left intentionally blank.



ALASKA DISTRICT  
CORPS OF ENGINEERS  
CIVIL WORKS BRANCH

ADP CURRENT METER LOCATIONS  
DELONG MOUNTAIN TERMINAL, ALASKA

Draft Feasibility Report  
Appendix A: Hydraulic Design, Delong Mountain Terminal, Alaska

**TABLE A-14. Table of Storm Extremes for DMT Station 5 see figure 28 for station 5 location.**

RANK	DATE*	H <sub>mo</sub> ft (m)	T <sub>p</sub> [s]	θ <sub>MEAN</sub> [degree]	U <sub>10</sub> knots (m/s)	θ <sub>WIND</sub> [degree]
1	70112722	29.5 (8.98)	12.87	52.	45 (23.)	50.
2	96102902	21.9 (6.68)	12.42	44.	29 (15.)	14
3	73111101	21.9 (6.68)	11.43	103.	39 (21.)	113.
4	62083019	21.3 (6.50)	11.44	109.	39 (21.)	110.
5	74111213	20.5 (6.25)	10.26	354.	47 (24.)	339.
6	96110219	16.9 (5.14)	10.43	82.	33 (17.)	57.
7	93111701	15.7 (4.79)	11.03	111.	31 (16.)	104.
8	72102622	15.6 (4.74)	10.21	49.	31 (16.)	47.
9	90110319	15.5 (4.72)	10.06	53.	31 (16.)	56.
10	91102116	14.7 (4.49)	9.45	46.	33 (17.)	28.
11	97110117	14.6 (4.46)	9.21	10.	35 (18.)	340.
12	92100608	14.5 (4.42)	9.18	349.	39 (20.)	324.
13	90111801	13.8 (4.21)	16.58	46.	23 (12.)	7
14	57071708	13.3 (4.04)	8.80	46.	29 (15.)	29.
15	63082313	12.8 (3.91)	8.73	51.	31 (16.)	40.
16	78092601	12.7 (3.88)	8.83	41.	31 (16.)	25.
17	85102223	12.7 (3.87)	9.93	116.	29 (15.)	133.
18	97100418	12.6 (3.85)	11.09	102.	27 (14.)	142.
19	96111519	12.6 (3.84)	8.38	3.	37 (19.)	331.
20	73101614	12.2 (3.73)	8.85	43.	29 (15.)	13.
21	91101214	12.2 (3.72)	8.52	17.	31 (16.)	354.
22	90111111	12.2 (3.71)	8.58	31.	31 (16.)	4.
23	96110913	12.1 (3.69)	7.91	345.	41 (21.)	309.
24	61061813	11.9 (3.62)	9.24	50.	27 (14.)	40.
25	93112107	11.7 (3.58)	8.10	358.	33 (17.)	347.
26	96072401	11.7 (3.56)	8.06	358.	33 (17.)	344.
27	83100519	11.6 (3.55)	8.56	62.	29 (15.)	64.
28	94081408	11.3 (3.44)	8.64	41.	27 (14.)	15.
29	93082007	10.6 (3.23)	7.51	348.	37 (19.)	327.
30	93100302	10.4 (3.17)	8.10	101.	27 (14.)	99.
31	88081414	10.4 (3.16)	7.96	24.	27 (14.)	10.
32	90112308	10.2 (3.12)	7.76	353.	33 (17.)	326.
33	96072601	10.1 (3.09)	7.51	357.	31 (16.)	352.
34	89102013	10.0 (3.06)	7.45	147.	31 (16.)	173.
35	85101403	10.0 (3.06)	8.40	89.	23 (12.)	79.
36	90082711	10.0 (3.05)	7.97	70.	23 (12.)	65.
37	93091419	9.94 (3.03)	7.54	8.	22 (16.)	347.
38	94100604	9.88 (3.01)	7.44	160.	33 (17.)	186.
39	92112319	9.71 (2.96)	7.09	170.	37 (19.)	194.
40	89092907	9.71 (2.96)	7.67	5.	29 (15.)	347.
41	88073114	9.68 (2.95)	8.11	47.	23 (12.)	30.
42	86092022	9.68 (2.95)	8.63	100.	25 (13.)	96.
43	89102304	9.65 (2.94)	8.50	319.	37 (19.)	288.
44	96071517	9.51 (2.90)	7.97	50.	25 (13.)	26.
45	97100913	9.45 (2.88)	7.62	107.	29 (15.)	97.
46	93110319	9.38 (2.86)	7.66	349.	31 (16.)	328.
47	90110601	9.32 (2.84)	9.39	111.	25 (13.)	139.
48	85101701	9.22 (2.81)	7.21	160.	33 (17.)	184.
49	85092113	9.22 (2.81)	7.20	66.	27 (14.)	50.
50	73080201	9.19 (2.80)	7.80	46.	25 (13.)	30.

H<sub>mo</sub> = Significant wave height  
T<sub>p</sub> = Significant wave period  
θ<sub>MEAN</sub> = Direction of wave propagation  
U<sub>10</sub> = Wind speed at 10 meter elevation  
θ<sub>WIND</sub> = Wind direction

Draft Feasibility Report  
Appendix A: Hydraulic Design, Delong Mountain Terminal, Alaska

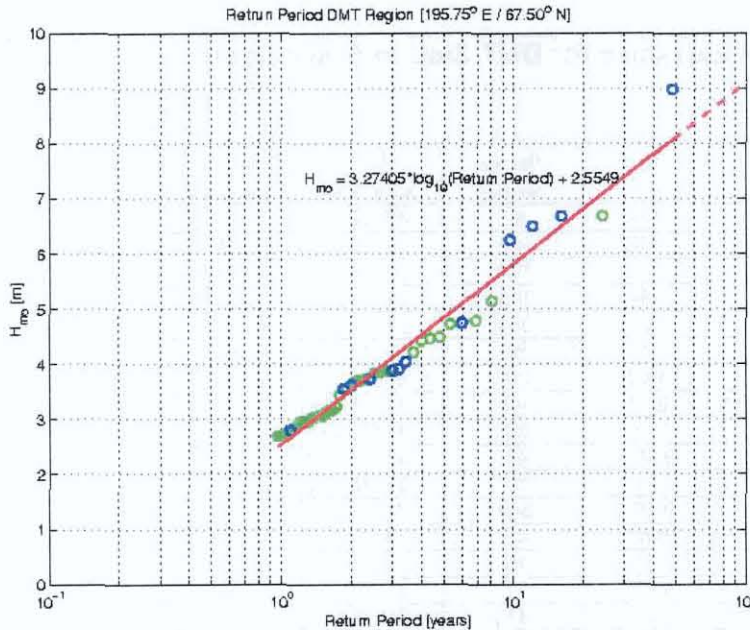


Figure 62 \*(1 m = 3.28 ft)

The storms that impact the project site are short duration storms generated by rapidly moving weather systems. The significant storms (defined as  $H_{mo} > 6.6$  feet [2 meters]) typically lasted between 24 to 48 hours. The largest storm of record in the extremal analysis occurred in November 1970 with a storm from the south. The peak wave was 29.5 feet (9 meters) with a 12 to 13-second period. A 19.7-foot (6-meter) wave from the same storm was sustained for over 14 hours and a 13-foot (4-meter) wave was sustained for over 20 hours. Examination of the least squares fit in figure 62 indicates that this storm may be an outlier, an extreme storm that occurred during the 47-year record but that may have a much longer mean return period.

The return period predicted by the extreme storm analysis is shown in table A-15. See figure 28 for the location of station 5 and figure 61 for the contour locations associated with the Snell's Law analysis. See the CHL report *Engineering Studies in Support of Delong Mountain Terminal Project* (ERDC/CHL TR-02-26) for details on the wave analysis.

TABLE A-15. Extreme Wave Height Analysis All DMT Sites					
RETURN PERIOD (yrs)	STATION 5 (h = 62 ft (19m))* ft (m)	h = 28 ft (8.5m)** ft (m)	h = 24 ft (7.3m)** ft (m)	h = 20 ft (6.1m)** ft (m)	h = 13 ft (4.0m)** ft (m)
1	8.37 (2.55)	7.55 (2.30)	7.61 (2.32)	7.74 (2.36)	7.51 (2.29)
5	15.88 (4.84)	15.16 (4.62)	13.65 (4.16)	11.71 (3.57)	7.87 (2.40)
10	19.13 (5.83)	15.98 (4.87)	13.94 (4.25)	11.81 (3.60)	7.91 (2.41)
25	23.39 (7.13)	16.11 (4.91)	14.14 (4.31)	11.94 (3.64)	7.97 (2.43)
50	26.61 (8.11)	16.40 (5.00)	14.53 (4.43)	12.20 (3.72)	8.10 (2.47)
100	29.89 (9.11)	17.52 (5.34)	15.06 (4.59)	12.57 (3.83)	8.23 (2.51)

\*WAM output point  
\*\*Snell's law analysis

## 5.7 Determination of Weather Days Based on Waves

The impact of loading delays on queuing was performed for the economic analysis and is presented in the economic appendix of this feasibility study. An analysis of weather days based on waves was performed to support the economic simulation performed for this project.

Waves greater than 3.3 feet (1 meter) are reported to cause too much motion for the barge loading operation. The termination of loading activities at the port site is based on sea and weather observations. If the seas appear to be building or weather worsening, loading may cease to wait out the conditions and see if they worsen. Weather systems move rapidly through the area, with seas quickly building and subsiding. This results in some occurrences where shipping stops and a storm never materializes.

The actual wave height that causes a shut down of loading activities is difficult to assess because waves arrive as a spectra of heights, and physical wave modifications at the dock face due to reflection can almost double the incoming wave height. Under the right conditions a clapotis or standing wave will exist as a result of the reflection. Horizontal velocities and vertical motions can become quite pronounced with very moderate approach wave heights and periods. Because of these conditions very small significant wave heights may be the cause of vessel reactions that curtail loading at the dock. The combined effects of reflections and lack of reliable criteria for observation of waves leaves doubt as to the actual wave height that closes the dock operation.

Once the barges are loaded and underway to the bulk container ships, waves up to 6.6 feet (2.0 meters) can be tolerated. At the ship, barges are able to conduct their loading operations in the lee of the ship, which provides adequate shelter and acts as a floating breakwater from the waves. It is a rare occasion when a loaded barge must go to the buoy to wait out a storm. All shipping shuts down in waves greater than 6.6 feet (2.0 meters).

The relationship between the percent occurrence of 3.3 feet (1 meter) and 1.6 feet (0.5 meter) waves in the hindcast as a basis for shut down during loading was checked against the weather days as reported by Foss Maritime, the company operating the tugs and barges. This analysis was performed to assess the potential for wave reflection being the basis for loading shut down. Table A-16 lists the percent occurrence of > 3 feet (1 meter) waves from the hindcast at the -62-foot (-18.9- meter) contour and table A-17 lists the percent occurrence of > 1.6 feet (0.5 meter) waves at the -20 foot contour. Table A-18 lists the usable shipping days (weather days subtracted) as reported by Foss Maritime and the usable days based on the hindcast weather days, defined as the percent occurrence of waves >3.3 feet (1 meter) and the percent occurrence of waves >1.6 feet (0.5 meter) at the -20 foot (-6.1 meter) contour. Percent occurrence of waves >6.6 feet (2.0 meters) is shown in table A-19.

Draft Feasibility Report  
Appendix A: Hydraulic Design, Delong Mountain Terminal, Alaska

There appears to be a better correlation between the percent occurrence of 3.3 feet waves at the -62 foot contour than the percent occurrence of 1.6 foot waves at the -20 foot contour. This leads to the belief that the shut down of loading activities at the site could be due in part to wave reflection off of the dock face.

**TABLE A-16. Percentage of time Hmo > 3.3 feet (1 meter) at the -62 foot (-19 meter) contour (Data from CHL hindcast statistics)**

Year	July	August	September	October
2000	15.2%	40.5%	24.8%	15.7%
1999	0.5%	6.3%	0.8%	3.5%
1998	3.5%	17.2%	24.7%	48.6%
1997	0.0%	9.0%	17.7%	22.3%
1996	19.2%	25.9%	26.8%	16.9%
1995	9.4%	2.9%	11.5%	6.3%
1994	0.0%	38.1%	30.6%	26.2%
1993	12.2%	12.7%	47.0%	30.2%
1992	4.0%	10.6%	14.6%	27.5%
1991	9.5%	13.0%	6.5%	40.4%
1990	11.9%	11.3%	23.7%	23.2%
1989	7.5%	9.7%	24.1%	28.3%
1988	11.1%	21.9%	20.1%	5.1%
1987	0.9%	15.8%	23.8%	27.2%
1986	8.9%	18.0%	32.3%	23.5%
1985	8.3%	12.2%	22.5%	45.6%

**Table A-17. Percentage of time Hmo > 1.6 feet (0.5 meter) at the -20 foot (-6.1 meter) contour (Data from CHL hindcast statistics)**

Year	July	August	September	October
2000	32.5%	48.9%	40.1%	43.4%
1999	0.3%	7.1%	4.4%	18.5%
1998	0.0%	24.2%	28.6%	37.2%
1997	6.2%	14.0%	14.0%	36.0%
1996	28.3%	40.1%	30.2%	19.7%
1995	35.3%	9.0%	15.0%	9.0%
1994	1.6%	50.2%	33.0%	38.7%
1993	22.4%	17.7%	63.9%	36.6%
1992	12.8%	24.6%	22.2%	36.1%
1991	16.2%	29.5%	4.4%	44.8%

Draft Feasibility Report  
Appendix A: Hydraulic Design, Delong Mountain Terminal, Alaska

**Table A-17. Percentage of time Hmo > 1.6 feet (0.5 meter) at the -20 foot (-6.1 meter) contour (Data from CHL hindcast statistics)**

Year	July	August	September	October
1990	19.7%	18.8%	36.4%	30.2%
1989	28.2%	21.5%	19.8%	39.1%
1988	30.9%	29.9%	26.2%	12.1%
1987	7.4%	22.1%	34.0%	13.4%
1986	26.0%	32.2%	53.7%	34.2%
1985	21.3%	18.5%	33.6%	39.5%

**TABLE A-18. Weather Day Comparison**

Year	Usable Days Based on Foss Report	Usable Days Based on Hmo > 3.3 ft (1 m) At 62 ft (19 m) contour	Usable Days Based on Hmo > 1.6 ft (0.5 m) At 20 ft (6.1 m) contour
	[days]	[days]	[days]
2000	67	64	55
1999	106	107	101
1998	75	80	79
1997	77	88	85
1996	62	63	55
1995	78	78	69
1994	70	66	59
1993	68	68	59
1992	66	73	64
1991	91	84	78
TOTAL	760	751	704

**TABLE A-19. Percentage of time Hmo > 6.6 ft (2 m) at the -62 foot (-19 m) contour Hmo = Significant Wave Height (Data from CHL hindcast statistics)**

Year	July	August	September	October
2000	1.1%	0%	1.8%	2.8%
1999	0%	0%	0%	0%
1998	0%	4.8%	3.5%	1.6%
1997	0%	2.5%	2.2%	8.5%
1996	10.1%	1.3%	0.6%	9.1%
1995	1.3%	0%	0%	1.7%
1994	0.0%	10.2%	3.5%	8.9%
1993	1.2%	1.7%	7.1%	3.8%

**TABLE A-19. Percentage of time Hmo > 6.6 ft (2 m) at the -62 foot (-19 m) contour  
Hmo = Significant Wave Height (Data from CHL hindcast statistics)**

Year	July	August	September	October
1992	0%	0%	4.2%	6.2%
1991	0%	0%	0%	13.3%
1990	3.8%	3.2%	0%	2.4%
1989	0%	4%	6.2%	6.3%
1988	3.8%	4.3%	3.7%	0%
1987	0%	1.5%	3.7%	2.1%
1986	0%	0.3%	9.0%	0.3%
1985	0%	3.9%	6.0%	11.7%

## 6.0 CURRENTS AND WATER LEVELS

Existing information on the currents and water level at the site was sparse. This information was needed to determine if non-storm currents and water level changes at the site are small enough in magnitude to allow for safe and efficient entry, loading, and departure of vessels at the Portsite. Information on currents and water levels at the site was also needed to determine if storm-induced currents, when coupled with waves, are of sufficient magnitude to erode, transport, and deposit unacceptable amounts of sediment into the proposed navigation channel and turning basin. Investigation of the currents consisted of a literature search for information in the area, deployment of instrumentation in 1998, 1999, and 2000, and modeling to characterize the site.

The Climactic Atlas of the Outer Continental Shelf Waters and Coastal Regions of Alaska Volume III indicates that a warm current enters the Chukchi Sea via the Bering Strait. The current concentrates near the surface and overlies dense, relic bottom water. It has a uniform velocity of 0.87 knots in the summer and 0.20 knots in the winter. Nearshore current patterns and velocities are complicated and variable because of coastal configuration, bathymetry, and winds.

### 6.1 Measured Currents

During the years 1998 to 2000, Acoustic Doppler Profilers (ADPs) were deployed by Peratrovich, Nottingham, and Drage, Inc. Engineering Consultants at the Port site to acquire data on the local current climate, including vertical structure of the current, which is captured by the ADP sensor. Details of these deployments can be found in AMEC's *Delong Mountain Harbor, Alaska Navigational Improvement Feasibility Study, Local Sponsor Facilities* Volume B4, 2002. Typically, instruments were deployed in shallower water during the open water season, and moved to deeper water before ice-cover moved in. Table A-21 lists the various deployments, and for each, the times of data collection and approximate water depth where the instrument was located. Figure 61 shows the instrument deployment locations.

<b>TABLE A-21. Prototype Current Meter Deployments</b>		
<b>Instrument</b>	<b>Depth, ft (m)</b>	<b>Deployment period</b>
ADP C47	29 (8.8)	8 April 1998 – 25 July 1998 ***
ADP C47	32 (9.8)	25 July 1998 – 30 September 1998 ***
ADP C47	42 (12.8)	5 October 1998 – 16 April 1999 ***
ADP C47	38 (11.6)	22 September 1999 – 25 June 2000 ***
ADP C55	44 (13.4)	8 April 1998 – 1 July 1998
ADP C43	65 (19.8)	18 September 1998 – 28 May 1999
ADP C43	59 (18.0)	22 September 1999 – 7 June 2000
ADP C43	34 (10.4)	31 July 2000 – 26 September 2000 ***

The CHL provided raw data analysis and constructed a composite time series by concatenating data sets acquired with the shallowest instruments (those closest to the proposed project site), where possible, but using deeper-water data to maximize the temporal data coverage. The data sets used to construct the record are indicated with asterisks in table 21.

Depth-averaged velocities, as well as averages over the upper 13 feet (4 meters) of the water column and middle and bottom thirds of the water column, were computed. These averages are illustrated in figures 63 through 66. The upper panel in these figures shows current speed in meters per second (m/sec). The lower panel shows current direction in degrees relative to true north. A direction of zero degrees indicates current flowing to the north; 180 degrees indicates current flowing to the south. The local shoreline azimuth at the study site is about 330 degrees. Therefore, currents with a direction of 330 degrees are moving along the coast to the north; currents with directions of 150 degrees are moving along the coast to the south. There seemed to be differences from deployment to deployment on the predominant northbound and southbound directions, suggesting that directional data for some of the deployment periods may be in error. But in all deployments there is about a 180-degree difference between persistent currents that primarily flow in one of two directions, presumably north and south along the coast.

The currents primarily appear to be wind generated. Fluctuations apparently associated with semi-diurnal astronomical tides are evident, particularly at low flows, but the peak magnitude of these fluctuations is only about 0.1 to 0.2 knots (0.05 to 0.1 m/sec) in terms of depth-averaged current. Wave hindcasting work suggested that the 1998-2000 period was not as energetic, in terms of wind and waves, as other years. Since currents at the project site are primarily forced by wind, it is reasonable to expect that extreme current magnitudes will be larger than those observed during 1998-2000.

For the most part, during the open water season, currents seem to flow along the coast, either northward or southward. Northward-flowing currents were found to occur approximately 70 to 75 percent of the time for the 1998-2000 data record, southbound currents occurred about 25 to 30 percent of the time. Peak currents to the north were

Draft Feasibility Report  
Appendix A: Hydraulic Design, Delong Mountain Terminal, Alaska

generally higher than peak currents flowing to the south. The highest recorded northbound current in the upper portion of the water column, where velocities tended to be greatest, was 2.3 knots (1.2 m/sec). The largest current flowing to the south, also measured in the upper part of the water column, was approximately 0.9 knots (0.45 m/sec).

Figure 63. Measured currents for July 1998  
\*(1 m/s = 1.9 knots)

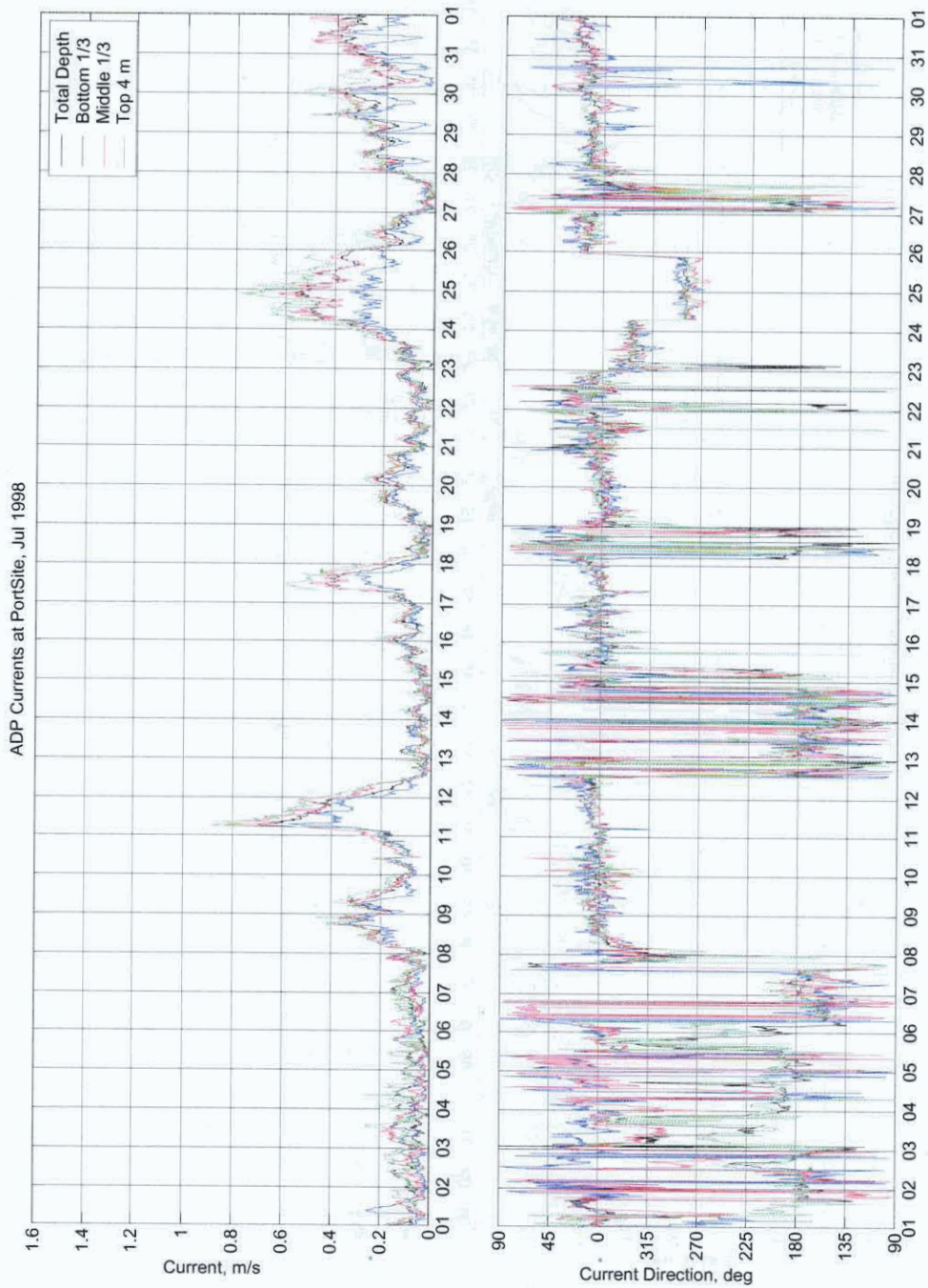


Figure 64. Measured currents for August 2000  
\*(1 m/s = 1.9 knots)

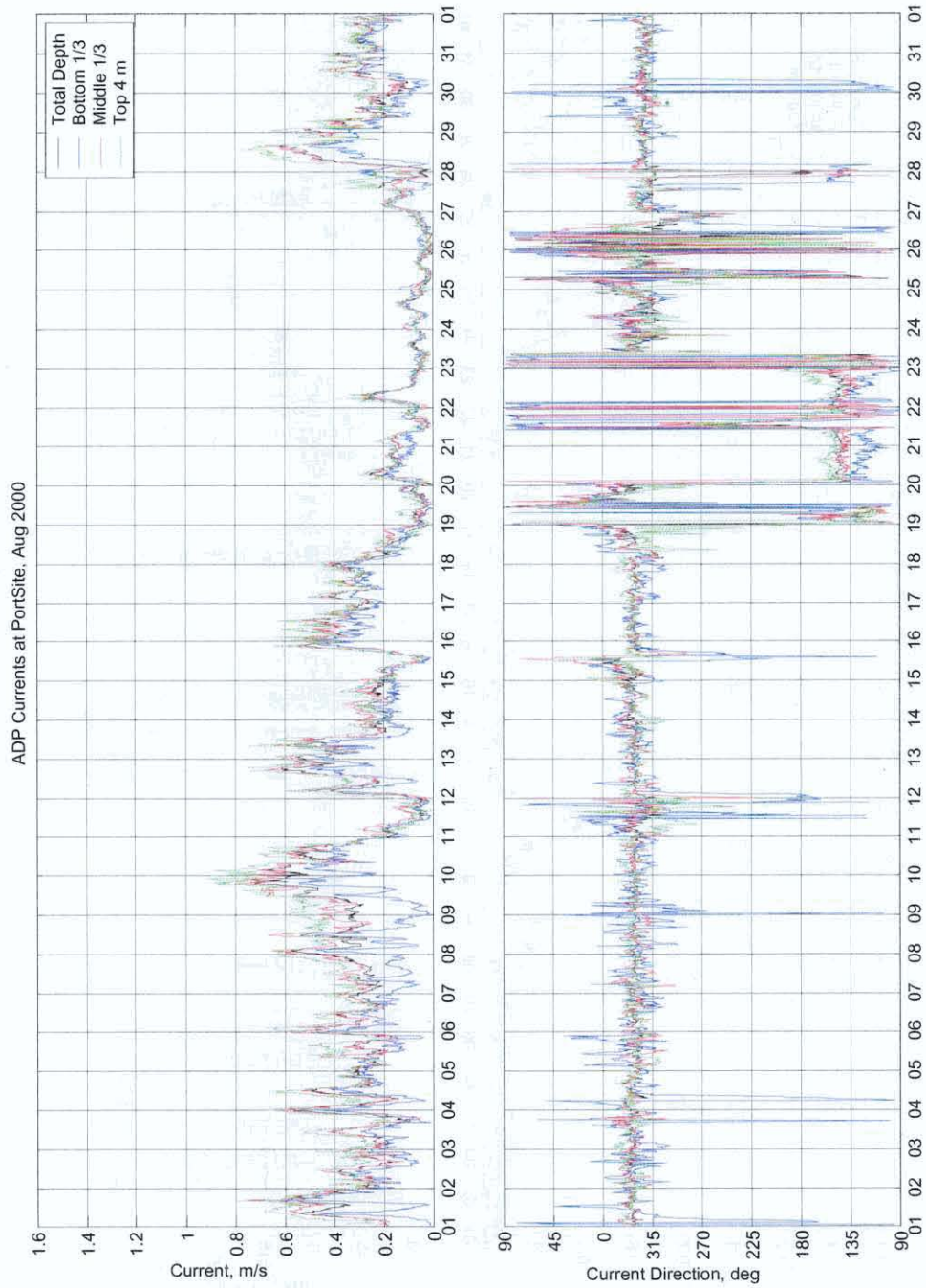


Figure 65. Measured currents for September 1998  
\*(1 m/s = 1.9 knots)

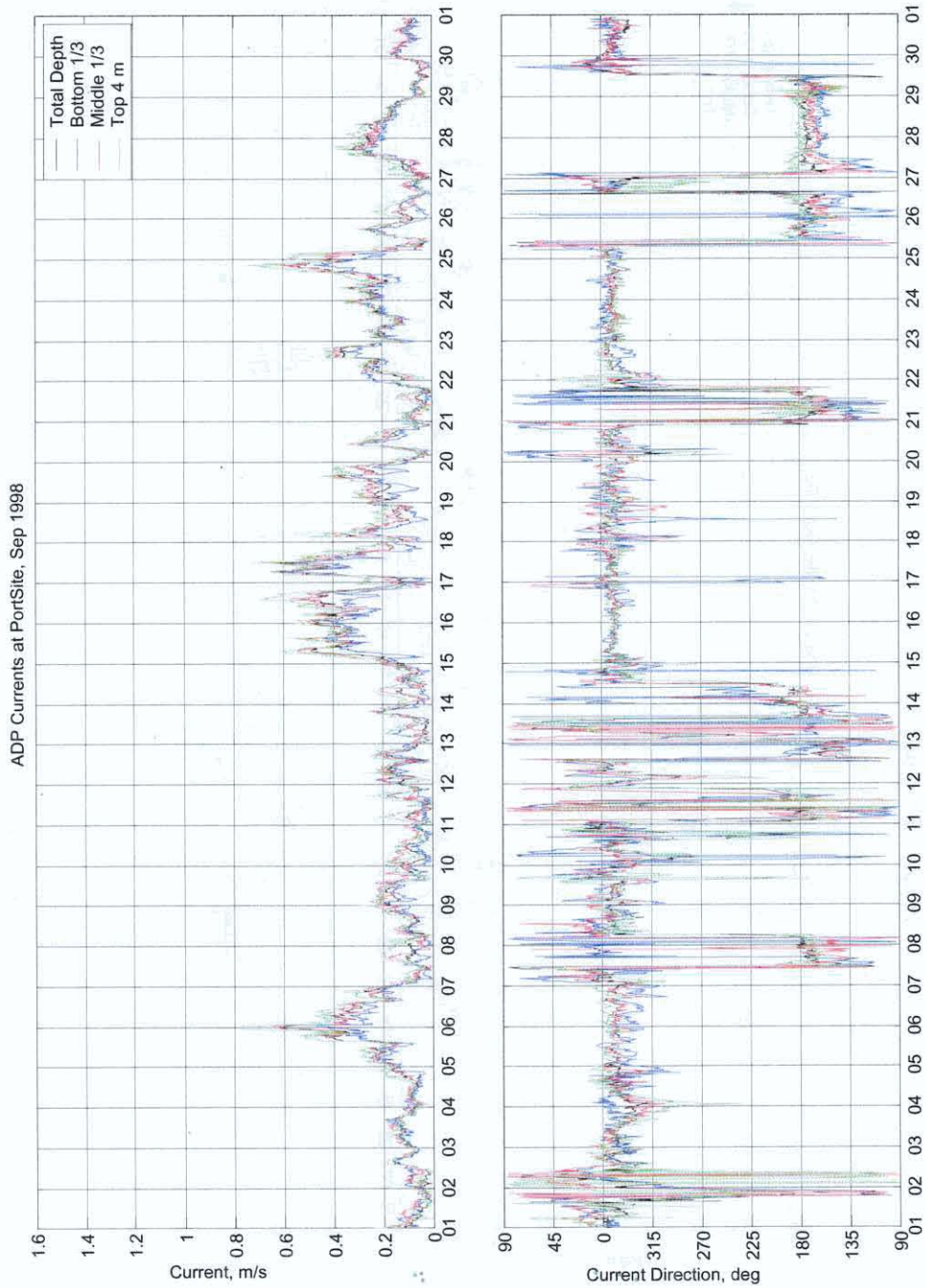
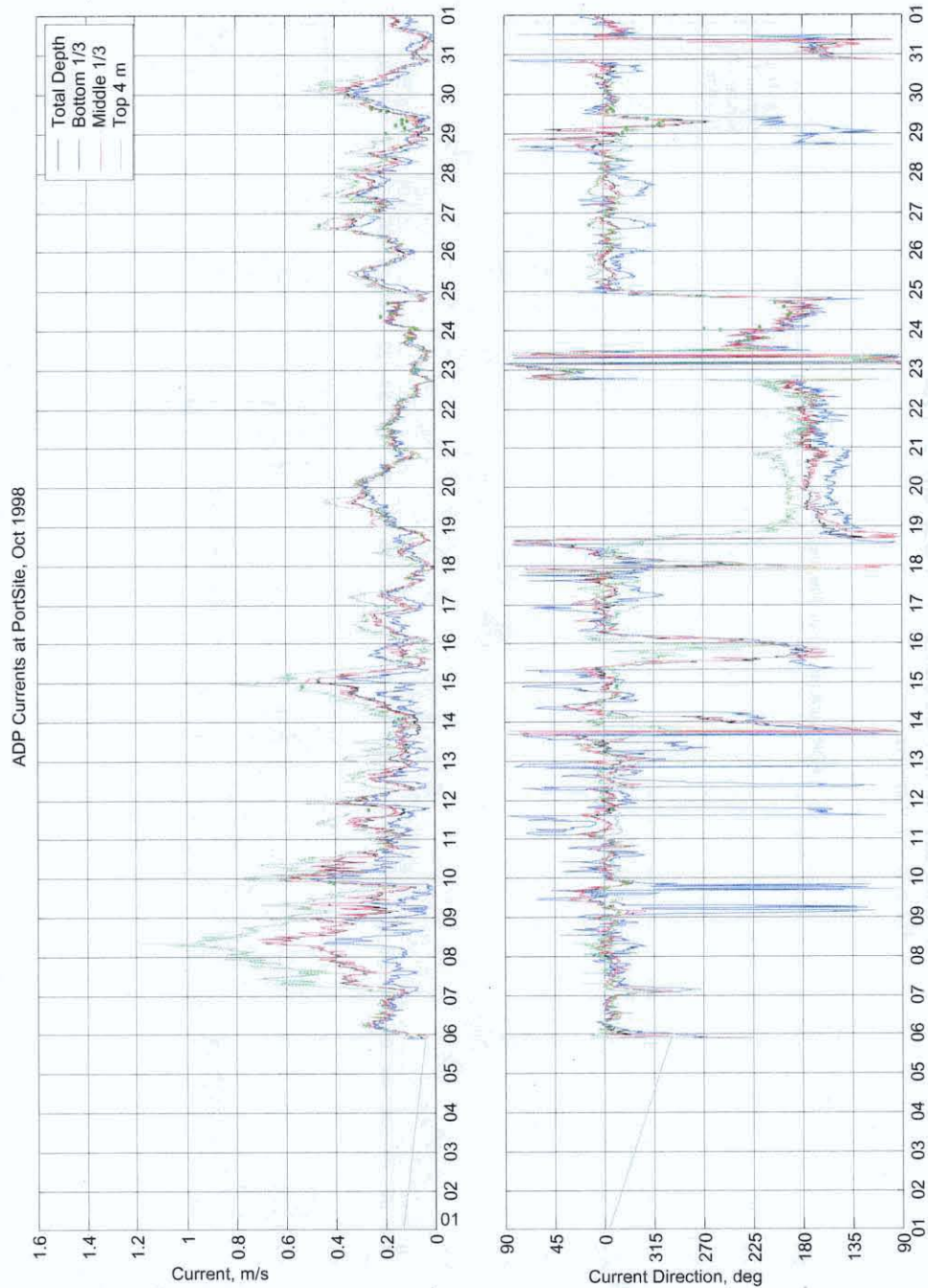


Figure 66. Measured currents for October 1998\*  
 (1 m/s = 1.9 knots)



### 6.1.1 Observations During Times of Ice Cover

In addition to current data from the open water season, current data was also collected in the middle of winter when one would expect extensive ice cover to exist. Temporal fluctuations in speed and direction were observed in the measured current speed and direction. Occasionally, high currents were measured when ice cover and low velocities were expected. It is assumed that the high currents are real, since low currents are

measured both before and after these anomalous events. It seems plausible that the currents are due to some ice-related phenomena, possibly formation of a lead in the ice in which water is being forced to flow to an open area. These flows may have significant implications on sediment transport and channel infilling. Wind-waves, which act to enhance sediment entrainment, are most likely not present during this time. These high currents are capable of moving sand.

Overall, flows were very small under the ice cover. There were a number of months in which flows were small, less than 0.2 knots (0.1 m/sec), for 90 to 100 percent of the month. As previously noted, the low flow periods were occasionally punctuated by a higher-current event.

## 6.2 Current and Water Surface Modeling

Currents and water surface for a hypothetical year and 37 storm events that had potential to move significant amounts of sediment were modeled. The water-surface elevations and currents for a hypothetical season and extreme storm events were computed by the CHL using the large-domain, long-wave hydrodynamic Advanced CIRCulation (ADCIRC) model (Luettich, Westerink, Scheffner, 1992).

The ADCIRC model is an unstructured-grid, finite-element, long-wave model developed under the U.S. Army Corps of Engineers (USACE) Dredging Research Program (DRP, Griffis et al. 1995). The model was developed as a family of two- and three-dimensional codes with the capability of:

- a. Simulating tidal circulation and storm surge propagation over large computational domains, while simultaneously providing high resolution in areas of complex shoreline and bathymetry. The targeted areas of interest include continental shelves, nearshore areas, and estuaries.
- b. Representing all pertinent physics of the three-dimensional equations of motion. These include tidal potential, Coriolis, and all nonlinear terms of the governing equations.
- c. Providing accurate and efficient computations over periods ranging from months to years.

The ADCIRC model solves its governing equations with a finite element algorithm over arbitrary bathymetry encompassed by irregular sea and shore boundaries. This algorithm allows for flexible spatial resolution over the entire computational domain and has demonstrated robust stability characteristics. The advantage of this flexibility in developing a computational grid is that larger elements can be specified in the open ocean regions where less resolution is needed, whereas smaller elements can be applied in the nearshore areas where finer resolution is required to resolve hydrodynamic details. The bathymetry and boundaries for the computational grid are shown in figure 67. The ADCIRC grid resolution near the project site is shown in figure 68 and the grid resolution

of the channel is shown in figure 69. Details on the ADCIRC modeling performed can be found in CHL report, *Engineering Studies in Support of Delong Mountain Terminal Project*, 2002, ERDC/CHL TR-02-26.

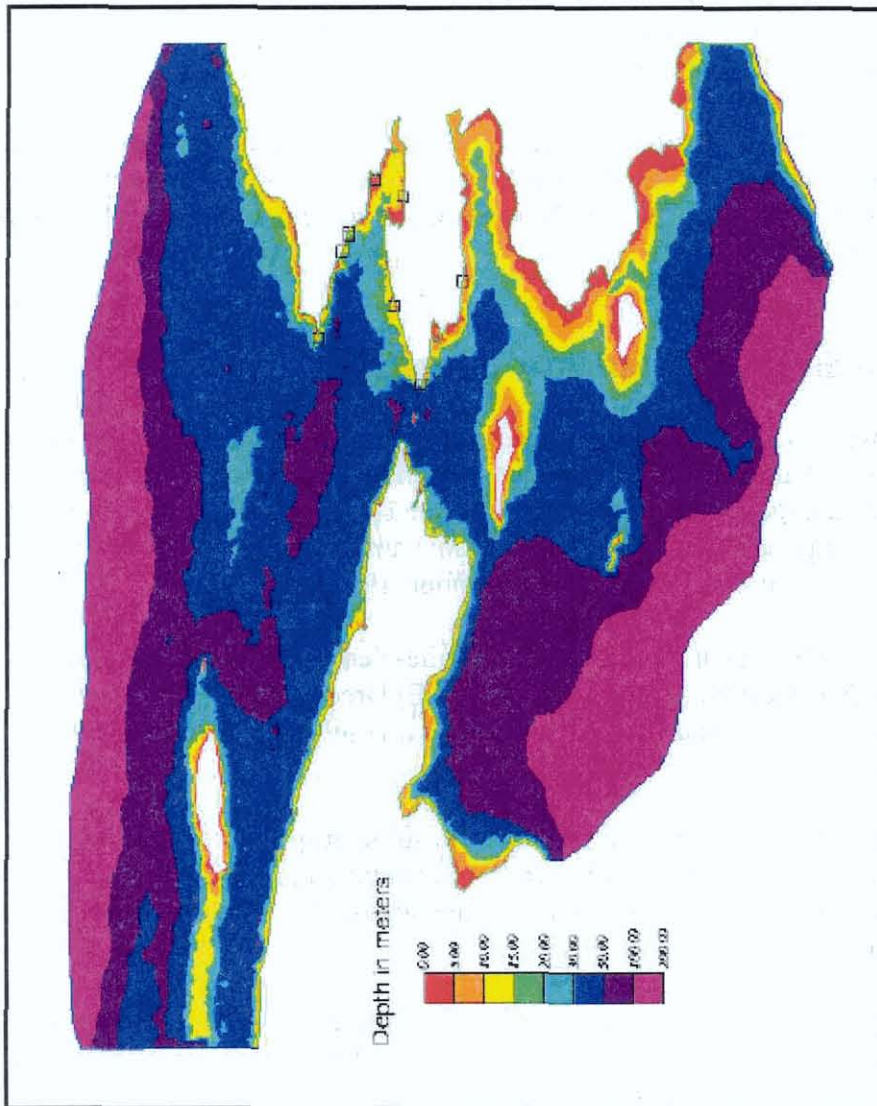


Figure 67 Bathymetry and boundaries used for the ADCIRC model

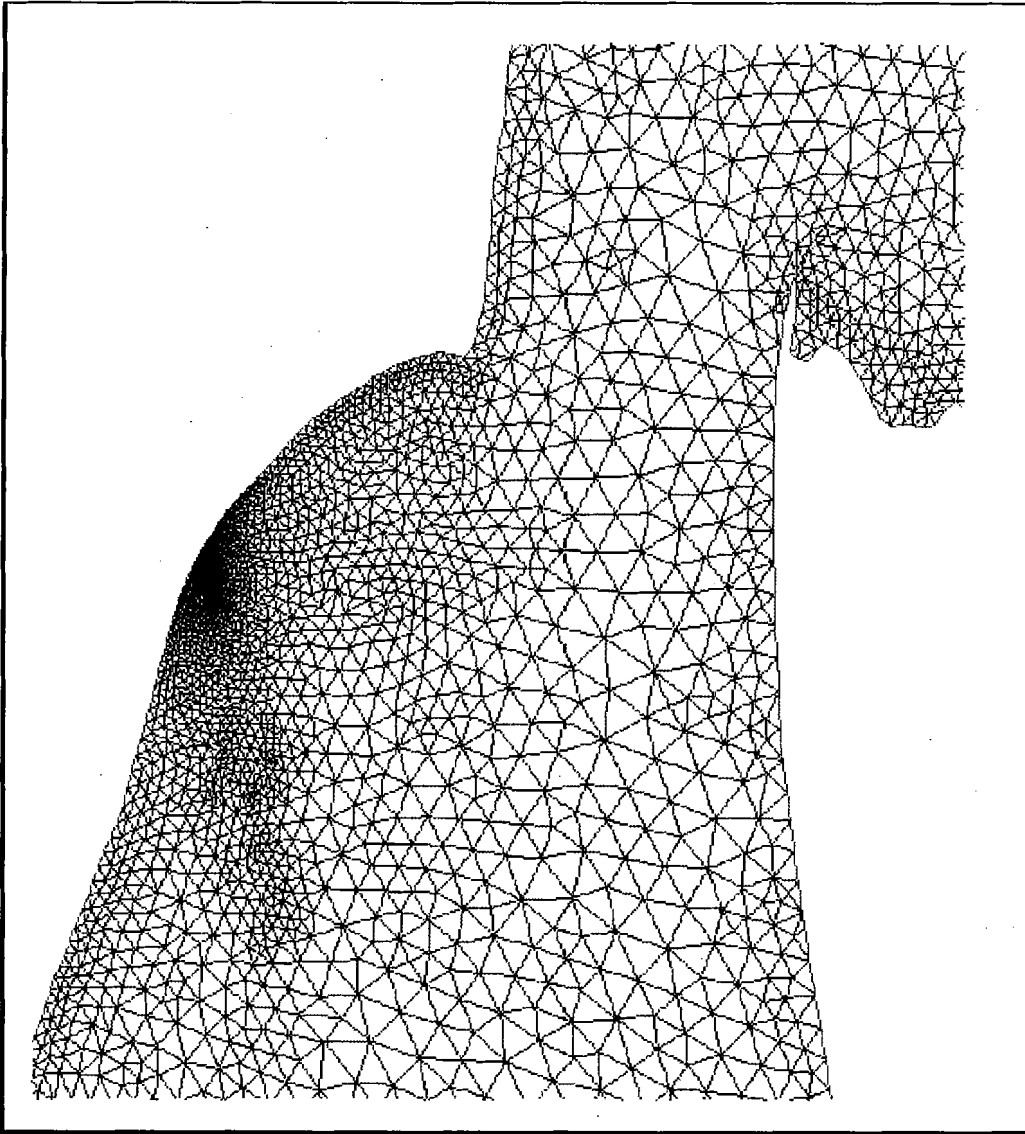


Figure 68 Grid resolution near the project site

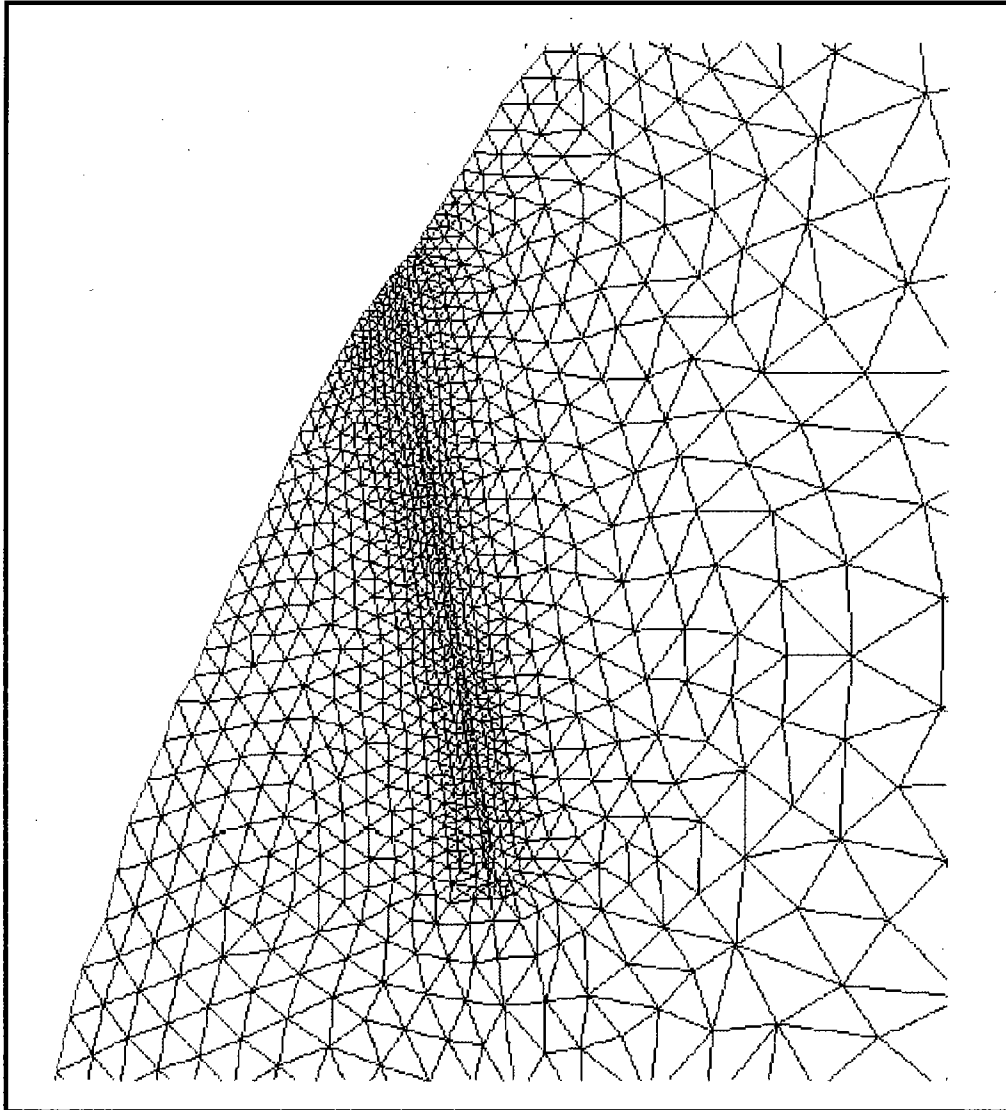


Figure 69 Grid resolution of the proposed channel.

### 6.2.1 Model Verification

Work on the water level and circulation modeling began with model verification to demonstrate that grid resolution, bathymetry, and boundary conditions are adequately described to reproduce known or observed hydrodynamic conditions.

#### *Literature Review*

A literature review identified the existence of a mean slope in the ocean surface between the Bering Sea and the Arctic Ocean that forces a long term mean south to north flow. Long term sea level differences have been reported to be on the order of 0.5 m (Stigebrandt 1984) to 1.0 m (Weingartner and Proshutinski 1998); with average flows through the Bering Strait reported to be approximately 0.8 Sv to the north (1 Sv =  $10^6$

cu m/sec), and having an annual transport cycle amplitude of 0.6 Sv. This results in an annual variability of transport rate of 0.2 to 1.4 Sv to the north with a corresponding mean current speed in the range of 0.1 to 0.5 m/sec. Although current reversals to the south occur during periods of strong wind from the north, these mean values to the north are well documented (Wilimovsky and Wolfe 1966, Stigebrandt 1984, Coachman and Aagaard 1988, and Weingartner and Proshutinski 1998).

A surface slope and corresponding mean flow to the north was incorporated in the model by imposing a surface elevation differential of 3.3 foot (1.0 meter) between the southern and northern boundaries of the computational grid (the southern boundary was raised by 3.3 foot (1.0 meter) and the northern boundary maintained at 0.0 m MSL). The mean velocity through the Bering Strait, simulated by the model in response to this static head differential, is approximately 0.5 m/sec, which is in agreement with published data. The impact to flow magnitude at the DMT in the model simulations, however, is only on the order of 0.06 m/sec.

#### *Tidal Circulation*

Tides at the DMT are shown to only have an average surface elevation amplitude of approximately 0.39 foot (0.12 meter) with a corresponding current amplitude on the order of 0.2 knots (0.10 m/sec). This contribution to the currents at the site was considered to be negligible, so a decision was made to omit tides from further consideration in the modeling. This decision was based on the fact that tidal influence at the site is small in comparison to wind effects and that databases used to specify tidal boundary conditions for the model and the harmonic analysis data used to verify model results appear to be in error. Therefore, the verification analysis concentrated on comparisons of model results to measured wind-driven circulation data.

#### *Wind Driven Circulation*

A composite time series of near shore, depth averaged currents (magnitude and direction) for 1998-2000 was compiled for this verification. The OWI wind fields were used as a surface boundary condition input into the ADCIRC model via a computed shear stress. The result of that comparison was that the model under predicted the maximum currents to the north and to the south. The results suggested that the wind stress was not great enough to accurately reproduce the observed north and south current; therefore an increase in shear stress was investigated. Shear stress is a linear function of air density. It is conceivable that commonly used wind stress formulations were not developed for the low temperature conditions and air sea temperature differences that characterize the Portsite area. The investigation resulted in the drag coefficient in the shear stress formula being increased by 50 percent.

Simulations using the OWI winds and modified drag coefficient resulted in current magnitudes that were approximately on half those measured at the site for the larger magnitude events of mid July through September. The sensitivity of the wind magnitude on the simulated currents in the study area was investigated by increasing the hindcast wind magnitudes 50 and 100 percent. Comparison of the results indicated that the increase of 50 percent produced acceptable results for currents directed to the north but that flows directed to the south were over predicted.

Reanalysis of the original simulations with the hindcast winds showed that currents directed to the south were well represented by the model, and that it was only the large magnitude events driven by winds to the north that resulted in an underestimated northerly current. This result suggests that there may be a land/water interface effect that is not accounted for in the hindcast winds. The increase in the winds directed to the north reflects an assumption that something in the wind forcing within the local generating area, or the treatment of wind forcing in the model is inaccurate. The use of the unadjusted hindcast winds directed to the south over the eastern Chukchi Sea could reflect a sheltering effect by the coastal mountain range. The selective increase in wind speeds to the north was used and results for the simulations are shown in figures 70 through 73.

The model generally reproduced measured data well with few exceptions. Measured current data indicate persistent “spikes” that are presumably forced by wind gusting. Simulations generally match trends and reproduce many of the measured peak magnitudes.

Comparisons of computed data to measured data can only be made for open water periods when currents are almost exclusively a function of wind because the ADCIRC model has no provision for ice cover. Ice cover substantially impacts the flow regime by eliminating wind forcing over portions of the domain, resulting in altered circulation patterns and possibly concentrated flows in the vicinity of breaks in the ice.

Figure 70. Hindcast (red dashed line) versus measured-DMT (solid black line) wind magnitude and direction for 1 June - 31 August 1998 \* (1 m/s = 1.9 knots)

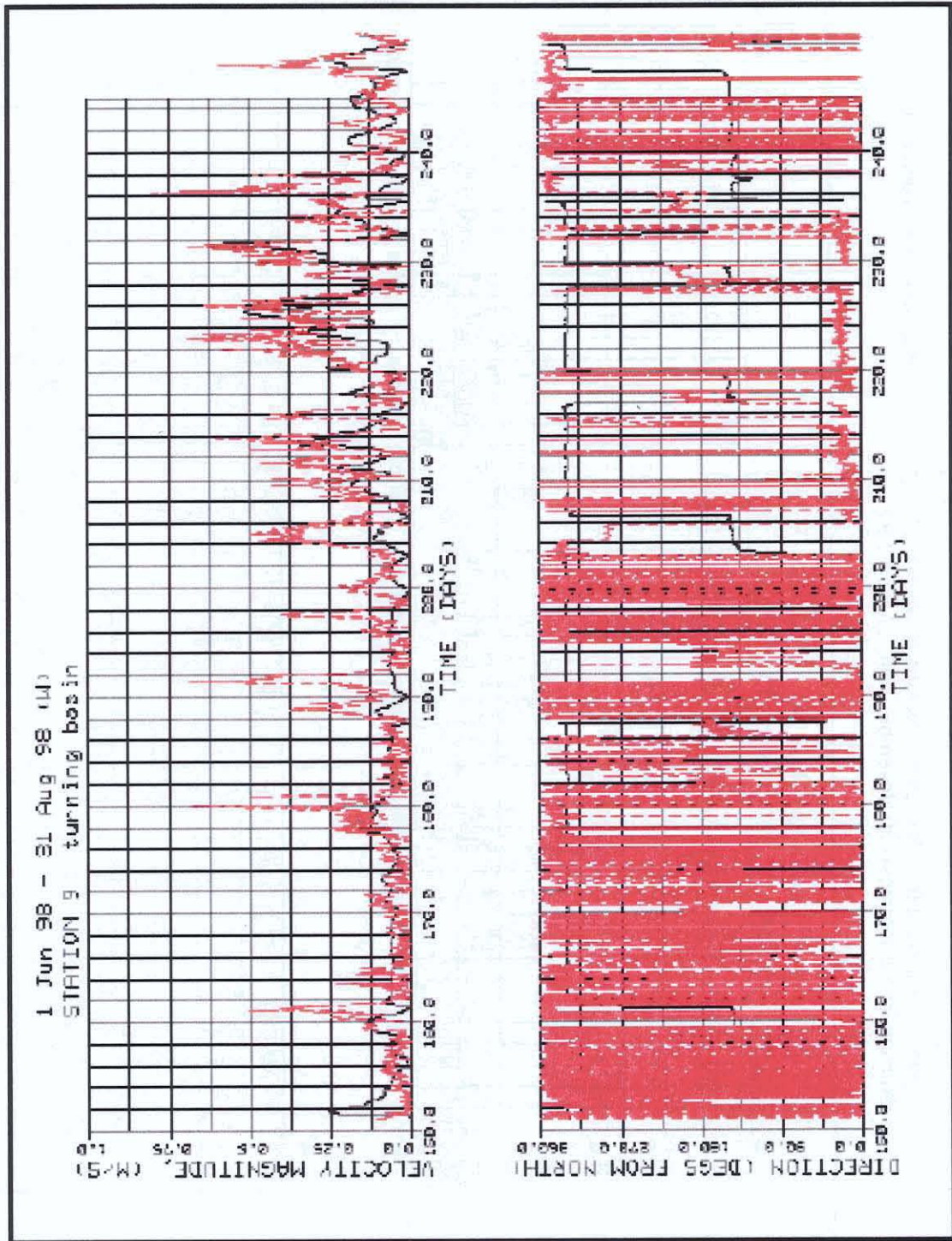


Figure 71. Hindcast (red dashed line) versus measured-DMT (solid black line) wind magnitude and direction for 1 September- 30 November 1998 ( $1 \text{ m/s} = 1.9 \text{ knots}$ )

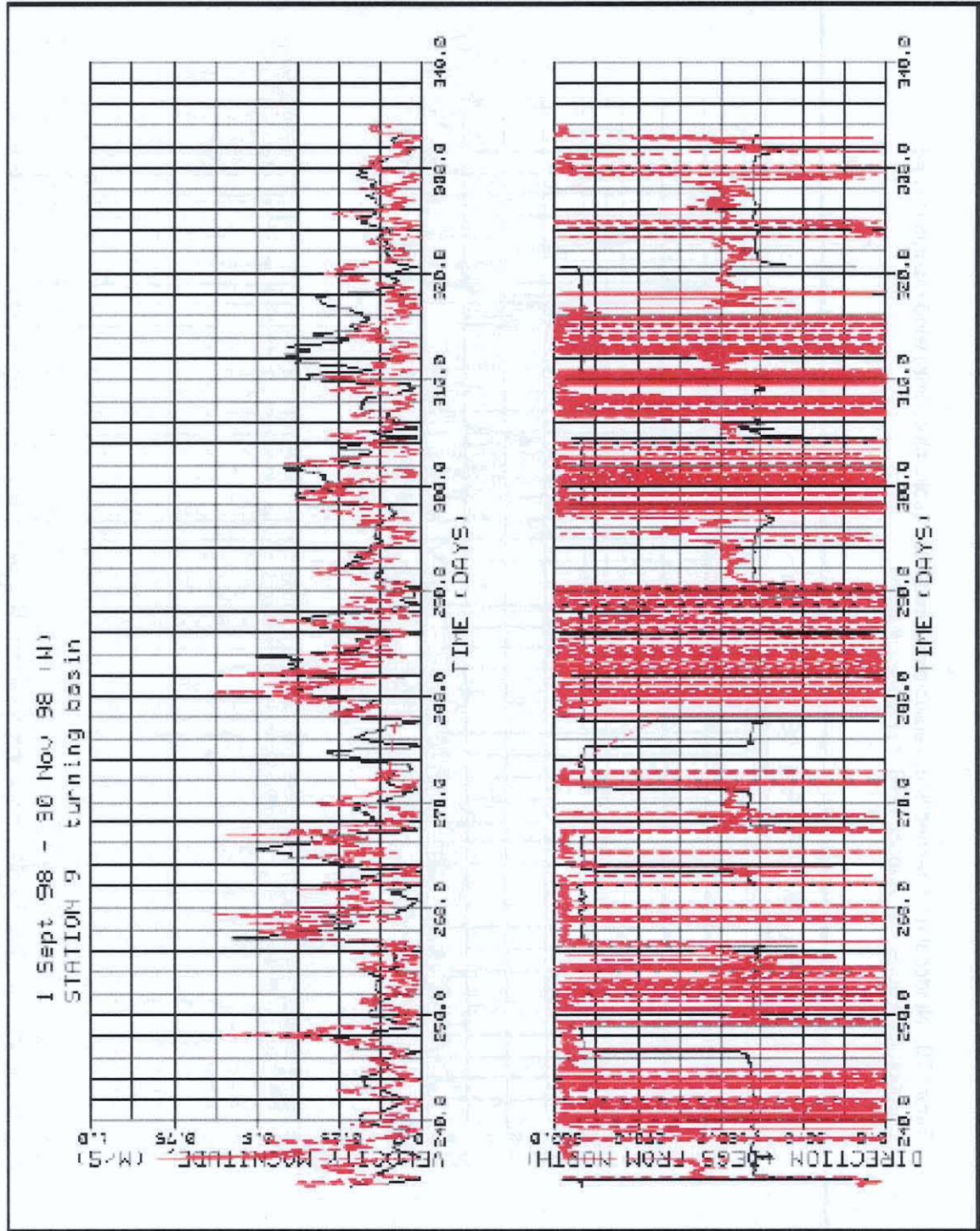


Figure 72. Hindcast (red dashed line) versus measured-DMT (solid black line) wind magnitude and direction for 22 September - 30 November 1999 ( $1 \text{ m/s} = 1.9 \text{ knots}$ )

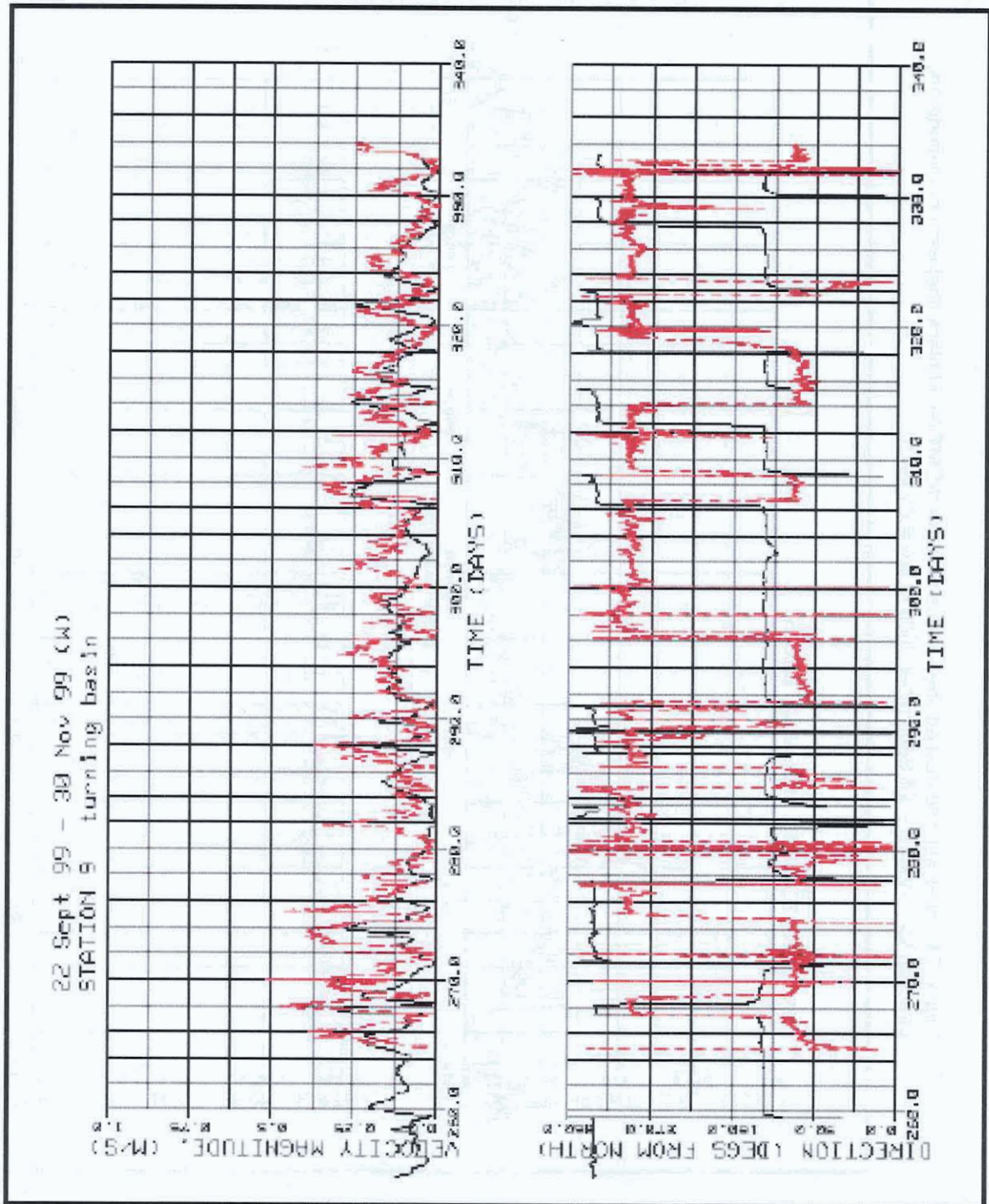
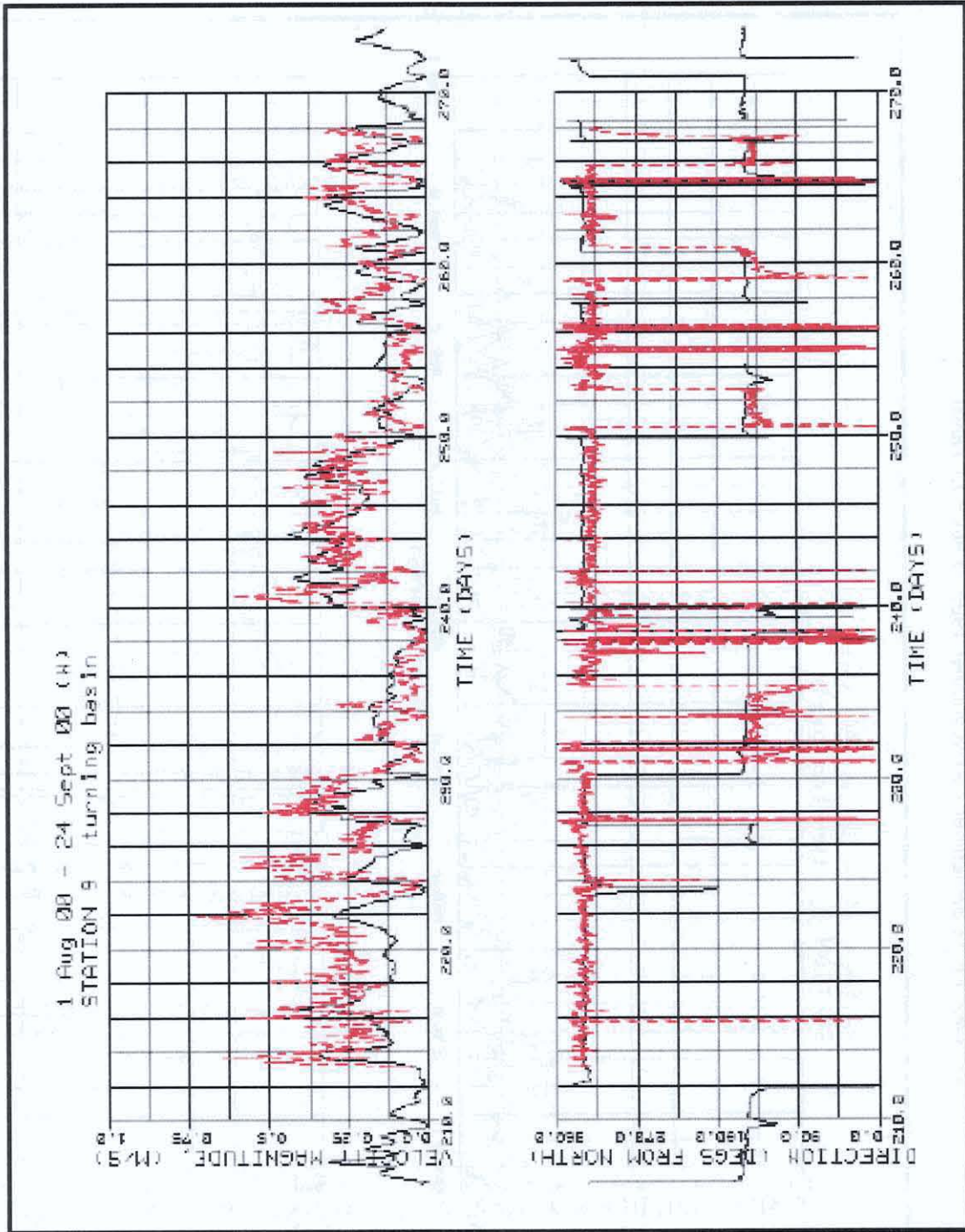


Figure 73. Hindcast (red dashed line) versus measured-DMT (solid black line) wind magnitude and direction for 1 August - 24 September 2000 ( $1 \text{ m/s} = 1.9 \text{ knots}$ )



### ***Water Surface Elevation***

Water surface elevation is an important issue regarding channel use. Negative elevation changes (set-down) resulting from offshore winds affect the minimum channel depth available to a fully loaded vessel. Water surface elevation time series for the open water years of 1998, 1999, and 2000 were computed and compared to model results. Figure 74 shows a comparison of surface elevation model results to the raw elevation data collected 7 July 1998 through 30 November 1998. The model generally reproduces measured data well.

In light of difficulties and uncertainties involved in the simulation of wind-driven circulation, a decision was made to primarily utilize measured current data to define the environmental conditions to be considered in the navigation and ship-simulator studies.

However, the ADCIRC model was used to simulate water levels and currents during the open water season, the latter for the purposes of examining potential sedimentation rates. The model was also used to simulate water level changes and currents for storm events that occurred outside the 3-year window for which current measurements were available. This information was also used in the sediment study.

## **6.3 ADCIRC Currents for Hypothetical Year**

Rather than generate a 16 year wind driven current climatology for input into the channel infilling analysis, it was deemed more feasible to select a hypothetical year based on the existing 16 year wave hindcast and available current point source measurements. The hypothetical open-water season was comprised of the following months: July 1998, August 2000, September 1998, October 1998, and November 1990. November 1990 was selected because it was a rather energetic year for storm activity. Substantial ice cover usually begins to form in November. Late fall also is the time when more severe storm events begin to occur in the region. If ice cover does not form, storm events have an increasing likelihood of producing high currents. High currents, coupled with higher waves that are also generated by these storms, increase the channel-infilling potential of fall storm events. For this reason, an energetic November, November 1990, was included.

For the first 4 months, measured current data were used to estimate currents at the site. From the perspective of sediment transport and channel infilling, bottom currents are of interest. Velocities from the bottom bin that were sensed by the ADPs were used to represent near-bottom currents for the times when measurements were available. The ADCIRC model was used to simulate currents during November 1990, using hindcast winds as input. The model only computes depth-averaged currents, so the conservative assumption was made that the currents represented bottom currents.

Southbound currents for the hypothetical year occurred approximately 29 percent of time, ranging from a low of 17 percent during July 1998 to a high of 44 percent during November 1990. For southbound currents, the maximum near-bottom current was 0.6

knots (0.3 m/sec). The mean southbound current for the entire season was 0.2 knots (0.11 m/sec).

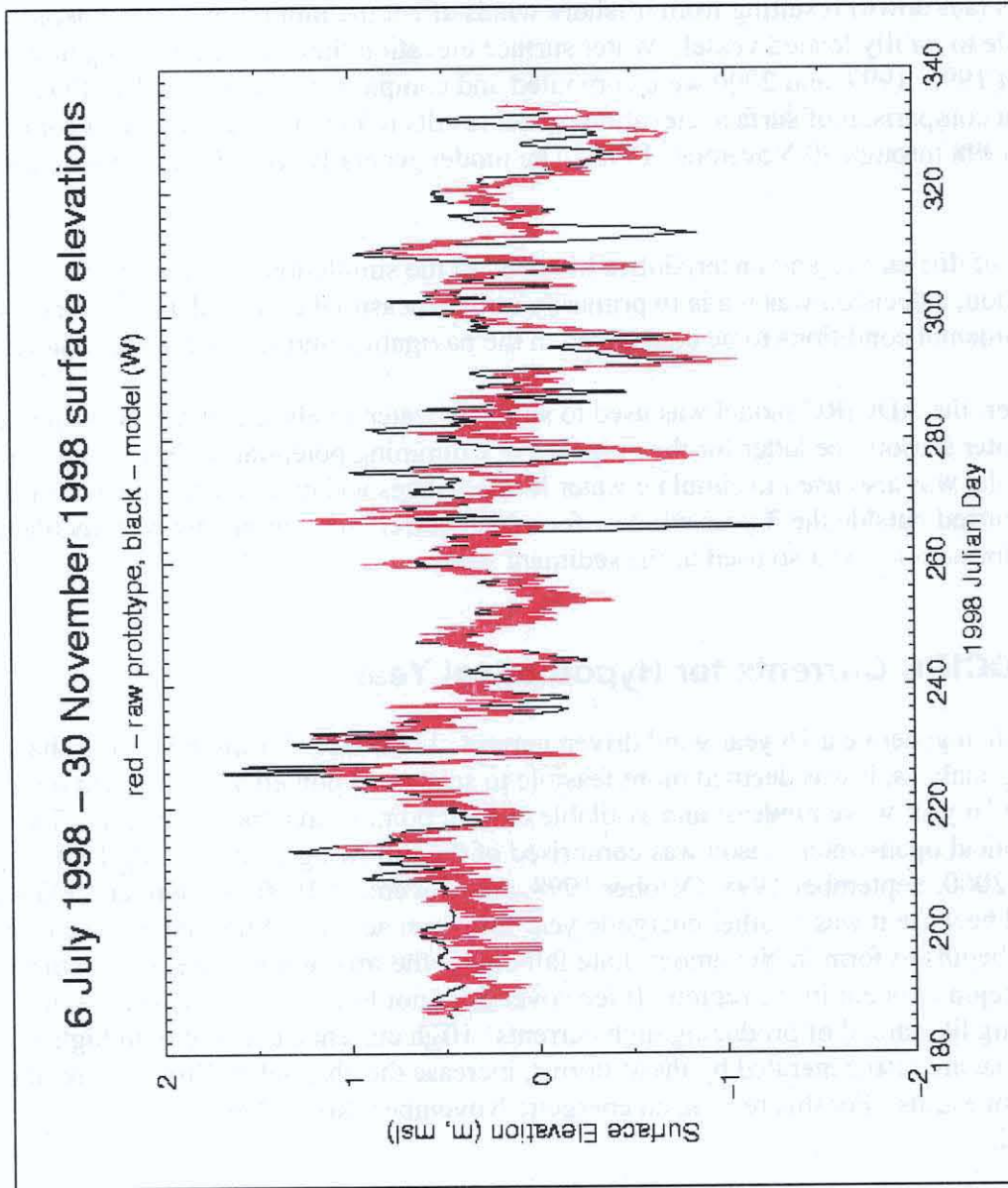


Figure 74. Model/measured water surface elevation comparison, 6 July - 30 November 1998  
\* (1 m = 3.28 ft)

Northbound currents occurred 71 percent of the time on average. The seasonal mean northbound current was 0.3 knots (0.16 m/sec), with monthly means ranging from a low of 0.2 knots (0.1 m/sec) in July 1998 to a high of 0.5 knot (0.28 m/sec) in November 1990. The maximum current was in November 1990 and was 1.3 knots (0.65 m/sec).

#### 6.4 ADCIRC Currents for Storm Events

In addition to the hypothetical open-water season simulations, storm events were modeled to provide input to the sedimentation analysis. Current hydrographs for each storm were computed and archived. Details about those storms and the associated currents are presented in Appendix 4B of the CHL report.

## 6.5 ADCIRC Water Surface Elevation

The ADCIRC model was also used to predict water surface elevation at the port site for the hypothetical season. Water level could affect the degree of loading that could be accommodated to maintain safe under-keel clearance while transiting the channel. The upper panel of figure 75 shows frequency of occurrence for water level set-down (negative water surface relative to a zero value). Water surface set-up (a positive water surface elevation relative to the same zero value) is shown in the lower panel. Substantial set-down could require light-loading of vessels; set-up would provide additional under-keel clearance. Note that these water levels, both set-up and set-down, and their frequencies of occurrence, are very dependent on the water surface differential that was imposed on the north and south boundaries of the model domain. The information presented below is based on a very limited data set. For the season as a whole, set-up occurred 60 percent of the time; set-down 40 percent of the time. Water levels during storm events were computed, but it was assumed that channel transit would not be performed during storm events.

For the times when set-down occurred, it exceeded  $-4.92$  feet ( $-1.5$  meters) less than 2 percent of the time;  $-3.28$  feet ( $-1.0$  meter) about 3 percent of the time; and  $-1.64$  feet ( $-0.5$  meter) only 14 percent of the time. For 75 percent of the time when set-down occurred, it was less than  $-1.15$  feet ( $-0.35$  meter). The maximum set-down gradually increased with each month,  $-0.98$  foot,  $-1.97$  feet,  $-2.30$  feet,  $-3.61$  feet,  $-7.55$  feet ( $-0.3$  meter,  $-0.6$  meter,  $-0.7$  meter,  $-1.1$  meters,  $-2.3$  meters) for July 1998 through November 1990, respectively. This is consistent with the trend of decreasing mean elevation that also was observed in the 1999-2000 simulations. However, the total percentage of time set-down occurred was 45 percent, 51 percent, 48 percent, 34 percent, and 23 percent for each of the months, July 1998 through November 1990, perhaps showing a slight decreasing trend.

Draft Feasibility Report  
 Appendix A: Hydraulic Design, Delong Mountain Terminal, Alaska

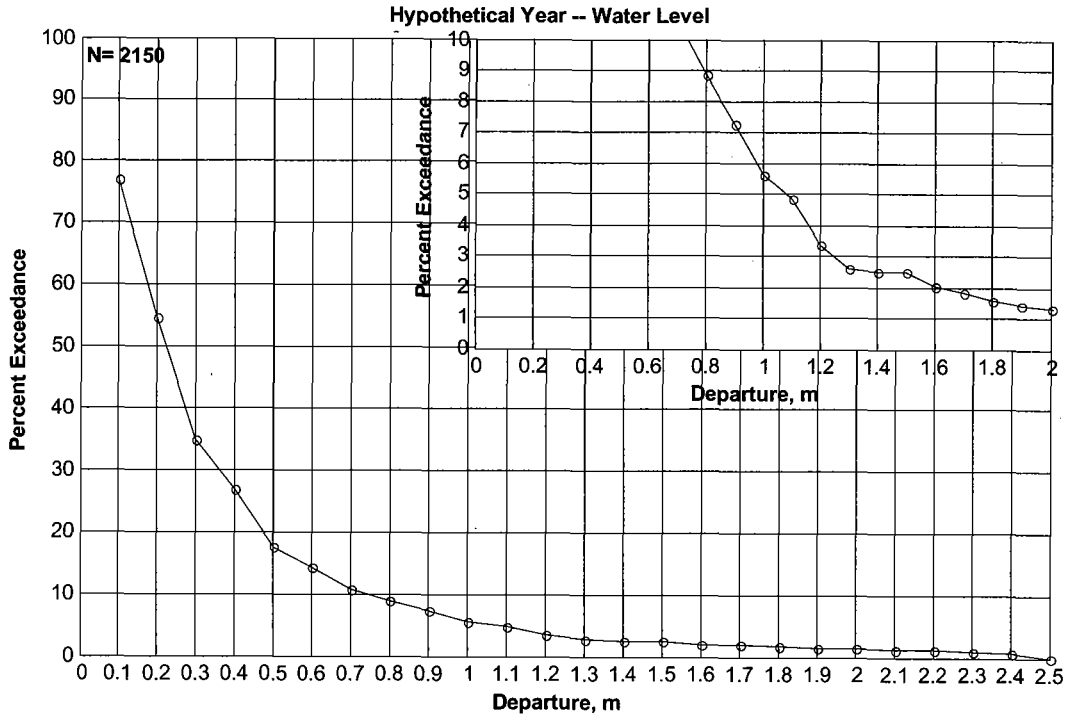
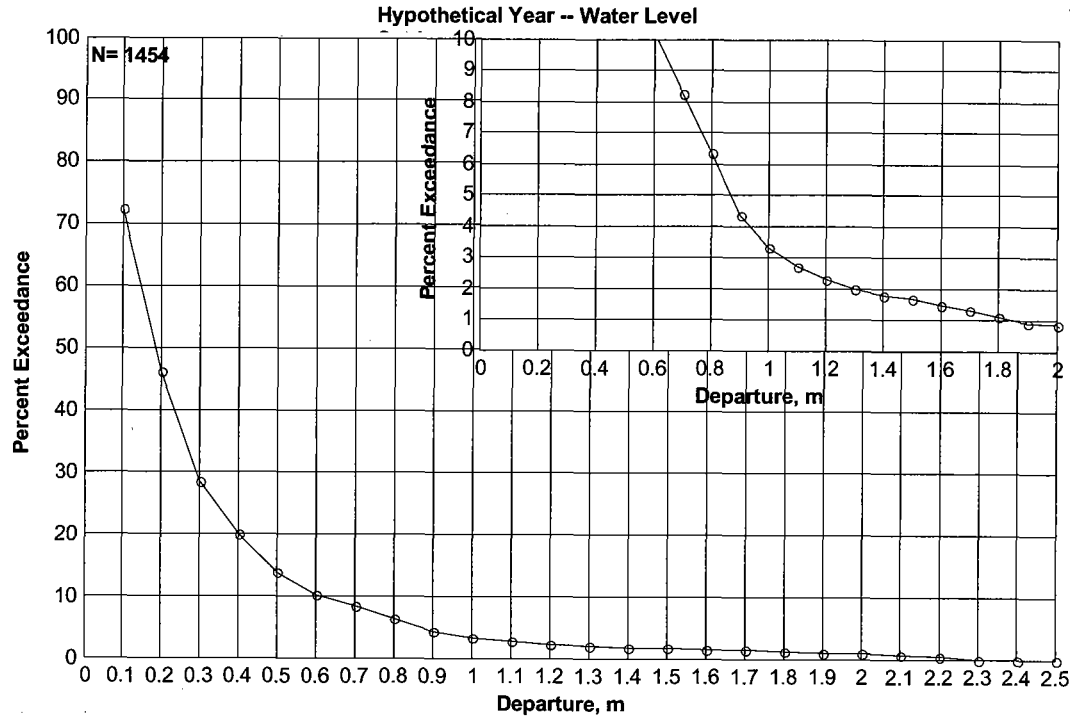


Figure 75. Frequency-of-occurrence for water level set-down and set-up – hypothetical open-water season. Upper panel shows water level set down, lower panel shows water surface set up.  
 \* (1 m = 3.28 ft)

When set-up occurred, it exceeded 4.92 feet (1.5 meters) 2.5 percent of the time; exceeded 3.28 feet (1.0 meter) 5.5 percent of the time, and exceeded 1.64 feet (0.5 meter) 17 percent of the time. For 75 percent of the time, set-up was less than 1.31 feet (0.4 meter) when it occurred. The total percentage of time set-up occurred was 55 percent, 49 percent, 52 percent, 66 percent, and 77 percent for July 1998 through November 1990, respectively. The maximum set-up was 9.19 feet (2.8 meters) in November 1990. Maximum set-up in the other months was 1.31 feet, 2.30 feet, 2.95 feet, 3.28 feet (0.4 meter, 0.7 meter, 0.9 meter, and 1.0 meter) for July 1998 through October 1998, respectively.

## 7.0 SEDIMENT MOVEMENT

The predictions of sediment transport rely heavily on the estimated environmental conditions at the site, specifically the wave hindcasting work and the simulations of circulation in the Chukchi Sea. The sediment properties along the length of the channel were determined from shallow core sampling and on-site erosion rate experiments. The combined environmental conditions and sediment property information were then used in a sediment transport model. Model-estimated channel infilling volumes were analyzed to determine the along-channel distribution of sediment infilling and the return intervals for infilling volumes. In addition to the channel infilling rates, longshore sediment transport was estimated from the 16-year wave hindcast. The estimated rates of longshore transport will assist in estimating sediment bypassing at structures that interrupt the longshore transport (such as the shallow-water dock located at the port facility).

### 7.1 Nearshore Sediment

The nearshore sediment classes at the DMT site range from fine gravel to silt. The bulk of the coarse-grained material is found from the shore face to the 34 to 39-foot (10.5 to 12.0-meter) contour. Offshore of the 39-foot (12-meter) contour, the sediment bed is predominantly composed of silt, with some fraction of gravel and sand.

### 7.2 Sediment Grain Size and Spatial Distribution

In 1998, Peratrovich, Nottingham, and Drage (PN&D) sampled surface sediments at 24 locations along a cross-shore profile inline with the proposed channel location and at three locations approximately 17,060 feet (5,200 meters) south of the proposed channel location. In July/August 2000, six shallow core samples were collected at four locations along the proposed navigation channel. The 1998 and 2000 sampling locations, summary of the sediment grain size distributions, and percentile diameters for each sample are shown in Chapter 4 of the CHL report, *Engineering Studies in Support of Delong Mountain Terminal Project, 2002*, ERDC/CHL TR-02-26 and in the Geotechnical Appendix of this Feasibility Study.

Along the proposed channel, the surface-sample data indicate sandy and gravelly sediments between 20 and 33 feet (6.1 and 10 meters) water depth, with patchy distributions of fine gravel and sand. Between a 34-foot and 39-foot (10.5-meter and 12-

meter) water depth, the sediments begin to contain a higher fraction of fines ( $d < 0.0025$  in or  $d < 0.063$  mm) and transition to a relatively uniform bed composed of silt and fine sand at approximately the 39-foot (12-meter) water depth. NW-GEO Sciences (1999) performed a side-scan sonar survey in June and September 1998 that suggests a patchy distribution of gravel, sand, and silt. The interpretation of the sonar reflectivity was ground-truthed to a limited distribution of sediment samples, and there was insufficient information from the survey to develop a quantitative model of the sediment bed.

### 7.3 Erosion Rate Data

To address the site-specific nature of the mobility of the silty sediments along the offshore portion of the proposed navigation channel, a sediment erosion study was conducted. Six shallow core samples approximately one foot in length were collected along the length of the proposed channel. One sample was collected at 35 feet (10.7 meters), two at 40 feet (12.2 meters), one at 45 feet (13.7 meters), and two at 50 feet (15.2 meters). These samples were tested during the 2000 sampling season using SEDFLUME.

SEDFLUME is a false-bottom flume that allows the determination of shear-stress/erosion relationships of minimally disturbed sediment samples. The operation and data obtained from the SEDFLUME analysis is detailed in Chapter 4 of the CHL report, *Engineering Studies in Support of Delong Mountain Terminal Project, 2002*, ERDC/CHL TR-02-26. Shear stress/erosion relationships were determined for each of the six core samples collected. Figure 76 shows the erosion rate/depth relationship developed for core CHL-40A. The inset legend shows the applied shear stresses, in Pascals. Note that the shear strength of the sediment increases with increasing depth until a depth of 6.7 inches (17 cm) is reached, then the shear strength decreases slightly. The decrease in shear strength at 6.7 inches (17 cm) corresponds with a layer of fine sediment with much higher gravel content. The stratification of field sediments commonly produces variations in shear-stress/erosion rate similar to that seen for this core. The complete SEDFLUME dataset is presented in the CHL report, *Engineering Studies in Support of Delong Mountain Terminal Project, 2002*, ERDC/CHL TR-02-26. The data obtained from the SEFLUME analysis was used to model the sediment transport at the site.

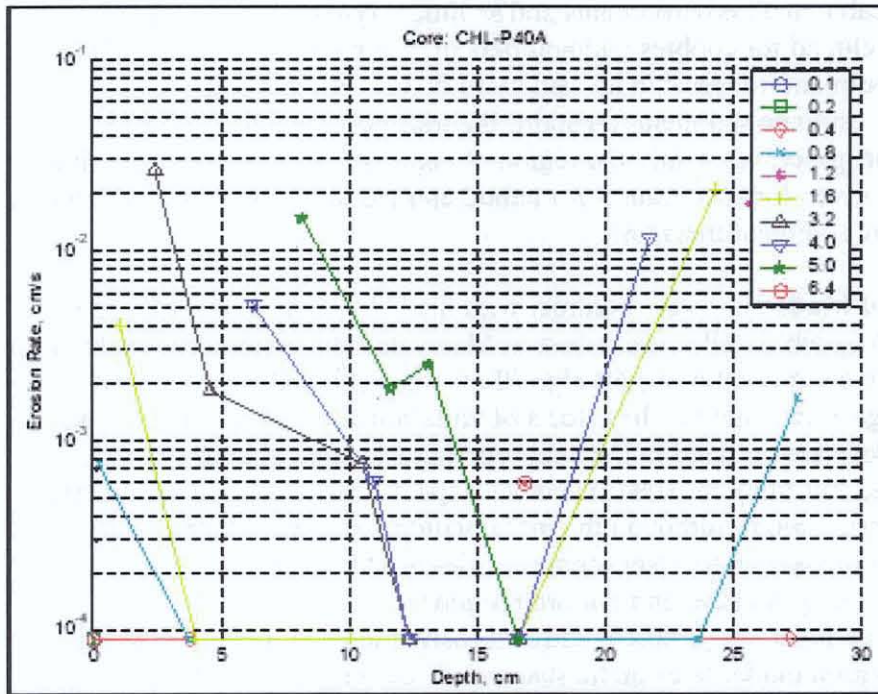


Figure 76 Erosion rate as a function of depth beneath the surface of the sediment core and bottom shear stress.

## 7.4 Sediment Transport Methods and Models

Currently, no sediment transport methods are universally applicable to all environments and sediment types. The gross sediment transport model used for the DMT analysis centered on the transport of Wilramanayake and Madsen, which was designed for sediment transport under the influence of currents and waves. The method of Van Rijn was applied for current dominated conditions, and the method of Soulsby was applied for conditions where bed load transport dominated. The longshore transport was estimated using the Damgaard and Soulsby longshore sediment transport method, which was developed for predicting the longshore transport of gravels. These are discussed in depth in the CHL report, *Engineering Studies in Support of Delong Mountain Terminal Project*, 2002, ERDC/CHL TR-02-26.

To estimate the rate of sediment infilling of the proposed navigation channel, predictive techniques must be applied with available knowledge of the environmental conditions and sediment properties. This section will describe the sediment transport methods incorporated into the sediment transport models, which produced the channel infilling estimates.

### Transport Methods

The algorithms that estimate sediment movement under specific wave and current conditions are referred to in this chapter as transport methods. Transport methods are algorithms designed to estimate the quantity of sediment movement under conditions within a specific transport regime. Presently there are no sediment transport methods that

are universally applicable to all environments and sediment types. For instance, a transport method developed for cobbles and boulders in an alpine stream is not likely to correctly represent sediment transport in an estuary or open-coast application. To correctly and reliably estimate sediment transport, the transport method must represent the important transport processes within the region of application. A general description and overview will be given for each transport method applied in the estimation of channel infilling and longshore sediment transport.

**Wikramanayake and Madsen.** Under contract with the U.S. Army Corps of Engineers, Dredging Research Program (DRP), researchers at Massachusetts Institute of Technology developed non-cohesive sediment transport algorithms for combined wave-current environment. The algorithms include the effects of variation between current and wave directions. The methods are outlined in DRP reports (Madsen and Wikramanayake, 1991; Wikramanayake and Madsen, 1994a) and were specifically designed for nearshore transport in high-energy regions, although the initial validation and calibration were performed outside the breaker zone. User input includes near-bottom orbital velocity, mean currents, bed slope, grain size, and bottom roughness.

The method uses a time-invariant turbulent eddy viscosity model and a time-varying near-bottom concentration model to estimate suspended sediment transport fluxes. A comparison to field data by Wikramanayake and Madsen (1994a) determined that the influence of time-varying bottom concentration are much more significant than the time-varying eddy viscosity. The method first calculates the bed roughness, using methods outlined by Wikramanayake and Madsen (1994b). Bed load and suspended sediment concentrations are then calculated using bottom shear stress. Estimates of vertical variation in suspended sediment concentration are based on a non-dimensional, time-varying, near-bottom reference concentration,  $C_r(t)$ . Wikramanayake and Madsen (1994a) stress that accurate prediction of reference concentration is critical to accurate transport calculations. This concentration can be estimated as:

$$C_r(t) = \frac{C_b \gamma_o (|\Psi^*(t)| - \Psi_{cr})}{\Psi_{cr}} \quad (1)$$

where  $C_b$  is the volume fraction of sediment in the bed,  $\gamma_o$  is an empirical resuspension coefficient,  $\Psi^*(t)$ , the Shield's parameter based on instantaneous, skin-friction shear stress, and  $\Psi_{cr}$ , the critical Shield's parameter. Laboratory experiments have demonstrated that  $\gamma_o$  decreases with increasing Shield's parameter based on wave skin friction shear stress. However, the data were insufficient to develop empirical methods to relate the resuspension coefficient to Shield's parameter. Therefore constant values of  $\gamma_o$  are applied for rippled and flat beds respectively. The Shield's parameters are defined by:

$$\Psi^*(t) = \frac{u^*(t)^2}{(s-1)gd_{50}} \quad (2)$$

$$\Psi_{cr} = \alpha_l \tan(\phi) \quad (3)$$

where  $u^*(t)$  is the bed shear velocity,  $\alpha_l$  is a coefficient dependent on the local Reynolds number,  $s$  is the specific gravity of sediment,  $d_{50}$  is the median grain diameter,  $g$  is gravitational acceleration, and  $\phi$  is the angle of repose of the sediment grains. The reference concentration is used to estimate vertically varying concentrations in the water

column due to steady and oscillatory currents. The estimated suspended sediment concentration is coupled with the vertically varying velocities to estimate the total suspended sediment flux.

The Wikramanayake and Madsen model includes a method for estimating the instantaneous bed-load flux based on the Meyer-Peter and Müller (1948) formula. This instantaneous bed-load flux,  $Q_b$  (cm<sup>3</sup>/cm·s), is estimated by:

$$\bar{Q}_b(t) = \frac{d_{50} \sqrt{(s-1)gd_{50}}}{2\pi} \frac{\delta(|\Psi^*(t)| - \Psi_{cr})}{1 + \tan \beta_L \frac{\cos(\Phi_t - \Phi_{sw})}{\tan \Phi_f}} \bar{\tau}_b(t) \quad (4)$$

where  $\beta_L = h/6\delta$ ,  $h$  is the water depth,  $\delta$  is the boundary layer length scale,  $\Phi_t$  is the angle between the current and the wave direction,  $\Phi_{sw}$  is the angle between the wave direction and bottom slope, and  $\bar{\tau}_b(t)$  is the instantaneous skin friction shear stress.

The wave-current model was originally developed for a single sinusoidal wave component. The method is extended to represent irregular waves by linearly superimposing two or more sinusoidal waves. Other than a constant in the bed-load calculation (incorporated into  $\alpha_f$  in Equation 3) and the resuspension coefficient, the model is completely deterministic. Available data, most of it from the laboratory, were used to estimate the bed-load concentration constants for both rippled and flat beds. Finally, the velocity profile, suspended sediment concentration profile, and bed-load calculations are used to estimate total transport.

Wikramanayake and Madsen (1994a) performed several tests to compare their results to field measurements in wave/current environments. Specifically, two data sets were used for sediment concentration profile verification: Vincent and Green (1990) measured at Holkham, UK, and another by Vincent and Osborne (unpublished) measured at Cornwall, UK. Additional laboratory data sets were used for verification of the bed roughness model and determination of  $\gamma_0$ . The results of these tests indicated that the model accurately predicted the mean (or current-related) and wave-related fluxes and their distributions in the water column. No verification was performed for the bed-load model estimates.

Field verification of the transport method has been performed against data sets from the Columbia River mouth, (Washington/Oregon) and in the surf zone at the Field Research Facility, Duck, North Carolina (Gailani, Smith, and Raad, in review) with favorable comparisons to field data. However, the Wikramanayake and Madsen transport method is unsuitable for conditions in which sediment suspension and/or wave-induced shear stresses are small, therefore other methods of approximating sediment transport were applied under conditions in which the transport was bedload-dominated or current-dominated.

**Soulsby bedload transport method.** Soulsby (1997) developed a formula for combined wave-current bedload by integrating the current-only bedload formula of Nielsen (1992) over a single sinusoidal wave cycle. The formula is expressed as follows:

$$\Phi_{x1} = 12\theta_m^{1/2}(\theta_m - \theta_{cr}) \quad (5a)$$

$$\Phi_{x2} = 12(0.95 + 0.19\cos 2\phi)\theta_w^{1/2}\theta_m \quad (5b)$$

$$\Phi_x = \text{maximum of } \Phi_{x1} \text{ and } \Phi_{x2} \quad (5c)$$

$$q_{bx} = \Phi_x \left[ g(s-1)d_{50}^3 \right]^{1/2} \quad (5d)$$

subject to  $\Phi_x = 0$  if  $\theta_{cr} \geq \theta_{max}$

where

$q_b$  = mean volumetric bedload transport rate per unit width

$\theta_m$  = mean Shield's parameter over a wave cycle

$\theta_w$  = amplitude of oscillatory component of  $\theta$  due to wave

$\theta_{max}$  = maximum Shield's parameter from combined wave-current stresses

$\theta_{cr}$  = critical Shield's parameter for initiation of motion

$\phi$  = angle between current direction and direction of wave travel

The Soulsby combined wave-current bedload transport method was applied when sediment suspension was estimated to be near zero.

**Van Rijn current-dominated transport method.** The Van Rijn (1984) current-only total transport method was parameterized from Van Rijn's comprehensive theory of sediment transport in rivers. Although the method was developed for sediment transport in the riverine environment, the method may also be appropriately applied in the marine environment under conditions for which waves contribute little to the bottom shear stress. The simpler, parameterized formulae presented here approximate the full theory within  $\pm 25$  percent and were developed for water depths between 1-20 m, velocities between 0.5 and 5 m/s,  $d_{50}$  between 0.1 and 2 mm, and for fresh water at 15 deg C. The resulting parameterized method estimates transport by the following simpler formulation:

$$q_t = q_b + q_s \quad (6)$$

$$q_b = 0.005 \bar{U} h \left\{ \frac{\bar{U} - \bar{U}_{cr}}{[(s-1)gd_{50}]^{1/2}} \right\}^{2.4} \left( \frac{d_{50}}{h} \right)^{1.2} \quad (7)$$

$$q_s = 0.012 \bar{U} h \left\{ \frac{\bar{U} - \bar{U}_{cr}}{[(s-1)gd_{50}]^{1/2}} \right\}^{2.4} \left( \frac{d_{50}}{h} \right) (D_*)^{-0.6} \quad (8)$$

where,

$$\bar{U}_{cr} = 0.19(d_{50})^{0.1} \log_{10} \left( \frac{4h}{d_{90}} \right) \left\{ \begin{array}{l} 0.1 \leq d_{50} \leq 0.5 \text{ mm} \end{array} \right.$$

$$\bar{U}_{cr} = 8.50(d_{50})^{0.6} \log_{10} \left( \frac{4h}{d_{90}} \right) \left\{ \begin{array}{l} 0.5 \leq d_{50} \leq 2.0 \text{ mm} \end{array} \right.$$

$$D_* = \left[ \frac{g(s-1)}{\nu^2} \right]^{1/3} d_{50}$$

$q_b$  = bedload transport

$q_s$  = suspended transport

$\bar{U}$  = depth-averaged current

$h$  = water depth

$g$  = gravitational acceleration

$s$  = specific gravity of sediment  
 $d_{90}$  = sediment diameter for which 90 percent is finer by weight  
 SI units are required for the Van Rijn current-dominated transport method.

**Damgaard and Soulsby longshore sediment transport method.** One of the most widely applied models of longshore sediment transport is the CERC equation, introduced in the *Shore Protection Manual* (CERC, 1984). The CERC formula is based on the premise that longshore transport is related to the longshore flux of wave energy. The CERC formula was calibrated to longshore transport data from primarily sandy coasts, where much of the longshore transport occurs in suspension. For a gravel and coarse sand beach, such as the beaches found at the DMT site, most of the longshore transport is expected to occur as bedload. Damgaard and Soulsby(1997) show that the CERC formula overpredicts longshore transport of shingle and gravel by a factor of 20, therefore a longshore transport model developed for predicting the transport of gravels was selected for this study.

Damgaard and Soulsby (1997) derived a physics-based formula for longshore sediment transport occurring as bedload. The basis of the formula was Soulsby's bedload formula (described above), and the parameterized model was developed with a number of simplifying assumptions made regarding the hydrodynamics of the surf zone. The resulting, analytical model was calibrated to measurements of longshore transport at Seaford Beach, UK. The model was subsequently verified to laboratory data and field data from Brighton, UK, indicating that most model predictions of longshore transport are within a factor 2 of the measured values. The formulation for the longshore transport method is as follows:

$Q_{LS}$  = maximum of  $Q_{LS1}$  and  $Q_{LS2}$

$$Q_{LS1} = \frac{0.19(g \tan \beta)^{1/2} (\sin 2\alpha_b)^{3/2} H_b^{5/2} (1 - \hat{\theta}_{cr})}{12(s-1)}, \text{ for } \hat{\theta}_{cr} < 1 \quad (9a)$$

$$Q_{LS1} = 0 \text{ for } \hat{\theta}_{cr} \geq 1 \quad (9b)$$

$$Q_{LS2} = \frac{0.24 f(\alpha_b) g^{3/8} d_{50}^{1/4} H_b^{19/8}}{12(s-1)T^{1/4}}, \text{ for } \theta_{wr} \geq \theta_{wsf} \quad (10a)$$

$$Q_{LS2} = \frac{0.046 f(\alpha_b) g^{2/5} H_b^{13/5}}{12(s-1)^{6/5} (\pi T)^{1/5}}, \text{ for } \theta_{wr} < \theta_{wsf} \quad (10b)$$

$$Q_{LS2} = 0 \text{ for } \theta_{max} \leq \theta_{cr} \quad (10c)$$

where,

$$\hat{\theta}_{cr} = \frac{16.7\theta_{cr}(s-1)d_{50}}{H_b(\sin 2\alpha_b)(\tan \beta)}$$

$$f(\alpha_b) = (0.95 - 0.19 \cos 2\alpha_b)(\sin 2\alpha_b)$$

$$\theta_{wr} = \frac{0.15H_b^{3/4}}{(s-1)g^{1/4}(Td_{50})^{1/2}}$$

$$\theta_{wsf} = \frac{0.0040H_b^{6/5}}{(s-1)^{7/5} g^{1/5} T^{2/5} d_{50}}$$

$\theta_w$  = maximum of  $\theta_{wr}$  and  $\theta_{wsf}$

$$\theta_m = \frac{0.1H_b(\sin 2\alpha_b)(\tan \beta)}{(s-1)d_{50}}$$

$$\theta_{max} = [(\theta_m + \theta_w \sin \alpha_b)^2 + (\theta_w \cos \alpha_b)^2]^{1/2}$$

$\theta_{cr}$  = threshold Shields parameter

$H_b$  = wave height at breaking

$\alpha_b$  = wave angle at breaking

$T$  = wave period

$\beta$  = beach slope

A wave transformation process described in the modeling section defined wave conditions at the breaking point.

## 7.5 Channel Infilling Assumptions, and Representations

To numerically estimate sediment transport, certain simplifying assumptions and representations of the natural processes must be developed. Making such approximations is not unique to sediment transport models, but is a common practice in the field of numerical modeling. The following discussion of the approximations developed for estimating channel infilling rates will be limited to general statements and descriptions of the approximations applied.

### 7.5.1 Representation of Bed Material

The bottom sediments at the DMT site can be generally classified into two types, cohesive and non-cohesive. The cohesive bed material has erosion resistance greater than the simple self-weight of larger, non-cohesive sediments.

Non-cohesive sediments (sand and gravel) typically exist on the sediment bed with a range of sediment particle sizes existing at one location. Analysis of bed samples collected along the length of the proposed channel defined the distribution of sediment grain sizes at each sample location. The appropriate representative particle diameters for each transport method were determined from grain-size distributions.

The availability of sediment to transport is also a key factor in estimating the sediment transport. Each of the transport methods employed assumes that an unlimited supply of sediment is available for transport. The transport model accounts for limits in sediment availability by reducing transport when the estimated thickness of the active sediment layer is less than the available non-cohesive sediment thickness.

The erosion resistance of cohesive bed material was approximated by the relationships developed from the SEDFLUME experiments. When the thickness of the overlying non-cohesive sediment layer is less than the estimated active depth of sediment transport, shear stresses are applied to the underlying cohesive sediment layer. When the bottom

shear stress on the cohesive layer is greater than the critical shear stress for erosion, the cohesive sediment layer will erode according to the relationships developed from the analysis of the SEDFLUME data. Cohesive bed information between the four sampling locations transitioned relatively smoothly between the four sampling locations, and erosion rate information was interpolated for modeling between the four sampling locations.

Visual inspection and grain-size analysis of samples extracted from the SEDFLUME experiments indicate that there is a significant amount of sand and occasionally gravel contained in the cohesive bed material. As the cohesive material erodes under high-energy conditions, this non-cohesive material will be released to the sediment bed, while the silt fraction will be suspended into the water column. The sand and gravel fractions released from the underlying cohesive bed were incorporated into the active non-cohesive bed layer by the model and made available for transport.

All transport methods assume that the bed conditions are locally uniform. Duplicate surface samples from the 1998 and 2000 surface and core sampling indicate that this assumption is appropriate. Furthermore, the transport model assumes that there is a uniform and unlimited supply of sediment existing both north and south of the proposed navigation channel.

### **7.5.2 Application of Environmental Conditions.**

Localized wave and current conditions were estimated from the wave hindcast and the ADCIRC circulation modeling. The wave hindcast supplied wave conditions offshore of the proposed channel in a water depth of approximately 62 feet (19 meters). The offshore wave conditions were transformed in shore using Snell's Law.

Circulation modeling provided estimates of depth-averaged current at a depth of 32.8 feet (10 meters) adjacent to the proposed navigation channel. The depth-averaged current was assumed to be uniform along the length of the proposed channel and was reduced with a mass-conservation expression to approximate the current within the deeper navigation channel. The circulation modeling also produced water-surface elevations at 32.8 feet (10-meter) water depth. This water-surface elevation was considered constant across the length of the proposed channel.

### **7.5.3 Other Parameters.**

Other parameters that enter into the sediment transport and channel infilling calculations include estimation of fluid properties (density, viscosity), estimation of bottom bed roughness, estimation of bottom current, and estimation of bottom shear stress. The estimation and approximations for these parameters were developed from published methods.

### **7.5.4 Model Accuracy and Uncertainty**

The accuracy and uncertainty of the channel infilling model is heavily dependent upon the accuracy of the wave and circulation modeling estimates, in addition to the estimates and representation of the sediment bed and sediment properties. Because of the highly non-linear relationship between environmental forcing conditions and sediment transport, the uncertainty of sediment transport prediction methods is relatively large. In general, the uncertainty in estimating sediment transport of non-cohesive sediments under combined waves and currents is a factor of five. Sensitivity of channel infilling to the input environmental conditions are presented with the model results to indicate the range of uncertainty associated with the channel infilling estimates.

## **7.6 Longshore Transport**

Longshore transport is classified as the quantity of sediment transported along the coast by the effects of breaking waves and the longshore currents that they generate. The method for estimating longshore transport of the gravel and coarse sand present along the shoreline at the Portsite is presented in Damgaard and Soulsby (1997).

### **7.6.1 Wave Transformation**

Wave transformation from the hindcast for the estimation of longshore transport was performed using Snell's Law approach. The longshore transport calculation requires wave height, wave period, and wave direction at breaking as input conditions. The breaking wave conditions were obtained by an iterative procedure, isolating the cross-shore position at which the transformed wave reaches the incipient breaking condition.

### **7.6.2 Beach Profile**

The cross-shore representation of the beach profile is required for both the wave transformation and estimation of beach slope. The beach profile was constructed from offshore and nearshore bathymetric surveys. Figure 77 presents the beach profile applied in the longshore transport model.

The primary requirement for the beach profile specification was the estimation of beach slope for the Damgaard-Soulsby longshore transport method. The slope was estimated as the mean slope over the surf zone, which was estimated by dividing the breaking wave depth by the distance from the point of breaking to the still-water line.

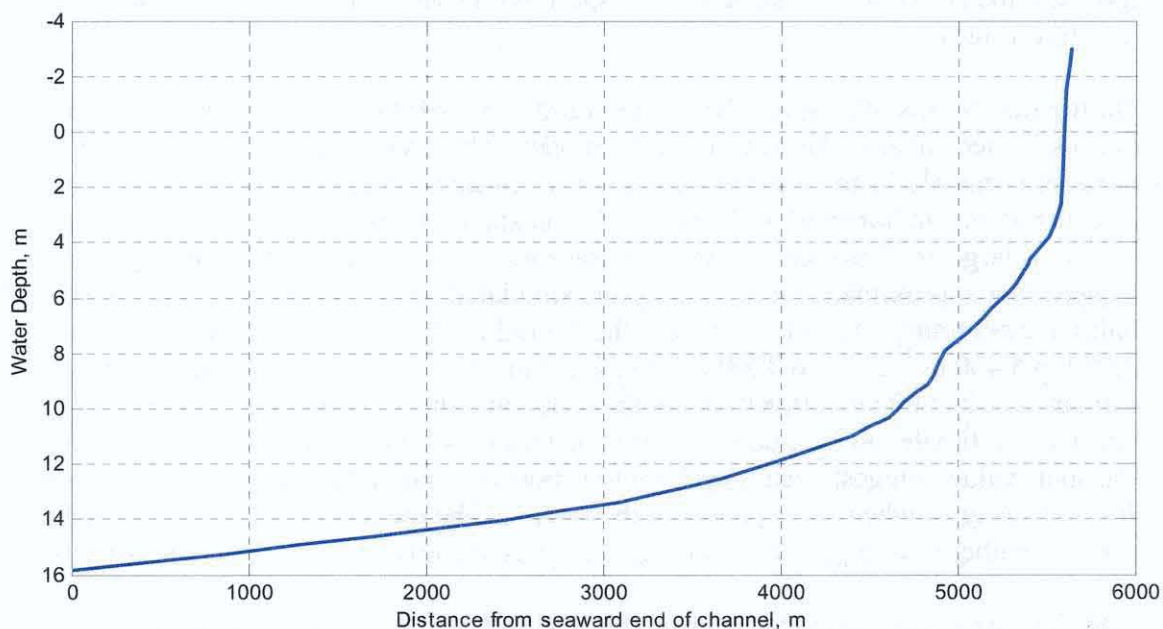


Figure 77 Beach profile applied for modeling of longshore transport. Negative values are above water surface; positive values are below water surface.

*\* (1 m = 3.28 ft)*

### 7.6.3 Longshore Transport Sediment Characteristics

Previous sediment sampling efforts did not collect sediment samples along the beach face. Observational evidence and a few casual samples of sediment from the beach face suggest that the median grain diameter,  $d_{50}$ , ranges between 0.02 and 0.80 inches (0.5 and 20 mm). The beach sediments were observed to be variable along the shore with regions of shoreline composed of gravel and other regions composed primarily of coarse sand. Documented characterization of beach sediments at Ogotoruk Beach by Moore and Scholl (1961) indicate that the beach sediments range in median diameter between 0.01 and 0.83 inches (0.2 and 21 mm).

### 7.6.4 Longshore Transport Estimates

Longshore transport was estimated by applying the 16-year offshore wave climate from the wave hindcasting study. The waves were transformed, and breaking wave conditions were supplied to the longshore transport model.

The gross and net longshore transport estimates are summarized on a monthly and annual basis in tables A-21 and A-22. Table A-21 contains longshore transport estimates for the 0.02 inches (0.5 mm) grain diameter simulation, and table A-22 contains the estimates for the 0.80 inches (20 mm) grain diameter simulation. Gross transport indicates the total volume of sediment transported, regardless of transport direction, and net transport

Draft Feasibility Report  
Appendix A: Hydraulic Design, Delong Mountain Terminal, Alaska

indicates the net volume of sediment transport, with southbound transport indicated as negative values.

During the months of June and November (and July 1998) transport is small or zero because of ice cover in the wave hindcast model. The average annual net transport rates are approximately 11 to 18 percent of the gross transport rate, indicating a weak overall directional bias in transport to the south. On an annual basis, however, the net transport can be as large as 70 percent of the gross transport. The annual net transport estimates suggest that approximately half of the years simulated have net transport to the north and half have net transport to the south, but the overall net transport averages approximately 3,000 to 5,400 cy<sup>3</sup> (2300 to 4200 m<sup>3</sup>) to the south. The maximum net transport was estimated at 26,000 cy<sup>3</sup> (20,000 m<sup>3</sup>) to the south, and the maximum net transport to the north was estimated to be much smaller at 6,100 cy<sup>3</sup> (4,700 m<sup>3</sup>). Reviewing the monthly transport values suggests that longshore transport is weakest during the months of June, July, and August when wave energy is the lowest. The months of September, October, and November have higher wave energy and consequently more longshore transport.

Anecdotal evidence exists that support the modeled results. First, since construction of the shallow-water dock in 1986, sediment has impounded on the north side of the dock, requiring mechanical bypassing of material to the south. (bypassing volumes are not available to verify the magnitude of transport.) This material impoundment suggests that the net longshore transport at the site is to the south, in agreement with the model predictions. In addition, Moore and Cole (1960) performed a study of longshore sediment transport for the northern Chukchi Sea coastline. The study concluded from analysis of historical deposits of sediment on Sheshalik Spit southeast of Cape Krusenstern that annual net transport of 14,649 cy<sup>3</sup> (11,200 m<sup>3</sup>) to the south must have occurred over the past 1,000 years to produce the formations on Sheshalik Spit. The conclusion from these anecdotal observations is that the transport estimates by the longshore transport model are in the correct direction, and within the limits and uncertainties of the estimates from the historical study.

**TABLE A-21. Longshore Transport for  $d_{50}$  = 0.02 in. (0.5 mm)**

Year	Gross Transport Volume, yd <sup>3</sup> (m <sup>3</sup> )						Annual
	June	July	August	September	October	November	
1985	0	1075 (822)	3348 (2560)	4944 (3780)	15597 (11925)	0	24965 (19087)
1986	179 (137)	1579 (1207)	4039 (3088)	10002 (7647)	4072 (3113)	1774 (1356)	21643 (16547)
1987	0	259 (198)	2017 (1542)	6412 (4902)	4333 (3313)	1011 (773)	14032 (10728)
1988	0	2412 (1844)	4090 (3127)	2972 (2272)	1015 (776)	872 (667)	11361 (8686)
1989	662 (506)	1771 (1354)	3318 (2537)	5212 (3985)	5694 (4353)	2939 (2247)	19596 (14982)
1990	2390 (1827)	3235 (2473)	2577 (1970)	5094 (3895)	2498 (1910)	19835 (15165)	35627 (27239)
1991	0	28181 (798)	83378 (2361)	10665 (302)	363282 (10287)	14020 (397)	499561 (14146)
1992	0	453 (346)	2560 (1957)	8125 (6212)	8564 (6548)	4336 (3315)	24039 (18379)
1993	331 (253)	2617 (2001)	1617 (1236)	16429 (12561)	8443 (6455)	21249 (16246)	50684 (38751)
1994	0	120 (92)	10466 (8002)	1983 (1516)	8690 (6644)	55 (42)	21314 (16296)
1995	909 (695)	2216 (1694)	422 (323)	1146 (876)	795 (608)	5291 (4045)	10778 (8240)
1996	2914 (2228)	6964 (5324)	4417 (3377)	4792 (3664)	12963 (9911)	14469 (11062)	46519 (35566)
1997	335 (259)	471 (360)	2526 (1931)	1457 (1114)	12572 (9612)	8508 (6505)	25871 (19780)

Draft Feasibility Report  
Appendix A: Hydraulic Design, Delong Mountain Terminal, Alaska

<b>TABLE A-21. Longshore Transport for <math>d_{50} = 0.02</math> in. (0.5 mm)</b>							
Year	Gross Transport Volume, $yd^3 (m^3)$						
	June	July	August	September	October	November	Annual
1998	0	0	2761 (2111)	5071 (3877)	4493 (3435)	143 (109)	12467 (9532)
1999	0	191 (146)	789 (603)	281 (215)	1311 (1002)	0	2573 (1967)
2000	473 (362)	5007 (3828)	4662 (3564)	4927 (3767)	5794 (4430)	1177 (900)	22040 (16851)
<b>Average</b>	<b>513 (392)</b>	<b>1838 (1405)</b>	<b>3293 (2518)</b>	<b>4953 (3787)</b>	<b>6893 (5270)</b>	<b>5136 (3927)</b>	<b>30168 (23065)</b>
Year	Net Transport Volume, $yd^3 (m^3)$						
	June	July	August	September	October	November	Annual
1985	0	1042 (797)	2008 (1535)	-4195 (-3207)	-15187 (-11611)	0 (0)	-16331 (-12486)
1986	109 (83)	1048 (801)	574 (439)	-2064 (-1578)	-2739 (-2094)	-1571 (-1201)	-4642 (-3549)
1987	0	50 (38)	-115 (-88)	-5705 (-4362)	-1832 (-1401)	-930 (-711)	-8533 (-6524)
1988	0	369 (282)	1812 (1385)	-1593 (-1218)	561 (429)	-735 (-562)	412 (315)
1989	-10 (-8)	1120 (856)	3033 (2319)	3293 (2518)	-3647 (-2788)	-1363 (-1042)	2424 (1853)
1990	1322 (1011)	3015 (2305)	-1037 (-793)	-4764 (-3642)	429 (328)	76 (58)	-959 (-733)
1991	0	411 (314)	-2761 (-2111)	-348 (-266)	3293 (2518)	-489 (-374)	107 (82)
1992	0	162 (124)	-394 (-301)	-8105 (-6197)	-65 (-50)	1628 (1245)	-6774 (-5179)
1993	-331 (-253)	383 (293)	179 (137)	-8107 (-6198)	-4579 (-3501)	-11978 (-9158)	-24431 (-18679)
1994	0 (0)	2719 (77)	4561 (3487)	-1937 (-1481)	-5416 (-4141)	55 (42)	-2637 (-2016)
1995	119 (91)	2144 (1639)	82 (63)	-385 (-294)	-216 (-165)	-3998 (-3057)	-2252 (-1722)
1996	-1329 (-1016)	6117 (4677)	530 (405)	-4349 (-3325)	5683 (4345)	-531 (-406)	6121 (4680)
1997	-188 (-144)	213 (163)	2452 (1875)	619 (473)	-10205 (-7802)	1142 (873)	-5967 (-4562)
1998	0	0	2586 (1977)	-272 (-208)	3165 (2420)	135 (103)	5614 (4292)
1999	0	167 (128)	778 (595)	-106 (-81)	-1287 (-984)	0	-446 (-341)
2000	459 (351)	-3681 (-2814)	1304 (997)	-27353 (-2091)	-1655 (-1265)	-777 (-594)	-7084 (-5416)
<b>Average</b>	<b>9 (7)</b>	<b>791 (605)</b>	<b>974 (745)</b>	<b>-2547 (-1947)</b>	<b>-2106 (-1610)</b>	<b>-1209 (-924)</b>	<b>-5448 (-4165)</b>

Draft Feasibility Report  
Appendix A: Hydraulic Design, Delong Mountain Terminal, Alaska

**TABLE 22. Longshore Transport for  $d_{50} = 0.79$  inches (20.0 mm)**

Year	Gross Transport Volume, $yd^3 (m^3)$						
	June	July	August	September	October	November	Annual
1985	0	959 (733)	2710 (2072)	4140 (3165)	15294 (11693)	0	23104 (17664)
1986	162 (124)	1317 (1007)	2739 (2094)	8769 (6704)	2829 (2163)	1188 (908)	17002 (12999)
1987	0	212 (162)	1984 (1517)	5352 (4092)	3004 (2297)	632 (483)	11183 (8550)
1988	0	2981 (2279)	4492 (3434)	2213 (1692)	755 (577)	553 (423)	10995 (8406)
1989	456 (349)	1452 (1110)	3354 (2564)	4932 (3771)	4280 (3272)	1978 (1512)	16454 (12580)
1990	1847 (1412)	2956 (2260)	2859 (2186)	3603 (2755)	1723 (1317)	22438 (17155)	35427 (27086)
1991	0	925 (707)	2237 (1710)	245 (187)	15344 (11731)	324 (248)	19074 (14583)
1992	0	400 (306)	1838 (1405)	6357 (4860)	7213 (5515)	3199 (2446)	19007 (14532)
1993	213 (163)	2275 (1739)	1161 (888)	12883 (9850)	7563 (5782)	24200 (18502)	48295 (36924)
1994	0	110 (84)	9545 (7298)	1390 (1063)	6389 (4885)	41 (31)	17474 (13360)
1995	790 (604)	1861 (1423)	391 (299)	757 (579)	531 (406)	4515 (3452)	8846 (6763)
1996	2260 (1728)	7619 (5825)	3511 (2684)	3258 (2491)	16764 (12817)	14947 (11428)	48361 (36975)
1997	288 (220)	330 (252)	1936 (1480)	1567 (1198)	12479 (9541)	7308 (5587)	23905 (18277)
1998	0	0	1889 (1444)	3955 (3024)	3344 (2557)	86 (66)	9273 (7090)
1999	0	140 (107)	528 (404)	190 (145)	777 (594)	0	1635 (1250)
2000	424 (324)	3921 (2998)	3341 (2554)	3538 (2705)	4149 (3172)	765 (585)	16137 (12338)
<b>Average</b>	<b>403 (308)</b>	<b>1716 (1312)</b>	<b>2782 (2127)</b>	<b>3947 (3018)</b>	<b>6402 (4895)</b>	<b>5136 (3927)</b>	<b>27181 (20781)</b>
Year	Net Transport Volume, $yd^3 (m^3)$						
	June	July	August	September	October	November	Annual
1985	0	923 (706)	1779 (1360)	-3614 (-2763)	-14976 (-11450)	0	-15886 (-12146)
1986	106 (81)	923 (706)	467 (357)	-2417 (-1848)	-1883 (-1440)	-1046 (-800)	-3849 (-2943)
1987	0	59 (45)	428 (327)	-4706 (-3598)	-1331 (-1018)	-568 (-434)	-6120 (-4679)
1988	0	1550 (1185)	2968 (2269)	-1010 (-772)	451 (345)	-442 (-338)	3516 (2688)
1989	739 (16)	999 (764)	3148 (2407)	3637 (2781)	-2752 (-2104)	-913 (-698)	4141 (3166)
1990	1054 (806)	2811 (2149)	-1526 (-1167)	-3305 (-2527)	331 (253)	3100 (2370)	2464 (1884)
1991	0	472 (361)	-1885 (-1441)	-211 (-161)	6729 (5145)	-313 (-239)	4795 (3666)
1992	0	160 (122)	-63 (-48)	-6350 (-4855)	1304 (997)	1439 (1100)	-3511 (-2684)
1993	-213 (-163)	634 (485)	237 (181)	-5246 (-4011)	-4832 (-3694)	-16692 (-12762)	-26111 (-19963)
1994	0	95 (73)	5172 (3954)	-1314 (-1005)	-3590 (-2745)	41 (31)	402 (307)
1995	98 (75)	1819 (1391)	143 (109)	-232 (-177)	-97 (-74)	-3492 (-2670)	-1628 (-1245)
1996	-574 (-439)	7051 (5391)	497 (380)	-2887 (-2207)	10772 (8236)	-3414 (-2610)	11446 (8751)
1997	-77 (-59)	146 (112)	1881 (1438)	1032 (789)	-10228 (-7820)	2087 (1596)	-5159 (-3944)
1998	0	0	1751 (1339)	204 (156)	2485 (1900)	86 (66)	4527 (3461)
1999	0	122 (93)	521 (398)	-72 (-55)	-763 (-583)	0	-192 (-147)
2000	424 (324)	-2709 (-2071)	1143 (874)	-1751 (-1339)	-1202 (-919)	-453 (-346)	-4548 (-3477)
<b>Average</b>	<b>60 (46)</b>	<b>940 (719)</b>	<b>1041 (796)</b>	<b>-1766 (-1350)</b>	<b>-1224 (-936)</b>	<b>-1286 (-983)</b>	<b>-2976 (-2275)</b>

### 7.6.5 Uncertainty in Longshore Transport Estimates

Uncertainty in the longshore sediment transport is illustrated in table A-23. Uncertainty in the estimates enters through the uncertainty in the environmental forcing (waves) and the uncertainty in the median grain diameter of the beach sediments. By sensitivity analysis, the uncertainty in median grain size produces approximately 10 to 20 percent uncertainty in the estimated longshore transport.

The best estimate of the combined uncertainties resulting from uncertainties in wave conditions and sediment grain size (assuming 20 percent error in wave height and 10 degree error in wave direction) is approximately  $\pm 60$  percent, and the maximum uncertainty estimate is  $\pm 90$  percent. The “best” estimate is derived by assuming that the errors in wave height, wave direction, and sediment diameter are completely independent. Conversely, the “maximum” uncertainty estimate is derived by assuming that all errors are correlated.

Wave Parameter	Wave Parameter Estimate		
	Longshore Transport Uncertainty, percent		
H <sub>b</sub>	5%	10%	25%
	12.5	25	50
θ <sub>b</sub>	5 deg	10 deg	20 deg
	13	27	53

## 7.7 “Hypothetical” Year Simulations

A hypothetical open-water season was developed and simulated to provide a preliminary estimate of the channel infilling. Wave and current conditions from the months July 1998, August 2000, September 1998, October 1998, and November 1990 were selected to represent the hypothetical year. Wave conditions for the hypothetical year were primarily obtained from the 16-year wave hindcast except for August 2000, for which wave data were available from the NDBC buoy. Because measured current and water level data were available during much of the hypothetical year, data from the ADP-collected current were applied when available. ADCIRC-simulated currents and water levels were substituted for periods when measurements were unavailable. Dates and sources of wave, current, and water level data are summarized in the following table.

Month	Waves		Currents and Water Level	
	Measured	Simulated	Measured	Simulated
July (1998)		X	X	
August (2000)	X		X	
September (1998)		X	X	
October (1998)		X	X (Oct 7-31)	X (Oct 1-6)
November (1990)		X		X

### 7.7.1 Hypothetical Year Channel-Infilling Results

Figure 78 presents the model-estimated channel infilling distribution along the length of the channel for the hypothetical year. The infilling line indicates the volume of sediment deposited in the channel per meter length of channel. Channel infilling is relatively low

along the outer 9,843 feet (3,000 meters) of the channel where the highly consolidated silty sediment is present. Infilling rates sharply increase near the 43-foot (13-meter) contour where sand and gravel appear on the sediment bed. Channel infilling decreases at approximately 15,748 feet (4,800 meters) with the increase in median grain diameter at the 31-foot (9.4-meter) water depth, and increases again with the rapidly decreasing water depth as the channel approaches shore. Three vertical lines in figure 78 indicate the location of the channel transition to ambient water depth for the three terminal depth alternatives examined in this study. Note that the infilling rates are increasing rapidly between these three alternatives, but the integrated infilling volume produced within these sections is small compared with the total length of the channel. For the hypothetical year, the 24.0-foot and 20.0-foot (7.3-meter and 6.1-meter) terminal depth alternatives result in a 5- and 16-percent increase, respectively, in the total infilling volume over the 28-foot (8.5-meter) alternative.

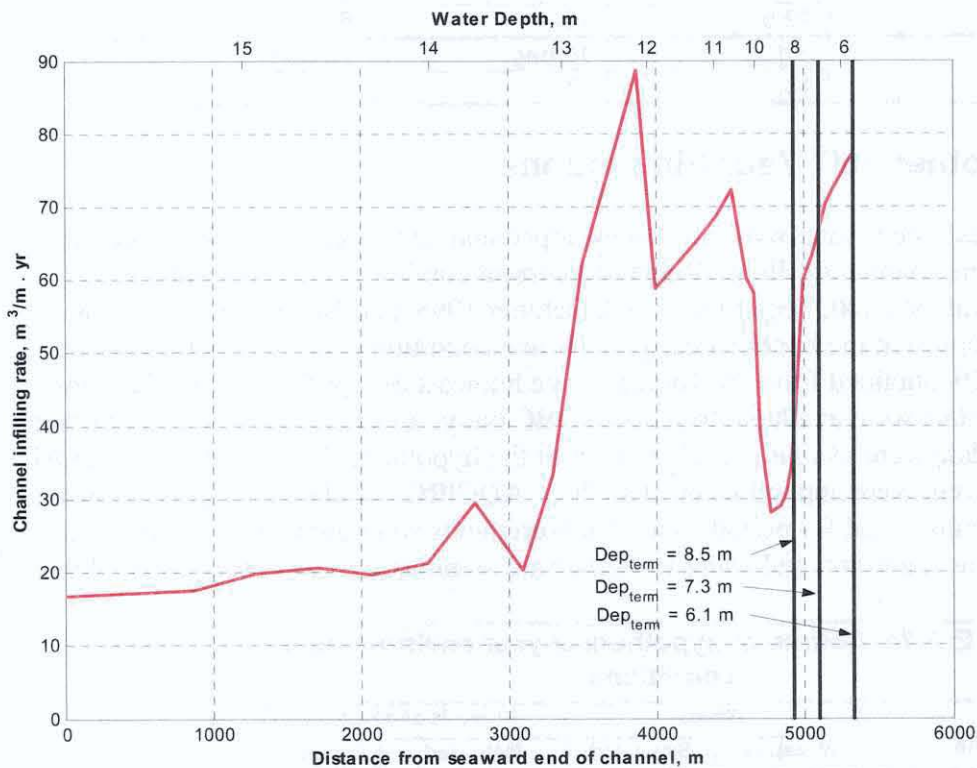


Figure 78. Spatial distribution of channel infilling for the hypothetical year.  
 \* (1 m = 3.28 ft)

Figure 79 presents the temporal distribution of channel infilling during the hypothetical year. Storms in September and November dominate channel infilling as indicated by the channel infilling rates in figure 79. Channel infilling from wave conditions exceeding 6.6 feet (2.0 meters) accounts for 86 percent of the total infilling volume, and infilling from wave heights exceeding 8.2 feet (2.5 meters) accounts for 73 percent of the total infilling volume. In light of the apparent importance of storms in defining the infilling of the proposed channel, more detailed analysis of storms at the DMT site were conducted.



Figure 79. Temporal distribution of channel infilling for the hypothetical year.

## 7.8 Channel Infilling Estimates for Extreme Events

Because channel infilling at the DMT site is characteristically an episodic process, extreme events contribute significantly to the infilling volume over time. The hypothetical year illustrated the significance of storms on sediment transport and consequently channel infilling. Another pertinent observation is that sediment transport along the length of the proposed channel is highly sensitive to bottom orbital velocities produced by waves. The near-bottom currents from circulation in the Chukchi Sea seldom exceed the threshold of motion for most sediment found along the length of the proposed channel. In light of these observations, extreme events in sediment transport are expected to be closely correlated to extremes in wave conditions. This relationship was examined to estimate the 1-year, 10-year, and 50-year events (as determined by peak significant wave height). Simulations of the 1-year, 10-year, and 50-year events (as determined by peak significant wave height) were performed to develop a frequency-of-occurrence relationship for channel infilling.

Two approaches were adopted in developing statistical associations for channel infilling rates. The first and most simple approach was to develop synthetic storms designed to represent the wave and current conditions representative of storms with particular return intervals. As mentioned previously, peak significant wave height is closely but imperfectly correlated to sediment transport. Other factors such as storm duration, wave period, wave direction, and current magnitude also factor into sediment transport. As a preliminary estimate of the channel infilling associated with the 1-, 10-, and 50-year

storms, the synthetic storm approach was applied. The second approach involved numerical simulation of waves and circulation for a suite of selected storm events. Wind fields for each of these events were input to WAM and ADCIRC. The waves and currents estimated by the models were then applied to the channel infilling model, and estimates of channel infilling for each storm were computed. The channel infilling estimates for the extreme events were then processed and frequency-of-occurrence estimates were developed for channel infilling.

### 7.8.1 Synthetic Storms

The first and most simple approach at quantifying the channel infilling resulting from the passage of storms was to develop synthetic storm conditions that represent the conditions of return intervals of interest. This analysis was performed prior to receipt of the extreme event sediment analysis and provided an idea of what storm events would move sediment. For the present study, the 1-, 10-, and 50-year infilling estimates are of interest. Input parameters of peak significant wave height, wave period, wave direction, storm duration, and current magnitude were specified to approximate the conditions represented by the 1-, 10-, and 50-year storms.

**Synthetic Storm Input Conditions.** Because the synthetic storm simulations do not represent actual events, many parameters were estimated from local experience or from indications from model simulations and measured data. The basis for the synthetic storm was developed around the peak significant wave height occurring during a storm of a certain return interval. Other wave and current parameters were estimated. A summary of the input conditions for the synthetic storms is presented in table A-26.

Wave period was estimated by review of conditions in the 16-year hindcast and local knowledge. In most storms, wave period is not constant throughout a storm, but varies with the passage of the meteorological system producing the waves. For simplicity in the development of the synthetic storm, wave period was held constant at the value estimated to coincide with the peak wave conditions. This approximation adds some degree of conservatism to the channel infilling estimates.

Wave direction, like wave period, is also dependent on the track and land speed of the storm. Wave direction was approximated as constant and waves were assumed to travel along a shore-normal path. This is also recognized as a conservative assumption because wave heights will not be reduced by wave refraction during transformation into shallower depths.

Total storm duration at the DMT site is estimated to be approximately 2 days. Many storms, especially in the 1- to 10-year return interval ramp up to a peak wave height and maintain the peak condition for some length of time. To represent this phenomenon, the wave height of the synthetic storms was ramped up to the peak condition and held for a specific duration. The duration of the storm was based on experience with storms in the vicinity, as well as a duration analysis of storm events contained in the 16-year wave hindcast. The duration analysis indicates that a wave height of approximately 9.8 feet (3 meters) during storm events remained above 80 to 85 percent of the peak significant

wave height for approximately 24 hours. For the 6- and 8-meter storms, wave conditions remained above 80 to 85 percent of the peak significant wave height for approximately 12 hours. The wave height of the synthetic storms was ramped to the peak value, held constant for the duration of the peak, and then ramped down.

Currents simulated for hindcast storm events were observed to frequently peak between 0.8 knots and 1.2 knots (0.4 and 0.6 m/s). For the idealized storm conditions, currents were approximated as temporally and spatially uniform with a magnitude of 1.0 knot (0.5 m/s) and a northward current parallel to shore. Water level for these simulations was assumed to be the mean water level, although it is recognized that some storm surge is anticipated with the more energetic storms.

**TABLE A-26. Summary of Environmental Conditions for Synthetic Storms**

Return Interval, (years)	Peak Wave Height, ft (m)*	Peak Duration (hours)	Wave Period (s)	Wave Direction (deg)	Water Surface ft (m)	Current Speed, knot (m/s)
1	9.8 (3.0)	24	8.0	0	0	1.0 (0.5)
10	19.7 (6.0)	12	10.0	0	0	1.0 (0.5)
50	26.3 (8.0)	12	12.0	0	0	1.0 (0.5)

\*This analysis was performed prior to the Snell's Law wave transformation, so all wave heights are based on hindcast data from the -62 foot (-19 meter) contour.

### 7.8.2 Synthetic Storm Results

Figures 80 through 82 present the channel infilling input conditions and results for each of the synthetic storms. The top two panels of the plots present time histories of hydrodynamic and wave conditions, where WSE represents water surface elevation,  $H_{m0}$  indicates energy-based wave height,  $T_p$  indicates peak spectral wave period, and  $\theta_p$  indicates wave direction in local polar convention (relative to shore-normal). All wave conditions were applied at a 16-meter water depth just offshore of the seaward end of the proposed channel. The third panel of each figure indicates time history of instantaneous channel infilling rate, expressed as the net volume of sediment deposited in the channel over one hour. The fourth panel presents the spatial distribution of channel infilling integrated over the duration of the simulation, indicating the net volume of sediment deposited in the channel per meter length of channel. Net channel infilling volumes estimated from the synthetic storm simulations are presented in table A-27.

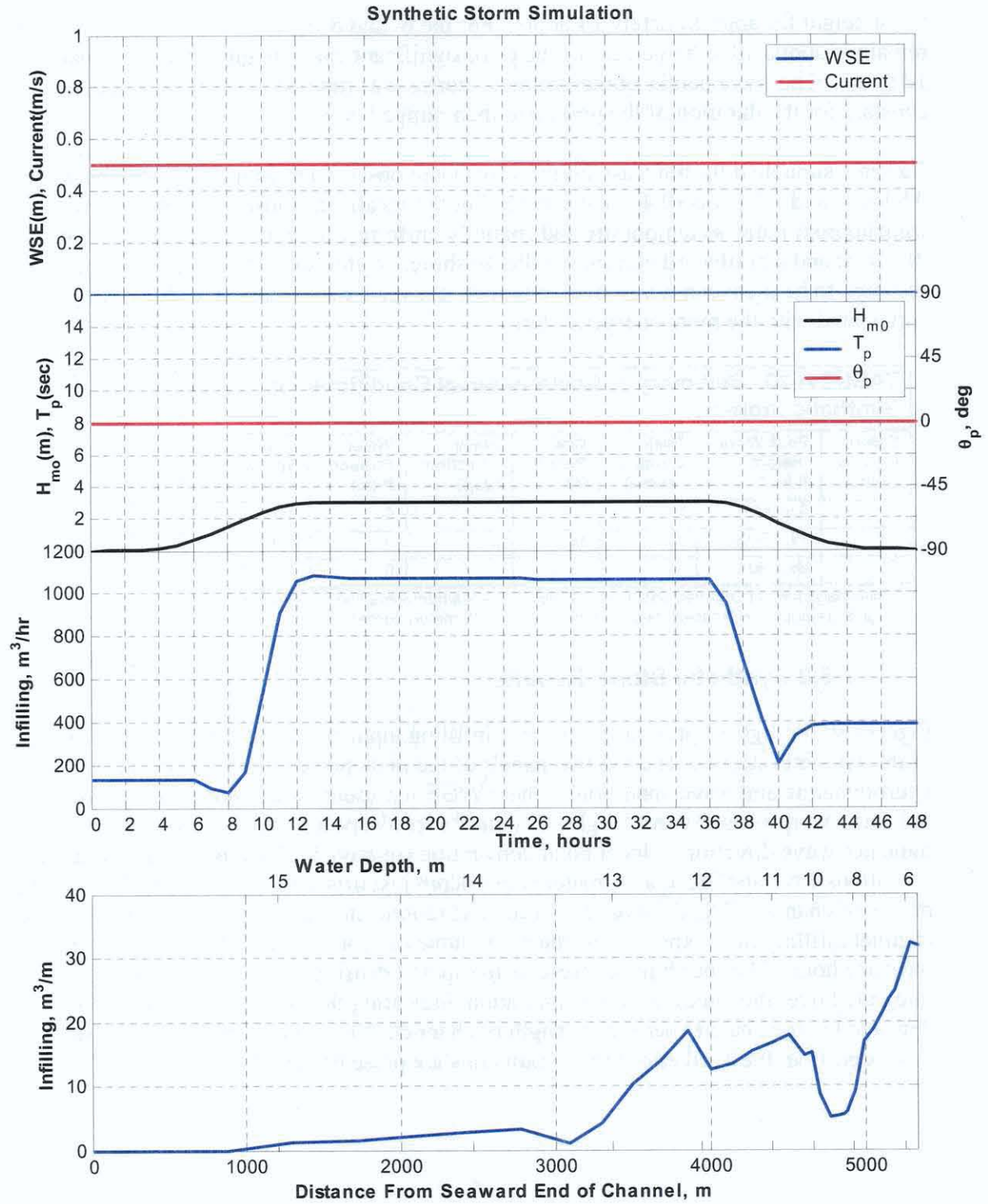


Figure 80 Input and output from 1 year return interval synthetic storm

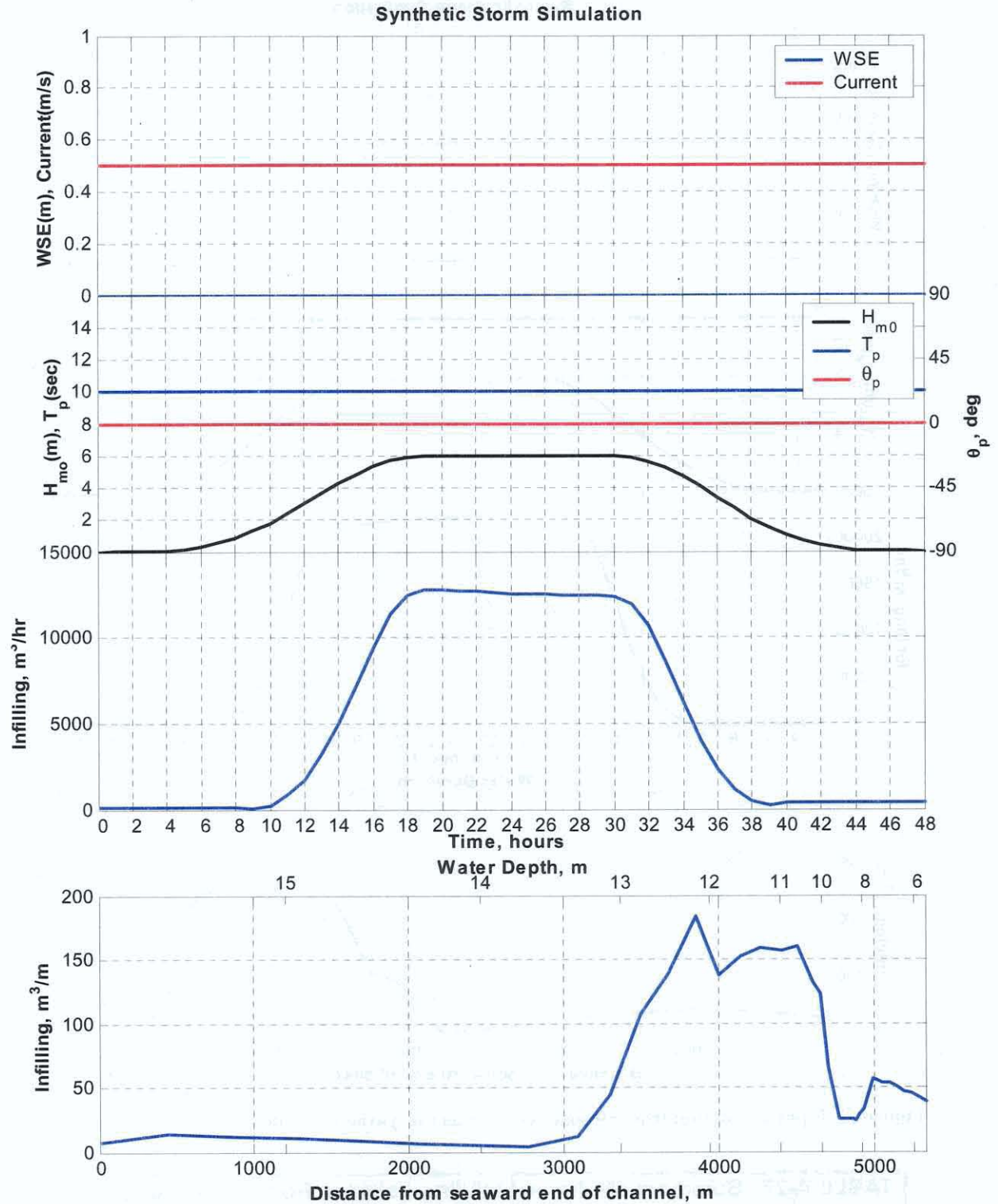


Figure 81 Input and output from 10 year return interval synthetic storm

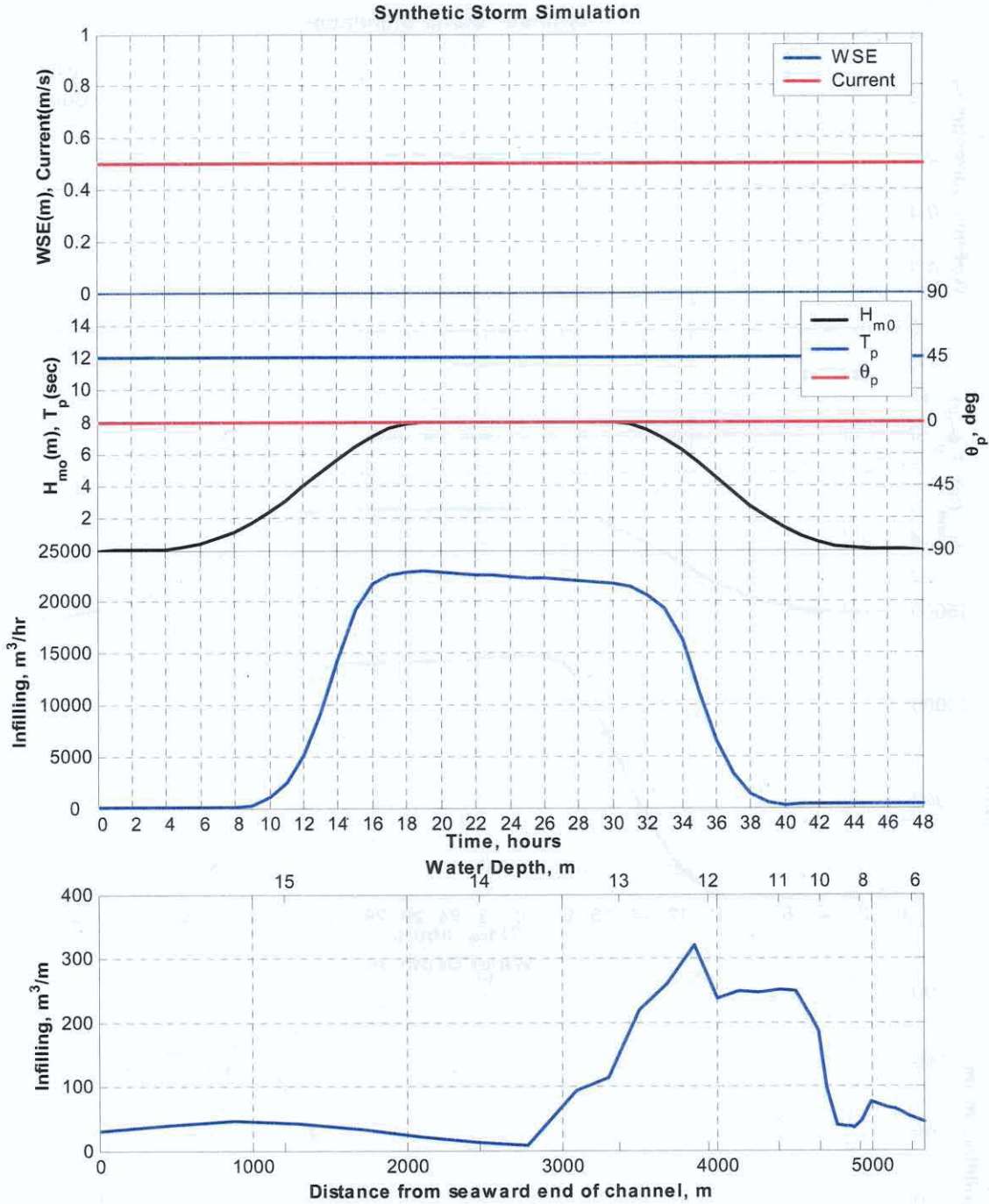


Figure 82 Input and output from 50 year return interval synthetic storm

<b>TABLE A-27. Summary of Channel Infilling Volumes from Synthetic Storm Simulations.</b>			
Return Period of Storm, yrs	Infilling Volume, $yd^3$ ( $m^3$ )		
	Terminal Depth = 28 ft (8.5 m)	Terminal Depth=24 ft (7.3 m)	Terminal Depth =20 ft (6.1 m)
1	33,222	36,884	45,255

**TABLE A-27. Summary of Channel Infilling Volumes from Synthetic Storm Simulations.**

Return Period of Storm, yrs	Infilling Volume, yd <sup>3</sup> (m <sup>3</sup> )		
	Terminal Depth = 28 ft (8.5 m)	Terminal Depth=24 ft (7.3 m)	Terminal Depth =20 ft (6.1 m)
	(25,400)	(28,200)	(34,600)
10	304,753 (233,000)	316,524 (242,000)	330,912 (253,000)
50	610,813 (467,000)	626,508 (479,000)	643,512 (492,000)

The most noticeable trend in the spatial distribution of channel infilling is the increase in channel infilling as approaching the nearshore end of the channel. The small infilling quantities in the first 9,843 feet (3,000 meters) of the channel are associated with the deeper water depths and transport resistance of the consolidated bed. The transition from consolidated bed to the gravel and sand bed at approximately 9,843 feet (3,000 meters) is evident in the sharp increase in channel infilling. Channel infilling generally increases between 9,843 feet (3,000 meters) and 14,764 feet (4,500 meters), and then decreases with an increase in sediment grain diameter. At approximately 16,076 feet (4,900 meters), infilling increases again under the effect of decreasing water depth and the associated increase in bottom shear stresses from the wave orbital motion.

**Uncertainty.** No detailed sensitivity or uncertainty analysis was performed on the synthetic storm simulations. Uncertainty in the synthetic storm simulations results from the recognized limitations of the sediment transport models and the approximation of the waves and currents to represent statistically relevant conditions. A general estimate of uncertainty in the estimated channel infilling quantities is a factor of 2 to 3.

## 7.9 Event-Based Extremal Analysis of Channel Infilling

A second, more rigorous approach in estimating the channel infilling associated with storm events is to simulate, or hindcast, the channel infilling caused by storms at the study site. By simulating sediment transport of actual storm events, the temporal variability and inherent correlation of wave and current conditions is incorporated into the analysis. With a sufficient record of storms, frequency-of-occurrence relationships can be developed for channel infilling.

### 7.9.1 Input Conditions

The same input conditions described for the synthetic storm simulations were required for the event-based simulations, specifically wave height, wave period, wave direction, current, and water surface elevation. Instead of approximating values and temporal variability of these parameters, conditions simulated by the wave model and circulation model were input to the channel infilling model. Wave spectra were saved from WAM at a position just offshore of the seaward terminus of the proposed channel in a water depth of 62 feet (19 meters). These spectra were processed to eliminate offshore-propagating wave energy, and the energy-based wave height, peak spectral frequency, and mean wave

Draft Feasibility Report  
Appendix A: Hydraulic Design, Delong Mountain Terminal, Alaska

direction were estimated from the half-plane spectra. Current and water surface elevation were estimated at the nominal 32.8-foot (10-meter) water depth and applied uniformly across the length of the channel.

Storms were selected from the results of the wave hindcasting simulations that spanned the years 1954 to 2000. Sediment transport has been previously demonstrated to be closely, but imperfectly, correlated to peak significant wave height. With this in mind, storm events were identified in the hindcast record and sorted by peak wave height. The smallest wave from the extremal storms had a peak significant wave height of approximately 9.2 feet (2.8 meters). Storms with peak significant wave heights greater than 9.84 feet (3 meters) allowed definition of storms with return intervals on the order of 1 to 50 years.

Table A-28 summarizes the 37 storms selected for the event-based analysis. The storm index indicates each storm's ranking by peak wave height. The date and time of the start, end, and peak of the storm are also presented in table A-29. The start and end times of the storm indicate the period simulated for the event-based analysis, and indicate the period of the storm for which wave heights exceed 4.9 feet (1.5 meters). Finally, peak wave heights for each selected storm are indicated, ranging from 9.84 feet to 29.5 feet (3 to 9 meters). Time histories of the wave and current conditions are presented for each storm in Appendix 4B of the CHL report.

ADCIRC simulations were selectively run to provide current and water surface estimates for the 37 events contained in table A-28. Model spin-up of approximately 5 days was applied prior to the start date to allow instabilities from the initial conditions to dampen before the wind fields of the storm were applied.

Index	Start	Peak	End	Peak $H_{m0}$ ft (m)
01	11/27/1970 02:00	11/29/1970 00:00	11/27/1970 22:00	29.5 (8.98)
02	10/27/1996 15:00	10/31/1996 02:00	10/29/1996 02:00	21.9 (6.68)
03	11/09/1973 13:00	11/12/1973 04:00	11/11/1973 01:00	21.9 (6.68)
04	08/28/1962 08:00	08/31/1962 16:00	08/30/1962 19:00	21.3 (6.5)
05	11/10/1974 19:00	11/14/1974 01:00	11/12/1974 13:00	20.5 (6.25)
06	11/01/1996 22:00	11/03/1996 20:00	11/02/1996 19:00	16.9 (5.14)
07	11/16/1993 04:00	11/18/1993 01:00	11/17/1993 01:00	15.7 (4.79)
08	10/24/1972 15:00	10/29/1972 14:00	10/26/1972 21:00	15.6 (4.74)
09	11/02/1990 13:00	11/06/1990 15:00	11/03/1990 19:00	15.5 (4.72)
10	10/20/1991 22:00	10/23/1991 10:00	10/21/1991 16:00	14.7 (4.49)
11	11/01/1997 03:00	11/02/1997 20:00	11/01/1997 17:00	14.6 (4.46)
12	10/05/1992 09:00	10/07/1992 18:00	10/06/1992 08:00	14.5 (4.42)
13	11/17/1990 02:00	11/20/1990 22:00	11/18/1990 01:00	13.8 (4.21)
14	07/15/1957 13:00	07/17/1957 23:00	07/17/1957 08:00	13.3 (4.04)
15	08/22/1963 23:00	08/24/1963 01:00	08/23/1963 13:00	12.8 (3.91)
16	09/24/1978 11:00	09/27/1978 00:00	09/25/1978 23:00	12.7 (3.88)

**TABLE A-28. Summary of Storms Selected from Wave Hindcast**

Index	Start	Peak	End	Peak H <sub>m0</sub> ft (m)
17	10/22/1985 10:00	10/25/1985 07:00	10/22/1985 23:00	12.7 (3.87)
18	10/04/1997 06:00	10/05/1997 15:00	10/04/1997 18:00	12.6 (3.85)
19	11/13/1996 22:00	11/16/1996 12:00	11/15/1996 19:00	12.6 (3.84)
20	10/15/1973 17:00	10/17/1973 09:00	10/16/1973 13:00	12.2 (3.73)
21	10/10/1991 23:00	10/13/1991 19:00	10/12/1991 14:00	12.2 (3.72)
22	11/10/1990 18:00	11/12/1990 20:00	11/11/1990 11:00	12.2 (3.71)
23	11/08/1996 20:00	11/11/1996 16:00	11/09/1996 13:00	12.1 (3.69)
24	06/17/1961 17:00	06/19/1961 07:00	06/18/1961 13:00	11.9 (3.62)
25	11/20/1993 09:00	11/21/1993 23:00	11/21/1993 07:00	11.7 (3.58)
26	07/23/1996 10:00	07/26/1996 10:00	07/24/1996 01:00	11.7 (3.56)
27	10/04/1983 15:00	10/07/1983 00:00	10/05/1983 19:00	11.6 (3.55)
28	08/13/1994 13:00	08/14/1994 22:00	08/14/1994 08:00	11.3 (3.44)
29	08/20/1993 00:00	08/20/1993 17:00	08/20/1993 07:00	10.6 (3.23)
30	10/02/1993 16:00	10/03/1993 15:00	10/03/1993 02:00	10.4 (3.17)
31	08/13/1988 22:00	08/15/1988 10:00	08/14/1988 14:00	10.4 (3.16)
32	11/22/1990 22:00	11/23/1990 19:00	11/23/1990 08:00	10.2 (3.12)
33	10/19/1989 23:00	10/21/1989 00:00	10/20/1989 13:00	10.0 (3.06)
34	10/13/1985 16:00	10/14/1985 15:00	10/14/1985 02:00	10.0 (3.06)
35	08/26/1990 14:00	08/28/1990 06:00	08/27/1990 11:00	10.0 (3.05)
36	09/14/1993 04:00	09/15/1993 20:00	09/14/1993 19:00	9.9 (3.03)
37	10/05/1994 11:00	10/07/1994 19:00	10/06/1994 04:00	9.9 (3.01)

### 7.9.2 Results of the Event-Based Analysis of Channel Infilling

The net channel infilling estimates of each storm from table 30 were incorporated into an extremal analysis of channel infilling. Net channel infilling volumes estimated from the event based storm simulations are presented in table A-29 along with the extremal analysis.

Return intervals for channel infilling were determined by frequency analysis and the following expression:

$$T_r = \frac{n+1}{m} \quad (11)$$

where  $T_r$  is the return interval in years,  $n$  is the number of years of record, and  $m$  is the rank (descending order) of the channel infilling volume produced by each storm. The return interval does not suggest that storms will recur on a fixed interval. It indicates the probability of a storm occurring in a given year. For example, the 50-year return interval has an annual probability of occurrence of 2 percent.

Draft Feasibility Report  
Appendix A: Hydraulic Design, Delong Mountain Terminal, Alaska

Storm Index	Return Interval (years)	Peak H <sub>mo</sub> ft (m)	Terminal Depth Alternative		
			28 ft (8.5 m)	24 ft (7.3 m)	20 ft (6.1 m)
1	16.00	29.5 (8.98)	335,332 (256,380)	345,971 (264,514)	359,871 (275,141)
2	48.00	21.9 (6.68)	636,468 (486,615)	656,241 (501,732)	680,355 (520,169)
3	6.86	21.9 (6.68)	93,699 (71,638)	98,213 (75,089)	104,643 (80,005)
4	9.60	21.3 (6.5)	128,855 (98,517)	135,419 (103,535)	144,090 (110,165)
5	24.00	20.5 (6.25)	423,942 (324,127)	443,578 (339,140)	473,189 (361,779)
6	1.66	16.9 (5.14)	5,343 (4,085)	5,890 (4,503)	6,831 (5,223)
7	3.00	15.7 (4.79)	28,978 (22,155)	31,536 (24,111)	35,410 (27,073)
8	12.00	15.6 (4.74)	115,516 (88,318)	122,749 (93,848)	135,976 (103,961)
9	2.53	15.5 (4.72)	17,007 (13,003)	18,400 (14,068)	20,943 (16,012)
10	4.36	14.7 (4.49)	56,322 (43,061)	59,958 (45,841)	66,788 (51,063)
11	8.00	14.6 (4.46)	74,585 (57,024)	78,030 (59,658)	83,832 (64,094)
12	3.43	14.5 (4.42)	27,663 (21,150)	28,358 (21,681)	29,154 (22,290)
13	6.00	13.8 (4.21)	55,097 (42,125)	58,675 (44,860)	64,613 (49,400)
14	1.30	13.3 (4.04)	179 (137)	217 (166)	271 (207)
15	2.40	12.8 (3.91)	15,459 (11,819)	16,491 (12,608)	18,447 (14,104)
16	4.00	12.7 (3.88)	42,830 (32,746)	45,347 (34,670)	49,473 (37,825)
17	1.71	12.7 (3.87)	5,452 (4,168)	5,901 (4,512)	6,702 (5,124)
18	1.92	12.6 (3.85)	9,118 (6,971)	9,842 (7,525)	1,193 (8,558)
19	4.80	12.6 (3.84)	46,001 (35,170)	48,347 (36,964)	52,284 (39,974)
20	3.69	12.2 (3.73)	40,600 (31,041)	43,389 (33,173)	48,700 (37,234)
21	2.29	12.2 (3.72)	9,518 (7,277)	10,116 (7,734)	11,097 (8,484)
22	3.20	12.2 (3.71)	29,620 (22,646)	31,418 (24,021)	34,623 (26,471)
23	5.33	12.1 (3.69)	49,456 (37,812)	51,351 (39,261)	53,145 (40,632)
24	2.67	11.9 (3.62)	18,003 (13,764)	19,383 (14,819)	22,027 (16,841)
25	1.33	11.7 (3.58)	124 (95)	153 (117)	192 (147)
26	2.18	11.7 (3.56)	10,948 (8,370)	11,509 (8,799)	12,427 (9,501)
27	2.82	11.6 (3.55)	25,788 (19,716)	27,783 (21,242)	31,642 (24,192)
28	1.41	11.3 (3.44)	875 (669)	985 (753)	1,154 (882)
29	1.85	10.6 (3.23)	1,279 (978)	1,545 (1,181)	1,853 (1,417)
30	1.45	10.4 (3.17)	943 (721)	1,037 (793)	1,197 (915)
31	1.37	10.4 (3.16)	753 (576)	845 (646)	980 (749)
32	2.09	10.2 (3.12)	6,546 (5,005)	6,885 (5,264)	7,429 (5,680)
33	2.00	10.0 (3.06)	2,931 (2241)	3,471 (2,654)	4,412 (3,373)
34	1.55	10.0 (3.06)	1,253 (958)	1,381 (1,056)	1,604 (1,226)
35	1.50	10.0 (3.05)	768 (587)	921 (704)	1,127 (862)
36	1.60	9.9 (3.03)	604 (462)	713 (545)	883 (675)
37	1.78	9.9 (3.01)	4,365 (3,337)	4,809 (3,677)	5,520 (4,220)

Because the 1-, 10-, and 50-year infilling quantities are of interest, the storms associated with these infilling quantities will be reviewed in detail. Details of all storms simulated are presented in Appendix 4B of the CHL report.

Figures 83 and 84 present the channel infilling input conditions and results for the 10-, and 50-year storms (from the perspective of channel infilling). The figures are similar in nature to the figures presented for the synthetic storm, but include the temporal variability of wave and currents inherent in storms. The top two panels of the plots present time histories of hydrodynamic and wave conditions, where WSE represents water surface elevation,  $H_{m0}$  indicates energy-based wave height,  $T_p$  indicates peak spectral wave period, and  $\theta_p$  indicates wave direction in local polar convention (relative to shore-normal). The sign of the current value indicates current direction, with positive currents being northbound and negative currents being southbound. Again, all wave conditions were applied at 62 feet (19 meters) water depth, just offshore of the seaward end of the proposed channel. The third panel of each figure indicates the history of instantaneous channel infilling rate, expressed as the net volume of sediment deposited in the channel over one hour. The fourth panel presents the spatial distribution of channel infilling integrated over the duration of the simulation, indicating the net volume of sediment deposited in the channel per meter length of channel.

Figure 83 presents the input conditions and estimated channel infilling for Storm04 (August 28-31, 1962). The net infilling volume of this storm was approximately 129,000  $\text{cy}^3$  (98,500  $\text{m}^3$ ), representing the 10-year event for channel infilling. Notice that the channel infilling rate is correlated to the peak wave height and peak wave period. The spatial distribution of channel infilling for this storm is similar to the distribution of the 10-year synthetic storm, but the magnitude of net infilling volume is approximately half that of the 10-year synthetic storm. Note that the transport direction for this storm is north-to-south (as indicated by the current direction).

Figure 84 presents the input conditions and estimated channel infilling for Storm02 (October 27-31, 1996). The net infilling volume for this storm was approximately 636,000  $\text{cy}^3$  (487,000  $\text{m}^3$ ). This infilling volume was the largest among the 37 storms simulated and represents the 48-year return interval. Notice that the peak infilling rate roughly coincides with the peaks in wave height and wave period. Note that the transport direction for this storm (south-to-north) is opposite of the transport direction of the 10-year storm. The spatial distribution of infilling is noticed to be similar to the 50-year synthetic storm. Figures 85 through 87 present the return-interval information for the 28, 24, and 20-foot (8.5-, 7.3-, and 6.1-meter) terminal depth alternatives, respectively. There are six plots on each figure representing uncertainty in the infilling estimates. The “best” estimate of the model is represented by the square symbols labeled “fine sediment distribution.” These model results are based on the bed characterization utilizing the finest grain-size distributions indicated by the surface sediment samples. In each figure, the channel infilling volume is plotted versus the return interval for each of the 37 storms of the extremal analysis.

The 50-year channel infilling volume is approximately 636,000  $\text{yd}^3$  (487,000  $\text{m}^3$ ). As discussed previously, the bulk of the infilling occurs seaward of the three terminal depth

alternatives for the most severe storms, resulting in only small differences in infilling volume between the three alternatives. For the 10-year storm, the channel infilling volume ranges between 120,000 to 145,000 cy<sup>3</sup> (90,000 to 110,000 m<sup>3</sup>), resulting in approximately a 10 percent increase between the 28-foot and 20-foot (8.5-meter and 6.1-meter) terminal depth alternatives.

Note that at approximately the 3-year return interval, there is a change in slope in the infilling/return-interval relationship, and a tailing off of the infilling volume as return intervals decrease below 2 years. Some of this effect is associated with the thresholds of motion for lower wave energy storms, and another portion of the trend is suspected to be associated with the limited number of storms simulated. To adequately resolve the 1-year return interval would require the simulation of 75 to 100 storms from the hindcast record, which is beyond the scope of this study. However, there is sufficient information in the extremal analysis to develop rough estimates of the 1-year infilling volume. One approach of estimating the 1-year infilling quantity is to extend the nearly linear trend in the infilling/return-interval relationship between 2 and 4 years to intersect the 1-year return interval, resulting in an infilling quantity of approximately 1,300 to 2,000 cy<sup>3</sup> (1,000 to 1,500 m<sup>3</sup>). A second estimate from the synthetic storm simulations suggests that the channel infilling for the 1-year return interval is approximately 32,699 cy<sup>3</sup> (25,000 m<sup>3</sup>). Therefore, with the limited information available, the channel infilling volume associated with the 1-year return interval is estimated to be within the range of 1,308 to 32,699 cy (1,000 to 25,000 m<sup>3</sup>).

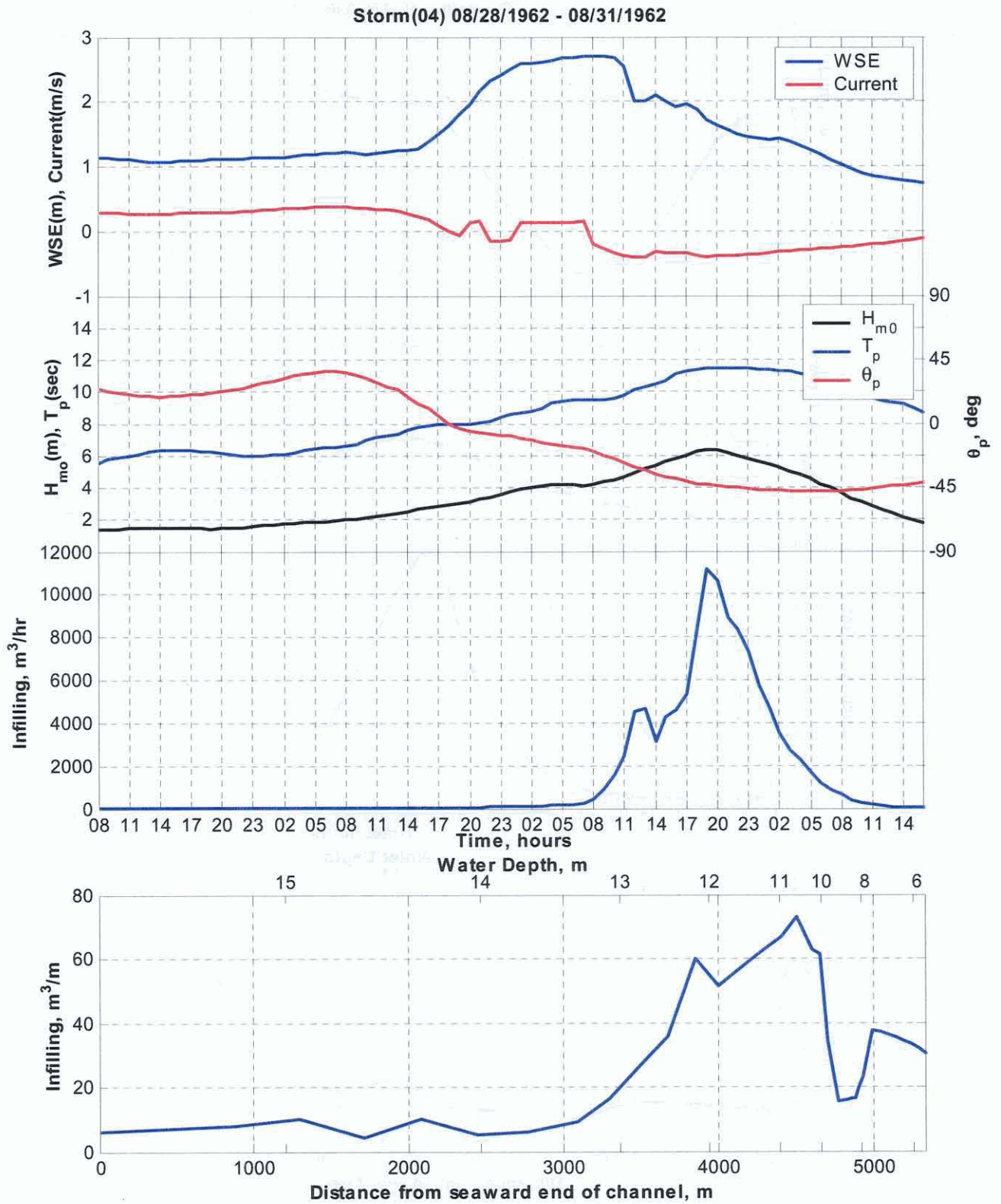


Figure 83. Input conditions and channel infilling for 10-year storm (Storm 04)  
 \* (1 m = 3.28 ft, 1 m/s = 1.9 knots, 1  $m^3/hr$  = 1.3  $yd^3/hr$ )

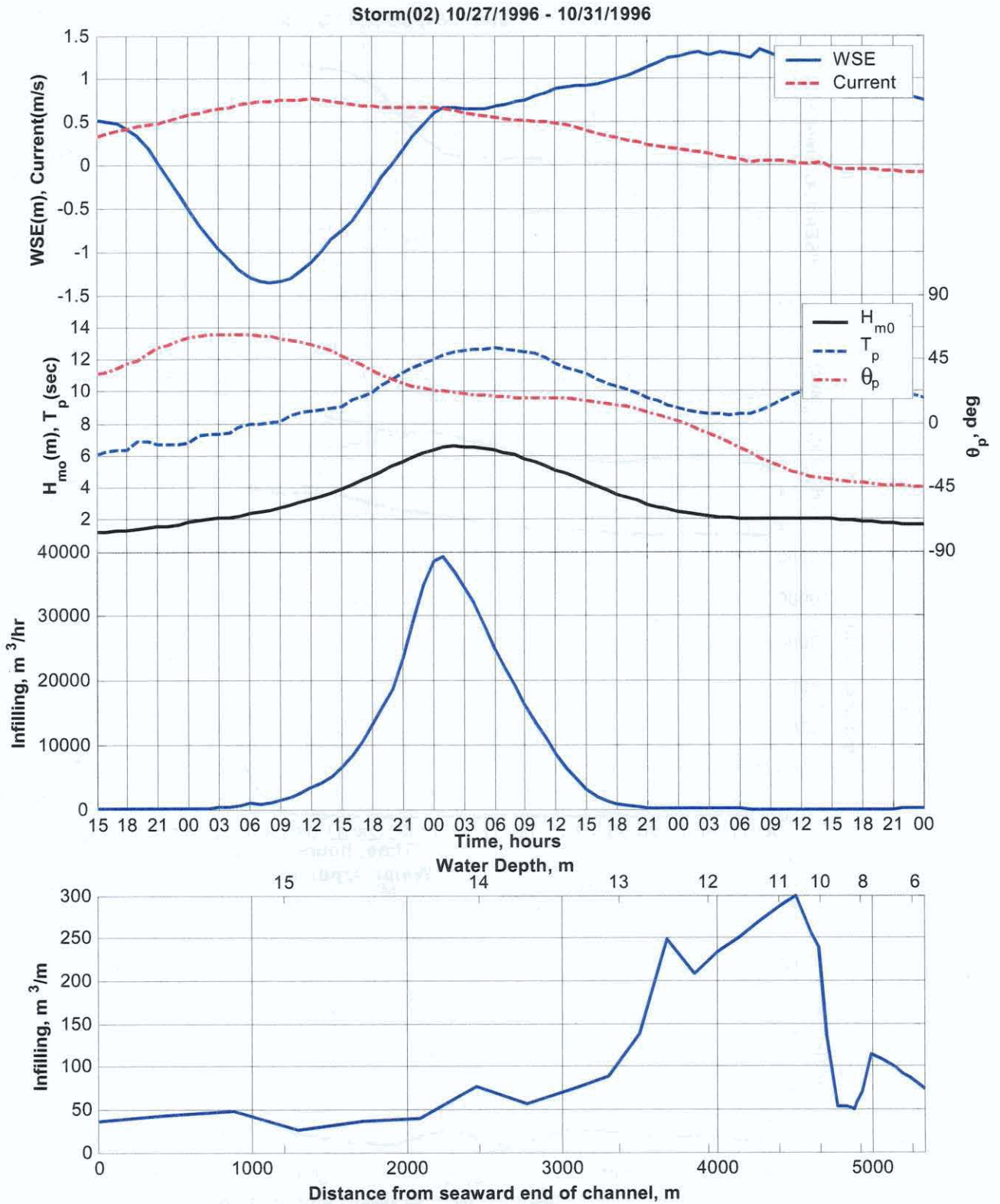


Figure 84 Input conditions and channel infilling estimates for 50-year storm (Storm02)

\* (1 m = 3.28 ft, 1 m/s = 1.9 knots, 1  $m^3/hr$  = 1.3  $yd^3/hr$ )

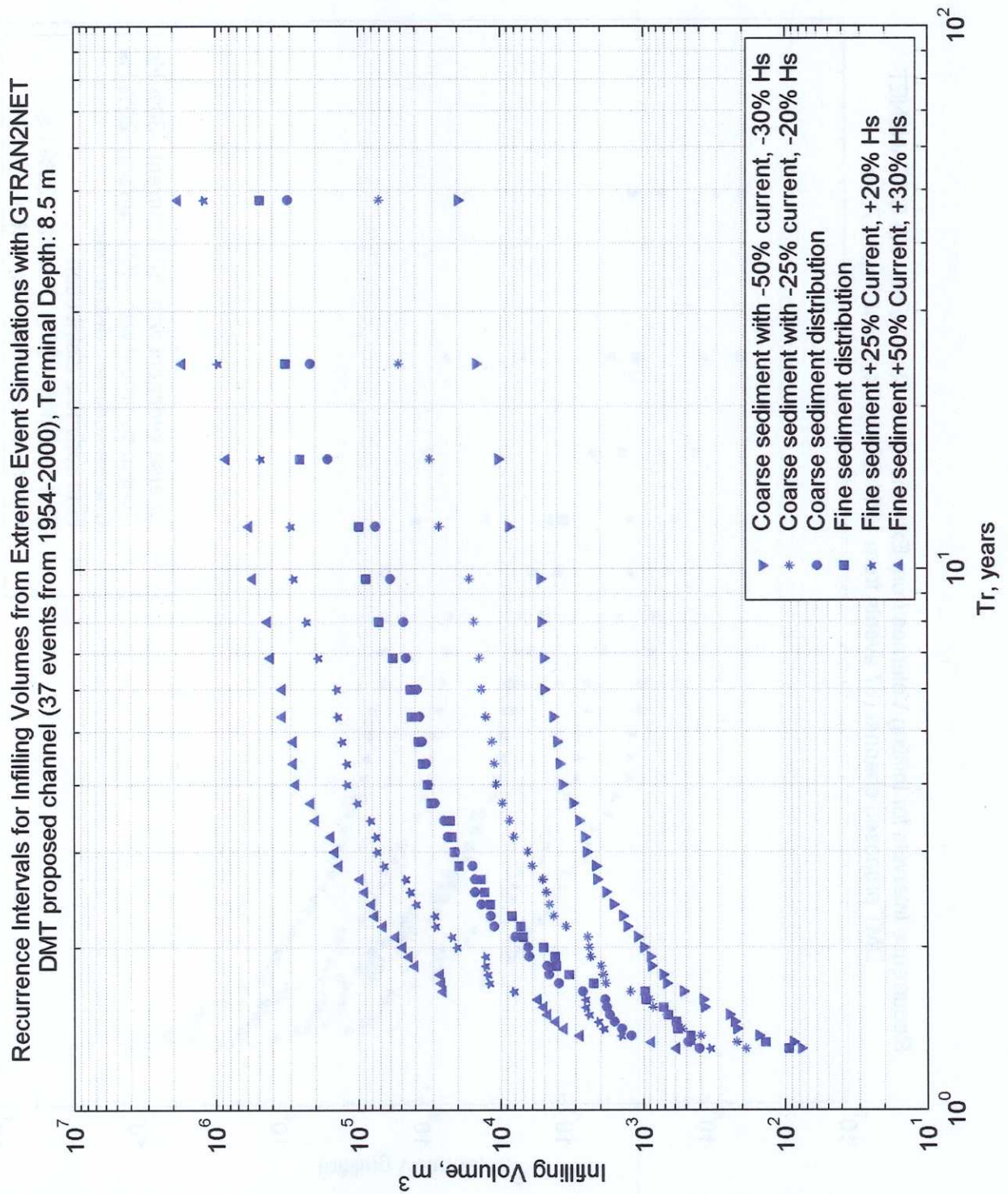


Figure 85 Frequency-of-occurrence relationships for channel infilling for the 28 foot (8.5-meter) terminal depth alternative.  
 \*(1 m<sup>3</sup> = 1.3 cy<sup>3</sup>)

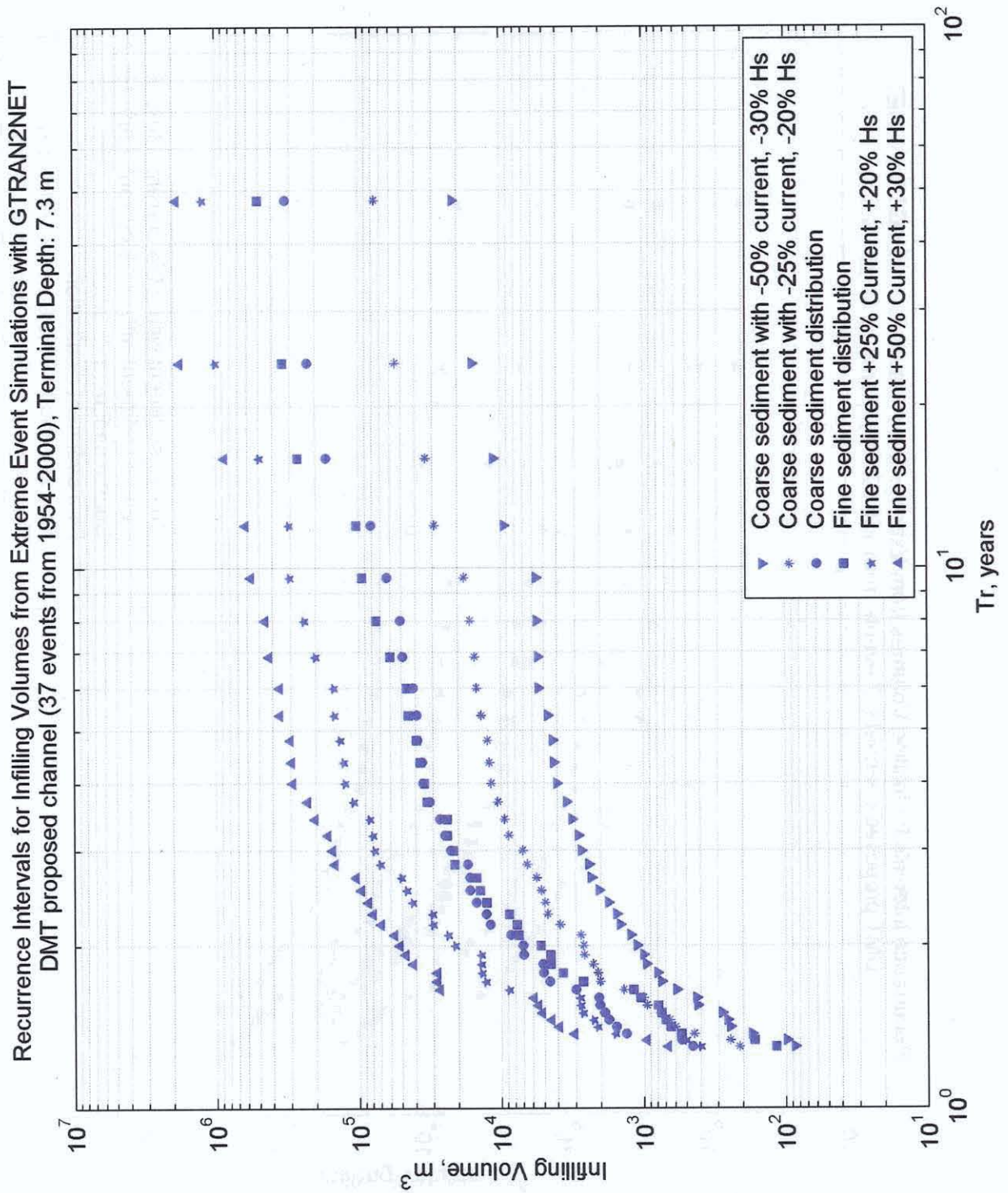


Figure 86 Frequency-of-occurrence relationships for channel infilling for the 24 foot (7.3-meter) terminal depth alternative.  
 \*(1 m<sup>3</sup> = 1.3 cy<sup>3</sup>)

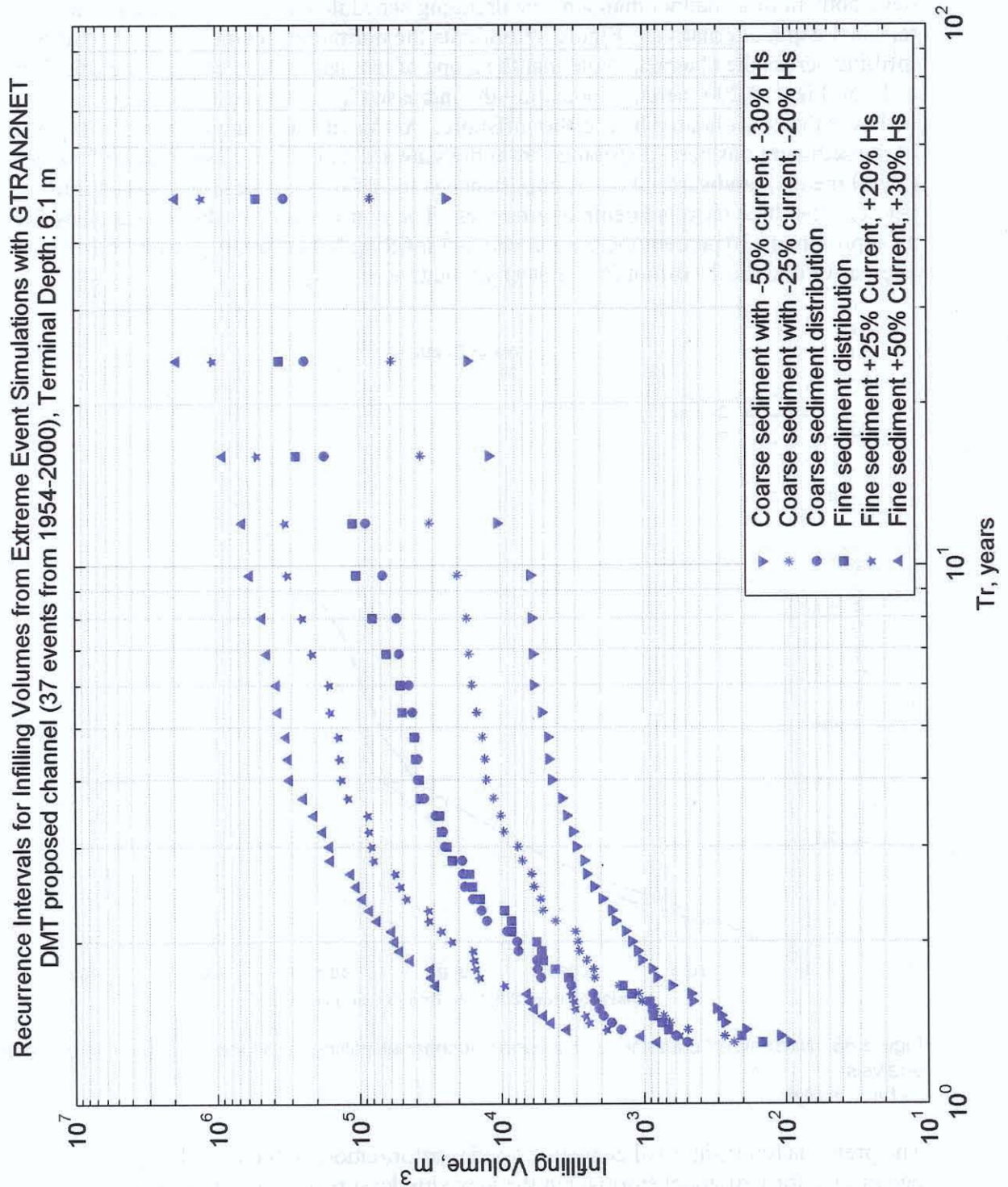


Figure 87 Frequency-of-occurrence relationships for channel infilling for the 20 foot (6.1-meter) terminal depth alternative.  
 \*(1 m<sup>3</sup> = 1.3 cy<sup>3</sup>)

The spatial distribution of channel infilling quantities is also of importance for development of a channel maintenance dredging schedule and consideration of the three terminal depth alternatives. Figure 88 presents the normalized cumulative distribution of infilling across the channel. Note that the slope of the distribution changes significantly at 10,500 feet (3,200 meters), indicating the increased infilling rate for the sand/gravel bed over the consolidated bed further offshore. At this distance approximately 30 percent of the sediment has been distributed from the seaward end of the channel to 10,500 feet (3,200 meters) landward. Also of importance is the relative increase in channel infilling between the three terminal depth alternatives. The normalized distribution suggests that an approximate 10 percent increase in channel infilling between the 28-foot (8.5-meter) alternative and the 20.0-foot (6.1-meter) alternative.

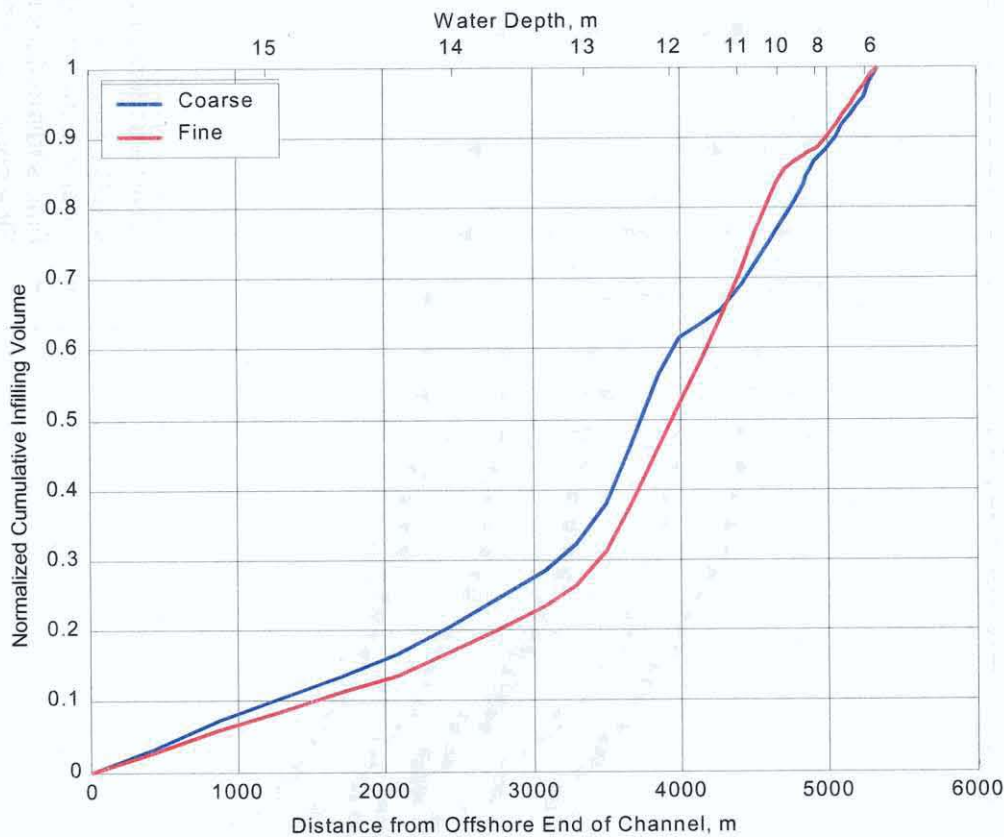


Figure 88. Normalized cumulative distribution of channel infilling for all storms in the event-based analysis

\* (1 m = 3.28 ft)

The previous return-interval analysis provides information on the probability of occurrence for individual storms, but the wave hindcast record suggests that cycles of increased storm activity exist. Table A-30 presents monthly and annual summaries of channel infilling during the 16-year hindcast period (1985-2000). The years 1985-2000 were selected because of the continuous record of wave hindcast conditions and the inclusion of the lower-return-interval storms. Two channel infilling estimates are presented that represent the best infilling estimate and an estimate that reflects an upper

Draft Feasibility Report  
Appendix A: Hydraulic Design, Delong Mountain Terminal, Alaska

bound of anticipated uncertainty. Note in the table, the wide variability in annual infilling rates from storms. The average annual infilling for the 16-year record is 75,000 to 211,000 cubic yards (57,000 to 162,000 cubic meters), but the maximum annual infilling volume is 805,000 to 2,080,000 cubic yards (615,000 to 1,590,000 cubic meters). There is also significant variation in the monthly infilling volumes, with storms during the months of October and November producing the highest infilling volumes.

**TABLE A-30. Monthly and Annual Summaries of Estimated Channel Infilling for the -20 foot (-6.1 meter) alternative) from Event-Based Analysis**

Year	Best Estimate of Channel Infilling, yd <sup>3</sup> (m <sup>3</sup> )						Estimate of Upper Bounds of Infilling, yd <sup>3</sup> (m <sup>3</sup> )					
	Jul	Aug	Sep	Oct	Nov	Annual	Jul	Aug	Sep	Oct	Nov	Annual
1985	0	0	0	8,305 (6,3501)	0	8,305 (6,350)	0	0	0	24,695 (18,881)	0	24,695 (18,881)
1986	0	0	0	0	0	0	0	0	0	0	0	0
1987	0	0	0	0	0	0	0	0	0	0	0	0
1988	0	980 (749)	0	0	0	980 (749)	0	2,396 (1,832)	0	0	0	2,396 (1,832)
1989	0	0	0	4,112 (3373)	0 (0)	4,112 (3373)	0	0	0	20,667 (15,801)	0	20,667 (15,801)
1990	0	1127 (862)	0	0	127,606 (97,562)	128,734 (98,424)	0	3,991 (3,051)	0	0	420,077 (321,172)	424,069 (324,224)
1991	0	0	0	77,885 (59,547)	0	77,885 (59,547)	0	0	0	255,368 (195,243)	0	255,368 (195,243)
1992	0	0	0	29,154 (22,290)	0	29,154 (22,290)	0	0	0	111,560 (85,294)	0	111,560 (85,294)
1993	0	1,853 (1,417)	883 (675)	1,197 (915)	35,602 (27,220)	39,535 (30,227)	0	12,469 (9,533)	4,073 (3,114)	3,382 (2,586)	108,890 (83,252)	128,815 (98,486)
1994	0	1,154 (882)	0	5,520 (4,220)	0	6,674 (5,102)	0	3,153 (2,411)	0	18,760 (14,343)	0	21,912 (16,753)
1995	0	0	0	0	0	0	0	0	0	0	0	0
1996	12,427 (9,501)	0	0	680,355 (520,169)	112,260 (85,829)	805,042 (615,499)	42,532 (32,518)	0	0	1,658,073 (1,267,688)	376,686 (287,997)	2,077,291 (1,588,203)
1997	0	0	0	11,193 (8,558)	83,832 (64,094)	95,025 (72,652)	0	0	0	34,751 (26,569)	279,172 (213,442)	313,923 (240,011)
1998	0	0	0	0	0	0	0	0	0	0	0	0
1999	0	0	0	0	0	0	0	0	0	0	0	0
2000	0	0	0	0	0	0	0	0	0	0	0	0
<b>AVG</b>	<b>777 (594)</b>	<b>319 (244)</b>	<b>55 (42)</b>	<b>51,126 (39,089)</b>	<b>22,456 (17,169)</b>	<b>74,734 (57,138)</b>	<b>2,658 (2,032)</b>	<b>1,376 (1,052)</b>	<b>255 (195)</b>	<b>132,953 (101,650)</b>	<b>74,051 (56,616)</b>	<b>211,294 (161,546)</b>

### 7.9.3 Sensitivity and Uncertainty

Sensitivity and uncertainty of the channel infilling model to anticipated uncertainties in the sediment characteristics, wave conditions, and current conditions was investigated by a sensitivity analysis. The sensitivity analysis involved repeating model simulations with modifications in the input parameters to represent the anticipated uncertainty in the model input.

The first variation in model input parameters involved the cross-shore specification of grain-size distributions. Variations in sediment grain-size distributions were evident in the sampling of the 1998 and 2000 surface sediment samples. To account for this

variability, the minimum and maximum distributions at each sampling depth were compiled to develop two cross-shore distributions of grain size, one with finer sediment and one with coarser sediment. These two distributions are indicated in Figures 85 through 87 by the circle and square plots. These two simulations include no uncertainty in the wave and current conditions.

To assess the maximum ranges of uncertainty in the wave and current conditions, the wave and currents were collectively varied by estimated ranges of uncertainty. Comparisons of ADCIRC-simulated currents to the relatively mild conditions of the 1998-2000 field measurements indicate that the model is accurate to within  $\pm 50$  percent. For more energetic conditions model accuracy is estimated to be on the order of  $\pm 25$  percent. Comparisons of WAM-estimated wave heights to available wave data indicate more favorable agreement, and the maximum model uncertainty is estimated to be on the order of  $\pm 20$ -30 percent. To estimate the maximum uncertainties in the channel infilling quantities, the estimated uncertainties in the current and the waves were applied as uniform biases and also applied in an additive fashion such that higher values of current correspond to higher values of wave height and vice versa. The inner bands of values (representing  $\pm 25$  percent current and  $\pm 20$  percent wave height) generally indicate a factor-of-5 uncertainty. The outer bands of uncertainty (representing  $\pm 50$  percent current and  $\pm 30$  percent wave height) generally indicate a factor-of-10 uncertainty. This is illustrated in figures 85 through 87 by the star and triangle plots. In each figure, the channel infilling volume is plotted versus the return interval for each of the 37 storms of the extremal analysis. The best estimate was used for the maintenance analysis presented later.

## 7.10 Infilling Under Ice Cover

The nearshore current measurements suggest that the currents under ice cover are typically much less than the critical velocities to produce sediment transport. However, measurements indicate that near-bottom, under-ice currents may reach velocities in excess of 1.9 knots (1 m/s) for up to a day in duration. These large, observed currents were directed offshore and are suspected to be associated with breaks, or leads, in the ice cover. There are no long-term statistics available for the occurrence of such phenomena at the DMT site, but the large, under-ice currents were observed in only one of the three winter deployments of the current meters. To assess the significance of such flows on channel infilling, sediment transport calculations were performed with the Van Rijn (1984) transport method for current-dominated regimes.

The integrated sediment transport over the duration of the simulation amounts to 410 ft<sup>3</sup>/ft (38 m<sup>3</sup>/m) for the 0.0055 inches (0.14-mm)  $d_{50}$ , and 2.48 ft<sup>3</sup>/ft (0.23 m<sup>3</sup>/m) for the 2.6-mm  $d_{50}$ . Put in terms of seaward displacement of the channel, if the channel is assumed to be approximately 32.8 feet (10 meters) deeper than the ambient bathymetry, 410 ft<sup>3</sup>/ft (38 m<sup>3</sup>/m) of infilling would result in a cross-shore migration of the channel terminus by approximately 13.1 feet (4 meters), a relatively small distance.

There are limited data to define the frequency of occurrence and magnitude of high-velocity, under-ice currents. The calculations and corresponding estimates of channel infilling from such flows are based on a single observation. Assuming that the observed event is representative of flows caused by surface ice leads, sediment transported by these events is not expected to produce significant infilling of the channel.

## 8.0 CHANNEL DESIGN

The purpose of dredging the channel is to directly load vessels from the concentrate conveyor, thereby removing the extra handling of the material that is currently occurring. The channel would also provide a means to import fuel to the area on tanker ships rather than on barges. The ultimate selection of a channel alternative requires the comparison of channel construction and maintenance costs to the transportation benefits for each different draft loading case. It is necessary to study constructible channel depths, which accommodate desired vessel draft.

### 8.1 Design Vessel Criteria

Design vessels are determined by examining the size of ships currently calling at the DeLong Mountain Terminal and those that can be reasonably expected to use the terminal in the future. The design vessel used is a joint decision made by engineering and economics.

The design vessel used for design considerations in engineering the channel is a 75,000 Dead Weight Ton (DWT) (68,000 meter-ton) Panamax bulk carrier with a fully loaded displacement of 45 feet (13.7 meters). The fuel bulk carrier used in design is a 30,000 DWT (27,200 meter-ton) bulk carrier with a loaded draft of 33 feet (10 meters). Vessels of this type currently call at the DMT and are expected to continue calling at the site. Pertinent information on the design vessel is shown in table A-31. Discussion on these vessels can be found in the economics appendix of this Feasibility Study.

**TABLE A-31. Design vessels for deepening and widening**

	Design Vessel – Panamax carrier	Design Vessel – Fuel bulk carrier
Length Overall ft (m)	781 (238)	593 (180)
Beam ft (m)	107 (32.6)	107 (32.6)
Loaded Draft ft (m)	45 (13.7)	33 (10.0)
30% Ballast Draft ft (m)	22 (6.7)	17 (5.2)

### 8.2 Configuration and Use

The channel design (figures 89 and 90) is a straight channel that expands from 500 feet to 760 feet where it becomes asymmetric with an expansion to 800 feet north of the centerline at the inshore end. A turning basing is located south of the asymmetric channel expansion. The channel leads to a berth on the north side of the concentrate conveyor. The prevailing current along the coast is to the north. With this in mind, the berth was placed north of the trestle to allow easier departure of the loaded ships. Berth configurations on the north and south of the trestle were tested during ship simulation at

Draft Feasibility Report  
Appendix A: Hydraulic Design, DeLong Mountain Terminal, Alaska

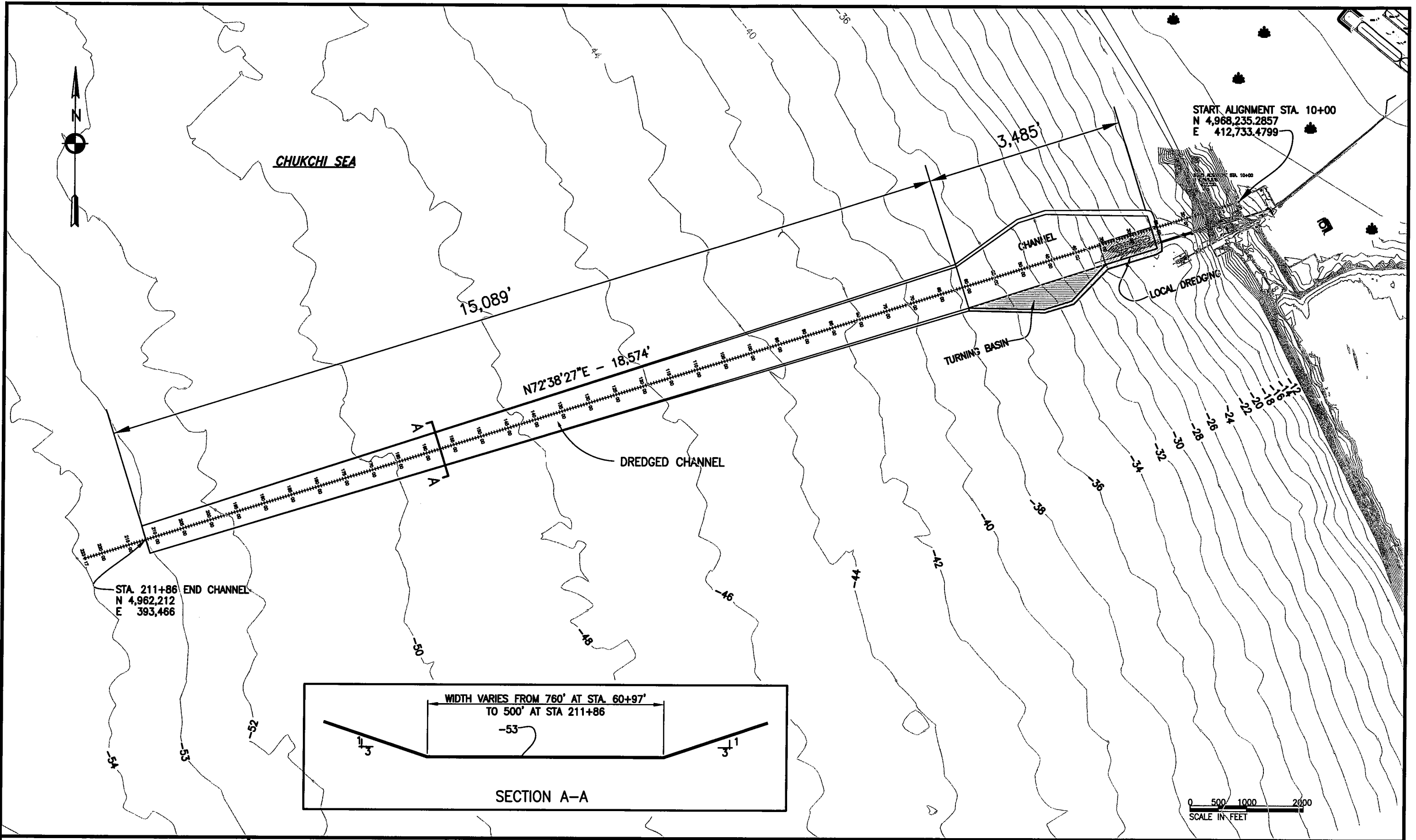
the Coastal Hydraulics Laboratory. A south-berthing configuration resulted in the ship being pushed against the dock during a majority of the time and resulted in the ship being pinned at the dock when currents were strong from the south during the ship simulation.

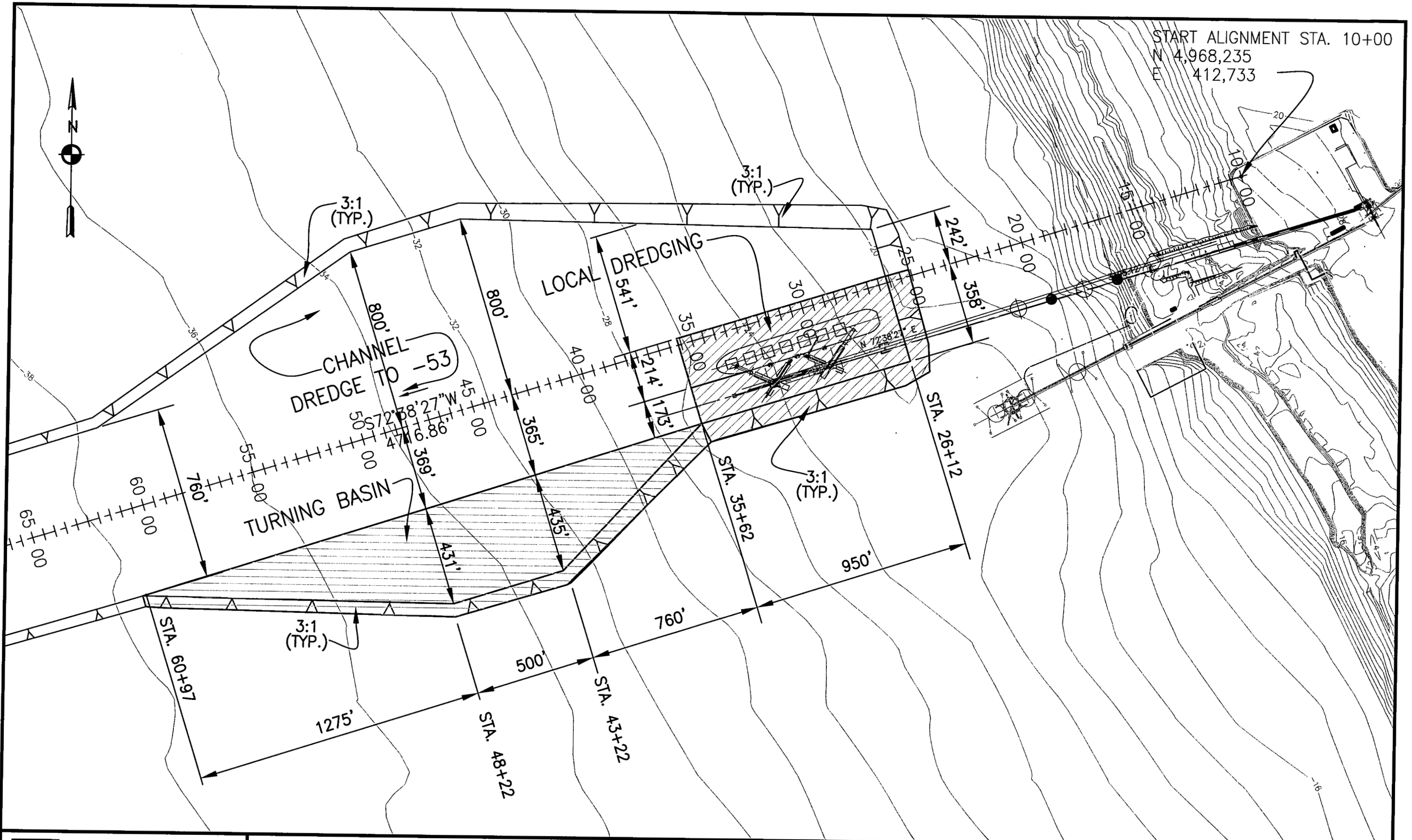
Departing loaded ships were used in the simulator and the tracks of the departing Panamax vessels established the navigation boundaries. The channel centerline begins at Station 10+00, with coordinates of N 4,968,235 E 412,733, and extends seaward on a bearing of N72°38'27"E. Station 10+00 is located on a bearing of 209°20'00" 54 feet from the northern most corner of the north Portsite dormitory/office complex. The seaward end of the channel begins at station 211+86 where it is established with widths perpendicular to centerline on 250 feet north and 250 feet south. The channel widens as it approaches shore to 380 feet north and 380 feet south of the channel centerline at station 60+97 (figure 90). The southern portion of the channel is tapered to 358 feet at station 35+62 where a 950-foot long by 214 foot wide mooring basin is located. The northern portion of the channel is widened to 800 feet at station 48+22 and maintains that width to station 43+22. From there it narrows to 242 feet at station 26+12.

South of the channel a turning basin is established beginning at station 60+97, widening to 431 feet at 48+22. The basin expands to a width of 435 feet at station 43+22 as a result of the channel tapering where it ties back into the channel at station 35+62.

Concentrate ships using the channel would enter the channel ballasted at drafts of approximately 22 feet. They would proceed to a turning basin where, with the tug assistance, they would turn 180 degrees and back into the berth. The loaded ship would leave the berth and proceed, with tug assistance, out of the channel. On occasion partially loaded ships may have to leave the berth due to anticipated weather conditions. In that case, after the storm, the partially loaded ship would have the option to return to the berth for final loading. The partially loaded ship would enter and berth in the same manner as an empty ship. In that case the turning basin would have to accommodate the draft of a partially loaded vessel.

Fuel ships would enter the channel loaded or partially loaded with drafts of approximately 33 feet (10 meters). They would turn in a similar manner to the ballasted Panamax with tug assistance in the turning basin and back into the berth. These ships would depart the site empty.





### 8.2.1 Channel Width

USACE guidance (EM 1110-2-1613) sets the channel at a width of 535 feet (163 meters) based on one way traffic, variable trench cross section, average aids to navigation, and currents upwards of 1.5 knots. The higher current range was used due to minimal current data at the site. Anecdotal information indicates that very strong currents (stronger than those measured to date) are experienced along the coast. These design criteria produce beam multiplier of 5. A beam of 107 feet (33 meters) and a multiplier of 5 produces a channel width of 535 feet (163 meters).

The channel width was checked using Permanent International Association of Navigation Congresses (PIANC) guidance. The PIANC width detailed in table A-32 shows the need for an approximate width of 600 feet (183 meters).

Condition	Site Description	Width Factor
Vessel Speed (knots)	slow (5-8)	0B
Prevailing Cross Wind (knots)	moderate 15-33	0.5B
Prevailing Cross Current (knots)	strong 1.5-2.0	1.3B
Prevailing Longitudinal Current (knots)	low $\leq 1.5$	0B
Significant Wave Height and Length (m)	$3 > H_s > 1$ and $\lambda = L$	0.5B
Aids to Navigation	moderate with infrequent poor visibility	0.2B
Bottom Surface	$< 1.5T$ and smooth	0.1B
Depth of Waterway	$< 1.25T$	0.2B
Cargo Hazard Level	Medium	0.5B
Additional Width for Bank Clearance (2x)	Sloping channel edges	0.6B
Basic Ship Maneuvering Lane	Poor Ship Maneuverability	1.8B
B=107	Total	5.7B
Width = 610 feet		

The final channel design is 500 feet (152.4 meters) at the seaward end to take advantage of the ship's speed and maneuverability at the seaward end. The channel increases to 760 feet (231.6 meters) at Station 60+97 as it extends shoreward to account for the decreased ship speed and maneuverability nearshore and the need for tug assisted or tug powered transit. Several unique conditions challenge the navigation in the channel. Currents perpendicular to the channel, adverse winds and an extremely short navigation period are part of the site conditions. The economic impact of not fully loading vessels and the costs associated with departing the dock and returning to dock under adverse weather conditions leads to an expectation that vessels will be retained in a loading configuration up until weather absolutely dictates leaving the dock. These adverse weather conditions

were considered in the simulation and the channel dimensions were set to allow safe transit of the channel. Ship transits were checked at both the 20-knot and 30 knot wind speeds. As a minimum two 4,000 horsepower tractor tug boats or three 3,000 horsepower tractor tugboats are necessary for safe navigation of the channel as shown in the ship simulation section of this appendix.

### **8.2.2 Channel Depth**

Vessels moving in navigation channels must maintain clearance between their hulls and channel bottom; accordingly, various navigational design parameters were analyzed. These design parameters such as squat, safety clearance, vertical motion due to waves, and water density effects were totaled and added to determine the minimum under-keel clearance. The final channel depth at the site is determined by the economic benefits of fully loading a ship versus partially loading a ship, and channel access 100 percent of the time versus limited access during negative surge events.

Considerations for channel design follow the standards of Engineering Manual (EM) 1110-2-1613, "Hydraulic Design of Deep-Draft Navigation Projects," and were checked against PIANC guidance. The first consideration is to define the fleet of vessels likely to use the prospective channel. Vessels now serving the DeLong Mountain Terminal include Panamax and handy sized bulk carriers. Dimensions of vessels representative of the fleet to call are presented in table 31. The dimensions chosen for the design vessel are a length over all (LOA) of 738 feet (225 meters), a beam (width) of 107 feet (32.6 meters), and a static draft of 45 feet (13.7 meters) in the Chukchi Sea.

Figure 91 illustrates the increments of channel depth design. The optimum elevation of an excavated channel bottom is determined by economic criteria.

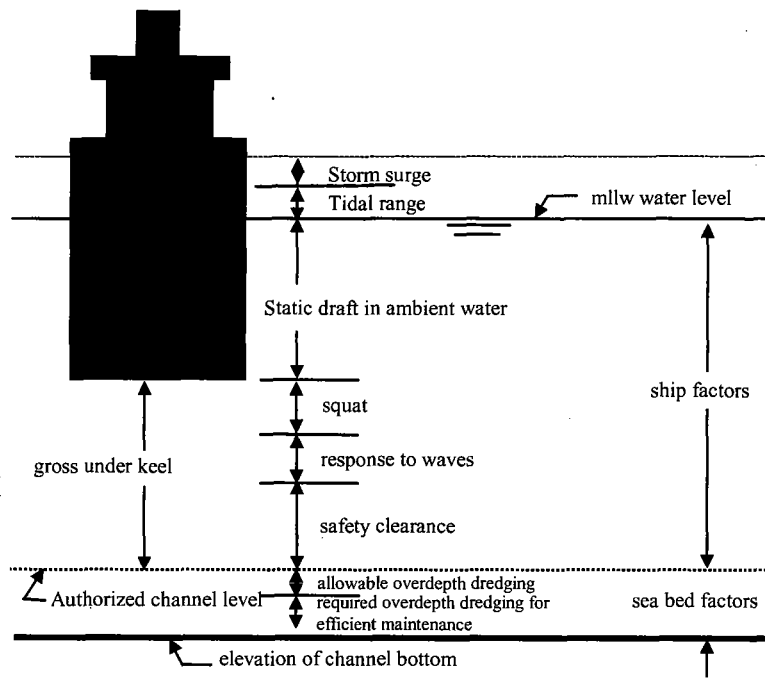


FIGURE 91. Channel depth design factors.

### 8.2.3 Ships Factors

**Draft.** Vessels now serving the DMT anchor at least 3 miles (4.82 km) from the barge loading pier in water depths of 50 to 72 feet (15.2 to 21.9 meters). Instructions to the ship masters calling on the DMT are that ships with drafts of up to 45 feet (13.7 meters) are intended to have an under-keel clearance of no less than 10 feet (3 meters). The maximum draft of ships that will serve the DMT is assumed not to exceed 45 feet (13.7 meters).

**Squat.** Vessel draft increases when vessel sailing depth adjusts to the energy balance between hydrostatic and kinetic energy due to the fluid velocity around and under the vessel hull. It is pulled down into the water column by the hydrodynamic pressure gradient. This phenomenon and related vertical hydrodynamic effects are defined here as "squat," which varies with vessel speed, water depth beneath the keel, and the ratio of the vessel cross-section area to the cross-section area of the channel. Computations for prediction of squat assume a channel width of 560 feet (171 meters), water depth of 53 feet (16.2 meters), vessel beam of 107 feet (32.6 meters), vessel draft of 45 feet (13.7 meters), and vessel speed of 8 knots. USACE calculations predict 1.3 feet (0.4 meters) of squat with these conditions. PIANC calculations also predict indicate that 1.9 feet (0.58 meter) of squat. A squat allowance of 2.0 feet (0.61 meter) for the DMT channel is estimated for the design ship. This squat value was also applied to the vessels in the turning basin and channel near the berthing area, as the ship must maneuver at near full power resulting in displacement of a vast amount of fluid. Even though the ship is not

operating at high relative bottom speed, the fluid motion around the hull is similar to a vessel traveling at high speed.

**Response to Waves.** USACE guidance estimates the effect of pitch, roll, and heave as being 0.5 to 2 times the wave height with a model estimate of 1.196 times the wave height. The USACE values were obtained from a Columbia River study, which primarily addressed long period waves. The wave hindcast indicated that the wave climate at the Ports site is generally comprised of young, short-period waves with wavelengths shorter than the design ship length. To account for this environment the pitch component of the USACE guidance was not included in the evaluation. This resulted in a ship excursion below the water surface of 0.70 times the wave height and resulted in 4-foot excursion below the water surface. During a previous ship simulation study performed by the sponsor, the ship excursion below the water surface was determined to be 2 feet (0.61 meter) in response to waves. To account for the conservative nature of the USACE calculations and the limited scenarios of the ship simulation study, the average between the ship simulation study and USACE guidance was used for a response to wave depth design value of 3 feet.

**Safety Clearance.** USACE guidance suggests a minimum net under-keel clearance of 2 feet (0.61 meter); however, for hard bottom conditions such as rock, consolidated sand or clay, 3 feet (0.91 meter) of net under-keel clearance is recommended. The channel bottom has been described in the geotechnical analysis as medium to dense material consisting of silt, sand, and gravel. Based on the description of the material and the geotechnical sampling data, a safety factor of 3 feet (0.91 meter) was used for this analysis.

**Set Down.** Modeling results indicate that severe set down events of up to 11.5 feet (3.5 meters) lasting for 12 hours are possible in the fall months. These events are more prevalent in the fall and are generally outside the shipping season window. By keeping the berthing area depth the same as the channel depth, set down events up to 5 feet during the shipping season can be tolerated by a ship at the dock and leave a 3 foot safety clearance.

**Total Clearance.** The subtotal of squat, response to waves, and safety clearance for the channel provides a design depth of 8.0 feet (2.4 meters). The sum of ship factors (figure 90) is 53 feet (16.2 meters) for the channel turning basin, and berthing area.

Dredging equipment and procedures cannot provide a smoothly excavated bottom at a precisely defined elevation. One foot (0.3 meter) of allowable over depth dredging was added to the target depth of excavation to guarantee mariners a least-depth equivalent to the sum of ship factors.

#### **8.2.4 Channel Location**

The channel for access to the DMT is nearly perpendicular to the bathymetry contours. Previous studies on vessel motion indicated that a parallel-to-shore berth orientation

would result in vessel motion problems from wave activity as well as concern for vessel docking and departure procedures.

### 8.2.5 Turning Basin

The ship pilots were very uncomfortable with a docking scenario that left the ship stern seaward at the berth. They preferred the ship bow to face seaward for a quick departure in the event that weather conditions made it unsafe to remain at the dock. The presence of the turning basin in the channel allows fully loaded fuel tankers and Panamax bulk carriers to approach the dock and turn and dock with the bow forward.

The ballasted ships transiting the channel provide a high profile for impact from the wind. Tracks from the ship simulation indicate that the full turning basin is needed to be able to turn and dock a ballasted ship during high wind and moderate current events. This is not an unlikely scenario since wind conditions at the site are highly variable and can build and die off quickly. Providing the ship the ability to transit the channel in a high wind, moderate current event allows the ship to transit the channel without the concern of being caught mid channel in a high wind event. Figure 94 shows a ship transiting the channel during a high wind, moderate current. The entire width of the turning basin is used for the turning maneuver.

### 8.2.6 Sideslopes and Bank Stability

The initial channel would be dredged with a side slope of 1 vertical to 3 horizontal. The material to be dredged has been characterized as medium to firm material with pockets of soft material. It is anticipated that this material will lay back on a 1 vertical to 10 horizontal slope in the short term. The channel is aligned such that the 1 vertical to 10 horizontal slope will not impact the existing sheet pile at the site. Over the long run the channel slope will likely lay back on slopes that are similar to the local subsurface conditions. In the event that this occurs, maintenance to stabilize the slope may be necessary to prevent further layback. This maintenance is not recommended until the channel slope has eroded to a 1 vertical to 10 horizontal slope. This scenario is viewed to be so far into the future that maintenance and maintenance costs associated with it are not addressed in this analysis.

## 8.3 Initial Dredging Quantity

The initial dredging quantity would vary with channel depth and location. Table A-33 shows the channel quantities associated with each scenario. The quantities presented include a one-foot dredging tolerance.

<b>TABLE A-33. Initial Dredge Quantities</b>		
Dredge Start Contour [feet] (meters)	Dredge Depth [feet] (meters)	Initial Construction Dredge Quantity [cy] (m <sup>3</sup> )
-28 (-8.5)	-53 (-16.2)	5,060,000 (3,868,648)
-26 (-7.9)	-53 (-16.2)	5,170,000 (3,952,749)

<b>TABLE A-33. Initial Dredge Quantities</b>		
Dredge Start Contour [feet] (meters)	Dredge Depth [feet] (meters)	Initial Construction Dredge Quantity [cy] (m <sup>3</sup> )
-24 (-7.3)	-53 (-16.2)	5,590,000 (4,273,862)
-22 (-6.7)	-53 (-16.2)	6,060,000 (4,633,202)
-20 (-6.1)	-53 (-16.2)	6,240,000 (4,770,822)
-28 (-8.5)	-50 (-15.2)	3,630,000 (2,775,334)
-26 (-7.9)	-50 (-15.2)	3,730,000 (2,851,790)
-24 (-7.3)	-50 (-15.2)	4,130,000 (3,157,612)
-22 (-6.7)	-50 (-15.2)	4,580,000 (3,501,661)
-20 (-6.1)	-50 (-15.2)	4,750,000 (3,631,636)
-28 (-8.5)	-47 (-14.3)	2,460,000 (1,880,805)
-26 (-7.9)	-47 (-14.3)	2,550,000 (1,949,615)
-24 (-7.3)	-47 (-14.3)	2,910,000 (2,224,855)
-22 (-6.7)	-47 (-14.3)	3,330,000 (2,545,968)
-20 (-6.1)	-47 (-14.3)	3,480,000 (2,660,651)

The volume of dredge material produced by various turning basin depths was analyzed and is shown in table A-34.

<b>Table A-34. Turning Basin Quantities</b>		
Vessel	Turning Basin Depth [ft]	Dredge Volume [cy]
Loaded Fuel Tanker	42.5	295,000
Empty Panamax	31.5	20,000
Partially Loaded Panamax	51	500,000
Full channel depth	53	555,675

## 8.4 CHANNEL NAVIGATION

### 8.4.1 Analysis of Currents With Respect to Navigation

Frequency-of-occurrence statistics were computed using the depth-averaged current, the current in the upper bin, and an average current representing the upper 13.1 feet (4 meters) of the water column. Table A-35 shows statistics that reflect a composite of all three open-water seasons (July through October) for the period 1998-2000, without regard to current direction. Monthly statistics were computed, and then weighted in the computation of open-water-season statistics to account for the fact that, during some years, data were not acquired in some months. Table A-36 lists the number of days currents flows were exceeded for the record of measured data. The measured data indicate that the higher velocity currents predominantly occur when the flow direction is from south to north.

The depth-averaged current speed exceeded 1.0 knot (0.5 m/sec) less than 2 percent of the time; and exceeded 0.5 knots (0.25 m/sec) 25 percent of the time. The surface current speed (top bin), which for most open water situations was the maximum speed in the water column, exceeded 1.5 knots (0.75 m/sec) less than 2 percent of the time; exceeded 1.0 knot (0.5 m/sec) about 11 percent of the time; and 0.5 knots (0.25 m/sec) 41 percent of the time. Depth-averaged current never exceeded 1.6 knots (0.8 m/sec) in the measured data record. The measured surface current did not exceed 2.2 knots (1.15 m/sec). It is worth noting that these statistics are based on a limited data record, and the years 1998-2000 may have been less energetic than other years.

Current Speed (m/sec)	Frequency of Exceedance (%)		
	Depth-Averaged	Average-Top 13.1 ft (4 m)	Surface Current
1.0 (2 knots)	0.00	0.02	0.03
0.9	0.00	0.1	0.3
0.8	0.01	0.5	0.9
0.75 (1.5 knot)	0.01	0.9	1.6
0.7	0.02	1.6	2.7
0.6	0.4	3.9	5.6
0.5 (1 knot)	1.8	8.8	11.0
0.4	6.3	16.4	19.5
0.3	17.0	28.3	31.8
0.25(0.5 knot)	25.0	37.0	40.7
0.2	35.2	46.3	50.8
0.1	64.0	72.6	76.8

	Current Flow From South to North [days]				Current Flow From North to South [days]
	≥0.75 knot	≥1 knot	≥1.25 knot	≥1.5 knot	≥0.75 knot
July 1998	3	2	0	0.25	0
August 1998	12	7	3	1	1.5
September 1998	5	3	0	0.25	0.75
October 1998	6	3	0	1	0
November 1998	0	0	0	0	0
October 1999	3	0.75	0	0	0
November 1999	0.25	0	0	0	0
August 2000	13	7	2	0.75	0
September 2000	4	0.25	0	0	0

### 8.4.2 Joint Probability of Currents and Wind

The combined influence of wind and current on vessels transiting the navigation channel and operations within the turning basin is of concern for project operation. The joint probability of the alongshore component of wind and alongshore-directed current was examined to assess the operating conditions of a ship in the channel. The average current in the upper 13.1 feet (4 meters) of the water column was used as the measure of current speed in the following discussion. The upper 13.1 feet (4 meters) of the water column

rather than the mid or entire water column was evaluated to add a degree of conservatism to a sparse current data set.

The source of wind data was wind speed from the hindcast. The current data were from the concatenated record representing the open water seasons. All current data outside the months of July-October were excluded from the analysis. Current data were available with 20-min resolution, and were paired to the wind data where current data were available. The wind speed is the alongshore component of wind, or the wind that would be acting on the beam of a vessel navigating the channel, which is nearly perpendicular to shore. Since the current was observed to flow along the coast, the current speed was not modified for direction.

Table A-36 shows the joint probability of the alongshore component of wind speed and the alongshore-directed current speed for all wind conditions for the 1998-2000 open-water seasons. Wind and current data are displayed in knots.

As an example of how to interpret information in table A-37, 13 percent of the time the wind speed is between 8 and 12 knots and the current speed is less than 0.5 knot. For 1.7 percent of the time, the wind speed is between 16 and 20 knots and the current speed is between 1.0 and 1.5 knots. By summing across a current-speed row, one can estimate the total percentage of time that the current is between certain speeds. For example, the current is between 0.5 and 1.0 knots, about 28.1 percent of the time, and less than 0.5 knot about 62.8 percent of the time.

**TABLE A-37. Joint Probability - Alongshore Wind and Current, in percent**

Current Speed (knots)	Wind Speed (knots)								
	4.0	8.0	12.0	16.0	20.0	24.0	28.0	32.0	36.0
2.5	0.0	0.0	0.0	0.0	0.0	0.0	0.0	0.0	0.0
2.0	0.0	0.2	0.1	0.0	0.2	0.3	0.2	0.0	0.0
1.5	0.7	0.8	1.9	1.2	1.7	1.4	0.5	0.1	0.1
1.0	0.6	1.9	6.7	5.5	6.6	4.5	1.5	0.6	0.2
0.5	2.8	10.7	13.0	12.8	12.9	7.5	1.9	1.1	0.1

By summing down a column, or columns, one can estimate the percentage of time the alongshore component of wind speed is in a certain range, or less than a certain speed. For example, the alongshore component of wind speed is between 20 and 24 knots, 13.7 percent of the time. The alongshore component of wind speed is less than 12 knots, 39.4 percent of the time (computed by summing percentages in the first three wind speed columns).

Table A-38 presents the same alongshore component of wind speed and current data in a slightly different format. The percentages listed are the total percent of time for which either the alongshore component of wind speed or the current speed exceeds the upper value of a particular bin. For example, 11.4 percent of the time, either the alongshore

component of wind speed exceeds 20 knots or the current speed exceeds 1.0 knot. For 26.6 percent of the time, either the alongshore component of wind speed exceeds 12 knots or the current speed exceeds 1.0 knot.

**TABLE A-38. Joint Probability of Exceedance for Alongshore Wind/Current, in percent**

Current Speed (knots)	Wind Speed (knots)								
	4.0	8.0	12.0	16.0	20.0	24.0	28.0	32.0	36.0
2.5	0.0	0.0	0.0	0.0	0.0	0.0	0.0	0.0	0.0
2.0	1.0	0.8	0.8	0.8	0.5	0.2	0.0	0.0	0.0
1.5	8.8	8.0	5.9	4.6	2.9	1.4	0.5	0.2	0.1
1.0	37.0	34.3	26.6	19.2	11.4	5.0	1.8	0.5	0.2
0.5	97.4	85.4	69.5	48.2	28.6	12.6	4.6	1.3	0.4

### 8.4.3 Ship Simulation

Ship simulation using a real time ship simulator, where events on the simulator require the same amount of time as they do in real life, was used to evaluate the Portsite terminal. The ship simulation was performed at the Waterways Experiment Station in 2001.

The simulations began with a design session that was used to test the model for reasonableness. Two pilots participated in the design session: a pilot from the Alaska Marine Pilots Association who works at the Portsite and who will be navigating the ship to the dock and a ship pilot consultant from Long Beach, California.

The formal testing program used four pilots to test the channel, two pilots from the Alaska Marine Pilots Association who work at the Portsite and who will be navigating the ship to the dock, a ship pilot consultant from Long Beach, California, and a ship pilot from Port Manatee in Florida. Ship navigation in Port Manatee includes cross current navigation similar to that expected at the Portsite. The Port Manatee pilot provided cross current navigation experience that the Alaska Marine Pilots had not had to date. Four different pilots were used during the formal simulation because different pilots will be used at the Portsite and each pilot will have variable reactions and methods of maneuvering the ships.

The simulator uses a three screen visual display that provides 140 degree field of view. The viewing angle is mariner controlled and can be rotated 360 degrees. Changing the view angle accomplishes the same effect as turning one's head in real life. The Ship/Tow simulator has two radar displays. One display has three variable scales, which are usually set to 1 1/2, 3/4, and 1/2 mile. The other radar display is 1/4 mile scale and is used to display tugs and thrusters as vectors either pushing or pulling the ship. The hydrodynamic model used in the marine simulator calculates the ship response to the variety of forces being exerted on the vessel. The model uses an iterative process that modifies flows in response to the changed topography caused by the channel incision and passage of a vessel. Wind effects are incorporated by applying either a steady state wind field or wind with gusts. Wind gusts can exceed the steady state condition during short bursts, which applies erratic forces on vessels that may not be accounted for in the model under steady wind forcing. Forces causing ship motion are both environmental and mariner controlled. Environmental forces

Draft Feasibility Report  
Appendix A: Hydraulic Design, Delong Mountain Terminal, Alaska

include: current, bank effects, wind, and waves. Mariner controlled forces include: rudder angle, propeller revolution, tugs, and bow and stern thrusters.

The model consisted of the channel, turning basin, and berthing area shown in figure 92 with a design depth of -53 feet. Two ships were used in the evaluation for the bulk concentrate ships: a 39.5-foot (12.04-meter) draft ship and a 44-foot (13.41-meter) draft ship. The 39.5-foot (12.04-meter) draft ship had similar ship dimensions to the design ship for the site; however, the draft was shallower than an actual fully loaded ship. The 44-foot (13.41-meter) draft ship had a similar design draft, but its length and beam were larger than the design ship. To resolve the problem, both ships were used. The 39.5-foot (12.04-meter) ship was used to evaluate ship handling when transiting the channel and the 44-foot (13.41-meter) ship was used to evaluate getting the ship off of the dock. The standard Panamax ship in the simulator was used to simulate the ballasted ship. A fully loaded fuel tanker was also simulated. Dimensions of the ships used in the simulator are listed in table A-39.

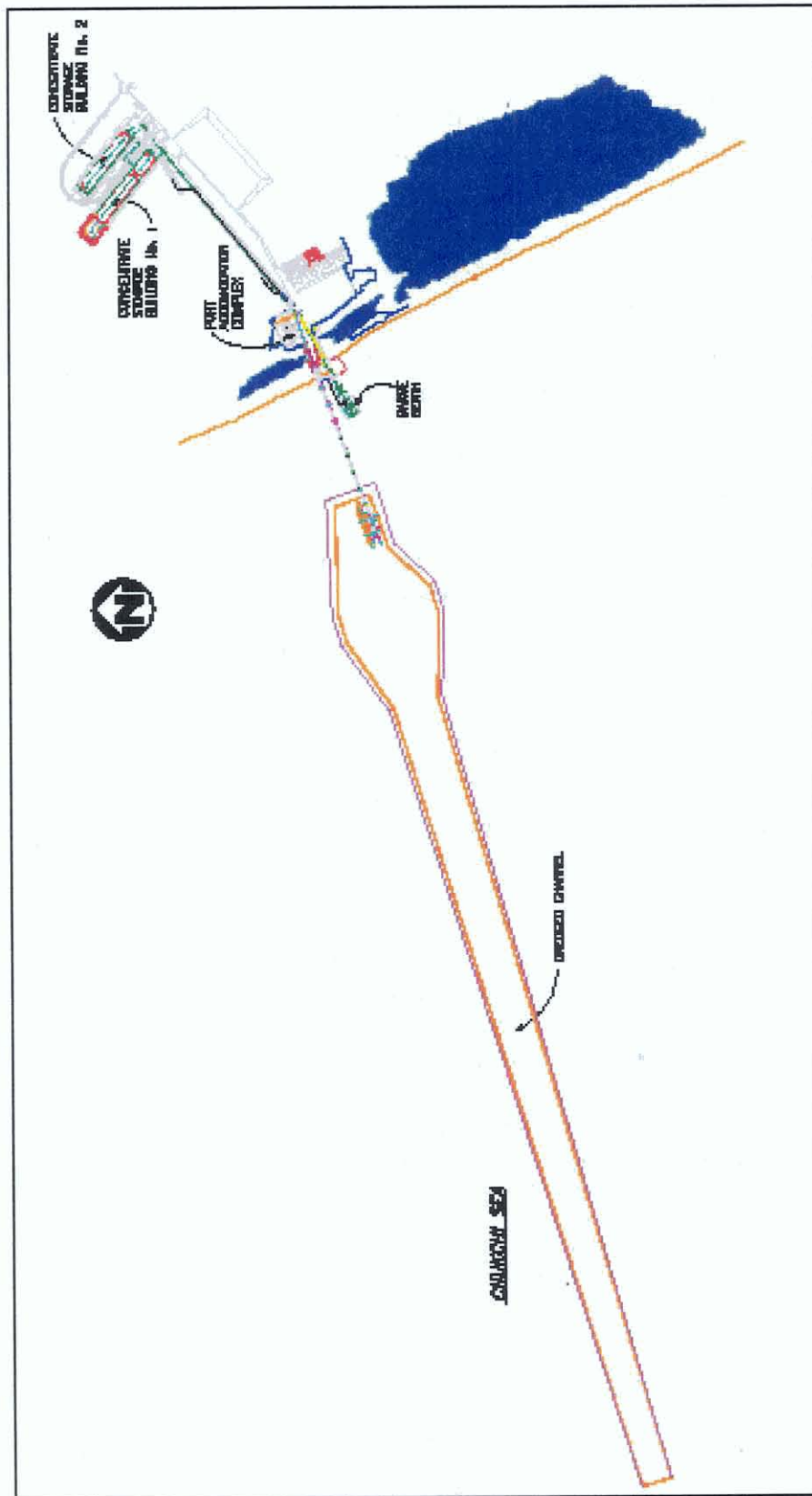


Figure 92. Ship simulation channel, turning basin, and berthing area.

**TABLE A-39. Simulator Ship Dimensions**

Dimensions	Panamax Loaded	Panamax Ballasted	Large Bulk Carrier Loaded	Fuel Tanker Loaded
Length Over All	775	775	810	610
Beam	107	106	125	94
Draft	39	25	44	36

The simulations were conducted with ideal sight conditions. Aids to navigation consisted of a series of buoys along the channel boundary. Winds used in the design session were steady state without gusts. Wind was input with gusting for the formal simulation session, which allowed the wind to fluctuate above and below the average wind speed by 70 percent. The average of the gusting winds never exceeds the average wind input.

The current data was input based on the measured currents in the top 4 meters of the water column. This current data was used to add conservatism to a sparse data set. Waves were not included in the simulation runs except to reduce the effectiveness of the tugs. The waves at the site are generally short period and will have greater impact on the tug operations than on the ship.

The design session tested the adequacy of the channel configuration and the tugs combinations to be used. The major outcome of the design session was that the berthing area was moved to the north side of the loading facility to take advantage of the predominately northward current flow. When the berthing area was located south of the loading facility, it was difficult to get the ship off the dock.

The simulation conditions tested in the formal simulation program are listed in table A-40. Simulation tracks associated with each of the runs are in the CHL report, *Engineering Studies in Support of Delong Mountain Terminal Project, 2002, ERDC/CHL TR-02-26.*

Run Number	Heading	Currents, Knots Direction to	Wind, Knots Direction from	Ship	Tugs	Pilots Participating			
						1	2	3	4
1	Outbound	1.5 North	30 South	Bulk Carrier 810X125X44	Three 3000-HP	x	x		
2	Outbound	1.5 North	30 South	Bulk Carrier 775X106X39	Three 3000-HP	x	x		
3	Outbound	1.5 North	30 South	Bulk Carrier 810X125X44	Two 4000-HP	x	x		

Draft Feasibility Report  
Appendix A: Hydraulic Design, Delong Mountain Terminal, Alaska

<b>Table A-40. Test Matrix for Formal Simulation Program.</b>									
Run Number	Heading	Currents, Knots Direction to	Wind, Knots Direction from	Ship	Tugs	Pilots Participating			
						1	2	3	4
4	Outbound	1.5 North	30 South	Bulk Carrier 775X106X39	Two 4000-HP	x	x		
5	Outbound	1.25 North	30 South	Bulk Carrier 810X125X44	Two 3500-HP	x	x		
6	Outbound	1.25 North	30 South	Bulk Carrier 775X106X39	Two 3500-HP	x	x		
7	Outbound	1.25 North	30 South	Bulk Carrier 810X125X44	Three 3000-HP	x	x	x	x
8	Outbound	1.25 North	30 South	Bulk Carrier 775X106X39	Three 3000-HP	x	x	x	x
9	Outbound	1.25 North	30 South	Bulk Carrier 810X125X44	Three 3000-HP	x	x	x	x
Note: Depth of Channel Near Berth is 60 feet.									
10	Outbound	1.25 North	30 South	Bulk Carrier 810X125X44	Two 4000-HP	x	x	x	x
Note: Depth of Channel Near Berth is 60 feet.									
11	Outbound	1.0 North	30 South	Bulk Carrier 810X125X44	Three 2500-HP	x	x		
12	Outbound	1.0 North	30 South	Bulk Carrier 775X106X39	Three 2500-HP	x	x		
13	Outbound	1.0 North	30 Southwest	Bulk Carrier 810X125X44	Two 3000-HP	x	x		
14	Outbound	1.0 North	30 Southwest	Bulk Carrier 775X106X39	Two 3000-HP	x	x		
15	Outbound	1.0 North	20 South	Bulk Carrier 810X125X44	Two 3000-HP	x	x		
16	Outbound	0.75 South	30 Northwest	Bulk Carrier 810X125X44	Three 2500-HP	x	x		
Note: Waves reduce tug effectiveness to 60%.									
17	Outbound	0.75 South	30 Northwest	Bulk Carrier 810X125X44	Two 3000-HP	x	x		
Note: Waves reduce tug effectiveness to 60%.									
18	Inbound	1.0 North	30 Southeast	Bulk Carrier 775X106X25	Three 2500-HP	x	x		

Draft Feasibility Report  
Appendix A: Hydraulic Design, Delong Mountain Terminal, Alaska

<b>Table A-40. Test Matrix for Formal Simulation Program.</b>									
Run Number	Heading	Currents, Knots Direction to	Wind, Knots Direction from	Ship	Tugs	Pilots Participating			
						1	2	3	4
19	Inbound	1.0 North	30 Southeast	Bulk Carrier 775X106X25	Two 3000-HP	x			
20	Inbound	0.75 South	30 Northwest	Bulk Carrier 775X106X25	Three 2500-HP	x	x		
Note: Waves reduce tug effectiveness to 70%.									
21	Inbound	0.75 South	30 Northwest	Bulk Carrier 775X106X25	Two 3000-HP	x	x		
Note: Waves reduce tug effectiveness to 70%.									
22	Inbound	0.75 South	20 Northwest	Bulk Carrier 775X106X25	Three 2500-HP		x		
Note: Waves reduce tug effectiveness to 85%.									
23	Inbound	0.75 South	20 Northwest	Bulk Carrier 775X106X25	Two 3000-HP	x	x		
Note: Waves reduce tug effectiveness to 85%.									
24	Inbound	1.0 North	20 South	Tanker 610X94X36	Two 3000-HP	x	x		
Note: Waves reduce tug effectiveness to 60%.									
25	Inbound	0.75 South	20 North	Tanker 610X94X36	Two 3000-HP	x	x		
Note: Waves reduce tug effectiveness to 60%.									
26	Inbound	1.0 North	20 Southeast	Bulk Carrier 775X106X25	Three 2500-HP	x	x		
Note: Waves reduce tug effectiveness to 85%.									
27	Inbound	1.0 North	20 Southeast	Bulk Carrier 775X106X25	Two 3000-HP	x	x		
Note: Waves reduce tug effectiveness to 85%.									
28	Inbound	0.75 South	20 Northwest	Bulk Carrier 775X106X25	Three 2500-HP	x	x		x
Note: Waves reduce tug effectiveness to 85%.									
29	Inbound	0.75 South	20 Northwest	Bulk Carrier 775X106X25	Two 3000-HP	x	x		
Note: Waves reduce tug effectiveness to 85%.									
30	Inbound	0.75 North	40 East	Bulk Carrier 775X106X25	Three 2500-HP	x	x		

Draft Feasibility Report  
Appendix A: Hydraulic Design, Delong Mountain Terminal, Alaska

Run Number	Heading	Currents, Knots Direction to	Wind, Knots Direction from	Ship	Tugs	Pilots Participating			
						1	2	3	4
31	Inbound	0.75 North	40 East	Bulk Carrier 775X106X25	Two 3000-HP	x	x		
32	Inbound	1.0 North	20 South	Bulk Carrier 775X106X39	Two 3000-HP	x	x		
33	Inbound	0.75 South	20 North	Bulk Carrier 775X106X39	Two 3000-HP	x	x		
34	Outbound	0.75 North	40 East	Bulk Carrier 810X125X44	Three 2500-HP	x	x		
35	Outbound	0.75 North	40 East	Bulk Carrier 775X106X39	Three 2500-HP	x	x		
36	Outbound	0.75 North	40 East	Bulk Carrier 810X125X44	Two 3000-HP	x	x		
37	Outbound	0.75 North	40 East	Bulk Carrier 775X106X39	Two 3000-HP	x	x		
38	Outbound	0.75 North	30 South	Bulk Carrier 810X125X44	Three 3000-HP			x	x
39	Outbound	0.75 North	30 South	Bulk Carrier 775X106X39	Three 3000-HP			x	x
40	Outbound	0.75 North	30 South	Bulk Carrier 810X125X44	Two 4000-HP			x	x
41	Outbound	0.75 North	30 South	Bulk Carrier 775X106X39	Two 4000-HP				x
42	Outbound	1.25 North	30 South	Bulk Carrier 810X125X44	Two 4000-HP			x	x
43	Outbound	1.25 North	30 South	Bulk Carrier 775X106X39	Two 4000-HP			x	x
44	Outbound	1.0 North	30 South	Bulk Carrier 810X125X44	Three 3000-HP			x	x
45	Outbound	1.0 North	30 South	Bulk Carrier 775X106X39	Three 3000-HP			x	x
46	Inbound	1.0 North	30 South	Bulk Carrier 775X106X25	Three 2700-HP			x	x

Draft Feasibility Report  
Appendix A: Hydraulic Design, Delong Mountain Terminal, Alaska

Run Number	Heading	Currents, Knots Direction to	Wind, Knots Direction from	Ship	Tugs	Pilots Participating			
						1	2	3	4
47	Inbound	1.0 North	30 South	Bulk Carrier 775X106X25	Two 4000-HP			x	x
48	Inbound	1.0 North	30 Southeast	Bulk Carrier 775X106X25	Three 3000-HP			x	x
49	Inbound	1.0 North	30 Southeast	Bulk Carrier 775X106X25	Two 4000-HP			x	x
50	Inbound	0.75 South	30 Northwest	Bulk Carrier 775X106X25	Three 3000-HP			x	x
51	Inbound	0.75 South	30 Northwest	Bulk Carrier 775X106X25	Two 4000-HP			x	x
52	Inbound	0.75 South	20 Northwest	Bulk Carrier 775X106X25	Three 3000-HP			x	x
53	Inbound	0.75 South	20 Northwest	Bulk Carrier 775X106X25	Two 4000-HP			x	x
54	Inbound	1.0 North	20 South	Bulk Carrier 610X94X36	Two 4000-HP			x	x
55	Inbound	0.75 South	20 North	Bulk Carrier 610X94X36	Two 4000-HP			x	
56	Inbound	1.0 North	20 Southeast	Bulk Carrier 775X106X25	Three 3000-HP			x	x
57	Inbound	1.0 North	20 Southeast	Bulk Carrier 775X106X25	Two 4000-HP			x	x
58	Inbound	0.75 North	30 South	Bulk Carrier 775X106X25	Three 3000-HP			x	x
59	Inbound	0.75 North	30 South	Bulk Carrier 775X106X25	Two 4000-HP			x	x
60	Inbound	1.0 North	20 South	Bulk Carrier 775X106X39	Two 4000-HP			x	x
61	Inbound	0.75 South	20 North	Bulk Carrier 775X106X39	Two 4000-HP			x	x
62	Outbound	0.75 North	30 South	Bulk Carrier 810X125X44	Three 3000-HP			x	x

**Table A-40. Test Matrix for Formal Simulation Program.**

Run Number	Heading	Currents, Knots Direction to	Wind, Knots Direction from	Ship	Tugs	Pilots Participating			
						1	2	3	4
63	Outbound	0.75 North	30 South	Bulk Carrier 775X106X39	Three 3000-HP			x	x
64	Outbound	0.75 North	30 South	Bulk Carrier 810X125X44	Two 4000-HP			x	x
66	Inbound	1.0 North	20 South	Tanker 610X94X36	Two 4000-HP			x	x
67	Inbound	0.75 South	20 North	Tanker 610X94X36	Two 4000-HP			x	x
68	Outbound	1.0 North	20 South	Tanker 610X94X20	Two 4000-HP			x	x
69	Inbound	1.0 North	30 Southeast	Bulk Carrier 775X106X39	Three 3000-HP			x	x

Ship tracks from the simulations were analyzed to determine if there were any adjustments necessary to make the channel transit safer and determine the minimum safe engineering width. Locations where ships frequently made excursions from the channel were of interest as well as locations where the channel was not frequently used. A range of wind and current conditions were analyzed in the simulations. The depth of the channel was determined later during the economic optimization, but for the simulation a -53-foot (-16-meter) depth was used since that allowed full loading of the Panamax sized ships.

The simulations examined a variety of tug combinations to assist the ship transit. The initial combination of tugs used in the simulation consisted of three 2,500 horsepower tugs and two 3,000 horsepower tugs. These tug combinations were run with a variety of conditions (table A-40) and were determined to not be capable of providing safe transit for ballasted ships entering the channel. This is demonstrated by the ship track and pilot comments in figures 93 and 94. As a result, the tug combinations were changed to three 3,000 horsepower tugs and two 4,000 horsepower tugs.

During relatively benign wind and current combinations, the transit into and out of the channel did not require the full channel and turning basin width with the three 3,000 horsepower tugs and two 4,000 horsepower tugs. This is demonstrated by the ship tracks and pilot comments in figures 95 through 97. The most challenging maneuver for the pilots in the sea and weather conditions tested was entering the channel in a ballasted condition, turning and docking. A portion of the turning basin was typically used in this maneuver.

During severe weather events the ships fully used the channel and turning basin (figures 98 through 102). Figures 98 through 100 show a ship leaving the dock fully loaded and partially loaded under extreme conditions. The ship makes full use of the channel during its

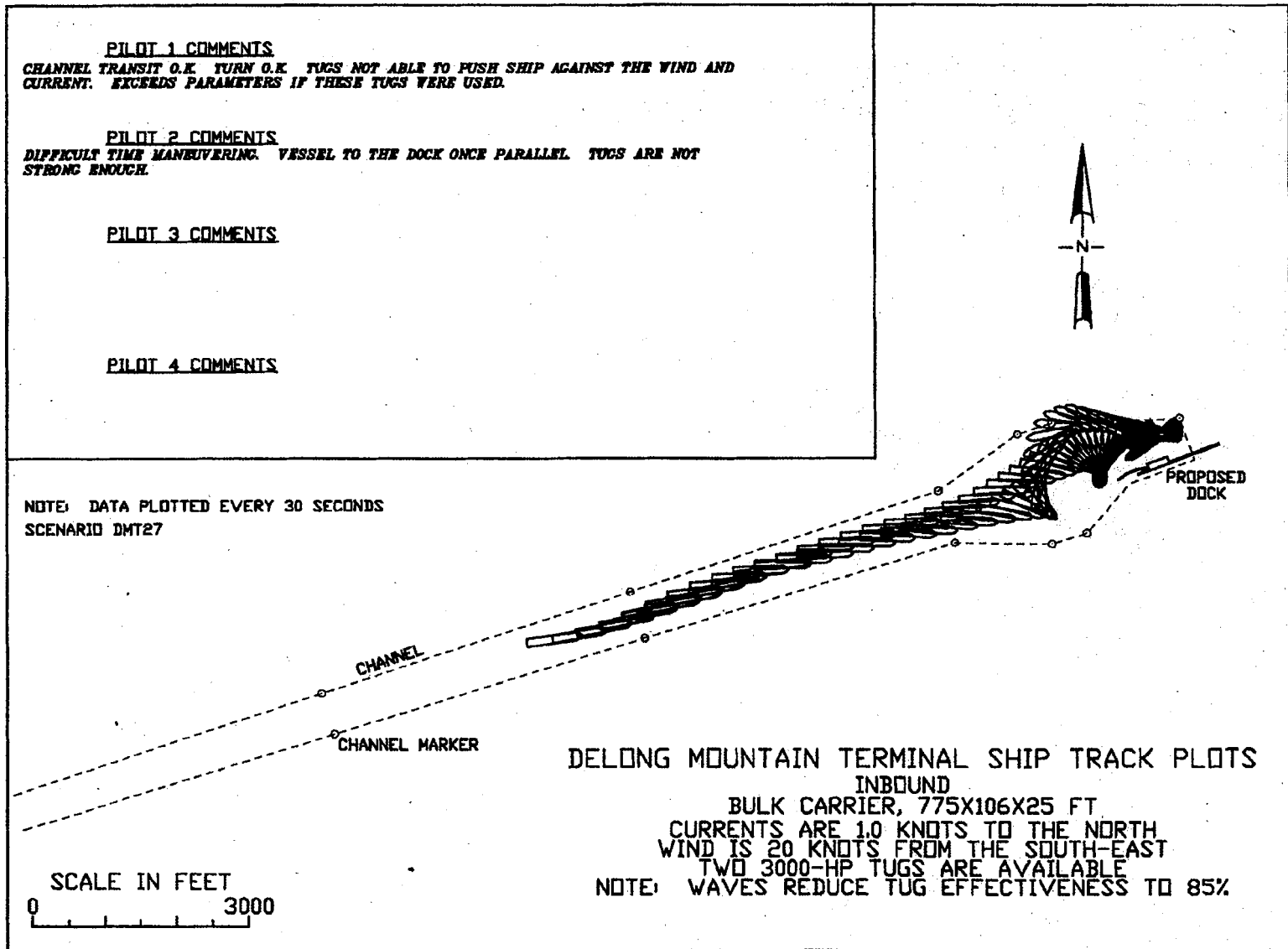
exit. Storms rapidly move into the Chukchi Sea, so it is feasible that a ship would be leaving the dock as a storm is moving into the area and extreme conditions are achieved.

Figures 101 and 102 show a ship entering the channel and using the full turning basin to turn and maneuver to the dock. The currents are moderate and the winds are strong. The pilot is able to safely transit the channel, but he needs the turning basin to complete docking.

The short loading season and the rapidly moving storm systems create a navigation environment that will result in a number of ships maneuvering in a channel during conditions that could be considered marginal. This consideration resulted in no changes to the channel configuration used in the formal simulation program. The ship tracks and pilot comments from the simulation program indicated the channel had been designed at its minimum width possible for safe transit in moderate to severe conditions that could be expected at the site.

The pilots commented during the simulation that tractor tugs would be necessary to safely navigate the channel. Of the tugs tested, the three 3,000 horsepower tractor tugs could handle the largest variety of weather. The three-tractor tug scenario provided more flexibility in the placement of the tugs. The two 4,000 horsepower tractor tugs were adequate to handle the majority of the weather, but did not have the safety margin that the three tug boat scenario provided. If one tug has engine problems the three tractor tug scenario has more horsepower available and retains flexibility, albeit reduced, in tug placement; whereas, the two tractor tug scenario would be reduced to a single force acting on the ship.

Figure 93. Ship tracks entering the channel with two 3,000 hp tugs.



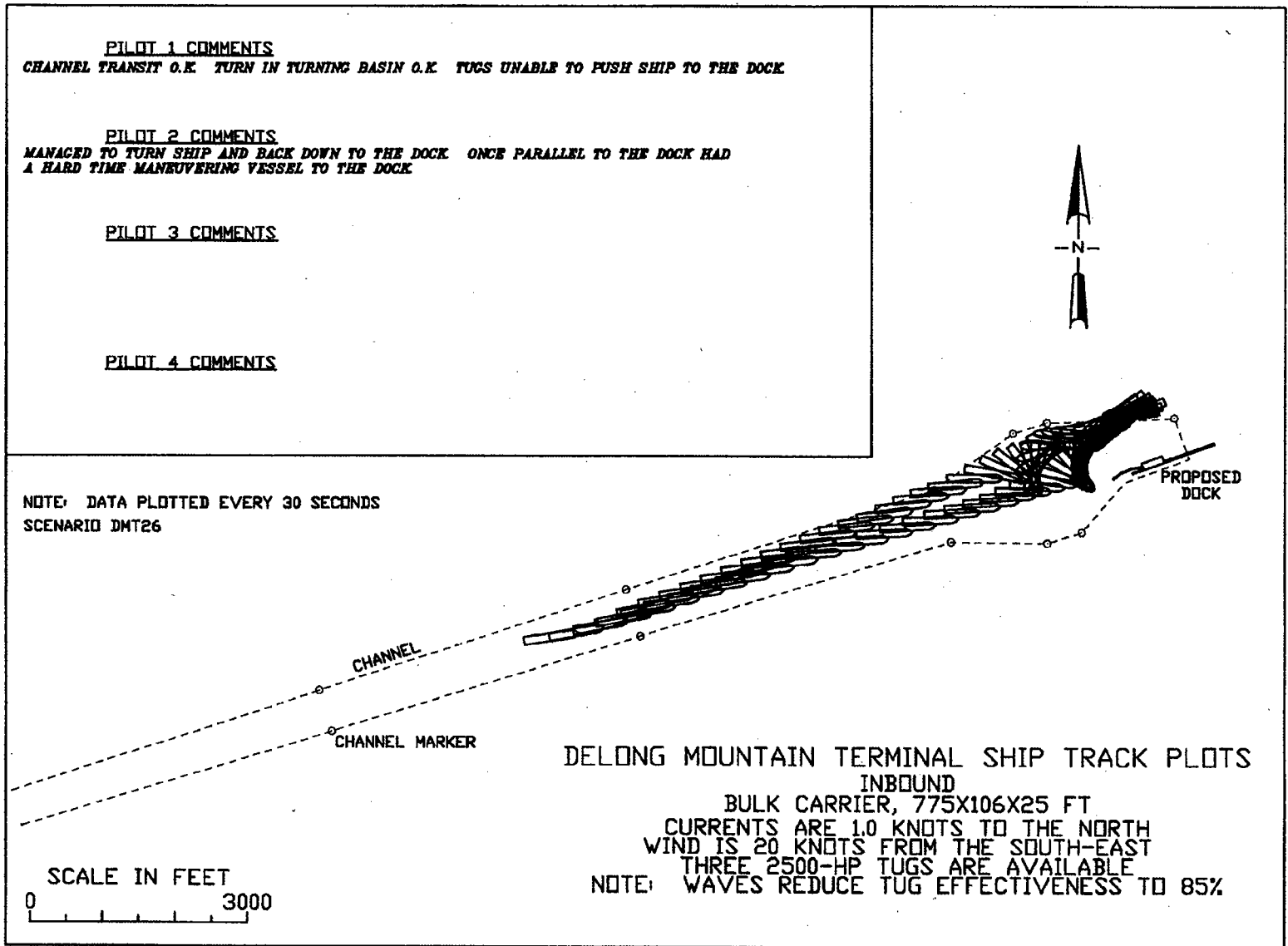


Figure 94. Ship tracks entering the channel with two 2,500 hp tugs.

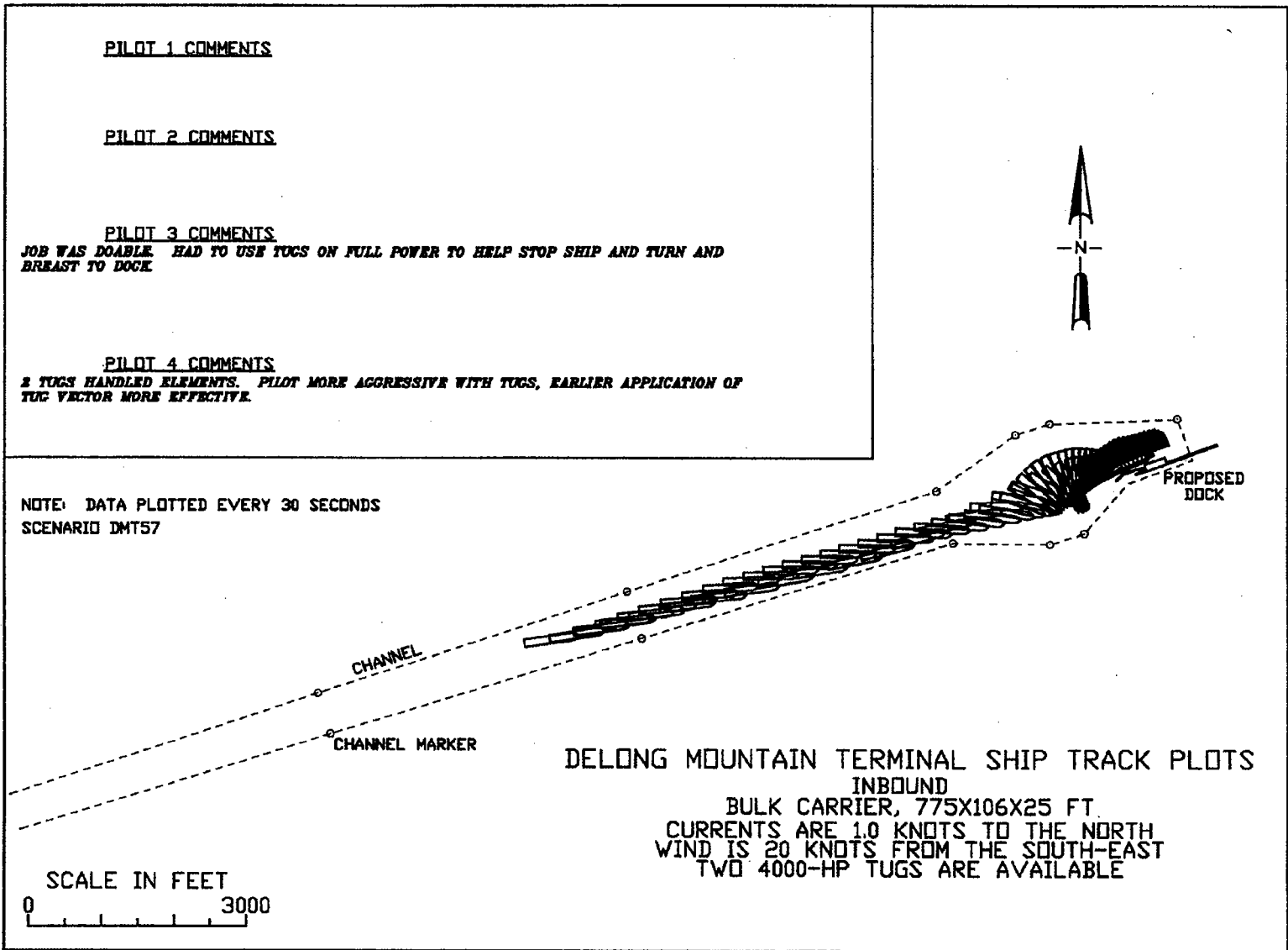


Figure 95. Ship tracks entering the channel.

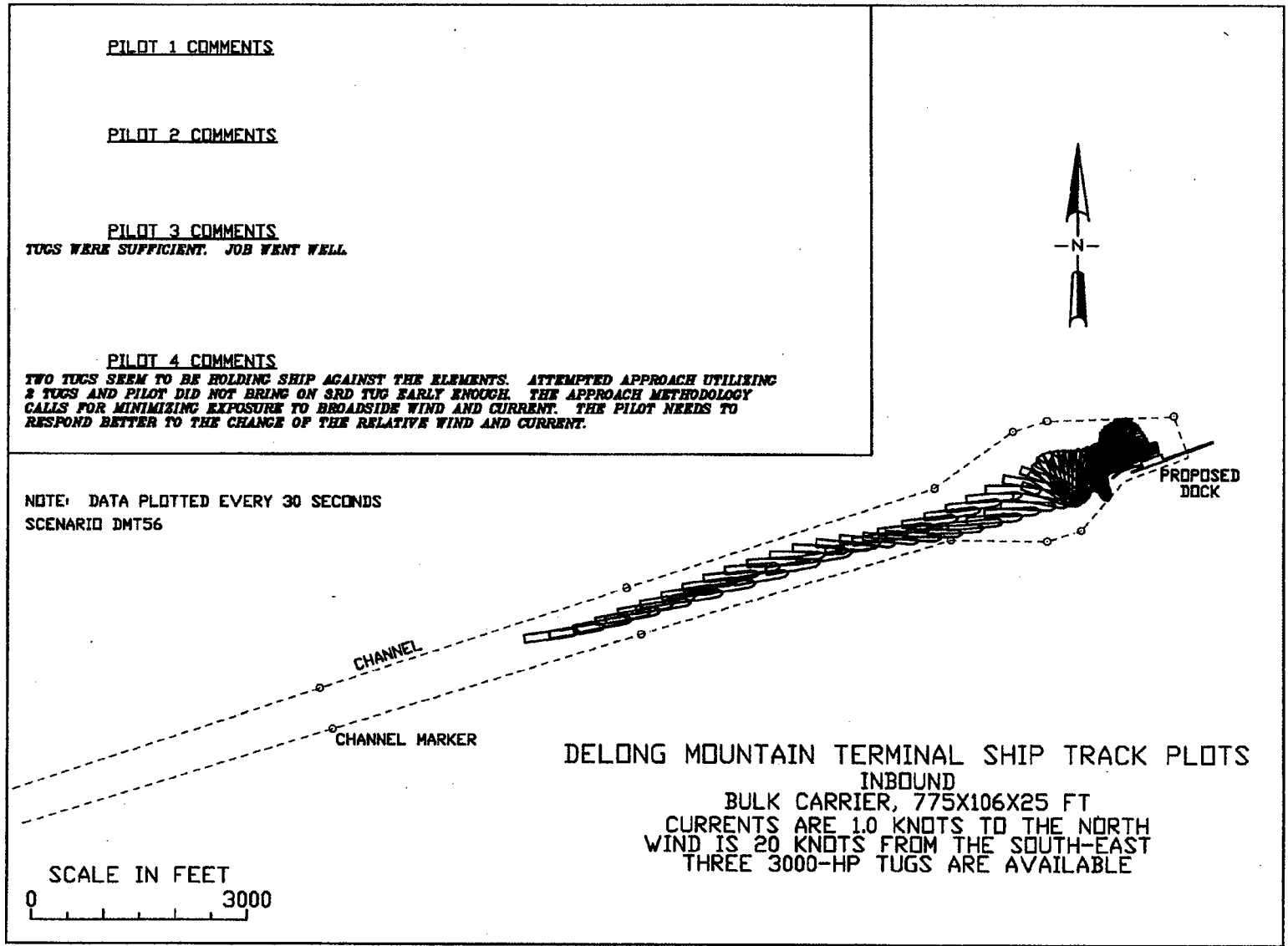


Figure 96. Ship tracks entering the channel.

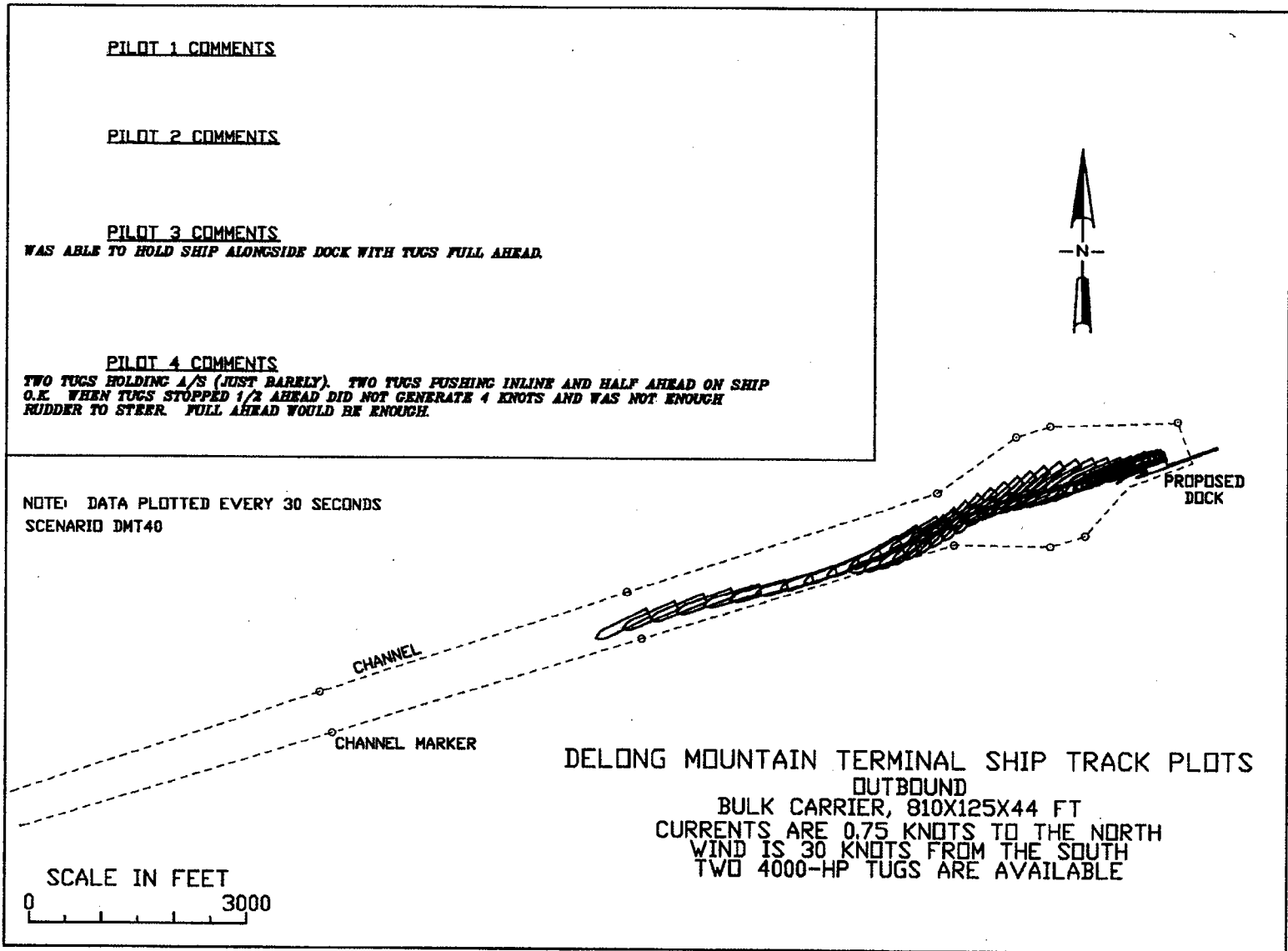


Figure 97. Ship tracks exiting the channel.

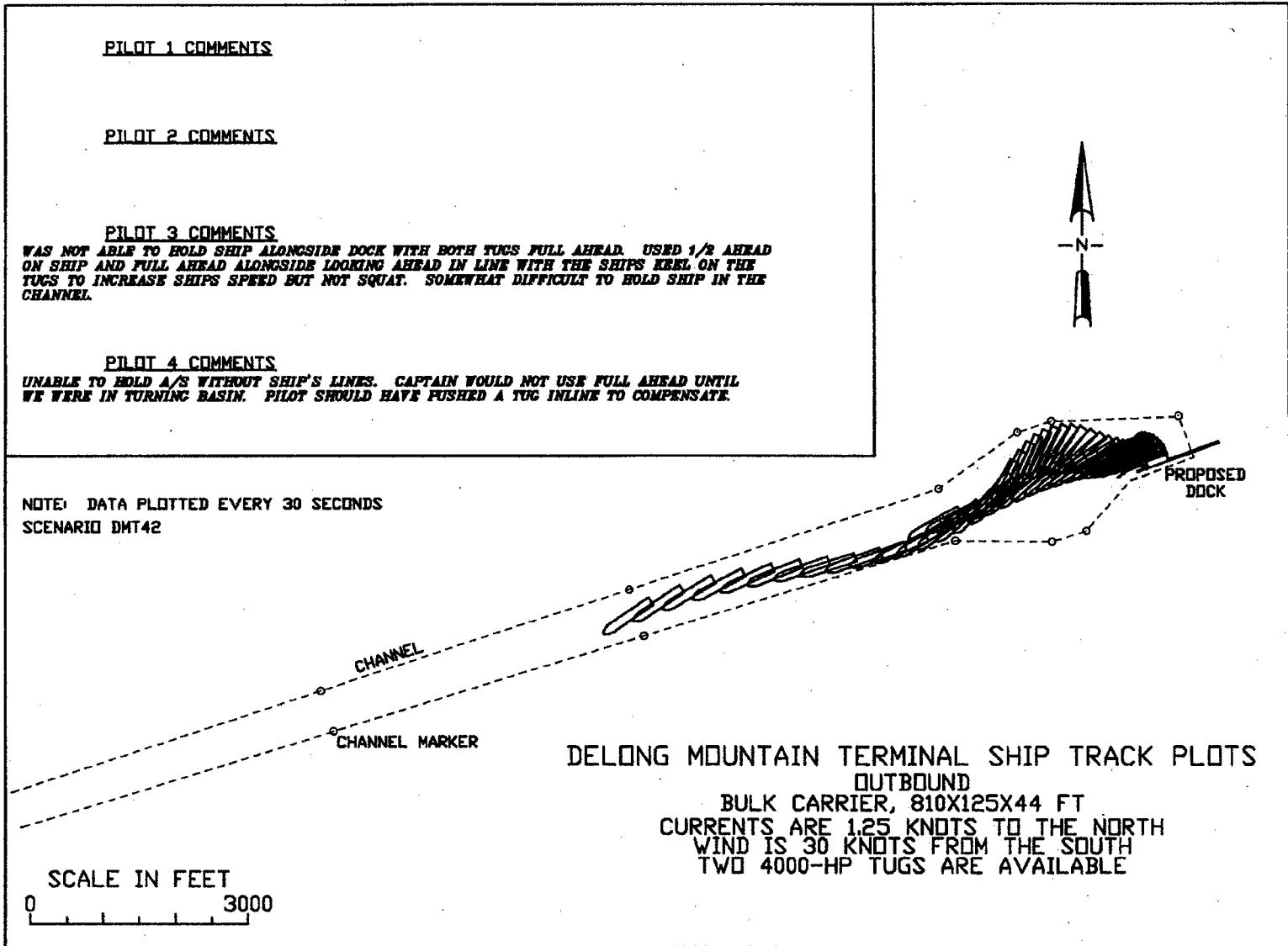


Figure 98. Ship tracks exiting the channel.

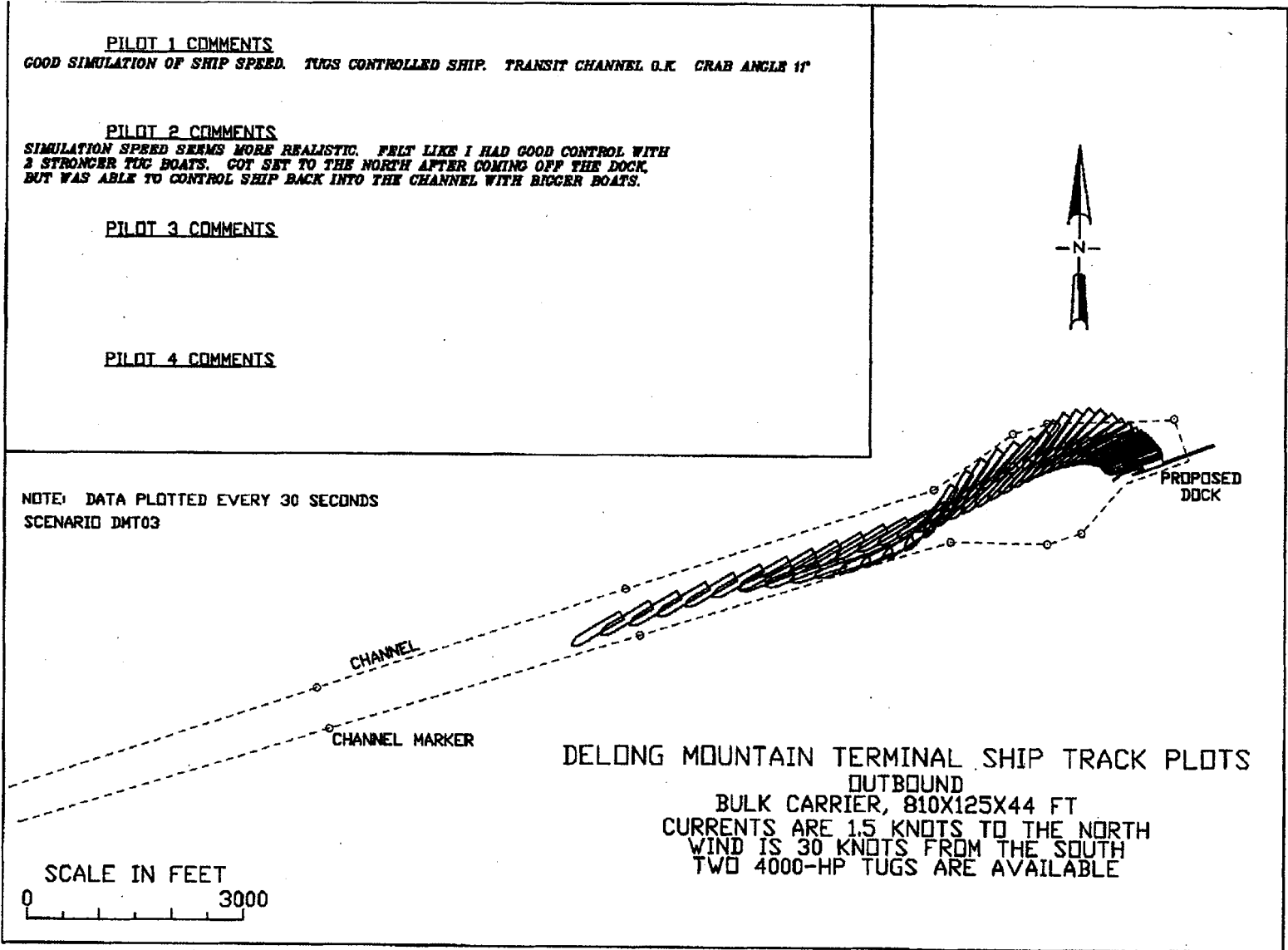


Figure 99. Ship tracks exiting the channel.

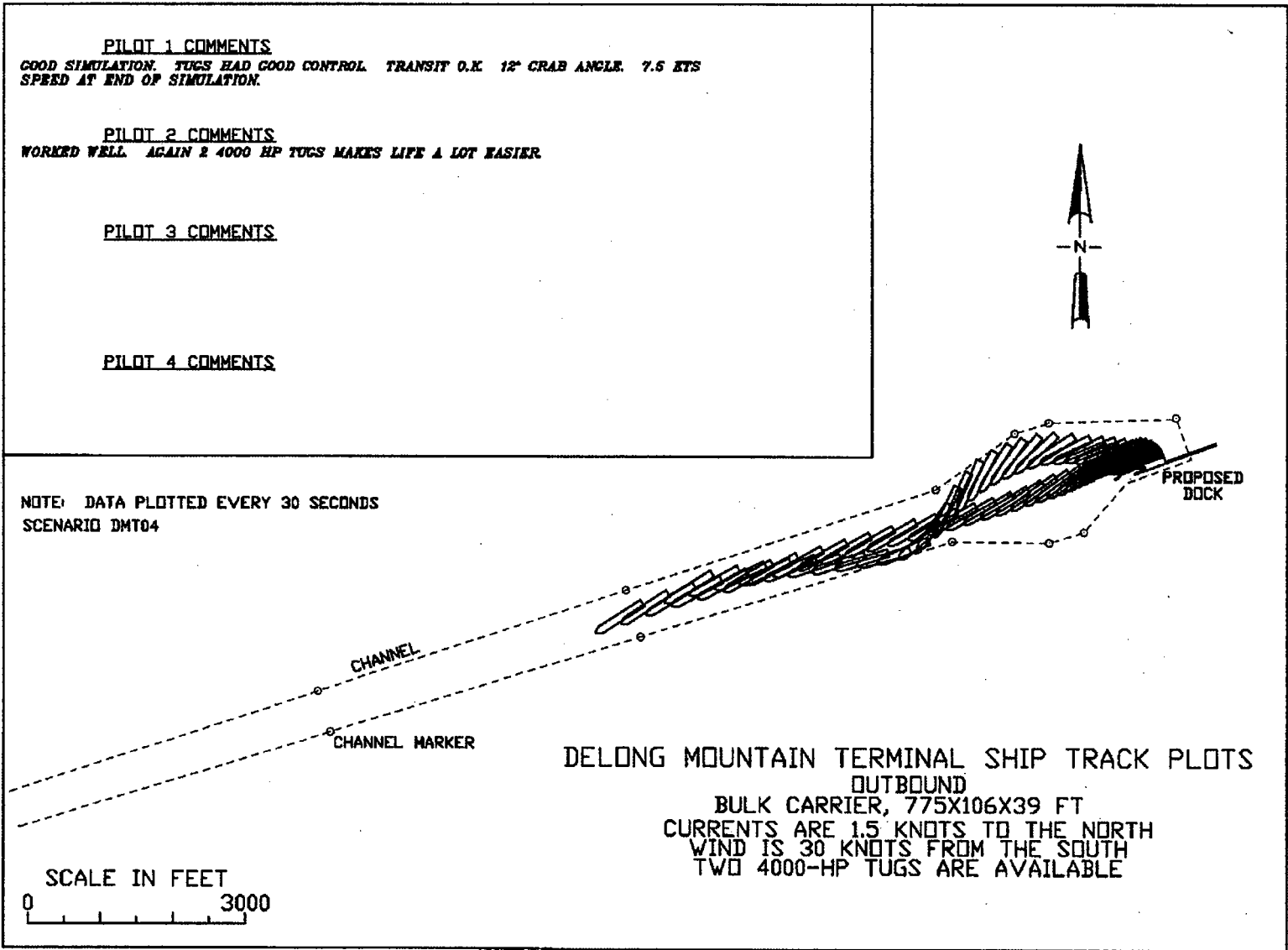


Figure 100. Ship tracks exiting the channel.

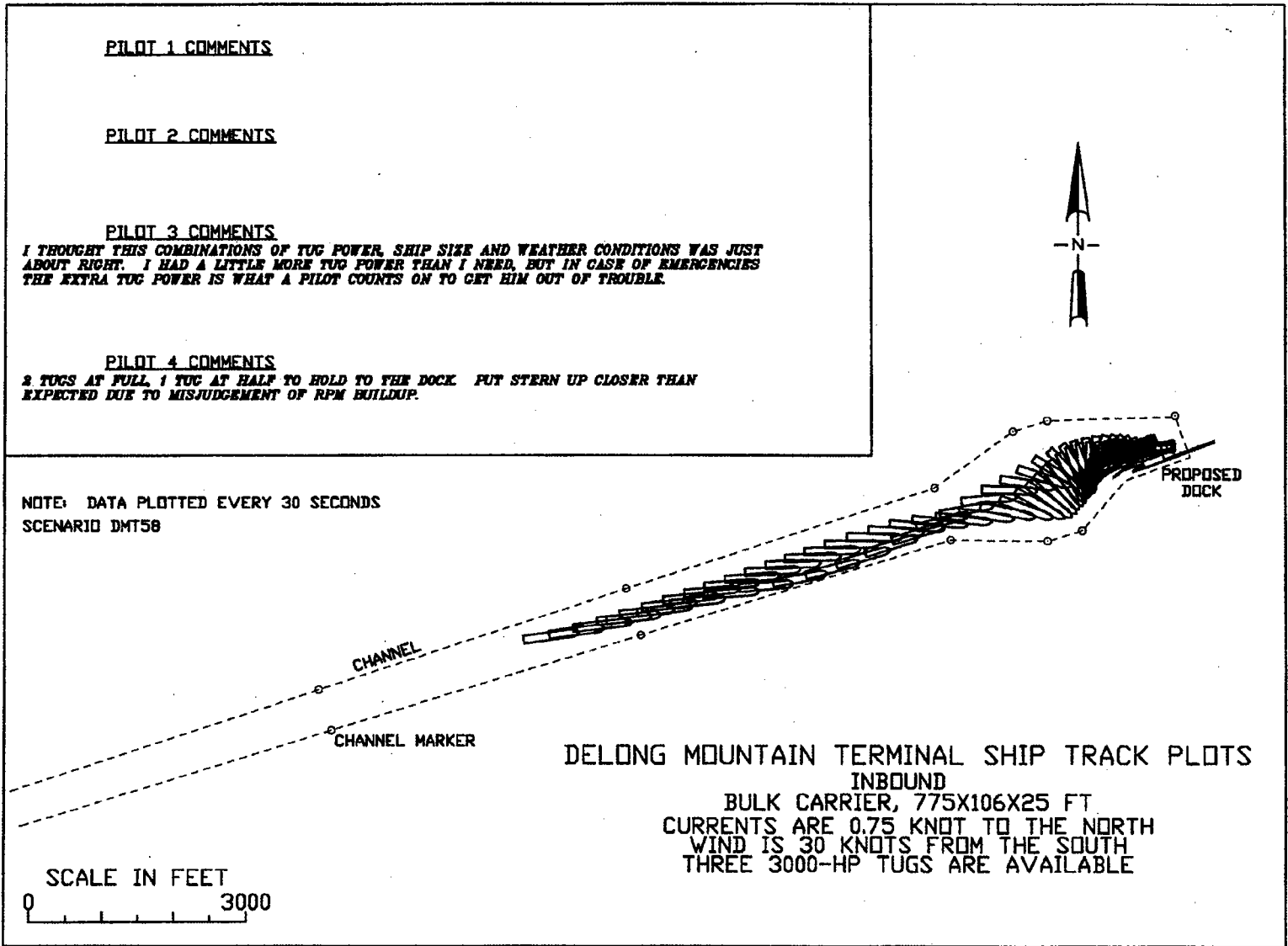
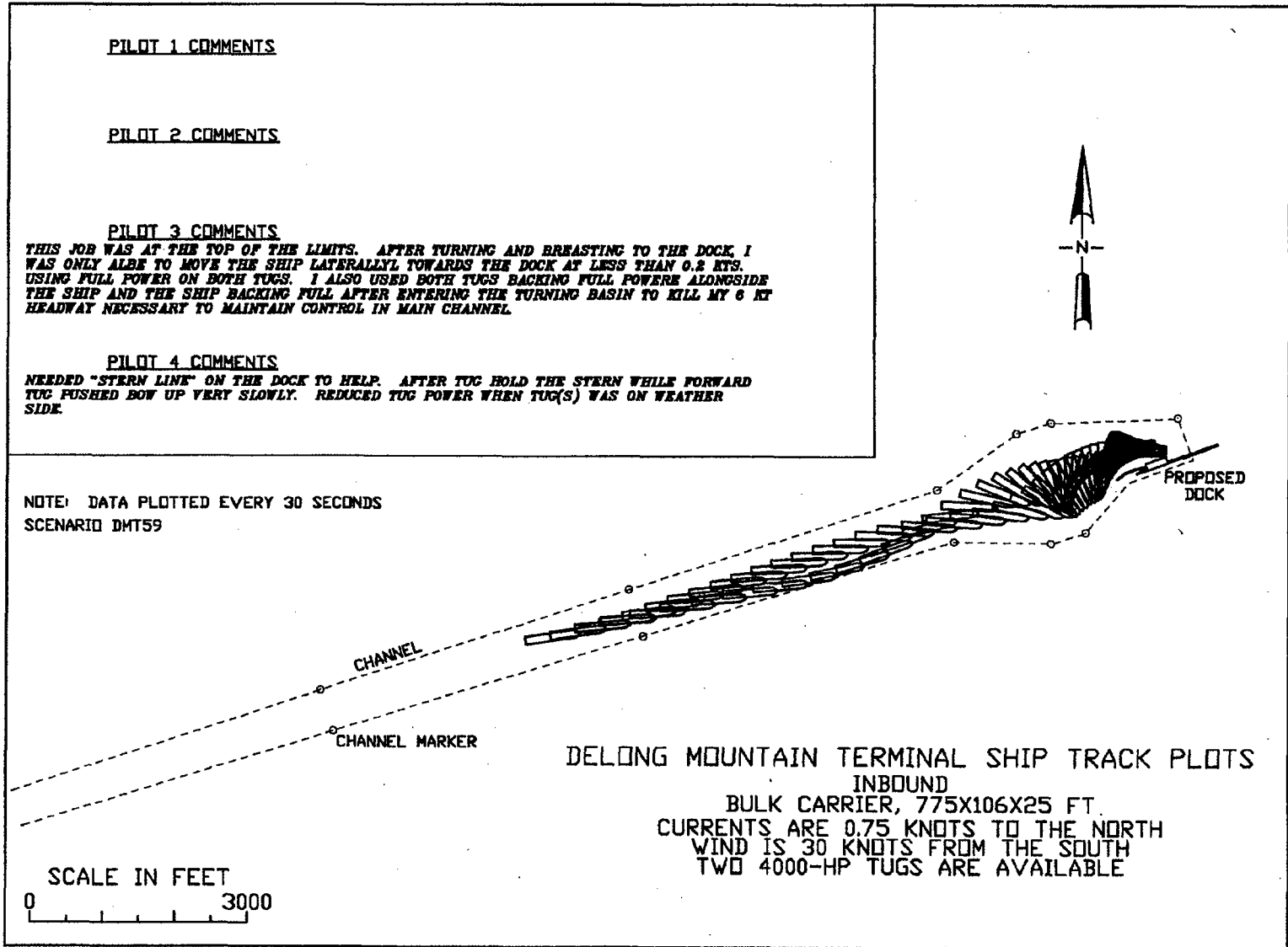


Figure 101. Ship tracks entering the channel.

Figure 102. Ship tracks entering the channel.



#### **8.4.4 Tug Boat Assistance**

The size and number of tug boats needed to assist the bulk carrier through the channel were evaluated during the ship simulation at WES. Initial evaluation of the tugs indicated that tractor type tugs were necessary for safe navigation of the channel. The following combinations of tugs were evaluated for use under varying weather conditions:

- Three 2,500 hp
- Two 3,000 hp
- Three 3,000 hp
- Two 4,000 hp

It became apparent during the simulation study that the three 2,500-horsepower tugs and the two 3,000-horsepower tugs were undersized and allowed no safety margin for channel transit. The pilots also noted that tractor type tugs were necessary for safe channel transit. The ship simulation was altered to test the Portsite conditions with three 3,000 horsepower tractor type tugs and two 4,000 horsepower tractor type tugs:

The three 3000-horsepower tractor type tugs had an upper operating limit of 30 knot winds with a 1 knot current inbound and outbound. The two 4,000-horsepower tractor tugs had an upper operating limit of 20-knot winds with a 1-knot current. The pilots tended to prefer the three-tug boat scenario over the two tugs. Operating limits of 28 knots or greater winds with a 1 knot or greater current at the site occurred 1.0 percent of the time using upper 13.12 feet (4 meters) from the year of concatenated currents for the open water season of July through October, while 20-knot or greater winds with a 1-knot or greater current occurred 2.6 percent of the time. According to a conversation with TCAK, the most likely scenario for the tugs is that they would contract for two 5,000-horsepower or greater tractor tugs since they would have a better chance of finding off-season work.

#### **8.4.5 Navigation Aids**

The Coast Guard requires a fixed navigation aid for the Portsite channel. This is due to the distance to the nearest Coast Guard Station. The navigation aid required for the site by the Coast Guard is two lighted range towers. Any navigation aid other than the Coast Guard required aid would be a local cost and maintenance responsibility.

The Alaska Marine Pilots Association (AMPA) has indicated that they prefer buoys spaced every 0.75 miles (1.21 km) as navigation aids at the site. According to the interim summary report by Simons, the AMPA recommended:

- A lighted bell buoy with Racon located in –55 feet (–16.76 meters) of water just outside the offshore entrance to the channel.
- A total of 10 lighted buoys.
- Center and shoulder ranges to provide visual alignment with the channel.
- A permanent current meter.

## 8.5 Vessel Motion Study

This study provided an estimation of vessel motions and mooring loads for the range of vessels expected to call at the proposed facility. The limiting wind, wave, and current environments for various marine operations (e.g., berthing, loading, and extreme loads) are inferred from these results. Details of the study performed and the model used can be found in volume B7 of the AMEC report *DeLong Mountain Harbor, Navigation Improvement Feasibility Study Local Sponsor Facilities*, 2002.

Triton Consultants, Ltd. performed the vessel response study for AMEC (Agra Simons). The purpose of the study was to examine the response of moored vessels and vessels underway to environmental conditions expected at the site. The objectives of the study were:

1. Determine the vertical motion of the keel of a vessel underway in the dredged channel.
2. Determine the response of moored vessels and their mooring components in the marine environment defining the upper limit of berthing and de-berthing (controlled by tug and vessel maneuverability)
3. Determine the response of moored vessels and their mooring components in the marine environment defining the upper limit of loading (controlled by shiploader shut-down wind speed, excessive vessel motion or excessive line or fender loads)
4. Define the extreme marine environment that the berth and moorings can withstand in the event that a vessel fails to leave the berth at the onset of deteriorating weather.

The investigation was conducted using the Atkins Quantitative Wave Analysis (AQWA) system, which is a floating structures analysis tool developed by Atkins Software of the United Kingdom.

### 8.5.1 Parameters Tested

#### *Vessels*

Three vessels were modeled in both loaded and ballasted states for a total of six vessel hulls:

- Panamax Bulk Carrier
- Handy-sized Bulk Carrier
- Small Tanker

The performance of large tankers and large general cargo vessel was inferred by use of the handy sized bulk carrier and the small tanker respectively. The design vessels used in the study are listed in table A-41.

<b>Table A-41 Vessel Motion Study Design Vessel Properties</b>				
<b>Parameter</b>	<b>Small Tanker</b>	<b>Large Tanker</b>	<b>Small Bulk Carrier -Handy</b>	<b>Large Bulk Carrier -Panamax</b>
Approximate Deadweight	15kDwt	37 kDWT	30 kDWT	75 kDWT
Length Overall	539 feet	580 feet	571 feet	738 feet
Length Between Perpendiculars	532 feet	562 feet	554 feet	716 feet
Beam	73 feet	100 feet	76 feet	106 feet
Draft – Fully Loaded	31 feet	36 feet	34 feet	45 feet
Draft Ballasted (30% loaded)	16 feet		15 feet	18 feet
Molded Depth	39 feet		49 feet	62 feet

*Water Levels*

The analyses performed for this study used a channel, berth, and turning area depth of –53 feet. These analyses are a function of water depth; however, variation in response to water level fluctuations different channel depths is expected to be minimal.

*Berth Configuration*

A single berth configuration was examined, except that the mooring components (e.g., fenders and number of lines) and the vessel location on the berth were varied during the study.

*Currents*

Beam-on currents are considered to be the single most important marine environmental consideration, with the loaded Panamax vessel being particularly important due to its modest underkeel clearances at low water levels which results in large loads on the mooring system components. Two current directions were considered, a north going current that tends to push vessels onto the fenders, and a south going current that tends to push vessels off of the berth. Draft-averaged current speeds up to 2 knots were considered with a resolution of 0.25 knots.

*Wind*

All eight cardinal wind directions were considered with sustained hourly winds up to 40 knots. The 30 second gust speeds (1.32 times the hourly value) associated with these hourly winds were used in the simulations.

*Waves*

The berth alignment is set roughly perpendicular to the shoreline such that waves become increasingly aligned with the berth as wave intensity increases. This is due to the fact that higher waves become are generally associated with longer wave periods that are more heavily refracted into this heading. Wave periods of 6, 8, 10, and 20 seconds were considered. Significant wave heights up to 13.1 feet (4 meters) were

considered with a resolution of 1.6 feet (0.5 meters). Wave directions were allowed to vary 45 degrees from the wind direction.

### **8.5.2 Vessel Motion in the Dredged Channel**

The case of vessels entering the channel with following seas gives the largest vertical motion. Assuming an approach speed of 9 knots, a significant wave height of 9.8 feet (3 meters), and an 8 second period, the maximum extreme downward movement of the bow is estimated to be about 3.7 feet (1.14 meters). Since escort tugs cannot operate in such conditions, a more realistic case is 6.6 feet (2 meters) significant wave and 8 second period, with an estimated maximum extreme downward movement of the bow of 2.6 feet (0.8 meters). Waves with a 20 second period and height of 1.6 feet (0.5 meters) have a maximum bow excursion of 3 feet (0.9 meters). This supports the use of a 3 foot allowance for a response to wave clearance in the channel depth calculation.

For dead-slow, fully loaded Panamax vessels leaving the berth in 6.5 feet, 8 second seas, the maximum significant downward movement of the bow is estimated to be about 1 foot (0.3 meters).

### **8.5.3 Moored Vessel Motion**

Moored vessels motions, mooring line forces and fender forces corresponding to a wind speed of 20 knots, significant wave height of 6.5 feet (2 meters) and draft average current speeds of 0.25 to 0.75 knots, do not exceed operating limits for any of the vessels tested, whether in ballasted or loaded condition.

The operating limit of the shiploaders is wind speed greater than 30 knots. While this wind speed should not be problematic for offshore wind direction, vessel motions, line loads and mooring loads frequently exceed normal operating limits when wind is in the onshore direction.

The effectiveness of adding additional mooring lines was tested for some of the extreme case conditions. When additional mooring lines are dispatched, all ships will be able to stay at the berth with the storm conditions tested.

## **8.6 Construction Considerations**

The channel construction is anticipated to take three years to complete, assuming a contract award in the fall. The construction contract will be an open invitation for bid. The type of dredge equipment used to perform the work will not be specified in the contract. It is anticipated that the bidders on the project will be dredgers with hopper dredges and/or clamshell dredges. Other dredge fleets may be used for portions of the project, but will likely not be used for the major portion of the dredging. Dredge plants used at the site will be limited by the wave climate and the lack of shelter to run to under storm conditions. Storms at the site move through the area very rapidly and there is no place to run for shelter. If shelter were made available either at Kivalina or at the Portsite, it is still unlikely that dredge plants sensitive to wave climate will be used at the

site. Storms move through the area so quickly that it is possible to get caught in the storm before shelter can be reached. This was experienced with a dredge in Barrow, which tends to be impacted by the same systems that impact the Portsite. Barrow's dredge was had a safe harbor dredged for access, but it ended up grounded and damaged during a storm in August 2000.

To attract a number of bidders, it is recommended that the project be advertised early to interest dredging contractors in bidding on this project. The contract should be awarded in the fall to allow the contractor the winter to prepare the logistics for the upcoming open water season.

The work season length, remote site location, wave climate, lack of local protection from wind and/or wave events are just some of the conditions that a contractor would need to consider when proposing on this contract. The start of the work season is based on the presence of whales and ice in the area. Based on previous years shipping records, the season typically begins in the beginning of July. It is anticipated that there would be approximately 100 days available for work before ice formation in the Bering Straits blocks travel from the site. Equipment would to be demobilized from the site before the Bering Straits ices and prevented travel to or from the site.

The Portsite is a remote location, so crew members would need to be flown to the site or ship up with the dredge equipment. Once on site the crew that will work on the project will need to have room and board provided. It may be possible for the contractor to put his crew up at the Portsite work camp. It anticipated that the dredges would work two shifts, 10 hours a day, 7 days a week.

The dredging contractor would need to make sure that there is fuel available for him at the site. He could bring up his own fuel barge, or he could make arrangements with AIDEA and Teck Cominco to purchase fuel from the site. Purchase of fuel from the site would need to be coordinated early in the year so that arrangements could be made to have additional fuel delivered to the site.

Once dredging work commences the contractor would need to coordinate his work with Foss and the barge loading operation. The barge loading operation would begin in early July at the same time as the dredging work, so there would be tugs and barges transiting the near shore area to approximately 3 miles off shore.

## **8.7 Disposal of Dredge Material**

Figure 103 shows the proposed dredged material disposal area. It is at a depth of 62 feet (18.9 meters) to approximately 72 feet (21.9 meters), approximately 30,000 feet (9,144 meters) west of the loading facility. This site is deep enough for disposal of the quantities to be excavated without significant impact on navigation or the coastal hydraulics of the area. Alternative ocean disposal sites were not considered since the sea floor conditions in the area are similar.

Modeling of the sediment transport during disposal and the fate of the disposal pile was performed. This work is detailed in the Environmental Impact Statement.

Gravel extraction from the dredged material for beneficial use was evaluated. Total gravel quantity available was estimated to be 614,000 cubic yards. This is slightly less than 10 percent of the total material being dredged. The gravel quantity available and the work required to separate the gravel from the fine material was not considered to be cost effective.

Alternative sites considered for disposal are detailed in Appendix 2 of the Environmental Impact Statement (EIS).

## **8.8 Dredged Channel Project Cost**

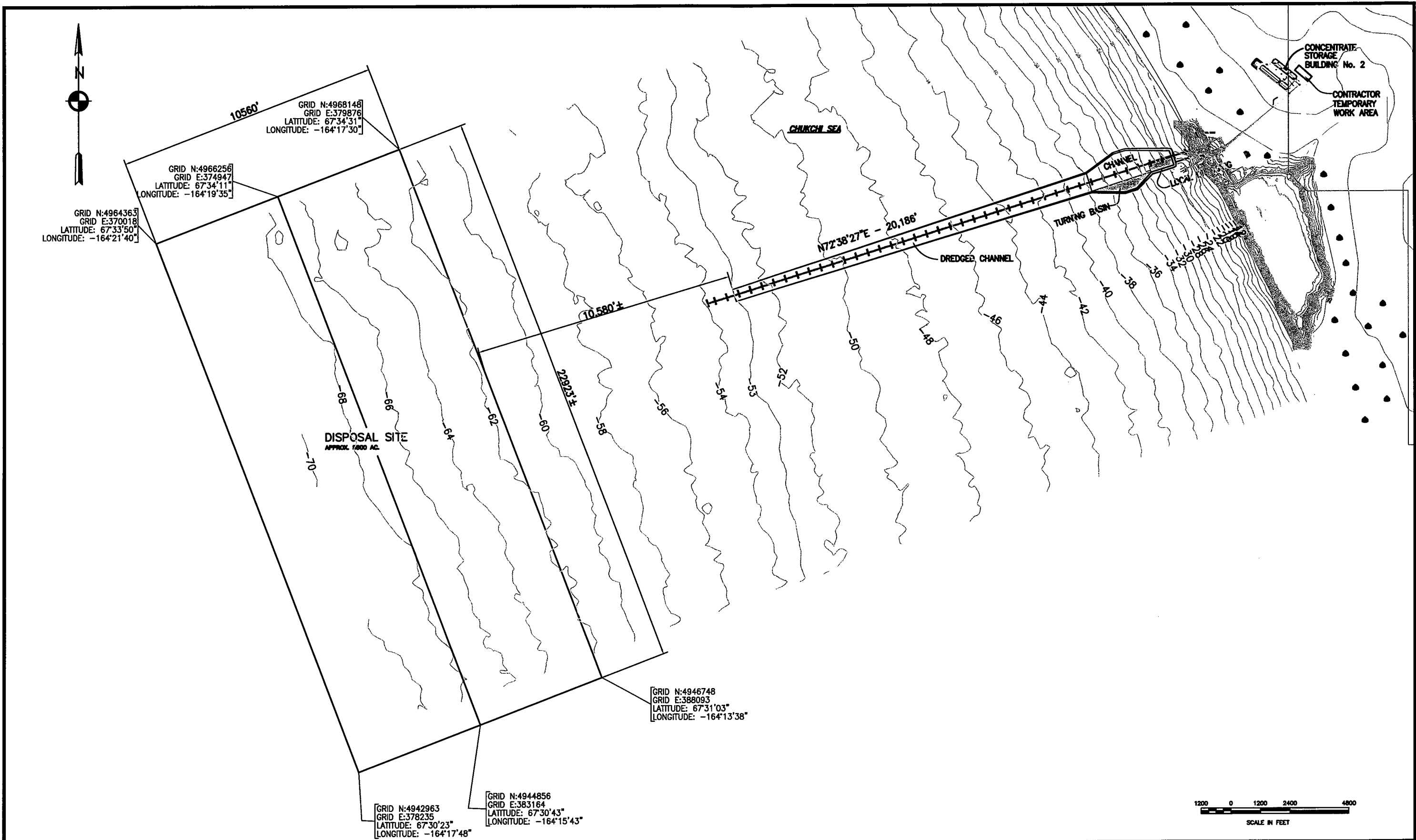
The Corps of Engineers Walla Walla District prepared the cost estimate for this project. Details for the project costs are in the Cost Engineering Appendix. Two dredging estimates were prepared. One uses a fleet of clamshell dredges and the other uses a clamshell and suction hopper dredge combination. The two scenarios were estimated to examine the price difference that could be experienced if no hopper dredges bid on the project. This is a possibility since the number of hopper dredges available to work on this project is limited. A cutter head dredge was not considered for this project. A cutter head is generally limited to a wave climate of 2 feet or less. The short construction season, lack of protection from waves, and the rapid progression of the weather systems through the area make the use of a cutter head unreliable for this project.

A channel dredged to -53 feet starting at the -20 foot contour is estimated to cost \$52 million. This assumes a dredge volume of 6,240,000 cubic yards at a cost of \$2.98 for hopper dredge dredging and \$8.03 for clamshell dredging. It is estimated that the construction will take three seasons. Mobilization and demobilization is assumed to be from the east coast of the United States at a cost of \$5.4 million per season. If the mobilization is from the west coast the mobilization and demobilization cost drops by about half.

An all clamshell fleet is estimated to cost \$81 million to dredge the same volume, and take three seasons to complete. Mobilization and demobilization of the all clamshell fleet is estimated to cost \$900,000 each season.

## **9.0 BREAKWATER DESIGN**

An alternative to the dredged channel is the construction of a breakwater. The breakwater would provide a calm loading climate for the barges at the site where the majority of the weather delays occur. The only delays that would be experienced would be when conditions prohibit the transit of the tug and barge to the ship. This is not a common occurrence since once at the ship the tug and barge are protected from the wave climate by loading in the lee of the ship.



ALASKA DISTRICT  
CORPS OF ENGINEERS  
CIVIL WORKS BRANCH

DREDGE DISPOSAL SITE, ENTRANCE CHANNEL, TURNING BASIN, AND LOCAL SPONSOR DREDGING  
DELONG MOUNTAIN TERMINAL, ALASKA

## 9.1 Alignment, Length & Usability

The centerline of the 2,800-foot (853-meter) breakwater straddles the -24-foot (-7.3-meter) MLLW contour in front of the barge-loading site (figure 104). This results in a protected barge maneuvering area of 620 feet (189 meters) between the breakwater and barge loader. The breakwater length is based on reducing a 6-foot wave to 3 feet (0.9 meter) at the barge loader approaching the shoreline at 30 degrees.

Comparisons of TCAK shipping data and the 9.8-foot (3-meter) buoy wave records for the 2000 shipping season indicated strong correlation of a 3.3-foot (1-meter) wave cut off for barge loading operations. The percent occurrence of a 6.6-foot (2-meter) wave based on the 15-year wave hindcast is roughly 3.1 percent (1 day a month). The percent occurrence of the 3.3-foot (1-meter) wave is 18 percent, which is roughly 5 to 7 days per month. The breakwater allows almost uninterrupted loading over the summer months. The 2000 shipping data also indicated the Panamax and handy size ore ships could be loaded uninterrupted in conditions with waves up to 6.6 feet (2 meters). Shut downs of loading at shore or ship would occur in events with waves greater than 6.6 feet (2 meters), which according to the 15-year hindcast occurred 0.5 day in July, 0.8 day in August, 1.0 day in September and 1.5 days in October.

The breakwater height is +10 feet (+3.1 meters) MLLW with a seaward slope of 1 vertical to 2 horizontal and a crest width of 18 feet (5.5 meters). This configuration is expected to overtop during storms. The breakwater only needs to protect up to 6-foot (1.83-meter) waves. It must withstand the 50-year wave for survivability only.

## 9.2 Underlayer Design

A 6.5-foot (1.98-meter) B rock layer of W-2 (2-ton) stone was used under the armor stone. The 3-foot (0.91-meter) filter layer between the bedding layer and bottom sands is composed of stone weighing 400 pounds (181 kg) or less. This filter layer has a wide gradation to act as both bedding and foundation filter under the toe. The stone weighing 400 pounds (181 kg) or less extends 10 feet (3.05 meters) seaward of the W-2 stone, and the W-2 stone extends 15 feet (4.57 meters) seaward of the primary armor layer. The core is quarry-run stone weighing 1 ton (3629 kg) or less.

## 9.3 Toe Design

The primary armor cover layer extends to the sea floor because water depth is less than 1.5 times the design wave height (USACE 1984b). The toe apron of armor stone is two layers wide and two layers thick, with each layer 6 feet (1.83 meters) thick. The toe stone is 10-ton (9072 kg). The toe stone must be parallel-piped stone.

## 9.4 Armor Stone

Armor stone size is based on a 50-year extreme wave at the -24 foot contour of 14.5 feet (4.4 meters). Using 1 vertical to 2 horizontal side slopes, 165 pounds per cubic foot

(2643 kg/m<sup>3</sup>) unit weight of stone, the wave height of 14.5 feet (4.4 meters) and a  $K_D$  of 3 for placement, (this value of  $K_D$  requires some special placement for the armor rock), results in a stone size of 20,000 pounds or 10 tons (9,072 kg). Ice studies performed at the University of Iowa showed 8-ton (7257 kg) stone was adequate to protect from ice at Nome and the causeway has performed adequately with no damage since 1986.

The armor stone is 10-ton (9.07-mton). The armor layer is two stones thick (12 feet [3.66 meters] thick). The armor stone must be parallel-piped stone. The cross section is shown in figure 105.

The breakwater nose is more susceptible to wave and ice damage than the breakwater trunk. The cross section design of the nose was recalculated to ensure stability. Based on the Hudson formula, the unit weights required for the primary armor on the breakwater nose are determined by using reduced  $K_D$  values, smaller structure slopes, or by adding a third layer of primary armor. In this analysis, reduced  $K_D$  values were used which resulted in 22 ton stone being used on the nose. If the breakwater alternative is selected for construction, the stability of the 22 ton stone on a 1 vertical to 2 horizontal slope will need to be analyzed along with the rock size suitability for the ice conditions.

## 9.5 Navigation Aids

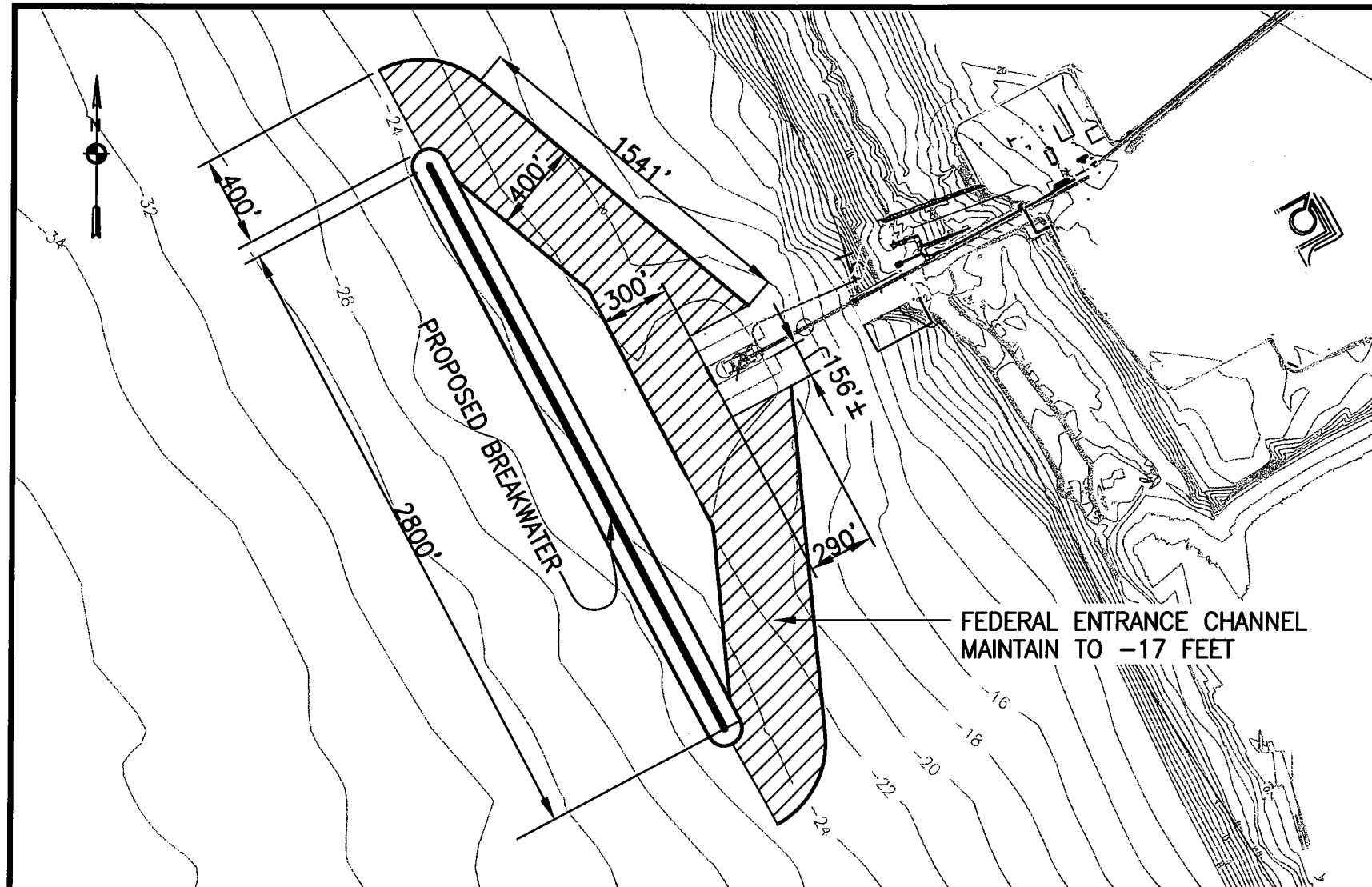
The Coast Guard requires a fixed navigation aid for the Portsite breakwater. The navigation aid required for the site by the Coast Guard is a light on each end of the breakwater. Any navigation aid other than the Coast Guard required aid would be a local cost and maintenance responsibility.

## 9.6 Construction Considerations

The breakwater construction is anticipated to take three years to complete, assuming a contract award in the fall. The construction contract will be an open invitation for bid. In order to attract a number of bidders, it is recommended that the project be advertised early to interest contractors to bid on this project. The contract should be awarded in the fall to allow the contractor the winter to prepare the logistics for the upcoming open water season.

The work season length, remote site location, wave climate, lack of local protection from wind and/or wave events are just some of the conditions that a contractor will need to consider when proposing on this contract. The start of the work season is based on the presence of whales and ice in the area. Based on previous years shipping records, the season typically begins in the beginning of July. It is anticipated that there will be approximately 100 days available for work before ice formation in the Bering Straits blocks travel from the site. Equipment needs to be demobilized from the site before the Bering Straits ices and prevents travel to or from the site.

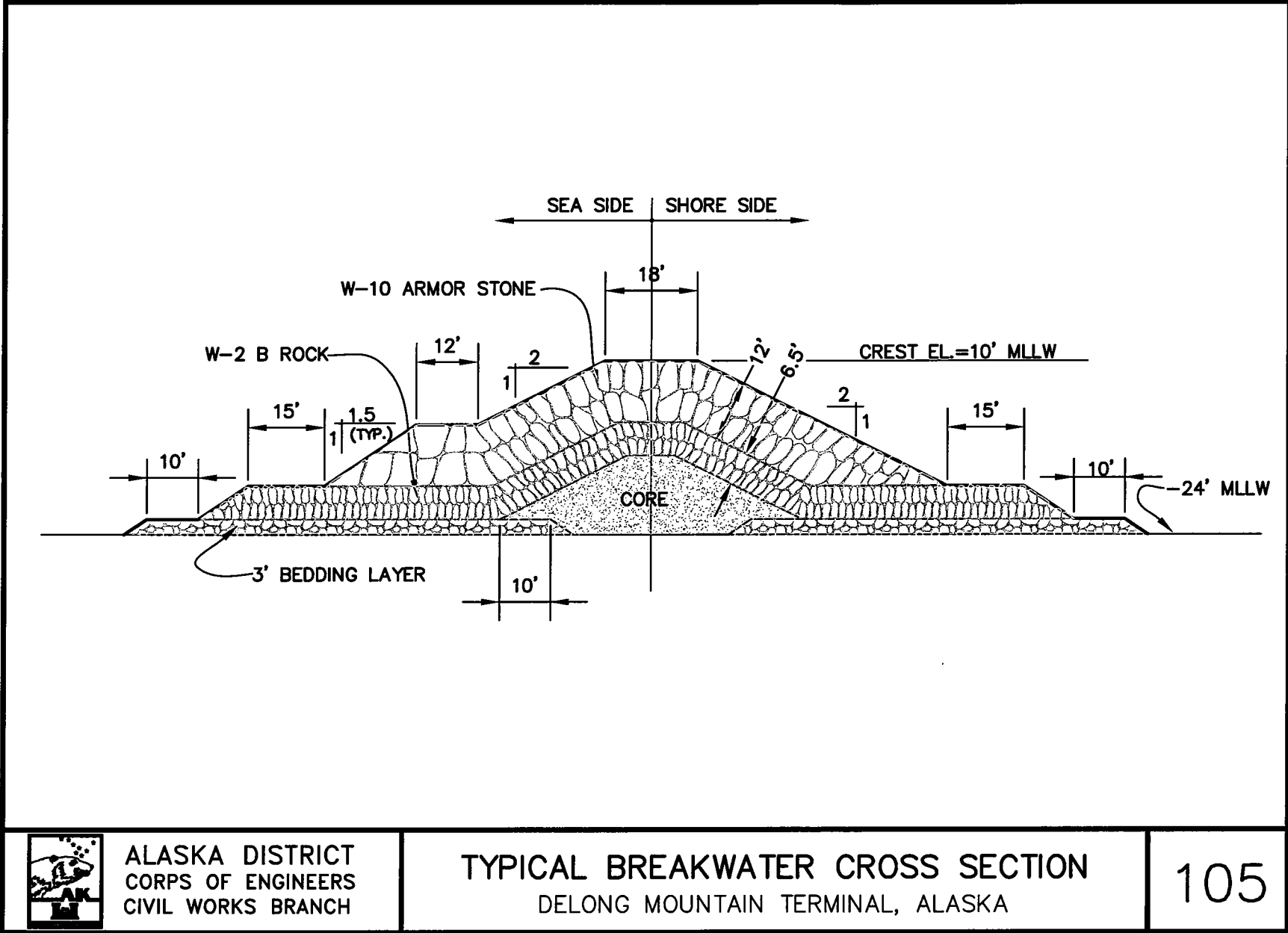
Storms at the site move through the area very rapidly and there is no place to run for shelter. Generally storms occur in the fall months. It is anticipated that the breakwater



ALASKA DISTRICT  
CORPS OF ENGINEERS  
CIVIL WORKS BRANCH

PRELIMINARY BREAKWATER DESIGN  
DELONG MOUNTAIN TERMINAL, ALASKA

104



ALASKA DISTRICT  
CORPS OF ENGINEERS  
CIVIL WORKS BRANCH

TYPICAL BREAKWATER CROSS SECTION  
DELONG MOUNTAIN TERMINAL, ALASKA

105

will be sufficiently constructed by the time the storm season begins to provide shelter for the contractor's water based equipment in the event of a storm.

The Portsite is a remote location so crew members will need to be flown to the site or ship up with the construction equipment. Once on site the crew that will work on the project will need to have room and board provided. It may be possible for the contractor to put his crew up at the Portsite work camp. It anticipated that the contractor will work two shifts, 10 hours a day, 7 days a week.

The contractor will need to make sure that there is fuel available for him at the site. He could bring up his own fuel barge, or he could make arrangements with AIDEA and Teck Cominco to purchase fuel from the site. Purchase of fuel from the site would need to be coordinated early in the year so that arrangements could be made to have additional fuel delivered to the site.

Once breakwater work commences the contractor will need to coordinate his work with Foss and the barge loading operation. The barge loading operation will begin in early July at the same time as the breakwater construction work, so there will be tugs and barges transiting the near shore area to approximately 3 miles offshore.

It is expected that the stone for the breakwater will come from Nome. The stone can be offloaded at the Portsite dock and stockpiled. At the end of each construction season, the breakwater will need to be finished with armor stone to protect it from damage over the winter. The armor stone will be removed at the start of the next construction season to continue work.

## **9.7 Breakwater Cost**

The estimated cost of the breakwater alternative is \$69.6 million. This includes a 3 year construction window. The 22-ton stone for the breakwater nose was estimated to cost \$112 per cubic yard. It is estimated that 6,120 cubic yards of 22-ton stone will be used. This included seasonal loss for the temporary placement of 22-ton stone at the end of each season. At the end of the first and second construction season the incomplete end of the breakwater will be protected with temporary armor rock that will be salvaged to the maximum extent possible at the start of the following construction season.

The armor stone used for the trunk armor is estimated to cost \$102 per cubic yard for 136,000 cubic yards. The B rock layer was estimated to cost \$84 per cubic yard for 119,400 cubic yards and the 54,900 cubic yards of core was estimated at \$73 per cubic yard. Bedding gravel was estimated to cost \$42 for 55,200 cubic yards of material.

## **10.0 GEOTECHNICAL CONSIDERATIONS**

### **10.1 Site Geology and Soils**

The sea bottom at the site is gently sloping with large areas of sand/silt interspersed with sand areas and sand/gravel areas. The coarser gravel areas are concentrated in the nearshore area in water depths less than 45 feet (13.7 meters).

The upper soil layer generally consisted of fine-grained soils that varied from firm to very hard in consistency and sandy soils that were typically medium dense. Occasionally, organic soil layers and lenses of peat were encountered. Subbottom profiling and boreholes indicated that the subsurface materials are composed of a layer of sand/silt/gravel/clay materials (from 10 to 25 feet [3.05 to 7.62 meters] thick) overlying a denser layer of sand/gravel (from 10 to 100 feet [3.05 to 30.5 meters] or more thick) and a basement material of sandstone bedrock.

The deeper sand/gravel materials protruded near the surface in sporadic locations in the survey area. Geological evidence indicates that the sand/gravel materials may be alluvial deposits. The submerged gravel and coarse sands may be remnant gravel beaches.

The bedrock surface in the project area varies from north to south and east to west. Bedrock is 39 feet (11.9 meters) below the seabed at the shore end of the project and 90 feet (27.4 meters) below the seabed at the 40 to 45-foot (12.2 to 13.7-meter) depth contour. Beyond this water depth, rock was not detected with the equipment used.

Bedrock coring indicates that the upper several feet of bedrock is weathered and that the material becomes more competent with depth. Bedrock material was homogenous, and described as either lavender sandstone or gray sandstone.

### **10.2 Boring Locations and Material Summary**

The location of the soil borings and a description of the soil are included in the Geotechnical Appendix.

## **11.0 MAINTENANCE DREDGING**

The two development alternatives considered for evaluation of maintenance dredging at the DMT site consist of a shore connected direct loading facility for Panamax vessels and an offshore breakwater with barge transfer of materials to Panamax vessels.

The direct loading facility consists of a shore connected conveyor system to a depth of about 20 feet (6.10 meters) with a dock and loading facility at that depth. A channel and turning basin would be dredged to the loading facility.

The breakwater and barge loading system with transfer to Panamax vessels in deep water consists of the existing conveyor, dock, and barge loading system at the - 18-foot (-5.5-

meters) depth protected by a shore parallel breakwater about 2,800 feet (853 meters) in length with its inshore toe at the -23-foot (-7-meter) depth. The breakwater extends to a height of +10 feet (+3.05 meters) MLLW and reduces waves at the dock from 6.6 feet (2 meters) to less than 3.3 feet (1 meter).

The viability of each of the development alternatives is subject to the effects of sediment transport and the maintenance that results from the construction of either alternative. The sediment transport mechanisms that could affect the site include:

- Transport by waves and currents shoreward of the littoral zone. Considered as sediment moving inshore of the 20-foot (6.10 meter) depth.
- Wave and current transported sediment seaward of the littoral zone
- Channel side slope deflation exacerbated by ship and tug wakes and currents during transits and docking operations.

The disruption of the bathymetry from the channel is anticipated to create a reduced energy environment that is conducive to the development of a rip current. The estimation of channel infilling presented in this document omits the processes of cross-shore sediment transport by a rip current developed from the resulting wave asymmetry. The omission of this process is not entirely valid but the average magnitude of sediment transport involved should not seriously impact the calculations.

## **11.1 Sedimentation Associated With Shore Connected Direct Loading Facility**

### **11.1.1 Littoral Zone**

Sediment transport will be affected by each of the proposed alternatives. The channel and turning basin option will leave an energy deficient zone extending through the surf and to the outer limits of the turning basin during longer period waves (greater than 5-second waves). This will result in deposition of littoral zone material on the shoreline and seaward towards the channel to a greater degree than under natural conditions. Sediments, if left to accumulate, may impact shoreline erosion in a relatively short period of time and could impact the turning basin in the longer term. Shore side management of the littoral sediments to prevent shore erosion is required. Management after individual events would minimize the impacts to the coastline. The littoral zone can extend to the -15-foot (-4.6-meter) depth contour under extreme events. Care has been taken to limit the channel excavation including the required overdepth dredging so that side slope deterioration to a 1 on 10 slope would have minimal incision into the littoral zone.

If incision does occur, sediment transport to the channel and berthing area will dramatically impact the use of the port facility by initiating a seaward flow of currents and sediments. This is physically similar to a fixed position rip current. Shoreline

recession would accompany the sediment deposition in the channel and berthing area. The deposited sediment in the channel and berthing area would need to be removed prior to vessel use. The major storms that impact the Ports site are all late season events so sediment removal would not occur until the open ice season at the beginning of the next shipping season. It is estimated that 30 days of the shipping season will be lost annually if incision occurs. The landward extension of the channel has been limited to the -20-foot (-6.1-meter) contour to prevent incision and the associated ramifications.

The longshore transport of littoral materials was estimated by CHL during a numerical model study. Details on the model and work performed by the CHL may be found in Chapter 4 of *Engineering Studies in Support of the Delong Mountain Terminal Project*. The modeling indicated that the total and net transport quantities in the littoral zone are modest. A summary of that analysis is presented in tables 21 and 22. The longshore transport is dominated by September, October and November events, which coincide with increased storm activity at the site. The period of December through June was presumed to be ice covered and sediment transport was assumed to be negligible. The sensitivity of the model to the range of grain sizes observed on the beach was analyzed by varying the material D50 from 0.02 inches to 0.079 inches (0.5 mm to 2.0 mm).

Calculations were ground truthed by a review of literature documenting net accumulations at two nearby sites and a review of sedimentation experienced by the existing dock. The sedimentation values were small and if an error of 100 percent is assumed, the modeled values still remain small and manageable. For estimating purposes, 26,159 cubic yards (20,000 cubic meters) per year is assumed to require removal annually. This is close to the estimated average gross littoral transport. Transfer of material to bypass the port site after major storms would need to take place with a net transfer to the south. This bypass estimate probably exceeds the real management requirement, as some sediment will naturally bypass.

### **11.1.2 Wave and Current Induced Sediment Transport Seaward of the Littoral Zone**

The navigation channel, turning basin, and berthing area, would interrupt sediment transport in this region. The degree of interruption was numerically modeled by the CHL, and estimates were made of the amount of sediment that would be deposited with a shoreward start of the berthing area at -28 feet (-8.5 meters) MLLW, -24 feet (-7.3 meters) MLLW, and -20 feet (-6.1 meters) MLLW. Summaries of the channel infilling at the -28-foot and -20-foot (-8.5-meter and -6.1 meter) MLLW for years 1985 through 2000 are shown in table A-42. Variables within the estimates include increases and decreases in currents, wave energy, and grain size. The best estimate values were used to establish economics and project formulation. The maximum and minimum sediment transport values have to be evaluated to address risks in maintenance procedures and estimating possible project costs. Only information from 1985 to 2000 was used for estimating site conditions for maintenance, as the higher frequency storms were not well represented in years prior to 1985. The record before 1985 is also slightly reduced due to not evaluating sediment yield for storm threshold with less than about a 2.5-year return

frequency. Movement in the lower energy storms is modest and the error introduced is very minor.

Using the best estimate table and only the years from 1985 to 2000 the average infill rate from this source is about 68,013 cubic yards (52,000 cubic meters) per year for the – 28-foot (–8.5-meter) MLLW terminal and about 74,553 cubic yards (57,000 cubic meters) for a terminal located at the – 20-foot (–6.1-meter) MLLW depth. The small difference in quantity resulted in retaining only the shallower channel terminus –20-foot (–6.1-meter) MLLW for further examination. The minimum estimated infill is 0 cubic yards, and if one assumes that anything less than 6,540 cubic yards (5,000 cubic meters) is inconsequential, more than half the years do not contribute significant amounts of sediment. The maximum year is, however, more than 800,000 cubic yards (784,770 cubic meters). The major portion of deposition in all years occurs during the October and November period shortly before ice closes the area to construction and shipping. The late season deposition would require storage of transported sediment to prevent interference with shipping in the following season.

To arrive at the distribution of sediments along the channel, the sediment infilling from storm events was analyzed. The 16-year history between 1985 and 2000 was used to determine the amount of storage needed to allow sediment to accumulate in the channel. An example of a storm distribution is shown in figure 106. Storm distributions for extreme storm events can be found in appendix 4B of the CHL report, *Engineering Studies in Support of the Delong Mountain Terminal Project*. As can be seen from the distribution, the majority of channel infilling begins at the –43-foot (–13.1-meter) contour and continues shoreward into the turning basin and berthing area. A drop off in the infilling occurs between the 30-foot (9.1-meter) and 26-foot (7.9-meter) contour, but increases again shoreward of the –26-foot (–7.9-meter) contour. This pattern of infilling is typical along the channel for the storm events analyzed. The increase in sediment between a berth terminus at –20 feet and a berth terminus at –28 feet is approximately 10 percent of the average annual infilling or 7,109 cubic yards (5,435 cubic meters) per year. This volume of sediment is minor when compared with the cost of extending the dock to the –28-foot (–8.5-meter) contour.

Draft Feasibility Report  
Appendix A: Hydraulic Design, Delong Mountain Terminal, Alaska

Year	Best Estimate of Channel Infilling at -20 feet (-6.1m), yd <sup>3</sup> (m <sup>3</sup> )						Best Estimate of Channel Infilling at -28 feet (-8.5 m), yd <sup>3</sup> (m <sup>3</sup> )						Difference in Infilling m <sup>3</sup>
	Jul	Aug	Sep	Oct	Nov	Annual	Jul	Aug	Sep	Oct	Nov	Annual	
1985	0 (0)	0 (0)	0 (0)	8305 (6350)	0 (0)	8350 (6350)	0 (0)	0 (0)	0 (0)	6705 (5126)	0 (0)	6705 (5126)	1601 (1224)
1986	0 (0)	0 (0)	0 (0)	0 (0)	0 (0)	0 (0)	0 (0)	0 (0)	0 (0)	0 (0)	0 (0)	0 (0)	0 (0)
1987	0 (0)	0 (0)	0 (0)	0 (0)	0 (0)	0 (0)	0 (0)	0 (0)	0 (0)	0 (0)	0 (0)	0 (0)	0 (0)
1988	0 (0)	980 (749)	0 (0)	0 (0)	0 (0)	980 (749)	0 (0)	753 (576)	0 (0)	0 (0)	0 (0)	753 (576)	226 (173)
1989	0 (0)	0 (0)	0 (0)	4412 (3373)	0 (0)	4412 (3373)	0 (0)	0 (0)	0 (0)	2931 (2241)	0 (0)	2931 (2241)	1481 (1132)
1990	0 (0)	1127 (862)	0	0 (0)	127606 (97562)	128734 (98424)	0 (0)	768 (587)	0 (0)	0 (0)	108271 (82779)	109039 (83366)	19695 (15058)
1991	0 (0)	0 (0)	0 (0)	77885 (59547)	0 (0)	77885 (59547)	0 (0)	0 (0)	0 (0)	65840 (50338)	0 (0)	65840 (50338)	12045 (9209)
1992	0 (0)	0 (0)	0 (0)	29154 (22290)	0 (0)	29154 (22290)	0 (0)	0 (0)	0 (0)	27663 (21150)	0 (0)	27633 (21150)	1491 (1140)
1993	0 (0)	1853 (1417)	883 (675)	1197 (915)	35602 (27220)	39535 (30227)	0 (0)	1279 (978)	604 (462)	943 (721)	29102 (22250)	31928 (24411)	7607 (5816)
1994	0 (0)	1154 (882)	0 (0)	5520 (4220)	0 (0)	6673 (5102)	0 (0)	875 (669)	0 (0)	4365 (3337)	0 (0)	5240 (4006)	1434 (1096)
1995	0 (0)	0 (0)	0 (0)	0 (0)	0 (0)	0 (0)	0 (0)	0 (0)	0 (0)	0 (0)	0 (0)	0 (0)	0 (0)
1996	12427 (9501)	0 (0)	0 (0)	680355 (520169)	112260 (85829)	805042 (615499)	10948 (8370)	0 (0)	0 (0)	636468 (486615)	100800 (77067)	748216 (572052)	53827 (43447)
1997	0 (0)	0 (0)	0 (0)	11193 (8558)	83832 (64094)	95025 (72652)	0 (0)	0 (0)	0 (0)	9118 (6971)	74585 (57024)	83702 (63995)	11323 (8657)
1998	0 (0)	0 (0)	0 (0)	0 (0)	0 (0)	0 (0)	0 (0)	0 (0)	0 (0)	0 (0)	0 (0)	0 (0)	0 (0)
1999	0 (0)	0 (0)	0 (0)	0 (0)	0 (0)	0 (0)	0 (0)	0 (0)	0 (0)	0 (0)	0 (0)	0 (0)	0 (0)
2000	0 (0)	0 (0)	0 (0)	0 (0)	0 (0)	0 (0)	0 (0)	0 (0)	0 (0)	0 (0)	0 (0)	0 (0)	0 (0)
<b>AVG</b>	<b>777 (594)</b>	<b>319 (244)</b>	<b>55 (42)</b>	<b>51126 (39089)</b>	<b>22456 (17169)</b>	<b>74734 (57138)</b>	<b>684 (523)</b>	<b>230 (176)</b>	<b>38 (29)</b>	<b>47127 (36031)</b>	<b>19547 (14945)</b>	<b>67626 (51704)</b>	<b>7109 (5435)</b>

### 11.1.3 Side Slope Sloughing Due To Waves And Vessel Activity

Side slopes of the channel are expected to deteriorate from the 1 on 3 constructed slopes to a 1 on 10 slope in the short term. Over the long run, the channel slope will likely lay back on slopes that are similar to the local subsurface conditions. In the event that this occurs, maintenance to stabilize the slope may be necessary to prevent further layback. This maintenance is not recommended until the channel slope has eroded beyond a 1 vertical to 10 horizontal slope. Side slope deterioration quantities are greatest at the inshore end of the project. The quantities associated with sloughing of the inner 5,000 feet were examined for additional sediment contribution (table A-43).

Depth at terminal End	1 on 10
-28 MLLW	613,000 cubic yards
-24 MLLW	755,000 cubic yards
-20 MLLW	1,014,000 cubic yards

Side slope deflation has the potential to supply a significant amount of sediment to the channel. For estimating purposes, it is assumed that at least 70 percent of the slope decay to 1 on 10 would take place in the first 5 years after construction.

Draft Feasibility Report  
 Appendix A: Hydraulic Design, Delong Mountain Terminal, Alaska

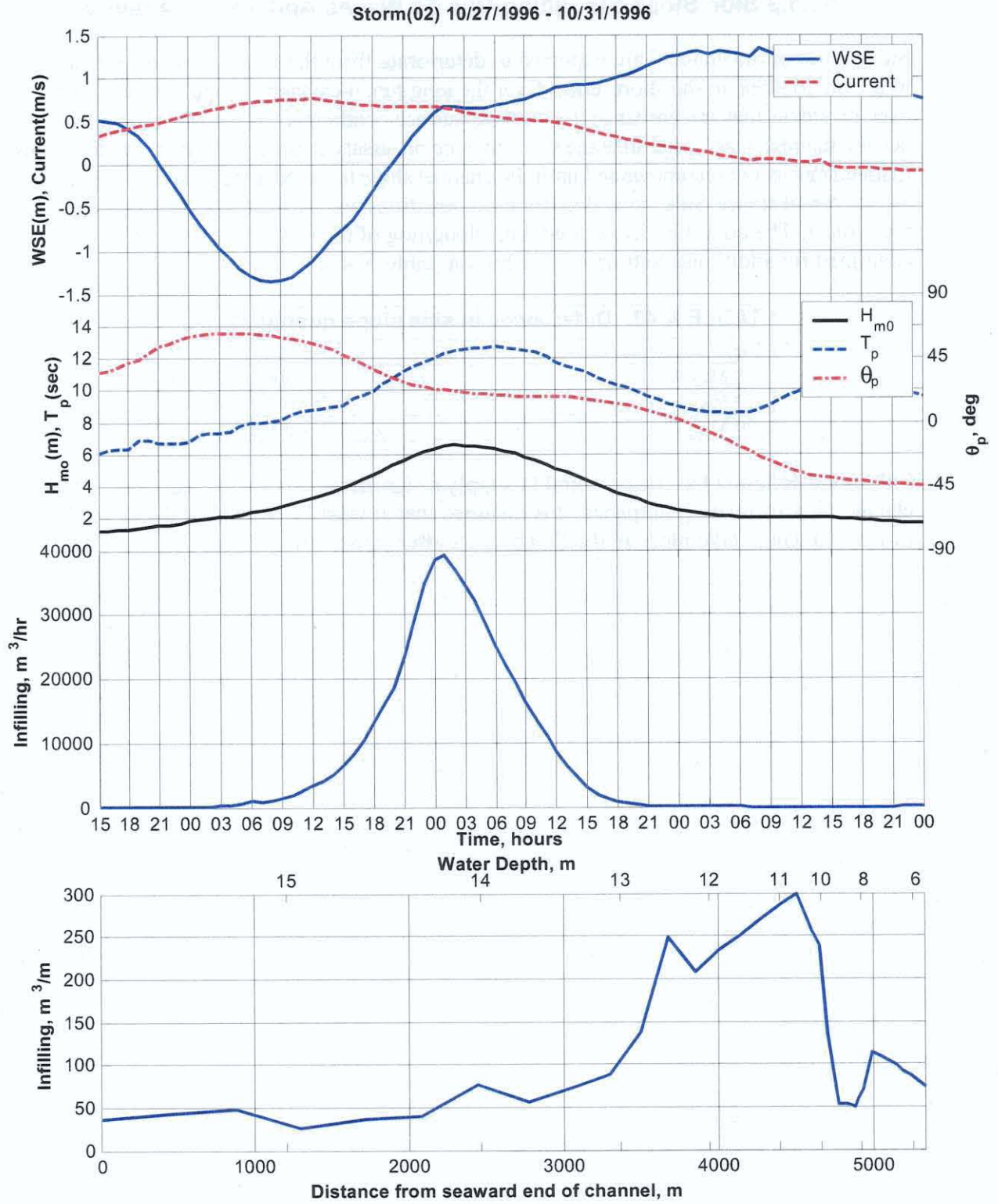


Figure 106  
 \*(1 m = 3.28 ft)

### 11.1.4 Required Overdepth Dredging Options

Maintenance dredging options evaluated for the site were limited by the meteorological and oceanic conditions at the site. Dredge equipment at the site is vulnerable to damage from rapidly changing climatic conditions. The beaching of a barge during a storm in October 2002 is an illustration of the damage that can occur during one short duration storm event.

The wave climate has been previously discussed in detail in this report. The winds at the site also pose a threat to equipment during the open water season. Summarized monthly wind information for one of the wave hindcast save points (site 5) is provided in tables A-44 through A-51. Significant hourly wind events up to 38.9 knots (20 meters per second) can occur during the open-water season. Gusts associated with those winds make non self-powered vessels vulnerable to damage. From this data it is evident that low cost hopper or cutterhead dredges without power would require either harbor protection or tug attendance during major storm events. The lack of such protection or attendance can result in the loss of the equipment as experienced by the North Slope Borough with the loss of their dredge in August 2000. A storm with winds up to 52 knots impacted the coast at Barrow, Alaska and resulted in damage to their dredge. The life of that particular dredge was less than five years. While sustained winds of 52 knots were not seen in the Portsite hindcast, the hindcast winds indicate that strong winds are experienced at the DMT site.

Table A-44 PERCENT OCCURRENCE OF WIND SPEEDS JUNE 1985 - 1999 LAT: 67.50 N, LONG: 195.75 E	
Wind Speed (knot (m/s))	TOTAL
0.00 - 4.84 (0.00 - 2.49)	38.22%
4.86 - 9.70 (2.50 - 4.99)	32.06%
9.72 - 14.56 (5.00 - 7.49)	19.17%
14.58 - 19.42 (7.50 - 9.99)	7.94%
19.44 - 24.28 (10.00 - 12.49)	2.17%
24.30 - 29.13 (12.50 - 14.99)	0.44%
29.16 - 34.00 (15.00 - 17.49)	0
34.02 - 38.86 (17.50 - 19.99)	0
38.88 - 43.72 (20.00 - 22.49)	0
43.74 - 48.58 (22.50 - 24.99)	0
48.60 - 53.44 (25.00 - 27.49)	0
53.46 - 58.30 (27.50 - 29.99)	0
58.32 - GREATER (30.00 - GREATER)	0
TOTAL	100.00

Table A-45 PERCENT OCCURRENCE OF WIND SPEEDS JULY 1985 - 1999 LAT: 67.50 N, LONG: 195.75 E	
Wind Speed (knot (m/s))	TOTAL
0.00 - 4.84 (0.00 - 2.49)	21.45%
4.86 - 9.70 (2.50 - 4.99)	33.44%
9.72 - 14.56 (5.00 - 7.49)	27.96%
14.58 - 19.42 (7.50 - 9.99)	13.01%
19.44 - 24.28 (10.00 - 12.49)	3.06%
24.30 - 29.13 (12.50 - 14.99)	0.75%
29.16 - 34.00 (15.00 - 17.49)	0.27%
34.02 - 38.86 (17.50 - 19.99)	0.05%
38.88 - 43.72 (20.00 - 22.49)	0

Draft Feasibility Report  
Appendix A: Hydraulic Design, Delong Mountain Terminal, Alaska

Table A-45 PERCENT OCCURRENCE OF WIND SPEEDS JULY 1985 – 1999 LAT: 67.50 N, LONG: 195.75 E	
Wind Speed (knot (m/s))	TOTAL
43.74 - 48.58 (22.50 - 24.99)	0
48.60 - 53.44 (25.00 - 27.49)	0
53.46 - 58.30 (27.50 - 29.99)	0
58.32 - GREATER (30.00 – GREATER)	0
<b>TOTAL</b>	<b>100.00%</b>

Table A-46 PERCENT OCCURRENCE OF WIND SPEEDS AUGUST 1985 – 1999 LAT: 67.50 N, LONG: 195.75 E	
Wind Speed (knot (m/s))	TOTAL
0.00 - 4.84 (0.00 - 2.49)	11.51%
4.86 - 9.70 (2.50 - 4.99)	26.99%
9.72 - 14.56 (5.00 - 7.49)	31.34%
14.58 - 19.42 (7.50 - 9.99)	17.42%
19.44 - 24.28 (10.00 - 12.49)	9.46%
24.30 - 29.13 (12.50 - 14.99)	2.42%
29.16 - 34.00 (15.00 - 17.49)	0.75%
34.02 - 38.86 (17.50 - 19.99)	0.11%
38.88 - 43.72 (20.00 - 22.49)	0
43.74 - 48.58 (22.50 - 24.99)	0
48.60 - 53.44 (25.00 - 27.49)	0
53.46 - 58.30 (27.50 - 29.99)	0
58.32 - GREATER (30.00 – GREATER)	0
<b>TOTAL</b>	<b>100.00%</b>

Table A-47 PERCENT OCCURRENCE OF WIND SPEEDS SEPTEMBER 1985 – 1999 LAT: 67.50 N, LONG: 195.75 E	
Wind Speed (knot (m/s))	TOTAL
0.00 - 4.84 (0.00 - 2.49)	2.11%
4.86 - 9.70 (2.50 - 4.99)	17.89%
9.72 - 14.56 (5.00 - 7.49)	31.89%
14.58 - 19.42 (7.50 - 9.99)	25.00%
19.44 - 24.28 (10.00 - 12.49)	14.44%
24.30 - 29.13 (12.50 - 14.99)	6.28%
29.16 - 34.00 (15.00 - 17.49)	2.17%
34.02 - 38.86 (17.50 - 19.99)	0.22%
38.88 - 43.72 (20.00 - 22.49)	0
43.74 - 48.58 (22.50 - 24.99)	0
48.60 - 53.44 (25.00 - 27.49)	0
53.46 - 58.30 (27.50 - 29.99)	0
58.32 - GREATER (30.00 – GREATER)	0
<b>TOTAL</b>	<b>100.00%</b>

Table A-48 PERCENT OCCURRENCE OF WIND SPEEDS OCTOBER 1985 – 1999 LAT: 67.50 N, LONG: 195.75 E	
Wind Speed (knot (m/s))	TOTAL
0.00 - 4.84 (0.00 - 2.49)	2.47%
4.86 - 9.70 (2.50 - 4.99)	16.61%
9.72 - 14.56 (5.00 - 7.49)	28.49%
14.58 - 19.42 (7.50 - 9.99)	24.30%
19.44 - 24.28 (10.00 - 12.49)	17.37%
24.30 - 29.13 (12.50 - 14.99)	7.90%
29.16 - 34.00 (15.00 - 17.49)	2.15%
34.02 - 38.86 (17.50 - 19.99)	0.54%
38.88 - 43.72 (20.00 - 22.49)	0.16%
43.74 - 48.58 (22.50 - 24.99)	0
48.60 - 53.44 (25.00 - 27.49)	0

Draft Feasibility Report  
Appendix A: Hydraulic Design, Delong Mountain Terminal, Alaska

Wind Speed (knot (m/s))	TOTAL
53.46 - 58.30 (27.50 - 29.99)	0
58.32 - GREATER (30.00 – GREATER)	0
TOTAL	100.00%

Wind Speed (knot (m/s))	TOTAL
0.00 - 4.84 (0.00 - 2.49)	2.89%
4.86 - 9.70 (2.50 - 4.99)	14.89%
9.72 - 14.56 (5.00 - 7.49)	22.72%
14.58 - 19.42 (7.50 - 9.99)	23.17%
19.44 - 24.28 (10.00 - 12.49)	19.56%
24.30 - 29.13 (12.50 - 14.99)	10.72%
29.16 - 34.00 (15.00 - 17.49)	4.50%
34.02 - 38.86 (17.50 - 19.99)	1.33%
38.88 - 43.72 (20.00 - 22.49)	0.22%
43.74 - 48.58 (22.50 - 24.99)	0
48.60 - 53.44 (25.00 - 27.49)	0
53.46 - 58.30 (27.50 - 29.99)	0
58.32 - GREATER (30.00 – GREATER)	0
TOTAL	100.00%

Two methodologies for maintaining the project have been examined and a matrix (table A-50) has been established to examine their merits. The methodologies are:

- A non-powered project dedicated dredge that would use tugs for mobility
- A conventional contract hopper dredge

**Table A-50 Project Maintenance Matrix**

Dredge Type	Good Features	Bad Features
Non powered project dedicated	Low first cost if sized for average conditions	Storm vulnerable Loss expectation high unless assigned a helper tug.
		Not flexible enough to adapt to range of yearly expectations without the addition of required overdepth dredging area
		Not flexible enough to adapt to the possible error range in expected deposition
	Mobilization cost are minimized	Need local moorage or upland storage during the off season and need tug boat assistance during extreme adverse weather
		Requires either a dedicated tug boat or establishes the need for a 3 tug boat array to manage the system.
		Requires outlay of capital before experience can dictate real time requirements Under or oversizing a distinct possibility.
Contract Hopper Dredge	Retains flexibility to accommodate a reasonable error range in estimates	Mobilization costs are high unless there is adequate sediment storage in a required overdepth dredging area to make mobilization infrequent.

**Table A-50 Project Maintenance Matrix**

Dredge Type	Good Features	Bad Features
	Requires no initial outlay of capital investment.	Requires significant lead time to contract for services. Up to 2 years advanced notice
	Requires no attendant tug boat to operate and can ride out storms without help or damage.	
	With an area dredged for required overdepth it can accommodate a large range of events.	Requires overdepth dredging area.

The use of a project-dedicated dredge was not pursued beyond development of the matrix, as it does not provide the flexibility that project uncertainties make desirable.

### 11.1.5 Required Overdepth Dredging For Efficient Maintenance

To minimize the impact of repeated mobilizations, required overdepth dredging for efficient maintenance should be performed on the channel to create a sediment storage area that is sized to accommodate the seasonal capacity of a dredge that is available to move the sediment and have the reserve capacity to sustain a major infill event between dredging cycles. A dredge with a capacity of 1,200,000 cubic yards per season should be used to perform the required overdepth dredging work. A sump size of 1,900,000 cubic yards (1,453,000 cubic meters) would allow full use of the dredge equipment by accommodating sediment deposition from channel side slope sloughing and infilling while still providing storage for sediment infilling from a major storm event.

The best, or most likely infilling estimate for 1985 through 2000 (table A-42) was used to analyze the volume and location of sediment deposition along the channel. A 1,900,000 cubic yard sump is large enough to accommodate the average annual yield of 74,734 cubic yards (57,138 cubic meters) and bank sloughing for a period of years. It would also provide containment of the most probable worst-case infill for a 50-year event 688,355 cubic yards (520,169 cubic meters).

Bank sloughing is anticipated to layback the channel side slopes to a 1 on 10 over time. For estimating purposes the side slopes are expected to contribute about 725,000 cubic yards (554,302 cubic meters) of sediment in the initial five years of operation. This volume, with an added 373,670 cubic yards (285,691 cubic meters) from average seasonal infilling during the same five year period, would occupy 1,098,670 cubic yards (839,994 cubic meters) of the sump, and leave 801,300 cubic yards available to accommodate a 50 year event.

The maximum infilling estimate (table A-30) for the same five years would require a 725,000-cubic yards (554,302-cubic meters) sump for bank sloughing plus a 1,056,000-cubic yard (807,000-cubic meters) sump to store the average sediment transport of 211,294 cubic yard per year. A 1,900,000 cubic yard (1,453,000 cubic meters) sump adequately addresses the maximum sediment infilling scenario, provides dredging deferment to reasonable mobilization periods, and contains a quantity that can be excavated within one construction season without interfering with navigation. The only

Draft Feasibility Report  
Appendix A: Hydraulic Design, Delong Mountain Terminal, Alaska

provision that is lacking is additional storage for a 50 year sediment infilling event for the entire five years.

The sump size should also be able to retain sediment from a reasonably severe event without interfering with navigation during the time it takes to contract and remove sediments. Hopper dredges are normally fully utilized, and to acquire reasonable bids, a 2-year advance notice on procurement is desirable. A 1,900,000 cubic yards (1,453,000 cubic meters) sump allows this advance planning. Table A-51 shows the dredging cycles, the infilling expected between the cycles, and the remaining sump capacity. Note that dredging is performed to maintain a sump capable of storing a 50 year event using the best infilling estimate.

Table A-51. Required Overdepth Dredging

Year	Dredged Volume [cy]	Side Slope Sloughing [cy]	Seasonal Infilling [cy]	Volume Available for Infilling [cy]
0	1,900,000	145,000	74,734	1,680,266
1		145,000	74,734	1,460,532
2		145,000	74,734	1,240,798
3		145,000	74,734	1,021,064
4		145,000	74,734	801,330
5	1,098,670	145,000	74,734	1,680,266
6		145,000	74,734	1,460,532
7		0	74,734	1,385,798
8		0	74,734	1,311,064
9		0	74,734	1,236,330
10		0	74,734	1,161,596
11		0	74,734	1,086,862
12		0	74,734	1,012,128
13		0	74,734	937,394
14		0	74,734	862,660
15		0	74,734	787,926
16		0	74,734	713,192
17	1,186,808	0	74,734	1,825,266
18		0	74,734	1,750,532
19		0	74,734	1,675,798
20		0	74,734	1,601,064
21		0	74,734	1,526,330
22		0	74,734	1,451,596
23		0	74,734	1,376,862
24		0	74,734	1,302,128
25		0	74,734	1,227,394
26		0	74,734	1,152,660
27		0	74,734	1,077,926
28		0	74,734	1,003,192
29		0	74,734	928,458
30		0	74,734	853,724
31		0	74,734	778,990
32		0	74,734	704,256
33	1,195,744	0	74,734	1,825,266
34		0	74,734	1,750,532
35		0	74,734	1,675,798
36		0	74,734	1,601,064
37		0	74,734	1,526,330
38		0	74,734	1,451,596
39		0	74,734	1,376,862
40		0	74,734	1,302,128
41		0	74,734	1,227,394
42		0	74,734	1,152,660
43		0	74,734	1,077,926
44		0	74,734	1,003,192
45		0	74,734	928,458

Draft Feasibility Report  
Appendix A: Hydraulic Design, Delong Mountain Terminal, Alaska

Table A-51. Required Overdepth Dredging

Year	Dredged Volume [cy]	Side Slope Sloughing [cy]	Seasonal Infilling [cy]	Volume Available for Infilling [cy]
46		0	74,734	853,724
47		0	74,734	778,990
48		0	74,734	704,256
49	1,195,744	0	74,734	1,825,266
50		0	74,734	1,750,532

The distribution of sediment infilling along the channel, combined with an estimate for bank sloughing, was used to develop an area for the required overdepth dredging. Analysis of the sediment distribution along the channel and the plot of the normalized infilling volume shown in figure 107, indicates that 70 percent of the storage development for required overdepth dredging should be provided in the area between the -20-foot (-6.1-meter) contour and the -43-foot (-13.1-meter) contour. A profile of the required overdepth dredging on the channel is shown in figure 108. From the -43 foot contour landward 1,307,000 cubic yards is removed from the original dredge area, resulting in an increased depth of five feet. From the -43 foot contour seaward 577,000 cubic yards of material is removed from the channel resulting in an increased depth of two feet.

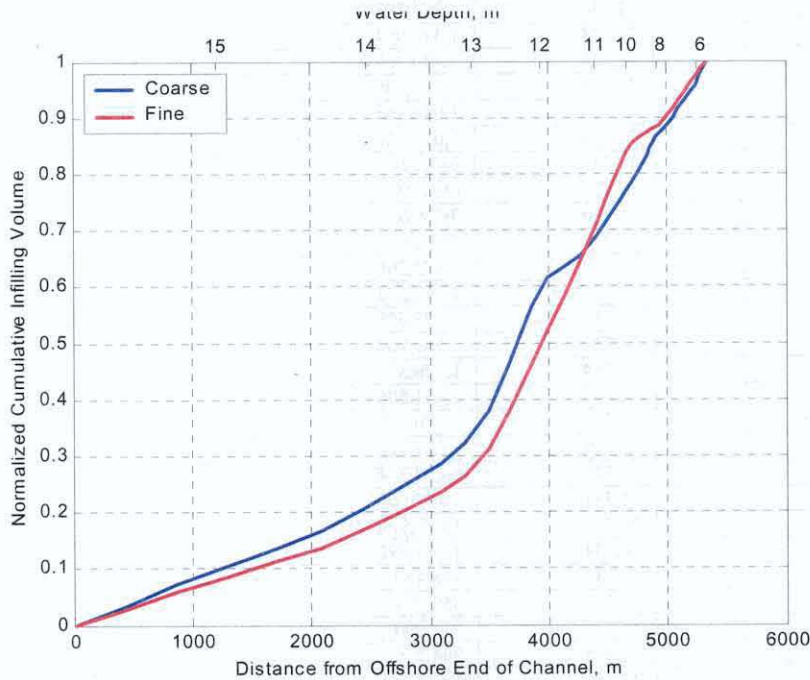
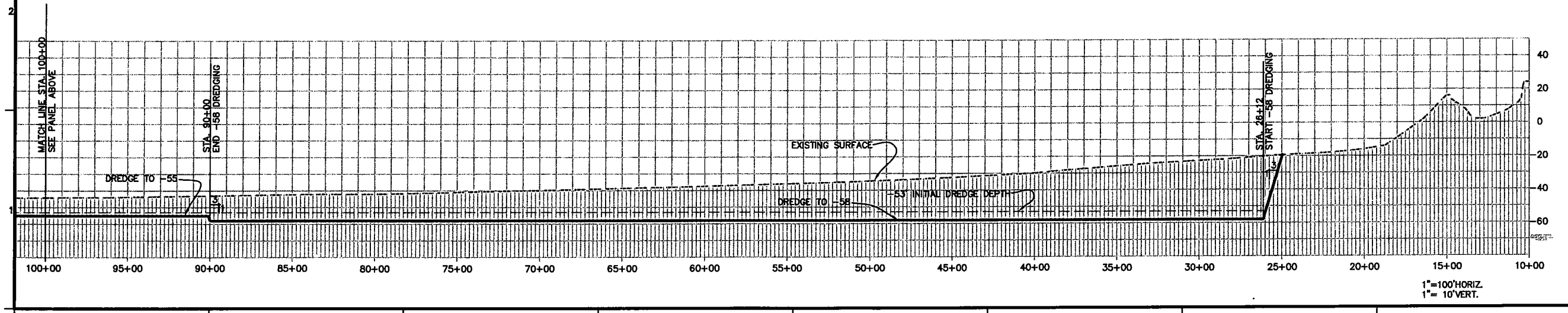
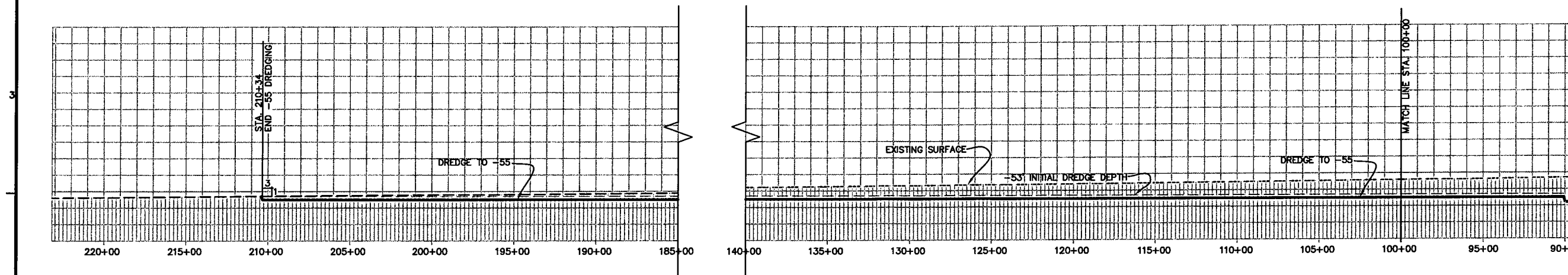
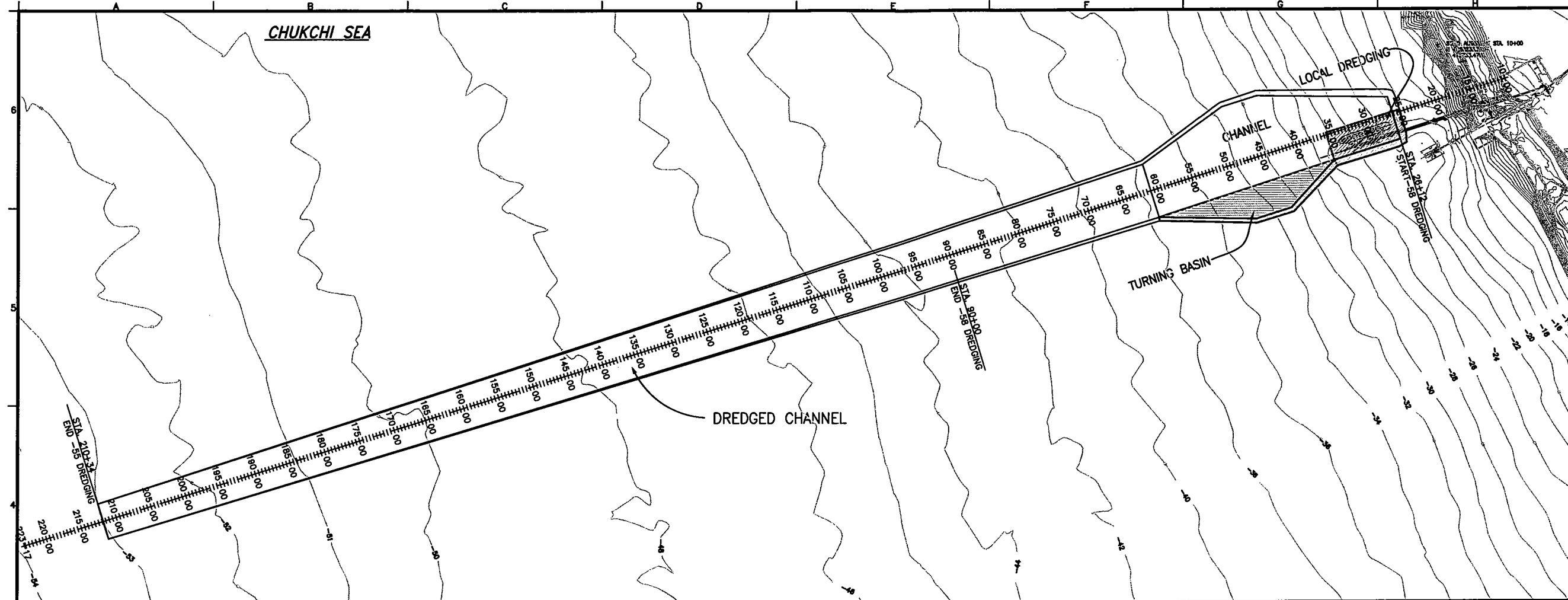


Figure 107 Normalized infilling volume

\*(1 meter = 3.28 feet)



  
 US ARMY CORPS OF ENGINEERS ALASKA DISTRICT  
 PROJECT NO. \_\_\_\_\_  
 DRAWING NO. \_\_\_\_\_  
 SHEET NO. \_\_\_\_\_ OF \_\_\_\_\_  
 DATE \_\_\_\_\_  
 DESIGNER \_\_\_\_\_  
 CHECKER \_\_\_\_\_  
 APPROVER \_\_\_\_\_  
 TITLE \_\_\_\_\_  
 INV. NO. DACABS-XX-B-XXXX

DELONG MOUNTAIN TERMINAL ALASKA  
 DELONG MOUNTAIN HARBOR IMPROVEMENTS  
 HYDRAULICS & HYDROLOGY  
 ADVANCE MAINTENANCE PLAN AND PROFILE I

Reference number:  
**108**  
 Sheet - of

1" = 100' HORIZ.  
 1" = 10' VERT.

### 11.1.6 Annual Dredging Cost For Deep Water Facility

The annual costs of the required overdepth dredging for the sump and littoral drift bypassing were evaluated to determine the least cost dredging alternative. The periodic dredging to clean out the sump, and the annual bypassing of 26,000 cubic yards of littoral material were included in the annual cost of each alternative. The initial sump construction cost will be part of the initial construction. The sump sizes that were evaluated were:

- 2,250,000 cubic yard,
- 1,900,000 cubic yard,
- 1,450,000 cubic yard,
- 1,250,000 cubic yard.

A sump sized larger than 1,900,000 cubic yards risked interruption of shoreline processes by incision into the littoral zone, so the analysis of the 2,250,000 cubic yard sump was performed as an academic exercise to determine the economic advantage of the sump size. A plot of the annual dredging costs and the associated sump size is shown in figure 109.

The annual cost for the 1,250,000 cubic yard sump provides storage for a 50-year sedimentation event and reflects dredging every other year for six years and again in year 11 to clean out average annual sedimentation and side slope sloughing. Annual littoral bypassing of 26,000 cubic yards is also included in the cost. After the side slopes have stabilized, dredging will be performed every seven years. The average annual cost associated with cleaning out the sump, and the yearly bypassing is \$1,965,000.

The annual cost for the 1,450,000 cubic yard sump provides storage for a 50-year sedimentation event and reflects dredging in years three, six, and fourteen to clean out average annual sedimentation and side slope sloughing. Annual littoral bypassing of 26,000 cubic yards is also included in the cost. After the side slopes have stabilized (after dredging in year fourteen), dredging will be performed every ten years. The average annual cost associated with cleaning out the sump, and the yearly bypassing is \$1,580,000.

The annual cost for the 1,900,000 cubic yard sump provides storage for a 50-year event, average annual sedimentation, and side slope deterioration. Annual littoral bypassing of 26,000 cubic yards is also included in the cost. Channel dredging is reflected in years 5, 17, 33, and 49. The side slopes will have stabilized by year seventeen and will be on a sixteen-year dredge schedule afterwards. The average annual cost associated with cleaning out the sump, and the yearly bypassing is \$1,245,000.

The annual cost for the 2,250,000 cubic yard sump provides storage for a 50-year event, average annual sedimentation, and side slope deterioration. Annual littoral bypassing of 26,000 cubic yards is also included in the cost. Channel dredging is reflected in years 7, 28, and 49. The side slopes will have stabilized by year seven and will be on a twenty one-year dredge schedule afterwards. The average annual cost associated with cleaning out the sump, and the yearly bypassing is \$1,120,000. As can be seen in figure 109 the

average annual costs continue to decrease with increasing sump size. This reflects the ability of the sump to store more sediment, which reduces the frequency of major dredging. The practicality of dredging a 2,250,000 cubic yard sump becomes the limiting factor. This size sump risks incision into the littoral zone, which would result in increased sedimentation and disruption of the shoreline processes.

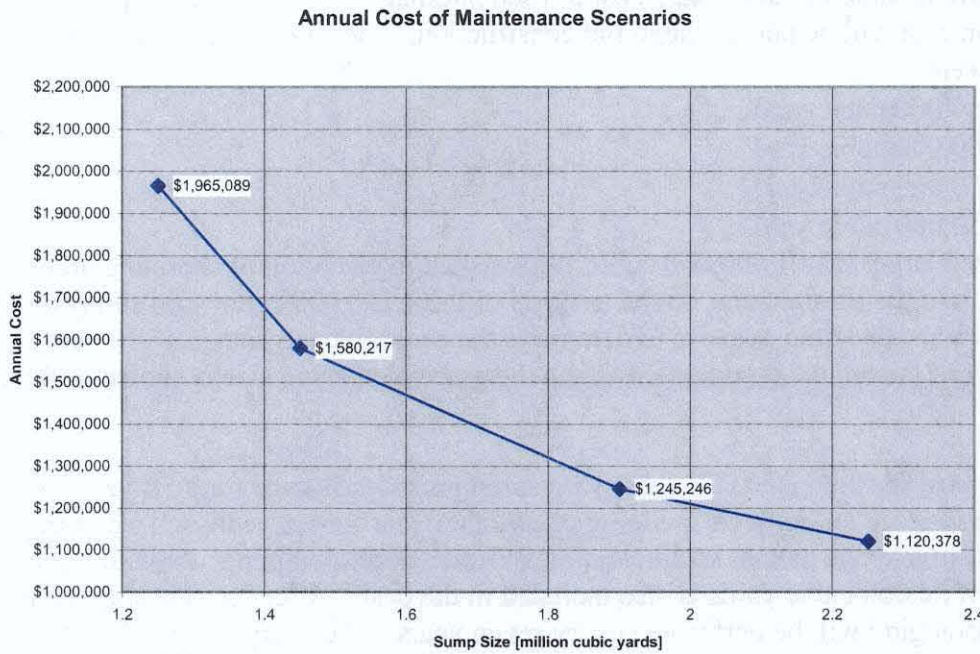


Figure 109. Annual Cost of Sump Dredging Scenarios

### 11.1.7 Dredge Required for the Shore Connected Direct Loading Facility

The quantity of sediment that must be handled is estimated to be on average 26,159 cubic yards (20,000 cubic meters) per year in the littoral zone and 74,553 cubic yards (57,000 cubic meters) per year seaward of the littoral zone. The offshore sediment transport variance within the 16 year hindcast used for estimating, calculated 805,044 cubic yards (615,500 cubic meters) as the maximum amount of channel deposition in one year (1996). A 10-year return event could contribute approximately 131,000 cubic yards (100,000 cubic meters), and a 50-year event could contribute 680,000 cubic yards (520,000 cubic meters).

Littoral zone sediment transfer requirements are calculated to be much smaller than the offshore depositions and can be handled from the shore side with a land-based equipment. The dredge equipment for the channel dredging must be ocean capable under extreme conditions or a local refuge needs to be established for protection during adverse climatic conditions. The range of sediment infilling estimates for the channel is listed in table A-52 to illustrate the flexibility that may be required to maintain a project. The upper bound of infilling from 1985 to 2000 is detailed in table A-53 as it is the maximum infilling that the project should be able to handle.

Draft Feasibility Report  
Appendix A: Hydraulic Design, Delong Mountain Terminal, Alaska

**Table A-52 Maximum, minimum, and best infilling estimate**

Best Estimate yd <sup>3</sup> (m <sup>3</sup> )				Lower Bound Estimate Coarse Sediment -25% current. -20% wave height				Upper Bound Estimate Fine Sediment + 25% currents + 20 wave height			
Average 1985- 2000	10 year event	20 year event	50 year event	Average 1985- 2000	10 year event	20 year event	50 year event	Average 1985- 2000	10 year event	20 year event	50 year event
74,000 (57,000)	131,000 (100,000)	392,385 (300,000)	680,355 (520,169)	14,387 (11,000)	32,699 (25,000)	52,318 (40,000)	104,636 (80,000)	211,888 (162,000)	405,465 (310,000)	980,963 (750,000)	1,658,073 (1,267,688)

**Table A-53 Estimate of upper bounds of infilling cubic yards (cubic meters)**

Year	Jul	Aug	Sep	Oct	Nov	Annual
1985	0	0	0	24,695 (18881)	0	24,695 (18881)
1986	0	0	0	0	0	0
1987	0	0	0	0	0	0
1988	0	2,396 (1832)	0	0	0	2,396 (1832)
1989	0	0	0	20,667 (15801)	0	20,667 (15801)
1990	0	3,991 (3051)	0	0	420,077 (321172)	424,068 (324224)
1991	0	0	0	255,368 (195243)	0	255,368 (195243)
1992	0	0	0	111,560 (85294)	0	111,560 (85294)
1993	0	12,469 (9533)	4,073 (3114)	3,382 (2586)	108,890 (83252)	128,815 (98486)
1994	0	3,153 (2411)	0	18,760 (14343)	0	21,912 (16753)
1995	0	0	0	0	0	0
1996	42,532 (32518)	0	0	1,658,073 (1267688)	376,686 (287997)	2,077,291 (1588203)
1997	0	0	0	34,751 (26569)	279,171 (213442)	313,923 (240011)
1998	0	0	0	0	0	0
1999	0	0	0	0	0	0
2000	0	0	0	0	0	0
<b>AVG</b>	<b>2658 (2032)</b>	<b>1376 (1052)</b>	<b>255 (195)</b>	<b>132,953 (101650)</b>	<b>74,050 (56616)</b>	<b>211,294 (161546)</b>

## **11.2 Sedimentation Associated With The Breakwater And Barge Loading Facility**

### **11.2.1 Sediment Transport Within the Littoral Zone.**

The shore-parallel breakwater would block sediment transport within the littoral zone. For estimating purposes, 26,159 cubic yards (20,000 cubic meters) per year is assumed to require removal annually. This is close to the estimated average gross littoral transport and is the same volume estimated for the littoral zone in the direct loading option. Transfer of material to bypass the port site after major storms would need to take place with a net transfer to the south.

### **11.2.2 Wave and Current Induced Sediment Transport Seaward of the Littoral Zone.**

The centerline of the breakwater straddles the -24-foot (-7.3-meter) MLLW contour in front of the barge loading site. Therefore a small amount of sediment in this category would impact the barge loading facility. This amount is estimated at 6,540 cubic yards (5,000 cubic meters) per year.

### **11.2.3 Annual Maintenance Cost For Breakwater and Barge Loading Facility**

The annual costs associated with the breakwater were analyzed. It was assumed that annual littoral sediment bypassing of 26,000 cubic yards would be performed using a shoreline operation. Sediment accumulation behind the breakwater is assumed to be cleaned out using tug boat prop wash.

Based on the history of other breakwater projects designed by the Corps of Engineers maintenance is anticipated to occur every 10 years with approximately 5% of the armor stones needing replacement. This is a more frequent annual maintenance schedule than typically experienced on Corps projects. The frequency was doubled to account for ice impacts on the breakwater.

The average annual cost associated with the breakwater and barge option is \$444,000 with armor stone replacement every 10 years for \$1,044,000.

### **11.2.4 Dredge Associated with the Breakwater/Barge Loading Facility**

The dredge associated with the breakwater and barge-loading facility can accomplish its task with floating equipment in protected water, but the dredging can also be accomplished with a shoreline operation. Similar to other estimates of sedimentation, the accuracy of estimates is minimal and the variance from year to year is large. It is recommended that the dredge have the capacity of 52,318 cubic yards (40,000 cubic meters) per year, which is double the annual expectation for infilling. It is assumed that

the dredging performed for the breakwater and barge-loading facility will use local shore based equipment.

## **12.0 RISK AND UNCERTAINTY**

The analysis performed for this appendix used historical information to assess the wind, waves, currents, sediment transport, and ice development at the DMT. Risk and uncertainty that directly affects this project is annual maintenance and is fully described in the sediment section of this appendix. The information gathered and analysis presented is the best data available.

In-shore dredge work will likely be very close to encountering bedrock. Based on the information available, it is assumed that bedrock will not be encountered. It is recommended that additional geotechnical work be performed during the plans and engineering design stage to determine the presence or absence of bedrock in the nearshore dredge footprint. Figure 110 shows the nearshore borings and the assumed location of bedrock.

In recent years evidence has suggested that the arctic environment is experiencing a warming trend. The magnitude, duration, and effect of a warming trend is not known; however the Office for Naval Research, the Naval Ice Center, the Oceanographer of the Navy, and the Arctic Research Commission held a conference in 2002 which discussed the shrinking polar ice cap. They even indicated that the polar ice pack is projected to retreat to the extent that a new shipping route may be opened. This was addressed somewhat, but not entirely, for this project by performing the extreme storm analysis without the presence of ice cover.

Draft Feasibility Report  
Appendix A: Hydraulic Design, Delong Mountain Terminal, Alaska